



<https://theses.gla.ac.uk/>

Theses Digitisation:

<https://www.gla.ac.uk/myglasgow/research/enlighten/theses/digitisation/>

This is a digitised version of the original print thesis.

Copyright and moral rights for this work are retained by the author

A copy can be downloaded for personal non-commercial research or study, without prior permission or charge

This work cannot be reproduced or quoted extensively from without first obtaining permission in writing from the author

The content must not be changed in any way or sold commercially in any format or medium without the formal permission of the author

When referring to this work, full bibliographic details including the author, title, awarding institution and date of the thesis must be given

Enlighten: Theses

<https://theses.gla.ac.uk/>  
[research-enlighten@glasgow.ac.uk](mailto:research-enlighten@glasgow.ac.uk)

**LASER MICROBIAL  
INACTIVATION AND DETECTION**

**Allen, Chiew Beng Yeo B.Eng (Hons)**

**Submitted for the degree of  
Doctor of Philosophy**

**Department of Mechanical Engineering**

**Faculty of Engineering**

**University of Glasgow**

**© A. C. B. Yeo, 1999**

ProQuest Number: 10391437

All rights reserved

INFORMATION TO ALL USERS

The quality of this reproduction is dependent upon the quality of the copy submitted.

In the unlikely event that the author did not send a complete manuscript and there are missing pages, these will be noted. Also, if material had to be removed, a note will indicate the deletion.



ProQuest 10391437

Published by ProQuest LLC (2017). Copyright of the Dissertation is held by the Author.

All rights reserved.

This work is protected against unauthorized copying under Title 17, United States Code  
Microform Edition © ProQuest LLC.

ProQuest LLC.  
789 East Eisenhower Parkway  
P.O. Box 1346  
Ann Arbor, MI 48106 – 1346

GLASGOW  
UNIVERSITY  
LIBRARY

11635 (copy 2)

This is the original work of the author

Allen, Chiew Beng Yeo

To God and my mum...

## ACKNOWLEDGEMENTS

Over the years, many people have been kind enough to share their thoughts about my work with me and I take this opportunity to express my appreciation to them all.

I would like to express my extreme gratitude to my academic supervisor and friend, Dr. Ian Watson, for his guidance, encouragement and continual support in making this thesis come to pass.

Special appreciation also goes to my joint supervisor, Professor Duncan E. Stewart-Tull, whose constant help, enthusiasm and meticulous criticism have been invaluable throughout the duration of this project.

Many thanks to Professor Alastair Wardlaw and Dr. Glenn Ward for their constructive suggestions and constant optimism on my work.

The technical support given in this course of work was excellent and I would like to thank, especially Ian Peden, Jimmy Wilson (retired) and not forgetting the rest who contributed, one way or another towards my experimental work.

Acknowledgements are also extended to Pastor Winston Lee and Sis Eunice for their constant spiritual support and all my friends and colleagues, who have helped to create a friendly and enjoyable atmosphere both within and outwith my work place. Jessica Tan Peng Peng is also thanked for her unfailing support and patience throughout the course of my research and a special chapter of my life.

Special recognition must be given to Mr. Vincent Koh Hoon Hwee, who had assisted me in the necessary preparation towards the final completion of this project.

Never will I forget and appreciate the love, patience and provision from my dear distanced mum for without her, my long academic career will not be possible and a success.

This course of research was supported by the Overseas Research Scholarship (ORS) awarded by the Committee Vice-Chancellors and Principals of the Universities of the United Kingdom and University of Glasgow Engineering award. Part of this work will be furthered with the support and credit of the European Commission Cooperative Research proposal, FA-ST-8431.

## AFTERWORD

*Dear Lord, "thank You for giving me  
enough tears to keep me tender,  
enough hurts to keep me humane,  
enough failures to keep my hands in Thy tightly clenched arms and  
enough rewards to make sure that I walk with Thee moment by moment.  
In Thy Name sake, Amen."*

*2 Cor 1:3-7*

# SYNOPSIS

The experimental work in this thesis was aimed at optimising both the Nd: YAG and CO<sub>2</sub> laser-bacteria sterilisation systems and to test synergistic bactericidal effects with other sources of electromagnetic waves, namely ultra-violet and microwaves. Such novel applications could be used in decontamination and hygiene systems in the food and medical industries. A novel study of laser-bacteria detection method, speckle, was used to detect the level of contamination before a decontamination process could be optimised.

First, the absorption properties of water were investigated. This was necessary because water is the main constituent in any living bacterial cells. Water is often the main interactor with laser light in processes such as photolysis, photocoagulation and photo-thermal medical and dental treatments. The efficacy of laser irradiation is governed also by the penetration and absorption abilities of the cells. The knowledge of such optical properties will enhance the efficiency of laser-cell interaction processes. The temperature dependency of the extinction coefficient of water was found between 25 to 70 °C at 1.064 μm. The  $\alpha_T$  decreased with temperature and there was an apparent sudden transition from 0.060 cm<sup>-1</sup> to 0.038cm<sup>-1</sup> between about 40-45 °C. The scattering coefficient did not decrease at this temperature, but did with increasing temperature.

The laser parameters, namely pulse repetition frequency (PRF), pulse energy, exposure time and beam diameter of 400 W Nd:YAG laser were investigated to quantify the bactericidal effects of *S. aureus* on agar plates. The effects of varying the applied energy density from 800 Jcm<sup>-2</sup> to 2700 Jcm<sup>-2</sup> were investigated by changing the pulse repetition frequency and pulse energy. Zones of clearing observed on lawned agar plates after incubation at 37 °C for 24 hr were measured and the energy density at which 50 % (IA<sub>50</sub>) of the beam area was inactivated determined. An increase in PRF and/or pulse energy increased the area of clearing. The IA<sub>50</sub> values were dependent on the pulse energy, frequency and exposure time. Nd: YAG irradiation produced rapid sterilisation without damaging the substrate.

A method of modelling the three dimensional beam output characteristic of the Nd:YAG high power laser with a two dimensional pyroelectric detector array scanning slit was described. The three dimensional beam profiles of both sets of

laser parameter were superimposed from the detector array to the lawned agar plates' positions. A two dimensional energy density profiles across the burn print diameters along the highest peak plane obtained at the lawned agar plate position were mapped onto the IA<sub>50</sub> values beam diameters of the lawned clearance for both sets of laser parameter used.

With the CO<sub>2</sub> laser, the biocidal activity on different contaminated biomaterials namely, polypropylene, polyethylene, polyvinyl chloride and stainless steel was investigated. Complete inactivation of *S. aureus* was achieved before damage was induced on the substrate surfaces with the exception of polyvinyl chloride.

Two different types of high power CO<sub>2</sub> scanning mechanism were used to study the bactericidal effects on nutrient agar, collagen film and stainless steel; both systems produced sterilisation. Complete killing was achieved at 1.3 and 0.9 cm s<sup>-1</sup> scanning speed with *E. coli* and *S. aureus* on stainless steel respectively.

With 15 W low power CO<sub>2</sub> system, similar work was done to compare with the high power CO<sub>2</sub> and to quantify the inactivation effect over various powers (2 to 13.4 W) and speed from 3 to 100 mm s<sup>-1</sup>. The investigation showed the feasibility of scaling down the sterilisation capability at this wavelength of laser light to minimise laser cost and increase portability.

The novel and efficacious use of lasers as sterilisation tools can be further exploited. By combining emerging processes, effective minimal processing and decontamination may be achieved more effectively than conventional techniques. As such, the synergistic effect and the performance of a sterilisation system combining high power CO<sub>2</sub>, ultra-violet and microwave was critically evaluated in this study. The bactericidal effects of the individual sub-systems, combined simultaneous and sequential systems were examined and results showed that the combined treatment process reduced the variability as compared to the performances of individual sub-systems. This study suggests that a minimal combined processing system which have the advantages of the individual technologies (laser, ultra-violet and microwaves), could be developed.

The bactericidal effect and mechanism of *S. aureus* on stainless steel discs was further exploited. The heat transfer kinetics of thermal microwave irradiation implies that the microorganism has power density at least 51 folds more than its surrounding liquid suspension. Heat conduction from the stainless steel to the bacteria was believed to be the mode of bacteriostasis.

A low power Helium Neon laser (10 mW), with a charge coupled device ( CCD ) array camera set-up was used to capture the biological images and quantify the state of activities of *Escherichia coli* with and without the addition of Hibitane disinfectant solution using different laser speckle algorithms and techniques. This set-up could potentially be coupled with a laser sterilisation system to provide real time controlled decontamination processes.

The studies in this thesis have elucidated the problems associated with laser sterilisation procedures. In particular the dependency of microbial inactivation with laser parameters and the laser energy distribution. With the speckle methodology to detect the level of contaminant and the combined laser system with ultra-violet and microwaves, this thesis has achieved greater insights into laser-bacteria interaction which shows the market potential of such an approach in food and medical applications.

# NOMENCLATURE

$\alpha_{AB}$	Absorption coefficient at $\lambda, T$ ( $\text{cm}^{-1}$ )
$\alpha_S$	Scattering coefficient ( $\text{cm}^{-1}$ )
$\alpha_T$	Extinction coefficient ( $\text{cm}^{-1}$ )
$A$	Beam area ( $\text{cm}^2$ )
$A_m$	Area of bacterium ( $\text{m}^2$ )
$C$	Decorrelation coefficient (dimensionless)
$C_{pl}$	Specific heat capacity of distilled water ( $\text{Jkg}^{-1}\text{K}^{-1}$ )
$C_{pm}$	Specific heat capacity of bacterium ( $\text{Jkg}^{-1}\text{K}^{-1}$ )
$c_t$	Speckle contrast (dimensionless)
$D$	Beam diameter (cm)
$E$	Energy (J)
$ED$	Energy density ( $\text{Jcm}^{-2}$ )
$ED_v$	Energy density with translational velocity ( $\text{Jcm}^{-2}$ )
$f$	Pulse repetitive frequency ( $\text{s}^{-1}$ )
$h_m$	Convective heat transfer coefficient of bacterium ( $\text{Wm}^{-2}\text{K}^{-1}$ )
$\langle I \rangle$	Mean intensity of pattern ( $\text{Wcm}^{-2}$ )
$I$	Intensity transmitted by sample of water thickness ( $\text{Wcm}^{-2}$ )
$I_0$	Maximum intensity output ( $\text{Wcm}^{-2}$ )
$I_r$	Rate of inactivation ( $\text{cm}^2\text{s}^{-1}$ )
$k$	Thermal conductivity ( $\text{Wm}^{-1}\text{K}^{-1}$ )
$\lambda$	Laser wavelength (nm)
$L$	Water thickness (cm)
$M^2$	Beam quality factor (dimensionless)
$P_e$	Pulse energy (J)
$P_0$	Power output (W)
$q$	Complex beam parameter (m)
$Q$	Power absorbed (W)
$q_l$	Power density of distilled water ( $\text{Wm}^{-3}$ )
$q_m$	Energy absorption rate per unit volume or power density ( $\text{Wcm}^{-3}$ )
$\rho_l$	Density of distilled water ( $\text{kgm}^{-3}$ )
$\rho_m$	Density of bacterium ( $\text{kgm}^{-3}$ )
$R$	Radius of curvature of wavefront (m)
$r_m$	Radius of micro-organism (m)
$S(X)$	Digital signal at position X (dimensionless)
$S_r$	Distance between rotating mirror and agar plate (cm)
$\sigma$	Standard error of the mean (dimensionless)
$\sigma_I$	Standard deviation of (spatial) intensity variation ( $\text{Wcm}^{-2}$ )
$t$	Exposure time (s)
$T$	Temperature ( $^{\circ}\text{C}$ )
$T_f$	Final equilibrium temperature of bacterial-liquid sample (K)
$T_I$	Initial temperature of bacteria-liquid sample (K)
$V_m$	Volume of bacterium sampled ( $\text{m}^3$ )
$V_t$	Translational velocity ( $\text{cms}^{-1}$ )
$V_{uk}$	Decorrelation speed ( $\text{s}^{-1}$ )
$w$	Beam waist radius (m)
$W_c$	Width of clearance (mm)
$w_0$	Minimum beam waist radius (m)
$x$	effective heat transfer width (m)
$z$	Distance away from the beam waist (m)

# LIST OF FIGURES

- Figure 1.1.1** Number of surviving bacteria,  $N$  with time
- Figure 1.1.2** Linear (logarithmic) relationship of survival rate of bacteria with time
- Figure 1.1.3** Diagram illustrating the different parameters of a logistic curve for bacterial thermal death
- Figure 2.1.1** Laser beam interaction with water
- Figure 2.1.2** Schematic of the experimental setup
- Figure 2.1.3** Example of trace of a typical transmitted signal detected by the LECROY 9400, 125 Mhz digital oscilloscope from photodiode 2
- Figure 2.1.4** Graph of  $\ln \int V dt$  (mVs) versus the depth of water in the vessel
- Figure 2.1.5** The extinction coefficient,  $\alpha_T$  of water as a function of temperature
- Figure 2.1.6** The scattering coefficient,  $\alpha_S$  of water versus temperature
- Figure 2.2.1** Schematic representation of the experimental system
- Figure 2.2.2** Burn print characteristic with 400 W Nd:YAG laser
- Figure 2.2.3** A culture plate lawned with *S. aureus* after 6 Nd:YAG laser exposures and then incubated for 24 hr
- Figure 2.2.4** Photograph showing section of the lawned plate of *S. aureus* after laser exposure at 30 J (300W) for 16 s
- Figure 2.2.5** Series of graphs showing the area of inactivation of *S. aureus* as a function of the exposure time of Nd:YAG laser
- Figure 2.2.6** Graph of pulse energy as a function of the exposure time for  $IA_{50}$  values for PRF of:  $\blacklozenge$ , 5;  $\blacksquare$ , 10;  $\blacktriangle$ , 15;  $\times$ , 20;  $*$ , 25 and  $\bullet$ , 30 Hz
- Figure 2.3.1** Experimental set-up. A fraction  $R_f$  of the main beam is reflected via a wedge and a mirror onto a 2-D pyroelectric detector array located at  $z=1664.0$  mm.
- Figure 2.3.2** Diagram shows the 2-D series of pyroelectric detector used to capture the intensity profile of both 10 Hz 10 J and 20 Hz 5 J respectively
- Figure 2.3.3** Graph showing the threshold energy density of each pyroelectric detector of approximately  $9 \text{ Jcm}^{-2}$  at 8 ms pulse width which is used for both 10 Hz 10 J and 20 Hz 5 J
- Figure 2.3.4** The various burn print diameters were plotted as a function of optical  $z$  positions away from the collimating lens for 10 Hz 10 J,  $\blacksquare$  and 20 Hz 5 J,  $\blacklozenge$  at single pulse shot to  $z = 851.0$  mm
- Figure 2.3.5** 3-dimensional view of the energy density profile at pyroelectric detector position ( $z=1664$  mm) of 10 Hz 10 J
- Figure 2.3.6** 3-dimensional view of the energy density profile at pyroelectric detector position ( $z=1664$  mm) of 20 Hz 5 J
- Figure 2.3.7** 3-dimensional view of the energy density ( $IA_{50}$  value= $2488.04 \text{ Jcm}^{-2}$ ) profile of the laser beam at 10 Hz 10 J imposed on *S. marcescens* seeded on nutrient agar plate
- Figure 2.3.8** 3-dimensional view of the energy density ( $IA_{50}$  value= $3022.5 \text{ Jcm}^{-2}$ ) profile of the laser beam at 20 Hz 5 J imposed on *S. marcescens* seeded on nutrient agar plate
- Figure 2.3.9** Various burn print radii plotted as function of optical  $z$  positions away from the collimating len for 10 Hz 10 J,  $\blacksquare$  and 20 Hz 5 J,  $\blacklozenge$  at single pulse shot to  $z = 851.0$  mm after which no distinct burn print was observed

- Figure 2.3.10** Graph of percentage areas of inactivation of *S. marcescens* with respect to exposure times (A) and energy densities applied (B)
- Figure 2.3.11** The  $1/e^2$  locus gives a beam diameter of 1.5 cm at 10 Hz 10J with the energy density across as shown with the continuous line
- Figure 2.3.12** The  $1/e^2$  locus gives a beam diameter of 1.28 cm at 20 Hz 5 J with the energy density across as shown with the continuous line
- Figure 3.1.1** Diagram showing the set-up of *S. aureus* on disc substrate with CO<sub>2</sub> laser
- Figure 3.1.2** Killing pattern curves of overnight cultures of *S. aureus* as wet film with 380 W CO<sub>2</sub> laser on polypropylene, PP (■), polyethylene, PE (◆) and stainless steel (▲)
- Figure 3.1.3** Killing pattern curves of overnight cultures of *S. aureus* as wet film with 980 W CO<sub>2</sub> laser on polypropylene, PP (■), polyethylene, PE (◆) and stainless steel (▲)
- Figure 3.2.1** A set of five contaminated unexposed stainless steel strips
- Figure 3.2.2** Scanning system of contaminated nutrient agar plates and collagen skins
- Figure 3.2.3** Scanning system of *E. coli* and *S. aureus* on stainless steel strips
- Figure 3.2.4** Killing pattern of width clearance versus scanning speed with *S. aureus* on sausage skin, (■) and nutrient agar, (◆)
- Figure 3.2.5** Killing pattern of percentage width clearance versus scanning speed with *S. aureus* on sausage skin, (■) and nutrient agar, (◆)
- Figure 3.2.6** Killing pattern of width clearance versus energy density applied with *S. aureus* on sausage skin, (■) and nutrient agar, (◆)
- Figure 3.2.7** Killing pattern of percentage width clearance versus energy density applied with *S. aureus* on sausage skin, (■) and nutrient agar, (◆)
- Figure 3.2.8** Killing pattern of rate of inactivation against scanning speed with *S. aureus* on sausage skin, (■) and nutrient agar, (◆)
- Figure 3.2.9** Killing pattern of rate of inactivation against energy density applied with *S. aureus* on sausage skin, (■) and nutrient agar, (◆)
- Figure 3.2.10** Killing curve of *E. coli*, (●) and *S. aureus*, (▲) seeded on stainless steel strip with different CO<sub>2</sub> laser beam translational velocities
- Figure 3.2.11** Response curve of *E. coli*, (●) and *S. aureus*, (▲) seeded on stainless steel strip with different CO<sub>2</sub> laser beam translational velocities
- Figure 3.2.12** Response curve of *E. coli*, (●) and *S. aureus*, (▲) seeded on stainless steel strip with rate of inactivation to CO<sub>2</sub> laser irradiation
- Figure 3.2.13** Killing curve of *E. coli*, (●) and *S. aureus*, (▲) seeded on stainless steel strip with applied CO<sub>2</sub> laser energy density
- Figure 3.3.1** Experimental set-up of low power, 15 W CO<sub>2</sub> laser scanning system
- Figure 3.3.2** Diagrams of stainless steel strips for laser scans
- Figure 3.3.3** Figure showed a section of a laser treated zone of *E. coli* lawned on nutrient agar plate at laser setting 10 W 60 mms<sup>-1</sup> after over incubation at 37 °C
- Figure 3.3.4** Sub-lethal inactivation shown on the laser scanning track with 40 mms<sup>-1</sup> occurred at 4 and 3 W for both *S. aureus* and *E. coli*

- Figure 3.3.5** Width of clearance,  $W_c$  on nutrient agar plates seeded with *E. coli* (solid line) and *S. aureus* (dotted line) over a range of laser power output with  $V_t$  at 40 (×), 60 (▲), 80 (■) and 100  $\text{mms}^{-1}$  (◆)
- Figure 3.3.6** Graph of area of inactivation versus power output at various  $V_t$ , namely, at 40 (×), 60 (▲), 80 (■) and 100  $\text{mms}^{-1}$  (◆) with *E. coli* (solid line) and *S. aureus* (dotted line)
- Figure 3.3.7** Relationship of varying laser energy density with the inactivated width of clearance,  $W_c$  with *E. coli* (solid line) and *S. aureus* (dotted line) at 40 (×), 60 (▲), 80 (■) and 100  $\text{mms}^{-1}$  (◆)
- Figure 3.3.8** Rate of inactivation,  $I_r$  of *E. coli* (solid line) and *S. aureus* (dotted line) against energy density applied with various  $V_t$  at 40 (×), 60 (▲), 80 (■) and 100  $\text{mms}^{-1}$  (◆)
- Figure 3.3.9** Rate of inactivation,  $I_r$  against translational velocity,  $V_t$  with *E. coli* (A) and *S. aureus* (B) at 13 (solid line; ◆), 12 (solid line; ■), 11 (solid line; ▲), 10 (solid line; ×), 9 (solid line; \*), 8 (solid line; ●), 7 (solid line; +), 6 (dotted line; ◆) and 5 W (dotted line; ■)
- Figure 3.3.10** Graph showed the relationship of laser inactivation parameters of *S. aureus* ( --◆-- ) and *E. coli* (solid line; ◆) between power,  $P_o$  and translational velocity,  $V_t$  corresponding to  $IA_{50}$  value of the beam characteristic
- Figure 4.1.1** Experimental setup of single and combined treatment with  $\text{CO}_2$  laser light, UV and microwave radiation
- Figure 4.1.1** Experimental setup of single and combined treatment with  $\text{CO}_2$  laser light, UV and microwave radiation
- Figure 4.1.2** Samples of unexposed apple
- Figure 4.1.3** Samples of unexposed potato
- Figure 4.1.5** Samples of uncontaminated potato cuts with exposure time up to 30 ms with 200 W  $\text{CO}_2$  laser
- Figure 4.1.6** Samples of uncontaminated apple cut with exposure time up to 30 ms with 200 W  $\text{CO}_2$  laser
- Figure 4.1.7** Samples of uncontaminated tomato cut with exposure time up to 50 ms with 200 W  $\text{CO}_2$  laser
- Figure 4.1.8** Bacterial viable reduction of contaminated samples namely, apple; ●, potato; ■, tomato; ▲, with initial bioburden of approximately  $6 \times 10^7$  cfu *S. aureus* (15  $\mu\text{l}$ ) exposed to 200 W  $\text{CO}_2$  laser up to 30 ms
- Figure 4.1.9** Response killing patterns of *S. aureus* on apple; ●, potato; ■, and tomato; ▲ samples with 800 W conventional microwave oven
- Figure 4.1.10a** Tomato sample exposed to 5 s microwave radiation
- Figure 4.1.10b** Tomato sample exposed to 6 s microwave radiation
- Figure 4.1.10c** Tomato sample exposed to 7 s microwave radiation
- Figure 4.1.11** Graph of *S. aureus* response killing pattern with ultra-violet radiation up to 90 s exposure time with apple; ●, potato; ■, and tomato; ▲, sample
- Figure 4.1.12** Boxplots of the individual results extracted from Table 4-1-2 with potato, box 1, 2, 3; apple, box 5,6, 7 and tomato, 9, 10, 11, and the permutations of combined treatments with potato, box 4; apple, box 8 and tomato, box 12. Box 13 showed the statistical results for the controls

- Figure 5.1.1** Representation of cell viability, ● (primary, left y-axis) and temperature measurements (secondary, right y-axis) of stainless steel, ◆; with broth, ▲; distilled water, ■ and bacteria-liquid suspension, × against microwaves exposure time
- Figure 6.1.1** Experiment set-up for detecting the state of bioactivity in *E. coli* suspension with and without disinfectant solution
- Figure 6.1.2** From each frame, each horizontal line consisting of 128 pixel at 25<sup>th</sup> position was extracted (at 3 s interval) and group to form a resultant STS image which contains both spatial and temporal information
- Figure 6.1.3** STS patterns of *Escherichia coli* suspension with 1/6000 at T<sub>0</sub> (b1) and T<sub>30</sub> (c1) min; 1/4000 at T<sub>0</sub> (b2), T<sub>15</sub> (c2) and T<sub>30</sub> (d2) min; 1/40 at T<sub>0</sub> (b3) and T<sub>15</sub> (c3) min and concentrated Hibitane disinfectant solution at T<sub>0</sub> (b4) and T<sub>15</sub> (c4) min
- Figure 6.1.4** Absorbance values for *E.coli* liquid culture with increasing concentration of HIBITANE disinfectant solution
- Figure 6.1.5** Contrast level characteristics of pure *E.coli* suspension (a), with 1/6000 (b), 1/4000 (c), 1/40 (d) and concentrated (e) Hibitane disinfectant solution at T<sub>0</sub> min corresponding to 128 temporal positions or array element number of 3 s interval
- Figure 6.1.6** Temporal decorrelation speed, V<sub>uk</sub> of pure *E.coli* suspension (a), with 1/6000 (b), 1/4000 (c), 1/40 (d) and concentrated (e) Hibitane disinfectant solution at T<sub>0</sub> min corresponding to 128 temporal positions or array element number of 3 s interval
- Figure 6.1.7** Temporal decorrelation speed, V<sub>uk</sub> of *E. coli* (solid line) with 1/6000 diluted Hibitane disinfectant solution at T<sub>0</sub> (dash line) and T<sub>15</sub> (dotted line) min corresponding to 128 temporal positions of 3 s interval
- Figure 6.1.8** Temporal decorrelation speed, V<sub>uk</sub> of *E. coli* (solid line) with 1/4000 diluted Hibitane disinfectant solution at T<sub>0</sub> (dash line) and T<sub>15</sub> (dot-dashed line) and T<sub>30</sub> (dotted) min corresponding to 128 temporal positions of 3 s interval
- Figure 6.1.9** Temporal decorrelation speed, V<sub>uk</sub> of *E. coli* (solid line) with 1/40 diluted Hibitane disinfectant solution at T<sub>0</sub> (dotted line) and T<sub>15</sub> (dashed line) min corresponding to 128 temporal positions of 3 s interval
- Figure 6.1.10** Temporal decorrelation speed, V<sub>uk</sub> of *E. coli* (solid line) with diluted Hibitane disinfectant solution at T<sub>0</sub> (dotted line) and T<sub>15</sub> (dashed line) min corresponding to 128 temporal positions of 3 s interval

# LIST OF TABLES

<i>Table 1-1-1</i>	Different sources of ionisation radiation on bacteria
<i>Table 1-1-2</i>	Various types of microbial heat treatment
<i>Table 2-3-1</i>	The calibration for each set of laser parameters were measured using a power/energy meter (FILEDMASTER™, Coherent, U.K.)
<i>Table 2-3-2</i>	Table shows the minimum diameter, $w_0$ , corresponding to $z = 0$ mm with energy density falling on the pyroelectric detector for 8.1 and 4.1 J pulse energy which is below the threshold level of the detector array of $9 \text{ J cm}^{-2}$
<i>Table 2-3-3</i>	Table shows the detail of the 3-D energy density profile, integrated pulse energy and reflected fraction of the main beam, $R_f$ for 8.1 and 4.1 J respectively
<i>Table 2-3-4</i>	Both the beam diameter using Gaussian beam propagation equation with $M^2$ compensation factor theoretical diameter, $2w_{\text{theor}}$ and actual diameter, $2w_{\text{detector}}$ obtained via the pyroelectric detector are shown for 8.1 and 4.1 J respectively
<i>Table 3-1-1</i>	Total inactivation of approximately $3 \times 10^7 \text{ cfu ml}^{-1}$ of <i>S. aureus</i> with $\text{CO}_2$ laser energy applied onto polypropylene, PP, polyethylene, PE and stainless steel, SS at 380 (A) and 980 W (B)
<i>Table 3-2-1</i>	Width of clearance of <i>S. aureus</i> lawn on nutrient agar plates
<i>Table 3-2-2</i>	Threshold killing level of clearance of <i>S. aureus</i> lawn
<i>Table 3-2-3</i>	Bacterial viability reduction of approximately $4 \times 10^9 \text{ cfu ml}^{-1}$ initial bioburden of dried <i>S. aureus</i> and <i>E. coli</i> inoculum on stainless steel strips with different suspending liquid medium
<i>Table 4-1-1</i>	Combined sequential experiments
<i>Table 4-1-2</i>	Simultaneously combined (COMB) effect of $\text{CO}_2$ laser, ultraviolet and microwaves radiation on <i>S. aureus</i> with potato, apple and tomato
<i>Table 4-1-3</i>	Sequential treatment of samples and the number of <i>S. aureus</i> which survived at each time and stage (in brackets)
<i>Table 5-1-1</i>	Rate of temperature rise, $R_T$ , with and without culture broth, distilled water or inoculum on stainless steel disc
<i>Table 5-1-2</i>	Comparison of power and power density conducted through stainless steel disc and inoculum with increasing temperature and microwaves irradiation
<i>Table 5-1-3</i>	Energy absorption rate ratio of <i>S. aureus</i> micro-organism to its surrounding suspending liquid, sterile distilled water, $q_m/q_l$ , with microwave irradiation at 50 to 65 °C
<i>Table 6-1-1</i>	Absorbant values measured at 600 nm wavelength of various dilutions concentration and concentrated HIBITANE disinfectant solution against sterile saline as blank
<i>Table 6-1-2</i>	Average temporal contrast values of <i>Escherichia coli</i> and with various strength of Hibitane disinfectant solution added
<i>Table 6-1-3</i>	Temporal decorrelation speed, $V_{\text{oks}}$ of <i>Escherichia coli</i> and with various strength of Hibitane disinfectant solution added

DEDICATION	i
ACKNOWLEDGEMENTS	ii
AFTERWORD	iii
SYPNOSIS	iv
NOMENCLATURE	viii
LIST OF FIGURES	x
LIST OF TABLES	xv
<b>I INTRODUCTION</b>	<b>1</b>
<b>1.1 STERILISATION</b>	<b>2</b>
1.1.1 KINETICS OF ANTI-MICROBIAL METHODOLOGY	2
1.1.2 MICROBIAL TERMINOLOGY	3
1.1.3 NON-IONISATION RADIATION	4
1.1.3.1 Ultra-violet rays	4
1.1.3.2 Microwaves	7
<i>Range of frequency inactivation</i>	8
<i>Bactericidal effects with 2450 MHz,                     microwaves</i>	9
1.1.3.3 Lasers	12
<i>Argon ion</i>	12
<i>CO<sub>2</sub></i>	13
<i>Excimer</i>	17
<i>He-Ne</i>	18
<i>Nd:YAG</i>	19
<i>Ruby</i>	22
<i>Other lasers</i>	23
<i>Photosensitization</i>	24
1.1.4 IONISATION RADIATION	25
1.1.5 OTHER PRACTICES OF MICROBIAL INACTIVATION	26
1.1.5.1 Heat	26
1.1.5.2 Gaseous	26
1.1.5.3 Novel methods	27
<b>II Nd:YAG LASER</b>	<b>29</b>
<b>2.1 LASER-WATER INTERACTION</b>	<b>30</b>
2.1.1 INTRODUCTION	30
2.1.2 EXPERIMENTAL SET-UP AND MEASUREMENTS	32
2.1.3 RESULTS	34
2.1.4 DISCUSSION	35

2.2	<b>INACTIVATION OF <i>STAPHYLOCOCCUS AUREUS</i> ON AGAR MEDIUM</b>	40
2.2.1	INTRODUCTION	40
2.2.2	MATERIALS AND METHODS	41
2.2.2.1	Culture preparation	41
2.2.2.2	Preparation of lawned plates	41
2.2.2.3	The Nd:YAG laser	41
2.2.2.4	Laser output beam area and energy density	43
2.2.2.5	Laser exposure of lawned plates	43
2.2.3	RESULTS	44
2.2.3.1	Frequency dependence of laser inactivation	51
2.2.3.2	Checks for viable but non-culturable microorganisms	53
2.2.4	DISCUSSION	54
2.3	<b>BEAM PROFILING / QUALITY ANALYSIS WITH <i>SERRATIA MARCESCENS</i></b>	58
2.3.1	INTRODUCTION	58
2.3.2	EXPERIMENTAL SET-UP	59
2.3.2.1	Nd:YAG laser delivery system	59
2.3.2.2	Signal detecting head	61
2.3.2.3	Signal processing system	61
2.3.2.4	Culture preparation	61
2.3.3	EXPERIMENTAL OPERATION AND PROCEDURES	63
2.3.3.1	Detector threshold energy density	63
2.3.3.2	Beam divergence	63
2.3.3.3	Beam profile	63
2.3.3.4	Beam quality factor, $M^2$	67
2.3.3.5	Laser parameters	68
2.3.3.6	Irradiation of lawned plates	68
2.3.4	RESULTS	69
2.3.4.1	Detector threshold energy density	69
2.3.4.2	Beam Divergence	69
2.3.4.3	Beam Profile	69
2.3.4.4	$M^2$	69
2.3.4.5	Laser inactivation of <i>S. marcescens</i>	77
2.3.5	DISCUSSION	77

### III CO<sub>2</sub> LASER 85

3.1	<b>SPOT TARGET STERILISATION SYSTEM WITH HIGH POWER CO<sub>2</sub> LASER</b>	86
3.1.1	INTRODUCTION	86
3.1.2	MATERIALS AND METHODS	87
3.1.2.1	Preparation of plastic and stainless steel discs	87
3.1.2.2	CO <sub>2</sub> Laser	87
3.1.2.3	Exposure of prepared discs	87

3.1.3	RESULTS	89
3.1.4	DISCUSSION	89
3.2	<b>LINEAR SCANNING STERILISATION SYSTEM WITH HIGH POWER CO<sub>2</sub> LASER</b>	95
3.2.1	INTRODUCTION	95
3.2.2	MATERIALS AND METHODS	95
3.2.2.1	<i>S. aureus</i> on collagen films	95
3.2.2.2	<i>S. aureus</i> and <i>E. coli</i> on stainless steel strips	96
3.2.2.3	CO <sub>2</sub> Laser	96
3.2.2.4	Bacterial viability assessment of dry and wet contaminated stainless steel strips	101
3.2.3	RESULTS	101
3.2.3.1	Nutrient agar and collagen film	101
3.2.3.2	Stainless steel strip	101
3.2.4	DISCUSSION	102
3.2.4.1	Nutrient agar and collagen films	102
3.2.4.2	Stainless steel strips	111
3.3	<b>LINEAR SCANNING STERILISATION SYSTEM WITH LOW POWER CO<sub>2</sub> LASER</b>	114
3.3.1	INTRODUCTION	114
3.3.2	MATERIALS AND METHODS	114
3.3.2.1	CO <sub>2</sub> laser	114
	<i>System design</i>	115
	<i>Experimental set-up</i>	115
	<i>Laser output beam and energy density</i>	115
	<i>Laser parameters</i>	117
3.3.2.2	<i>S. aureus</i> and <i>E. coli</i> on nutrient agar plates	117
3.3.2.3	<i>S. aureus</i> and <i>E. coli</i> on stainless steel strips	117
3.3.3	RESULTS	118
3.3.3.1	Laser exposed nutrient agar plates	118
3.3.3.2	Laser exposed stainless steel strips	129
3.3.4	DISCUSSION	129
IV	<b>LASER, ULTRA-VIOLET AND MICROWAVE SYSTEM</b>	132
4.1	<b>MINIMAL PROCESSES FOR BACTERIAL INACTIVATION WITH COMBINED UNIT OPERATION WITH LASER, ULTRA-VIOLET AND MICROWAVES</b>	133
4.1.1	INTRODUCTION	133
4.1.2	MATERIALS AND METHODS	134
4.1.2.1	Laser, ultra-violet and microwaves systems	134
4.1.2.2	Preparation of fruit samples	134
4.1.2.3	Inoculum	134

4.1.2.4	Exposure of prepared samples	135
	<i>Sub systems exposures</i>	135
	<i>Sequential combined system exposure</i>	135
	<i>Simultaneous combined system exposure</i>	139
4.1.2	RESULTS	140
4.1.3.1	Sub systems	140
	<i>CO<sub>2</sub> laser</i>	140
	<i>Microwaves</i>	140
	<i>Ultra-violet</i>	142
4.1.3.2	Combined simultaneous system	142
4.1.3.3	Combined sequential system	149
4.1.4	DISCUSSION	152
4.1.4.1	Sub systems	153
	<i>CO<sub>2</sub> laser</i>	153
	<i>Microwaves</i>	154
	<i>Ultra-violet</i>	154
4.1.4.2	Combined system	154
	<i>Simultaneous effect</i>	155
	<i>Sequential effect</i>	155
V	MICROWAVES IRRADIATION ON <i>STAPHYLOCOCCUS AUREUS</i>	156
5.1	HEAT TRANSFER ANALYSIS OF MICROWAVES RADIATION ON <i>S. AUREUS</i> LIQUID SUSPENSION	157
5.1.1	INTRODUCTION	157
5.1.2	MATERIALS AND METHODS	158
5.1.2.1	Bacterial samples	158
5.1.2.2	Microwaves	158
5.1.2.3	Temperature measurements	158
5.1.2.4	Heat transfer analysis	159
	<i>Thermal heat conduction</i>	159
	<i>Lumped analysis</i>	159
5.1.3	RESULTS	162
5.1.4	DISCUSSION	166
VI	LASER SPECKLE FOR CONTROLLING & MONITORING CONTAMINATION SYSTEM	170
6.1	BIODYNAMIC LASER-BACTERIA SPECKLE INTERACTION	171
6.1.1	INTRODUCTION	171
6.1.2	MATERIALS AND METHODS	173
6.1.2.1	Experimental set-up	173
6.1.2.2	Data acquisition of spatial time speckle (STS) pattern	173
	<i>STS pattern</i>	173
	<i>Data acquisition</i>	176
	<i>Data transfer</i>	176
	<i>Image processing</i>	176

6.1.2.3	Sample preparation	176
6.1.2.4	Hibitane disinfectant solution	176
6.1.2.5	Optical density measurement	177
6.1.2.6	Laser speckle statistical analysis techniques	177
	<i>First order statistic analysis: Spatial contrast analysis</i>	177
	<i>Second order statistics: Temporal decorrelation speed effect</i>	178
6.1.3	RESULTS	180
6.1.3.1	Spatial time speckle (STS) pattern	180
6.1.3.2	Optical density measurements	185
6.1.3.3	First order statistics: Spatial contrast analysis	185
6.1.3.4	Second order statistics: Temporal decorrelation speed effect	189
6.1.4	DISCUSSION	189
VII	CONCLUSION	201
VIII	REFERENCES	207
IX	APPENDICES	222
9.1	HEAT TRANSFER ANALYSIS	223

# I. INTRODUCTION

## 1.1 STERILISATION

### 1.1.1 KINETICS OF ANTI-MICROBIAL METHODOLOGY

Sterilisation is a treatment or process, which *frees the treated object of all living organisms*. Since in most common usage, 'sterilisation' or 'inactivation' is associated with microorganisms, it can be re-defined as *the complete destruction of all living microorganisms*. The criterion in this context is with the assumption that 'complete destruction' or 'death' is the *irreversible loss of the ability to reproduce* which is usually determined by quantitative plating methods with microbial survivors detected by the ability to form colonies (colony-forming units; 'cfu'). The kinetics of the death rates generally depends on which stage of viability or growth they are in. For example, the microbial population in the 'lag' phase will decrease with a lower dosage of treatment of an anti-microbial agent than one in its exponential growth condition. For this reason, all microorganisms investigated during this study were used during the exponential growth (conditions as described later) to ensure consistency and comparison between all experiments. It also implies that the laser action, if bactericidal, achieved sterilisation at the microbial population's most resistant state with the exception of the endospore stage in some species.

The *death kinetic rate* of a pure microbial population when exposed to a lethal agent always approximates to nearly exponential (**Figure 1.1.1**) and is commonly expressed in logarithmic form, **Figure 1.1.2**. With the logarithmic function expressed as a function of anti-microbial agent dosage, a straight line is obtained and the negative slope defines the *death kinetic rate*. It is noted that the pattern and rate of the graph differs with different bacteria. In the case of thermal related bactericidal activity, the temperature applied and the rate at which a certain lethal temperature is reached alters the shape of the killing curve. Nevertheless the death rate approximates exponential.

Consistent as it may be, there are certain exceptions to the general rule of logarithmic death which cannot be accounted for by experimental error or tolerance.

One such common phenomenon can be seen with food pathogens such as *Clostridium botulinum* and *Penicillin* species (Reed *et al.* 1951) and *Listeria monocytogenes* (Martin *et al.* 1993) with conventional water-bath, heat treatment conforming to a *sigmoidal* response pattern, **Figure 1.1.3**. Others have also reported such killing curves (Humphrey and Nickerson 1961, Hansen and Riemann 1963). Such non-logarithmic behaviour models the bacterial population decline based on log-logistic death kinetic assumptions; the initial and final population range plateau gradually with a centre linear decline slope. However, in this study, it is assumed that the response is linear between two successive D-values reduction in all experiments for simplicity unless otherwise stated.

### 1.1.2 MICROBIAL TERMINOLOGY

In 1922, Esty and Meyer were the first to show that the absolute thermal inactivation time increased with the initial number of microorganisms. They founded the definition, *D value*, decimal reduction time, which defined the time taken to reduce the number of microorganisms to 10 % of the initial population or a one  $\log_{10}$  reduction. *D value* is generally defined in minutes with microbial death kinetics. A *D value* is expressed at the particular temperature at which the lethal action occurred. The rate of microbial destruction is not always the same; i.e. heat treatment is more efficacious at higher temperature, implying that the *D value* will decrease with increasing temperature. To take this into account the *z value* is given:

$$z = \frac{T_1 - T_2}{\log D_2 - \log D_1} \quad (1.1.1)$$

in which  $T_1$  and  $T_2$  are the absolute temperature, in Kelvin and  $D_1$  and  $D_2$  the *D values* for temperature  $T_1$  and  $T_2$  of the microbes respectively. Therefore, the *z value* is the increase or change in temperature ( $^{\circ}\text{C}$ ) at which the *D value* is reduced by a factor of 10.

More often than not, the *F value* is related to the *D value*. The *F value* expresses an inactivation process (at any temperature) equal to a lethality effect of a certain number of minutes at a given temperature which is given by:

$$F = D (\log_{10} n_1 - \log_{10} n_2) \quad (1.1.2)$$

where  $n_1$  and  $n_2$  are the initial and final microbial population defined by the *D value*.

### 1.1.3 NON-IONISING RADIATION

#### 1.1.3.1 Ultra-violet (UV) rays

UV radiation has wavelengths which lie approximately between 100 and 400 nm. It has been divided, broadly, by the International Commission Illumination (CIE) into three regions: UVA (315 to 400 nm), UVB (280 to 315 nm) and UVC (100 to 280 nm). Wavelengths below 100 nm are generally absorbed in the air before they reach the earth. The most effective bactericidal range is much narrower, between 280 and 240 nm. The sensitivity of microorganisms to UV radiation vary with the wavelength of the radiation, although they all occur within a reasonable short range but optimum sensitivities of different geno-types do not occur at the same wavelength. In 1929, Gates reported that 265.2 nm was the optimum lethal wavelength for staphylococci while Duggar and Hollaender (1934) gave values between 265.2 and 280.4 nm for bacterial spores. Controversial as it may be, Gartner (1947) reported that the optimum lethal wavelength for all microorganisms was at 254 nm. Nevertheless, it seems that the wavelength of 254 nm is used world-wide for many bactericidal applications for the practical reason that most commercially produced quartz tube, low pressure Hg lamps that emit over 95 % of their total radiation at 254 nm.

The quantum photon energy radiated by UV rays is much higher compare to visible and infrared rays. However its penetration power is generally poor (approximately within the first 10 microns (Jagger, 1973) Nevertheless, the emission presents a very high risk of damage to unprotected skin and eyes.

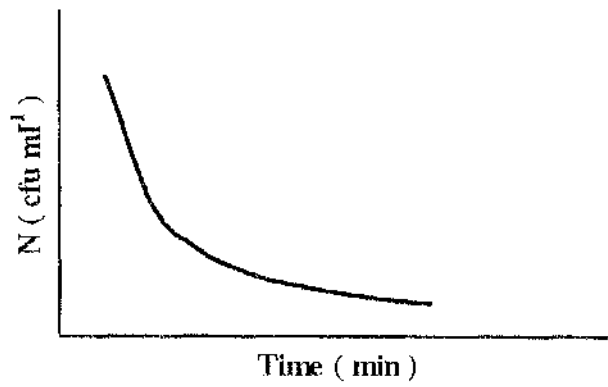


Figure 1.1.1 Number of surviving bacteria,  $N$  with time.

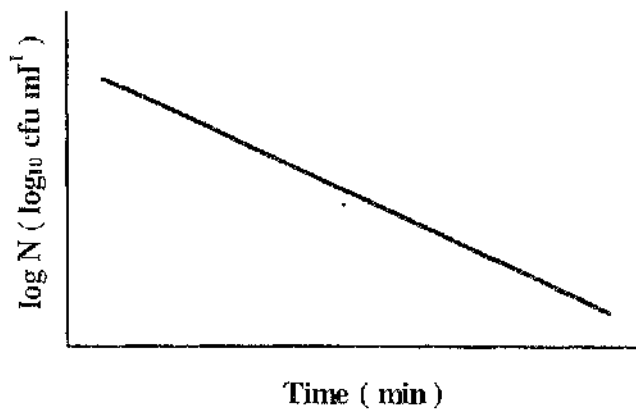


Figure 1.1.2 Linear (logarithmic) relationship of survival rate of bacteria with time.

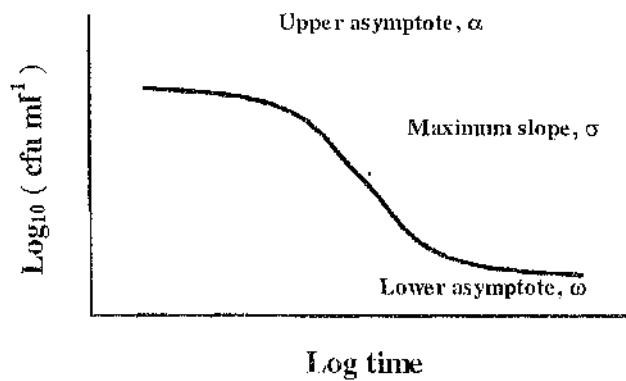


Figure 1.1.3 Diagram illustrating the different parameters of a logistic curve for bacterial thermal death.

In brief, the lethality effect is one of electron excitation and it is one where thymine dimers inhibit correct replication of the deoxyribonucleic acid (DNA) during the cell's reproduction. In 1930, Gates published the action spectra of the UV region for the bactericidal effect on *S. aureus* and *E. coli*. The highest spectra response was at around 254 nm wavelength which corresponded more closely to the absorption spectra of the nucleic acid bases than to those of the aromatic amino-acids of proteins. The actual killing is the result of formation of a linkage of two pyrimidine bases of the DNA which gives rise to substitution or deletion of DNA bases in reproductive-related genes and causes cell death.

Because of its ability to inactivate microorganisms at a relatively fast rate without a significant rise in temperature, UV irradiation is utilised in almost all medical fields where sterilisation is needed. Its widespread usage can also be accounted for by its portability (UV lamps).

UV rays have potential use in hospitals against air-borne pathogens and to combat cross-infection (Colebrook, 1955). Total bactericidal actions was reported with UV irradiation on *Escherichia coli* in drinking water after an exposure time of 1 min from a UV lamp emitting at  $0.7 \mu\text{Wcm}^{-2}$  at a distance of 7 cm (Cortelyou *et al.*, 1954). Similar works were also shown to be efficacious with UV radiation on *Salmonella typhimurium* and *Staphylococcus aureus* with *Bacillus subtilis* being the most resistant (Cortelyou *et al.* 1954). The bactericidal effect with UV has been commercially employed in the disinfection of drinking water since the 1960's (Sykes, 1965).

In 1992, Sobotka, reported the application of UV radiation for water disinfection and purification countrywide in Poland. A system was made to determine the influence of UV irradiation on bacterial water quality. In this system, recirculated water was infected with *E. coli*. Examination of water samples taken directly after the UV irradiation showed 50% reduction of bacteria after three water exchanges. The study also showed that water disinfection was achieved by means of ceramic filters in conjunction with UV irradiation. The combination of chlorine with ammonia and

UV irradiation was also tested in a pool of water and the result showed a reduction in the number of psychrophilic and mesophylic, as well as coliform, bacteria.

Recently, Shaban and his co-workers (1997) reported on the ability of UV to inactivate microorganisms in pure water and in turbid suspensions when combined with different factors affecting radiation. The effect of UV radiation on *E. coli*, *S. typhimurium*, *P. aeruginosa*, *S. aureus*, spore formers, *C. albicans*, *S. obliquus*, coliphage and vibrios was studied. Each organism in liquid suspension was exposed to UV in a batch experiment with variable turbidity and various flow rates of the contaminated suspension. A flow rate of 0.5 litre min<sup>-1</sup> with 1 min contact time was effective in killing all vegetative cells except *S. aureus* which required an additional 0.5 min contact. Spore-forming bacteria such as *Candida albicans* and coliphage were more resistant than vegetative cells to UV action. Increasing the turbidity of the suspension increased the cell resistance to UV irradiation.

Different materials contaminated with microorganisms have been seen to have different killing exposure times and energy requirement with UV irradiation. Hoerter and Eisenstark (1988) reported the susceptibility of *E. coli* and bacteriophage on polystyrene plastic and glass with far (FUV) and near ultraviolet (NUV) at 254 and 300-400 nm irradiation respectively. Significant differences were observed in FUV survival curves between cells or phage irradiated in glass and plastic with the organisms on plastic more susceptible. With NUV, at 90 % inactivation, the energy densities needed were 45 and 60 Jm<sup>-2</sup> on plastic and glass respectively. It was also suggested that no inherent toxicity was produced by the substrate except that due to the toxicity produced by the interaction of the polystyrene plastic and cells or phage during the irradiation. This implied that the sequence of interactions leading to toxicity required continuous 254 nm wavelength irradiation before bacteriostasis occurred; but the report did not state the UV lamp's power density or the exposure time with the killings observed.

### **1.1.3.2 Microwaves**

Microwaves are relatively long transverse waves as compared to infrared and UV region. Microwaves used in domestic ovens are in the same family of frequencies as

the signals used in radio and television broadcasting; although signal transmission in military radar systems use longer waves (approximately 300 MHz). It is well accepted and understood that microwaves are non-ionising and the mode of action onto the target via vibrational modes of the targeted atoms or molecules. The range of generated wavelengths is probably the most common encountered in the electromagnetic spectrum in our daily lives, besides radio waves.

### ***Range of frequency inactivation***

Microwaves generally extend over the range of 1 m to 1 mm in wavelength with frequency of 300 MHz to 300 GHz of the electromagnetic spectrum respectively; falling between the radio frequency and infrared region. Microwaves in the extremely short wavelength region are called submillimetre waves. The conventional microwave oven normally has a frequency of 2450 MHz and most of the sterilisation work on food and destruction of microorganisms reported are used with this frequency. However, the usage and application of microwaves does not limit it only to this frequency as described below.

Reports of microwaves inactivating microorganisms can be traced as far back as 1954 by Brown and Morrison. In 1968, Blackman and co-workers examined the colony forming ability of *E. coli* cells exposed to 1.70, 2.45, 68-74 and 136 GHz. The experiment was designed to study non-thermal effects on the biological system. The main result was that microwaves did not inhibit cell growth, but were responsible for cell growth enhancement, which was attributed to slight temperature rises due to absorbed microwave power in the cell system. Obviously, the power supplied was far from the killing threshold of the cells.

Culkin *et al.* (1975) reported the destruction of *Escherichia coli* and *Salmonella typhimurium* in microwave-cooked soups with two different frequencies at 915 and 2450 MHz. The objective of this experiment was to examine a possible non-thermal effect of microwaves. It was also stated that low frequency-range microwaves have better penetration into food than higher ones. For large industrial applications, 915 MHz is used for better penetration.

The effects of 2.6 to 4.0 GHz microwave radiation for ten hr at 26 °C on *E. coli* was studied by Corelli and co-workers in 1977. As the power used in this case was approximately 20 W, no effects were observed on the viability of *E. coli* as determined by colonies forming units (cfu) measurements and no molecular or conformational structure changes were noted in the molecular structure of *E. coli* measured by infrared spectroscopy.

In 1982, Hossain conducted a comparison of bacterial growth with high-intensity microwave exposure and conventional cooking. *E. coli* cells were exposed to 8.8 GHz microwaves pulsed at 1000 Hz and a specific absorption rate (SAR) of 40 Wkg<sup>-1</sup>, which increased the temperature of the cell culture by 7 °C. Two way analysis variance showed no significant difference between the growth rates of microwave-irradiated and thermally exposed cells. It was concluded that the 8.8 GHz pulsed microwave radiation at an average power density of 20 mWcm<sup>-2</sup> had no effect on the growth of *E. coli* beyond that associated with a temperature increase.

Nelson *et al.* (1994), reported on the microwave permittivity of fresh fruits and vegetables from 0.2 to 20 GHz. Microwave permittivity measurements were taken of 23 types of common fresh fruits and vegetables with an open-end coaxial-line probe in conjunction with a microwave network analyser. The dielectric constant (electric field distribution factor) decreased steadily with increasing frequencies, dropping more rapidly at frequencies above 5 GHz which suggested that even more microwaves are absorbed by the substrate below 5 GHz. Values for the loss factor (absorption rate factor) decreased as frequency increased above 0.2 GHz to a broad minimum in the 1-3 GHz region and then increase again as the frequency approached 20 GHz. The dielectric behaviour of the fruit and vegetable tissues appeared to be influenced by ionic conductivity and bound water relaxation at the lower frequencies and by free water relaxation at the higher end of the frequency range.

#### ***Bactericidal effects with 2450 MHz, microwaves***

The bactericidal effects on microorganisms after microwave radiation, operating at 2450 MHz, delivered by commercially equipment is reviewed below.

In 1977, Corelli *et al.* studied the sterilisation effect of 2.6-4 GHz microwave radiation on *E. coli*. The *E. coli* B cells were exposed to microwave radiation in a nutrient broth environment for cfu ml<sup>-1</sup> measurements, or exposed in an aqueous suspension for the study of molecular structure changes for 10 hr at a temperature below 26 °C at 20 mW. No effects were observed on the viability of the *E. coli* as determined by viable counts and no molecular or conformational structured changes were noted in the cell structure as measured by infrared spectroscopy.

Conversely, Fitzpatrick *et al.* (1978) reported the positive effects of microwave sterilisation after trials with a 2450 MHz commercial microwave oven. The experiments were initiated with *S. aureus* in saline suspension (5 ml), *B. subtilis* (dry spore) and *B. subtilis* (wet spore strip). The microorganisms were treated in the microwave oven with five successive doses of irradiation 12 seconds each. Sterilisation was achieved provided that the system employed a sealed container for the material being sterilised with sufficient moisture present for a thermal effect to take place.

Clothiaux in 1983 reported the inactivation of bacterial spores and vegetative cells via a microwave discharge system. Samples were prepared using stainless steel scalpel blades and microscope cover glasses contaminated with approximately 1 x 10<sup>7</sup> cfu of *S. typhimurium*, *P. mirabills*, *E. coli* and *P. aeruginosa*. Part of the samples was used as controls while others were treated in an autoclave or hot-air oven for comparison. The remaining samples were subjected to microwaves of 2450 MHz and power 600 W for different periods of time. The results showed complete sterilisation of the cover glasses and scalpel blades after the microwave exposure, with all enterobacteria examined being killed in a period of 2.5 min.

Soren and Flemming (1986) used microwaves to sterilise vials. In some experiments, the turntable was loaded with 66 vials and in others, it was fully loaded with 113 vials. In all experiments, five vials each were contaminated with dried spores of *B. stearothermophilus* and dried spores of *B. subtilis* or with 0.1 ml the suspension of spores in sterile water containing 6 X 10<sup>6</sup> to 6 x 10<sup>7</sup> spores ml<sup>-1</sup> were placed on various positions on the turntable. The initial number of spores per ml of

suspension was determined in every experiment as a control. The experiments were done with non-insulated wet vials and insulated dry vials. The difference in spore reduction at different positions on the turntable was also compared using both insulated and non-insulated turntable. In each series the microwave treatment time varied from 2 to 8 min. The results concluded that it is possible to sterilise vials by microwave heating as it showed a spore reduction of ( $2 \times 10^6$  cfu) within 2.7 min. The calculated D-value reduction time for  $1 \times 10^7$  spores was approximately 3 min and approximately 3.5 min for 66 vials with an end-point temperature of the vials at 160 and 170 °C respectively. The great difference in spore reduction between insulated and non-insulated vials suggested that the effect of microwave treatment on spores was due to a heating process. With the equipment used and with insulation of the vials, uniform spore reduction was observed regardless of the position of the vials which indicated a homogeneous treatment of the load.

Kazbekov and Vyacheslavov (1987) performed a series of experiments of *E. coli* and *B. subtilis* to demonstrate non-thermal effects induced by continuous microwave irradiation of a low power density. As the cell wall structures of the two species were rather different (*E. coli* was Gram-negative while *B. subtilis*, Gram-positive), it was of interest to compare the responses of identical biological processes in these bacteria to microwave irradiation. The samples were first heated to 25 °C to promote effective DNA uptake and exposed to microwave irradiation for 15 min before being transferred to agar plates and incubated at 37 °C. The colonies were counted and compared to the control values. Control cells were processed in parallel without irradiation. The data indicated that during irradiation the cell suspension, which was heated by 5 to 6 °C above the initial temperature, would induce a two to four-fold increase in the output of the DNA; considering all the data gathered, the authors concluded that the effects observed during microwave irradiation of the samples were thermal.

Wu *et al.*, (1994) reported the sterilising effect of high-power microwaves on bacteria and viruses on different materials with a specially-designed dis-infecter, at a frequency of  $2450 \pm 30$  MHz, at  $11.5 \text{ Wcm}^{-3}$  and  $6.2 \text{ Wcm}^{-3}$ . The bacteria and virus used were *B. subtilis*, *B. stearothermophilus*, *B. pumilis*, *S. aureus*, *B. cereus* and

HB<sub>A</sub>S<sub>g</sub> respectively. The items to be sterilised include china plates, popsicle sticks and food packaging synthetic plastics. The results indicated that on the same items with different energy densities, the time needed for killing all the microbes was unequal (ranging from 10 to 45 minutes). With the different bacterial strains on the same item, the time required for complete killing was different and with the same bacterial strain on different items, the time was different too.

Most reports have indicated that microwave energy does possess killing effects on microorganisms though a few did not find any effect. This may be due to the different parameters and conditions used, for example, different power settings. However, all reports which used the conventional microwave oven with 700 W power and frequency 2450 MHz did present killing effects on the microorganisms.

### 1.1.3.3 Lasers

#### *Argon ion*

The low power argon ion laser, operating in the visible region with principle emission at 488 and 514 nm, exhibited bactericidal capabilities. It has been used in medical applications and is set to replace the ruby laser since it is relatively less expensive. Powell and Whisenant (1991) used the argon ion laser for dental instrument sterilisation. An investigation was also made to compare the relative efficacy with CO<sub>2</sub> and Nd:YAG laser on *S. aureus*, *B. subtilis*, *P. aeruginosa*, *Strep. pyogenes*, *C. albicans* and *B. subtilis* spores seeded onto endodontic reamers. Five contaminated sets of the reamers were irradiated each with different laser parameters of time, power and laser source. Results showed that all three lasers were capable of disinfecting the microorganisms at 1 W power output with 60 s exposure time or greater. The argon laser radiation sterilised the reamers with spores at 120 J (59.6 Jcm<sup>-2</sup>) whereas with the CO<sub>2</sub> and Nd:YAG laser irradiation similar bacterial inactivation occurred at higher energy densities. Although the radiation of the three lasers showed bactericidal capabilities, the use of an argon ion laser was the most effective; requiring the lowest energy density of 29.8 Jcm<sup>-2</sup>. The argon ion laser radiation showed a more consistent killing trend than the other two lasers over the

five sets of experiments conducted. However, the authors did not fully state the laser parameters where the tests were not bactericidal. As such, the optimised parameters could not be deduced and compared for the three lasers used.

In another report, Yanagawa *et al.* (1992) investigated the bactericidal effect of an argon laser on various organisms namely, *Pseud. aeruginosa*, *Pseud. fluorescens*, *Acet. calcoaceticus*, *E. coli*, *Shigella. sonnei*, *Salm. typhimurium*, *Salm. enteritidis*, *Prot. mirabilis*, *M. morgani*, *Serr. marcescens*, *B. cereus* and *Staph. aureus*. The different kinds of bacteria were chosen as they are associated with nosocomial, opportunistic infection or various diseases. All species, lawned on Mueller Hinton agar, were tested with the argon laser set at 20, 40 and 60 mW for 30 min (72, 144 and 216 Jcm<sup>-2</sup> energy densities respectively). The laser beam spot size was 8 mm in diameter with the fibre optic cable tip at 30 mm from the surface of the agar plates. An inhibitory spot more than 6 mm in diameter or a deep inhibitory spot with less than 6 mm in diameter was considered bactericidal. The temperature rise with 70 mW for 30 min exposure time on the agar plate was less than 1 °C and generally, the organisms were killed with the laser irradiation. *P. aeruginosa*, which is often resistant to antibiotics, was found to be very sensitive to the low power irradiation, a bactericidal effect was seen with 144 and 216 Jcm<sup>-2</sup>. In contrast, *S. aureus* and *B. cereus* vegetative cells exhibited high resistance and no killing was observed when irradiated with energy densities up to 216 Jcm<sup>-2</sup>.

## CO<sub>2</sub>

Strong and Jako first reported the first use of a CO<sub>2</sub> laser with biological tissues on metal surfaces in 1972. One of the first groups to explore the susceptibility of microorganisms with this wavelength at 10.6 µm was Stellar *et al.* in 1974, living bacteria in tissue were vaporised and destroyed by CO<sub>2</sub> laser irradiation in a very short exposure time.

In 1979, Adrian and Gross reported the use of this laser on scalpel blades contaminated with spores of *Bacillus subtilis* and *Clostridium sporogenes*. Complete inactivation was observed with the laser set at 10 W in its continuous mode of action for 1.5 to 2 min. The 'sweeping motion' of the beam ensured all the

surfaces were exposed. However, the surface area of action was not specified and such experimental work and results could not be repeated and compared to other, similar laser-bacteria interactions.

CO<sub>2</sub> laser sterilisation has been favoured in dentistry where the need exists primarily for a rapid method of sterilising chair-side endodontic reamers which quickly become contaminated by contact with different patients' oral flora during treatment. Moreover, conventional bench-side sterilisation often does not provide consistent and reliable results (Dayoub and Devine, 1976, Winderler and Walter, 1975). Thus, Hooks and associates (1980) investigated whether endodontic reamers contaminated with *Bacillus subtilis* and *Bacillus stearothermophilus* spores could be effectively sterilised by CO<sub>2</sub> laser. The reamers were individually placed in a holding device in which full 360 ° angular rotation, at an interval of 90 ° sweep was made. For each surface section, a total of 3 s exposure was made at 10 W laser power. Longitudinal motion of the laser beam was made to interact with the reamers for complete laser treatments. Complete inactivation of the spores was recorded after incubation with normal growth taking place in unexposed reamers acting as controls. It was also proven that the reamers, being twisted would not prevent effective sterilisation since complete sterilisation was observed with the above mentioned settings.

Using the CO<sub>2</sub> laser, the effective time to achieve a bactericidal effect was found to be a few seconds less as compared to conventional methods. However, Mullarky (1985) pointed out that the observed puff of smoke, called a plume (the vaporisation of the microorganisms which causes the pyrolysed cellular debris to be released) due to the laser action, could contain infective microorganisms and as such could lead to cross-contamination during the sterilisation process. In his work, *S. aureus* and *E. coli* with initial concentrations of approximately  $3.7 \times 10^7$  cfu ml<sup>-1</sup>, were inoculated onto processed pig skin. The skin was laser-treated for 15 s at 25 W with a focused spot size of 0.2 mm and 10 s at 25 W with an unfocused spot size of 3 mm. In both cases no cells were recovered from the plumes with *E. coli* but some with *S. aureus*. The 68 viable *S. aureus* bacteria recovered may be attributed to the fact that staphylococci were more resistant than *E. coli*. Interestingly, the microorganisms

found, after laser treatment on the substrate, varied significantly with both focused and unfocused conditions at 3 D and 6-D-value microbial population reduction were observed respectively. Such killing patterns were due to the extremely high energy density applied; 1 MJcm<sup>-2</sup> and 3.5 kJcm<sup>-2</sup> for focused and unfocused beam respectively. Although one assumes that this would cause undesirable charring marks on the substrate after irradiation, the authors made no comment about this. Ironically, the unfocused beam with lower energy density of 3.5 kJcm<sup>-2</sup> produced a higher inactivation rate than the focused beam at 1 MJcm<sup>-2</sup>. This illustrates the ineffective experimental procedure used since the laser beam diameters (0.2 and 3 mm) were smaller than the 11 mm inoculated spot diameter. The bactericidal action of the laser radiation was not utilised to its fullest potential since most of the microorganisms killed were restricted to the 0.2 and 3 mm beam spot. The killing mechanisms was possibly due to heat conducted out from these small laser spot size areas in both focused and unfocused conditions rather than a direct effect of laser radiation on the cells. Nevertheless, the authors demonstrated the possibility of viable cells in the smoke emissions as a result of laser-bacteria interaction on pig skin substrate.

In 1986, Zakariasen and co-authors investigated the CO<sub>2</sub> laser interactions with three oral bacteria namely, *Streptococcus sanguis*, *Streptococcus mutans*, and *Actinomyces viscosus* and compared these with *Bacillus cereus*, *Staphy. aureus* and *Pseud. aeruginosa*. Exposure of all the six organisms on glass slides to CO<sub>2</sub> laser irradiation showed there was little significant difference in the energy densities required for inactivation. *Strep. sanguis* was found to be the most resistant: to achieve 99.9 % killing required 18.75 kJcm<sup>-2</sup>. With the exception of *Staph. aureus* at 9.37 kJcm<sup>-2</sup>, all organisms were completely inactivated at 6.25 kJcm<sup>-2</sup>. A correlation between laser alignment and bactericidal action was made experimentally and it was concluded that both related variables, namely, accuracy of alignment of the laser beam and physical characteristics of the prepared inoculum were important in determining the bacterial survival rate. For example, cell survival increased with increasing cell density for the same applied laser parameters. It was also concluded that there was no selective resistance of the organisms tested to the bactericidal action of CO<sub>2</sub> laser irradiation on glass slides or root canals of teeth.

A more detailed comparative approach of the bactericidal exposures and parameters on microorganisms with CO<sub>2</sub> laser light was investigated by Dederich *et al.* in 1990. Four clinically isolated oral bacteria, namely, *Actinomyces viscosus*, *Streptococcus mitior* (two strains), *Streptococcus sanguis*, *Streptococcus mutans* and two other microorganisms namely *Pseud. aeruginosa* and *Staphy. aureus* were tested. The results showed that *S. aureus* was the most resistant with 99.9 % killing at energy density of 159 Jcm<sup>-2</sup>. A comparison of equivalent energy exposures with different laser parameters was made on the bacterial viability but no significant statistical variations and differences were found in the energy needed to kill all the bacterial species. There were no susceptibility differences with respect to clinically or naturally occurring oral bacteria isolates with constant laser energy exposures. This implied that bacteria isolated from a particular ecological niche, and by implication possessing a cell envelope with maximal protection for the cell, were no more resistant to CO<sub>2</sub> laser wavelength than cells maintained in a laboratory culture sample. The work concluded that 'taxonomically unrelated bacteria of the same bacterial species were equally susceptible to CO<sub>2</sub> laser radiation.' The much lower energy densities applied for similar microbial killing as compared to Zakariasen *et al.* 1986 were due to proper laser alignment, with the beam spot size (2 mm) on the droplet of bacterial culture adhering to the substrate (1 to 1.5 mm in diameter). This ensures full action of the laser beam whose area encompasses the area of the inoculum.

In 1994, Talebzadeh *et al.* reported the use of CO<sub>2</sub> laser on *E. coli*, *Strep. mutans* and *B. stearothermophilus*. The aim was to investigate whether the 'susceptibility' or 'selectively' invariance findings of both groups of Gram-positive and Gram-negative bacteria to CO<sub>2</sub> irradiation, as reported by Dederich *et al.* 1990, was due to the selective absorption spectrum of the suspending liquid medium rather than the cells itself. Cell monolayers were prepared by placing atop filters which minimised the presence of extracellular water, no difference was observed between Gram types and his findings agreed with Dederich *et al.* (1990). However, much lower energy densities were reported at 19, 28 and 41 Jcm<sup>-2</sup> with *E. coli*, *B. stearothermophilus* and *S. mutans* to achieved 90 % cell reduction respectively.

### ***Excimer***

The excimer laser can emit coherent light at various wavelengths, namely, 193 nm (argon fluoride), 248 nm (krypton fluoride), 308 nm (xenon chloride) and 358 nm (xenon fluoride). Such lasers are known to induce photochemical and mutagenic effects on biological systems with sufficient energy to break chemical bonds. Moreover, high extinction coefficients in water were observed at these wavelengths implying a relatively higher absorption rate could be observed in living cells since water is the main constituent (Hale and Query, 1973). As such, the use of excimer lasers could provide a compromise with a strong bactericidal action while generating less heat in biological systems.

Sedarevic *et al.* in 1985, were the first to treat experimental *Candida keratitis* with an argon fluoride laser. In 1988, Keates *et al.* demonstrated the effectiveness of argon fluoride (ArF) laser emission on various bacterial strains-; namely *Serr. marcescens*, *Pseud. aeruginosa*, *Staph. aureus* and *Strep. faecalis* on tryptic soy agar. This work investigated the optimum laser parameters for the reduction in viability of these microorganisms. The laser was operated at 2 W, 10 Hz, 15 ns pulse duration with an energy density of 300 to 330 mJcm<sup>-2</sup> on single colonies inoculated on the agar plates. The time of exposure varied from 60 to 196 s. The results revealed that bacterial inactivation was achieved with all laser settings on all strains. However, localised melting of the agar was observed up to 2.6 mm depth. The time required rendering the bacteria inactive varied only slightly among the strains.

In another study, Frucht-Pery *et al.* (1993) investigated *Candida albicans* with the ArF laser radiation *in vitro*. The microorganisms were grown as colonies on Sabouraud agar plates. In the first experiment, the colonies were at least 5 mm apart, exposed to various energy densities at 10 Hz with a 2 mm focused beam to investigate the photoablation effect of the laser. In the second experiment, colonies of close proximity, i.e., 1 to 2 mm apart, were treated to investigate the laser effect on the colonies adjacent to the treated ones. In the third experiment, the bacterial effects were tested at 115 mJcm<sup>-2</sup> with an increase in the laser beam repetition frequency at 10, 20, 30, 40 and 50 Hz. The results showed that the laser could

destroy the bacterial species at relatively lower energy densities than reported by Keates *et al.* (1988). Sterilisation was achieved with 200 and 115 mJcm<sup>-2</sup> with a total of 400 pulses and 1500 pulses respectively. However, no inactivation was observed with 1000 or less pulses at 115 mJcm<sup>-2</sup>, and the bactericidal activity was not frequency dependent. Raising the frequency with constant energy density at 115 mJcm<sup>-2</sup>, 200 pulses did not sterilise the microorganisms on the plates which implied that energy density was the more important variable for bacterial killing. The elimination of a colony did not have a significant effect on the closely surrounding colonies.

The bactericidal action of a xenon chloride (XeCl) excimer laser on *Strep. mutans* was demonstrated by Stabholz *et al.* (1993) on well-culture and blood agar plates. The work reported was closely associated with dental applications. The laser, operating at 308 nm wavelength, was lasing at 15 ns pulse duration with spot size of 0.08 cm<sup>2</sup> and fluence up to 0.7 Jcm<sup>-2</sup>. Exposure times of up to 8 s were used. The killing of the microorganisms increased with an increased exposure time. A 7 D-value microbial reduction was observed with 8 s treatment. The antibacterial effects of the laser treatment were also more statistically significant than with 4 s. However, no statistically significant differences were observed with inactivation of the microorganisms on agar plates. The smallest and largest zones of inhibition were observed with 0.1 Jcm<sup>-2</sup> at 0.13 cm<sup>2</sup> and 1.0 Jcm<sup>-2</sup> at 0.42 cm<sup>2</sup>. The smallest area of clearance showed that the laser even at such a low energy level, was capable to induce bacterial inhibition without producing an indentation on the agar surface. Other similar reports were Kochewar (1992) and Karoutis *et al.* (1996).

### **He-Ne**

The low-power He-Ne laser radiation has shown biocidal abilities on microorganisms. Since the invention of the He-Ne laser in 1961 (Javan *et al.*, 1961), the effect of the monochromatic radiation on microorganisms was first reported by McGuff and Bell (1966). A 0.5 mW continuous wave He-Ne gas laser, operating at 632.8 nm with focussed and unfocussed beam spot diameters of 1.5 and 3 mm was incident on *Pseud. aeruginosa*, *Prot. vulgaris*, *Staph. aureus* and *B. subtilis*. However, no lethal effect of the laser energy on the bacterial growth on the agar

surfaces was detected. The longest exposure time was 120 (60 Jcm<sup>-2</sup>) and 300 (509 Jcm<sup>-2</sup>) min for unfocussed and focussed beams respectively. There was some retardation of pigment production by *Pseud. aeruginosa* after 300 min with the focussed beam system.

However, Okamoto *et al.* (1992) demonstrated that this low-power laser had an inhibitory action on cariogenic microorganisms. With the bactericidal effect determined by the formation of growth-inhibitory zones on Mitis-Salivarius (MS) agar, four stereotypes of *Strep. mutans* were tested with a 6 mW, 0.126 cm<sup>2</sup> area of irradiation from the He-Ne laser. Inactivation was achieved with 2, 5 and 10 min irradiation times with 5.7, 14.3 and 28.6 Jcm<sup>-2</sup> energy densities respectively; but the definition of the area of the cleared zones was unclear. The bactericidal effect, which was not achieved by McGuff and Bell, even with a relatively high energy density, could be due to the fact that the 0.5 mW laser had a much lower peak intensity on the microorganisms.

### **Nd:YAG**

McGuff and Bell (1996) studied the bactericidal effect of Ruby, He-Ne and Nd:YAG (1.064 µm) lasers on two positive and two negative species, namely, *Pseud. aeruginosa*, *Prot. vulgaris*, *Staph. aureus* and *B. subtilis*. All the microorganisms were inoculated on agar plates. The Nd:YAG laser used has a maximum energy output of 600 J but the peak or mean power was not mentioned. No bactericidal effect was observed for all species with an applied energy up to 100 J, 260 Jcm<sup>-2</sup>.

Schultz *et al.* (1986) investigated the susceptibility of three bacterial strains, *S. aureus*, *E. coli* and *Pseud. aeruginosa* with Nd:YAG laser irradiation, with and without added dyes. Water-bath thermal killing was also compared to laser-induced microbial death. In the first case, two artificial dyes, Congo red and methylene blue were added to the cells. The results showed that at a constant energy density, all the three strains exhibited different radiation tolerances with *Pseud. aeruginosa* being the most sensitive, followed by *E. coli* and *Staph. aureus*. Complete inactivation was approximately at applied energy of 2800 Jcm<sup>-2</sup> except with methylene blue and

*Pseud. aeruginosa* which was at  $2150 \text{ Jcm}^{-2}$ . It was believed that cell-produced or artificially simulated pigments enhanced the bactericidal action with Nd:YAG laser radiation. Such an assumption agreed with the radiation being absorbed more efficiently if a dark pigment was present (Polanyi 1983). The immersion of the microorganisms in the water-bath at  $60^\circ \text{C}$  for 10 s resulted in a two log D-value decline in cell viability compared to complete inactivation under the same conditions with a laser fluence of  $2778 \text{ Jcm}^{-2}$ . This could be associated with photochemical, photothermal, photoablative or photomechanical effects induced in the bacteria as suggested by Wilson (1993).

The Nd:YAG has been used in many dental applications. Anti-bacterial actions were reported with the microorganisms, *Actinobacillus actinomycetemcomitans*, *Porphyromonas gingivalis* and *Prevotella intermedia*, in the surface layer of microbial plaque in teeth by *in vivo* treatments (Cobb *et al.*, 1992). The Nd:YAG laser radiation appeared to vaporise subgingival plaques adherent to root and calculus surfaces as observed by scanning electron microscope (SEM). The  $320 \mu\text{m}$  fibre optic delivery probe was placed in contact with the microbial deposits. The parameters of the pulsed laser were set at 20 Hz, varying pulse energy of 3 to 1.75 J and exposure time of 1 to 3 min in a total of 18 patients treated. However, the effective laser contact area was not mentioned but if assumed, as with other microbial root surface treatments, to be 2 mm in diameter, the energy applied would be 3342 to  $5730 \text{ Jcm}^{-2}$ . Almost complete inactivation occurred except for some detectable cell viability with 1.75 J, 1 min exposure time. Relatively smoother surfaces were observed in the SEMs after laser treatment with lower laser settings and exposure time than higher settings. However, mechanical debridement was suggested to remove residual plaques after laser treatments.

Similar endodontic investigations were conducted by Rooney *et al.* (1994). *Enterococcus faecalis* on teeth were subjected to Nd:YAG irradiation with power ranging of 0.3 to 3 W, exposure time 20 to 60 s and the bactericidal effects were noted. Radiation dosages above 54 J at 1.8 W, 30 s exposure produced a 3.0-fold D value bacterial reduction. With non-toxic Suomi black ink, 25 J of laser energy, sterilisation was equally effective under the same conditions. Thus, Nd:YAG laser

could be an alternative dental technique to those currently employed if the presence of the dye produces increased intra-canal absorption effects with lower energy settings. This implies a reduction of any risk of unwanted side-effects with higher laser parameters on root treatments.

Recently, the penetration properties of Nd:YAG laser radiation on bacteria, operating at 1.06 and 1.32  $\mu\text{m}$ , were evaluated by Semenov *et al.*, 1996. Two mesophilic bacteria, *Staph. aureus* and *E. coli* were subjected to laser irradiation to assess the killing patterns on different thickness of agar medium. With 4400  $\text{Wcm}^{-2}$  power density, complete inactivation was observed up to a 4 mm depth of the agar followed by an increasing cell viability count observed with no inactivation at a depth of 30 mm. At 1.06  $\mu\text{m}$  wavelength, irradiation was more effective than at 1.32  $\mu\text{m}$  at each thickness of agar. The irradiation at these wavelengths did not cause elimination of R plasmids or any effect on the antibiotic resistance of the bacteria.

Similar work was done by Klinke *et al.* (1997). Sections of dental slices were made of different thickness (100-1000 $\mu\text{m}$ ) and artificially contaminated with *Strep. mutans*. The microorganisms were exposed to a 1.5 W, 15 Hz pulsed mode action laser irradiation with 10 to 20 s exposure time. When compared with un-irradiated controls, a significantly high microbial reduction was observed for all thickness after laser treatment with the antibacterial actions decreased with increasing thickness.

In all, Nd:YAG laser irradiation has the ability to inactivate a wide range of microorganisms. The pulsing mode of its action allowed for significant reductions in the amount of heat generated which could produce detrimental damage to the immediate surroundings. Furthermore, there is a window of low absorbency by air, water and solutions of proteins (Ward *et al.*, 1996) which suggested a more directional and selective action on any microorganisms with relatively deeper penetration properties.

## **Ruby**

The first publication of the use of laser radiation on living cells was in 1963. Saks and Roth demonstrated the irreversible damage on *Spirogyra* cells with a ruby laser operating at 694.3 nm wavelength. It was noted that the relative high transmissivity of the cell-wall to the laser wavelength caused a build-up internal pressure which then disrupted the cell wall. The laser had a maximum output of 20 mJ per pulse with pulse duration of 500  $\mu$ s. Complete disruption of the cell-walls, which also affected adjacent cells, was observed with full laser power. Microscopically, the cell-wall was split with nuclei and chloroplasts ejected into the surrounding medium. Smaller beam energies ranging from 1.4 to 2.5 mJ showed a less severe effect with cell-wall perforations of diameter 25  $\mu$ m. The cell-wall also appeared to be darkened and browned. No visible damage was seen with 0.3 mJ pulse energy or less. However, laser parameters such as exposure time and energy densities were not given making comparisons of the system's efficacy impossible. Although this investigation studied the action of laser irradiation on an algae, a multi-cellular organism, primarily aimed at microsurgery, the work has opened up avenues to many laser-living cell applications such as laser sterilisation and decontamination.

Three years later, Klein *et al.* (1965) demonstrated the effects of a ruby laser on several strains of microorganisms namely, *Serratia*, *Staph. aureus*, *Strep. pneumoniae*, *Pseud. aeruginosa* and *Asp. niger*. The irradiation constraints ranged from 3 to 76 J per pulse over a constant 1 ms pulse duration. Single and multiple exposures with 5 to 15 min pulse intervals were delivered focused, defocused and unfocused with a simple lens providing spot sizes of 8 to 14 mm in diameter on solid media. At 250 J, delivered as 5 exposures of 50 J per pulse, full bacterial inactivation was observed with *Pseud. aeruginosa*. The degree of inhibition varied from 60 J to 250 J. Although the authors did not state the beam diameters with these results, the energy densities could have ranged between 120.0 to 162.3 Jcm<sup>-2</sup>. *Pseudomonas* and *Serratia* strains showed variable and reversible decrease in pigment formation with single exposures of 60 J. The sensitivity of *Staph. aureus* to several antibiotics was not altered by the irradiation. With *Asp. niger*, no apparent sterilisation was seen with the laser. In all, the authors did show the biocidal effects

of ruby laser irradiation but did not give enough technical information on each laser treatment to allow a detailed comparison between each strain.

McGuff and Bell (1966) used three different kinds of ruby laser and a 0.5 mW continuous (CW) He-Ne laser, operating at 632.8 nm on two Gram negative and two positive bacteria, namely *Pseud. aeruginosa*, *Prot. vulgaris*, *Staph. aureus* and *B. subtilis*. The aim was two-fold: to investigate further the bacterial susceptibility to ruby light with different output powers and the effect of low-power laser light on microorganisms. The three types of ruby laser were, (1) a Maser Optics model with 2.5 ms pulse duration. The beam was focussed to 0.01 cm<sup>2</sup> spot size and 1.25 cm<sup>2</sup> with unfocussed condition, (2) a Q-switched ruby laser which delivered 10 MW, 40 ns pulse and (3), a twin lamp Q-switched type operating at 40 MW, 15 ns pulse duration. The He-Ne laser spot diameter sizes were 0.7 and 1.88 cm with focussed and unfocussed conditions with exposure times up to 300 min. However, no bactericidal effects were observed. The authors concluded that these negative findings could be due to overgrowth of viable cells on the agar plates prior to the exposures. Moreover, the energy densities were low since one and five pulses were applied to the microorganisms at 10 MW and 40 MW respectively. The results did indicate inhibition of the pigment-producing cells of *Pseud. aeruginosa* with He-Ne after five hours' exposure and a local increase in pigmentation with one burst of 40 MW ruby light.

### ***Other lasers***

Biocidal effects at other laser wavelengths have also been reported, however, the results in journal citations on laser-bacteria interaction were not comparable with due to the use of different lasers, laser parameters, experimental procedures and materials used; not to mention the complexity in combining these conditions. During this study, Watson *et al.* (1996) demonstrated the comparative bactericidal activities of lasers operating at seven different wavelengths namely 118, 10.6, 1.06, 0.810, 0.532, 0.488 and 0.355  $\mu\text{m}$  with *E. coli* on agar plates. This report was informative and provided a good overview of the efficiency of a wide spectrum of lasers under identical experimental conditions aiming to elucidate the lasers' bactericidal capability. The most effective was the 600 W CO<sub>2</sub> laser operating at

10.6  $\mu\text{m}$  which produced 1.2  $\text{cm}^2$  circular zones of inactivation at energy density approximately 8  $\text{Jcm}^{-2}$  in a 30 ms exposure. With Nd:YAG laser operating at 1.06  $\mu\text{m}$  wavelength, 20 Hz pulse repetitive frequency, 8 ms pulse duration and 10 J energy per pulse yielding energy density of 1940  $\text{Jcm}^{-2}$ , the area of clearance stood at only 0.7  $\text{cm}^2$  with 16 s exposure time. This vast difference was believed to be partly due to the much higher absorption rate of water in the bacterial cell and the surrounding underlying agar substrate. However, the far infrared (118  $\mu\text{m}$ ; 7.96  $\text{Jcm}^{-2}$ ), laser diode array (0.81 $\mu\text{m}$ ; 13750  $\text{Jcm}^{-2}$ ) and the argon ion (0.488  $\mu\text{m}$ ; 2210  $\text{Jcm}^{-2}$ ) laser were totally ineffective in sterilising the microorganisms.

### ***Photosensitisation***

It should be realised that all the above mentioned laser effects were due to the direct laser radiation treatment of the microorganisms. Because of the selective absorption nature of different monochromatic wavelengths to specific dyes or sensitisers, there have been various reports on exogenous photosensitizations on bacterial cells with laser radiation. The first laser effect of artificially induced dye-sensitised cells can be seen reported in 1963 by Saks and Roth. The localised burn effects on *Spirogyra* cell-walls of the Ruby laser radiation, operating at 694.3 nm, was enhanced by methylene blue chloride since the dye acted as a barrier to laser radiation penetration. Since then, various authors have reported feasible studies of cell destruction by light with endogenous photosensitisers.

With non-oral bacteria, Macmillan *et al.* (1966) reported that Gram-positive *Miclutus* and Gram-negatives *E. coli* and *Pseud. aeruginosa* species were inactivated by He-Ne laser irradiation (632.8 nm) when the microorganisms were stained with toluidine blue. The killing action was due to enhanced penetration capabilities of the dye since its maximum absorption peak was at 632 nm. In 1986, Mainetto *et al.* used haematoporphyrin as a photosensitiser and found that *Staph. aureus* and *E. coli* could be sterilised by He-Ne light. Similarly, Bedwell *et al.* (1990) achieved inactivation with aluminium disulphonated phthalocyanine (ADP) to sensitise *Helicobacter pylori* to killing by red light at 675 nm with a copper vapour pumped dye laser.

In dental applications, Wilson *et al.* (1992) showed the bactericidal capabilities of *Strep. sanguis* with 16 sensitising compounds. Killings were achieved with energy densities between 2.75 to 33 Jcm<sup>-2</sup> with a 7.3 mW He-Ne laser at 5 to 60 s exposure time. Of all the photosensitisers, toluidine blue O (TBO), methylene blue and azure B chloride were found to be relatively more effective synergistic bactericidal agents. There was no evidence of killing by the dyes themselves at concentration tested without the laser light.

Burns *et al.* (1992, 1993) found that cariogenic bacteria, namely, *S. mutans*, *Strep. sobiumms*, *Laet. casei* and *A. viscosus* when doped with TBO or ADP, could be killed by exposure to radiation from a 7.3 mW He-Ne and 11 mW Gallium Aluminium Arsenide (GaAs) laser for 60 s. The inactivation energy densities were as low as 34 and 1 Jcm<sup>-2</sup> respectively with 1 x 10<sup>6</sup> cfu organisms treated.

The photosensitisation of cells has been included in novel medical treatments against cancerous and malignant tissue cells through the process called photodynamic therapy (PDT). This advance methodology involves the use of dye molecules, for example photofrin<sup>™</sup> which has been extensively applied clinically for the last decade (Marcus, 1992; McCaughan *et al.*, 1990). Briefly, when these dyes were activated by laser radiation, they caused the formation of active forms of oxygen which resulted in the killing of cells in which the dyes were present. Its selective absorption characteristic allowed the killing of targeted cells while sparing the normal surrounding tissues. Today, PDT has been successful in the treatment of psoriasis (Kennedy *et al.*, 1990), gastrointestinal cancer (Loh *et al.*, 1993), cutaneous malignancies (Wieman *et al.*, 1994), and many more possible indications which are still in the pre-clinical stages (Levy, 1994). Thus with lasers, the technology has potential to be used as a treatment in many other disease conditions.

#### 1.1.4 IONISING RADIATION

Ionising radiation is a low-temperature sterilisation method, which is normally applied where conventional heat-treatment would cause unacceptable or detrimental

effects on products. Such sterilisation methods evolved from the discovery of X-rays in 1895. Since then, the potential for its lethal action to microorganisms has emerged. However, for economic reasons, non-ionising sterilisation techniques are used on industrial, large-scale development. Sceptical views by the public regarding the safety and toxicity aspects of such radiation has reduced the usage. It was in the field of sterilisation of medical products (plastics) that ionising sterilisation techniques were first demonstrated to be of significant practical advantage; it is superior to other sterilisation techniques where microorganisms may be difficult to reach with toxic gas sterilisation or the products cannot tolerate the temperature necessary for heat sterilisation (Artandi and Winkle, 1959). The ability to penetrate deeper into the substrate gives ionising radiation its practicality. **Table 1-1-1** shows the various forms of ionising radiation, its properties and bactericidal effects reported.

## **1.1.5 OTHER PRACTICES OF MICROBIAL INACTIVATION**

### **1.1.5.1 Heat**

Convention heat treatment, is by far the most reliable and widely used means of sterilisation and prevention of cross-contamination. If enough heat is applied, such conventional methods will destroy all forms of microbial life. However, heat sterilisation is often time-consuming and causes functional instability in many medical plastic products if treated (Hambleton and Allwood, 1976). It is often found with autoclaves that the effectiveness of rubber seals to glass in laboratory equipment is reduced after several heat treatments (Allwood *et al.*, 1975). Nevertheless, it is still widely practised due to its comparative ease of operation and control. **Table 1-1-2** summarises different forms of heat sterilisation.

### **1.1.5.2 Gaseous**

Gaseous sterilisation is another common form of anti-bacterial action which includes ethylene oxide (Phillips, 1977) and formaldehyde (Nordgren 1939, Weymes and White 1975).

### **1.1.5.3 Novel methods**

Other novel processes of sterilisation which has been used are, sonication (Sams and Fera, 1991), electrical stimulation (Lin *et al.*, 1984), pulse electric field (Zimmermann, 1986) and incoherent visible light (Mertens and Knorr, 1992).

**Table 1-1-1 Different sources of ionisation radiation on bacteria.**

Radiation	Source	Energy	Wavelength ( m )	Bactericidal actions
Radioactive Cobalt	<sup>60</sup> Co	1.17, 1.33 MeV	1.1X10 <sup>-12</sup> , 9.3X10 <sup>-13</sup>	Idziak, 1973; Bruck and Mueller, 1988.
Cathode rays	Electron accelerator	5-10 MeV	2.5X10 <sup>-13</sup> - 1.2X10 <sup>-13</sup>	Hannan 1955; Pivaev, 1990
X rays	X ray tubes	100 eV-0.2 MeV	1.2X10 <sup>-8</sup> - 6.2X10 <sup>-14</sup>	Dunn <i>et al.</i> 1948; Sato <i>et al.</i> 1993

**Table 1-1-2 Various types of microbial heat treatment.**

Types of heat treatment	Reports
Moist	Kelsey, 1958; Russell and Harries, 1967
Dry	Curran, 1952; Ernst, 1977
Infrared lamp	Darmady <i>et al.</i> , 1957; Darmady <i>et al.</i> , 1961

## **II Nd: YAG LASER**

## 2.1 LASER-WATER INTERACTION

### 2.1.1 INTRODUCTION

The increasing prevalence and complexity of laser use in all aspects of medicine necessitates an understanding of the effects of laser radiation in a wide variety of situations. Water is the main constituent of biological cells. Thus, the temperature dependency of the optical properties of water plays an important role in understanding laser-tissue and laser-bacteria interactions. Recent interests in laser inactivation or sterilisation (Watson *et al.*, 1995; Schultz *et al.*, 1986) have shown that lasers offer specific advantages over conventional sterilisation techniques, for example, autoclaves. The laser sterilisation mechanism has not yet been elucidated, but it is clear that the mechanism will be wavelength dependent. Lasers operating in the IR (Nd:YAG, CO<sub>2</sub>) have shown bactericidal capacity, the mechanism probably, being in part, thermal.

Present efforts to model the interaction between laser radiation and bacteria have been hindered by the availability of suitable data. To overcome this problem, the present work was initiated to determine the temperature dependence of the optical properties of water and used to develop models of the laser sterilisation process for the Nd:YAG laser operating at 1.064  $\mu\text{m}$ .

A schematic of the laser beam interaction with the water is shown in **Figure 2.1.1**. The incident radiation can be reflected, absorbed, scattered or transmitted. Absorbed photons are converted to heat energy via vibrational relaxation, increasing the temperature of the water. The relationship between the absorption, scattering and the extinction coefficient is given by:

$$\alpha_T(\lambda, T) = \alpha_S(\lambda, T) + \alpha_{Ab}(\lambda, T) \quad (2.1.1)$$

where  $\alpha_T$  ( $\text{cm}^{-1}$ ) is the extinction coefficient,  $\alpha_S$  ( $\text{cm}^{-1}$ ), the scattering coefficient and  $\alpha_{Ab}$  ( $\text{cm}^{-1}$ ), the absorption coefficient at wavelength  $\lambda$  and temperature T. Lambert's equation can be used to evaluate  $\alpha_S$  by using the relationship:

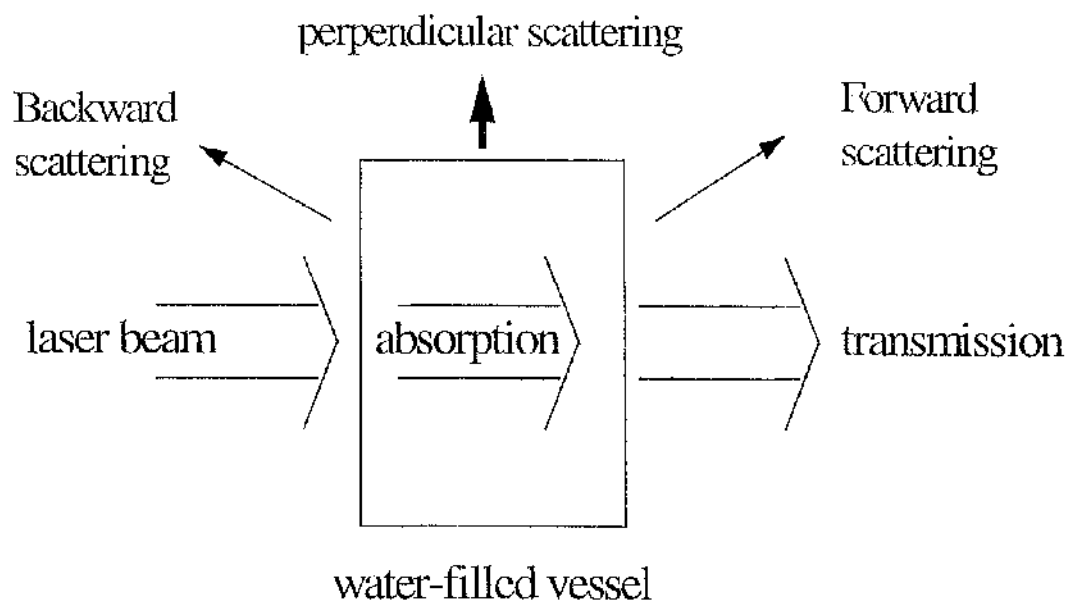


*Figure 2.1.1* Laser beam interaction with water.

$$I = I_0 \exp(-\alpha_T L) \quad (\text{at constant temperature}) \quad (2.1.2)$$

where  $I$  was the intensity transmitted by the sample of water,  $I_0$ , the maximum intensity output and  $L$ , the water sample thickness. Through **Eqn. 2.1.2**, the energy transmitted through a medium can be found. Alternatively by measuring the transmitted intensity through different thicknesses of material,  $\alpha_T$  can be found by plotting:

$$\ln I = \ln I_0 - \alpha_T L \quad (2.1.3)$$

The gradient of the resulting graph will give the value of  $\alpha_T$ .

### 2.1.2 EXPERIMENTAL SET-UP AND MEASUREMENTS

The experimental system to measure the temperature dependence of the absorption and scattering properties of water is shown in **Figure 2.1.2**

Radiation at  $1.064\mu\text{m}$  from a Lumonics MS850 laser was delivered through a fibre optic beam delivery system to a beam expanding telescope, operating in reverse. A collimated beam, about 1.7 cm in diameter was produced that matched the diameter of the water-filled vessel. A thermocouple was positioned in the side wall of the vessel such that it was in contact with the water, but not directly irradiated by the laser beam. The fraction of the beam transmitted through the water was reflected off of the two glass wedges and directed onto photodiode 1; photodiode 2 was located perpendicularly to the water-filled vessel to measure scattered intensity.

The depth of the water was varied, and for each depth its temperature was changed from 25 to 70 °C in 5 °C increments. The water was heated by the laser irradiation. For each temperature and depth, the radiation transmitted (photodiode 1) and scattered (photodiode 2) was detected by two BPX65 photodiodes. The signals were amplified and the voltage waveforms were integrated on a

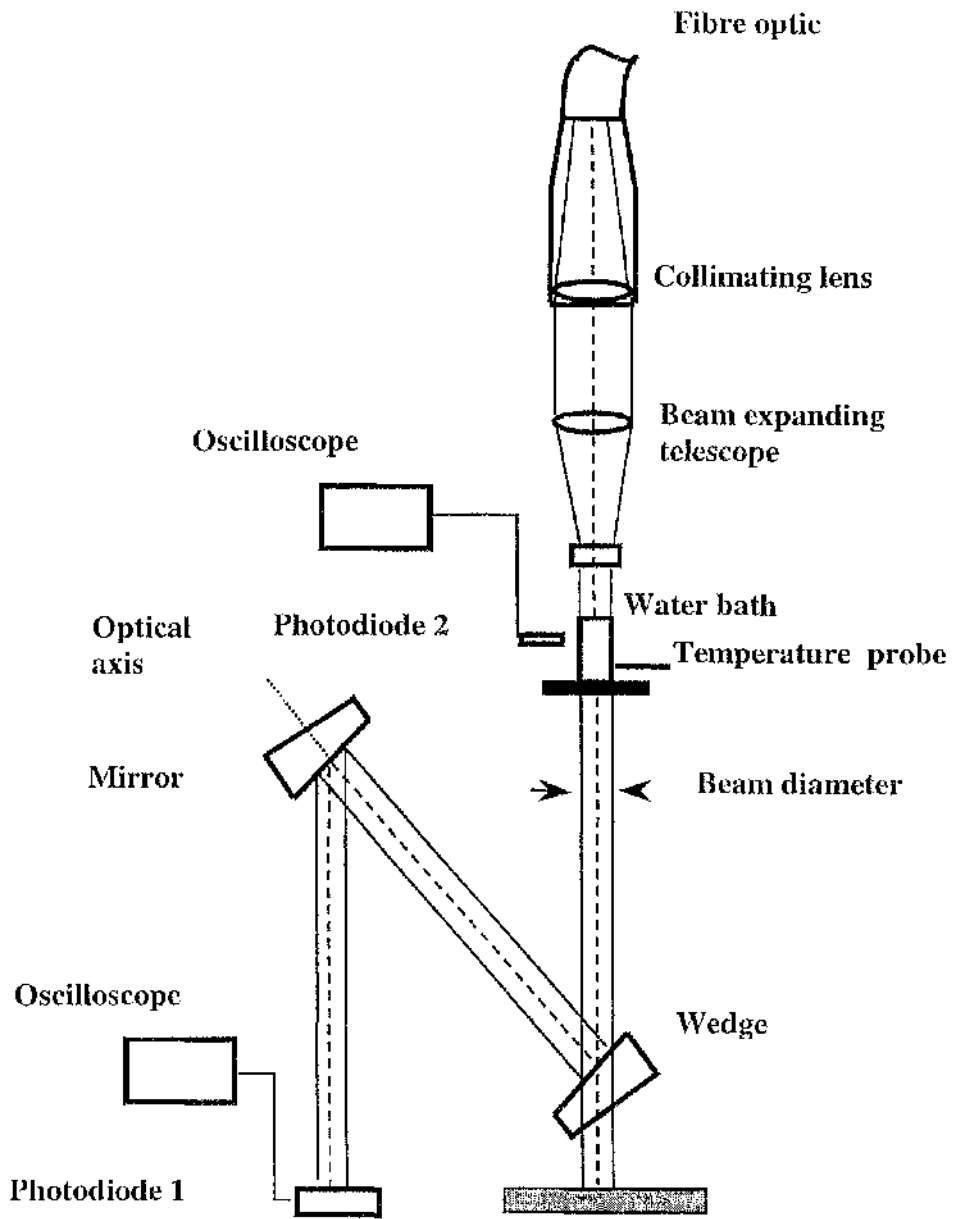


*Figure 2.1.2* Schematic of the experimental set-up.

LECROY 9400, 125 MHz digital oscilloscope, **Figure 2.1.3**. The intensity of the laser beam is proportional to the current gain responsivity of the photodiode for a given area. The photodiodes' gain then produced a voltage gain on the oscilloscope in which the integral of the voltage pulses from photodiode 1 and photodiode 2 gave a relative measure of the total energy transmitted and scattered respectively. As  $I \propto \int V dt$ , **Eq. 2.1.3** can be written as:

$$\ln \int V dt = \ln \int V_0 dt - \alpha_T L \quad (2.1.4)$$

where  $V_0$  is the respective voltage gain without any water in the vessel.

Consequently, the extinction coefficient,  $\alpha_T$  and the scattering coefficient,  $\alpha_S$ , were found by plotting the natural logarithm of the integrated voltage as a function of the depth of water for the different temperatures. The resulting gradients of these graphs gave a measure of the temperature dependency of the coefficients.

### 2.1.3 RESULTS

The beam detected via photodiode 1, the graphs  $\ln \int V dt$  plotted as a function of the depth of water, for temperature from 25 to 70 °C are shown in **Figure 2.1.4**. In each case, a best-fit line was plotted through the data and the extinction coefficient was found from the gradient of this line. The scattering coefficient,  $\alpha_T$  was also calculated this way.

**Figure 2.1.5** shows the extinction coefficient of water as a function of temperature. In general,  $\alpha_T$  reduced with increasing temperature. However, between about 40-45 °C, there was a sudden transition from about 0.060cm<sup>-1</sup> to 0.038cm<sup>-1</sup>.

The temperature dependence of the scattering coefficient of water was measured perpendicular to the incident beam. Here, the general trend was that  $\alpha_S$  reduced with increasing temperature, but a slight increase was observed between 50-55 °C, **Figure 2.1.6**. It should be noted that the reflection coefficient was not taken into

account for this analysis, and the scattering was only observed perpendicular to the incident beam.

#### 2.1.4 DISCUSSION

In the present case, normal tap water was used and the level of impurities was unknown. However, it is possible that the sharp transition in the extinction coefficient could be associated with a rapid increase in inhomogeneity of the liquid density. Such inhomogeneities may result from density gradients caused by the heating process (Hawkes and Astheimer, 1974). It was known that liquid water is composed of three components, namely monohydrol, dihydrol and trihydrol (Collins, 1922) which are later accepted, described and structurally similar as monomer, di-mer and tri-mer after the sixties (Draegert *et al.*, 1966; Ford and Falk, 1968; Curnutte and Bandekar, 1972). The relative amount of these constituents varies with the physical state of the water; i.e. pressure, temperature and/or the level of impurities. The only variable parameter in this experiment was temperature. The pressure differences were negligible and impurity levels were constant since the water samples taken were from the same source. As the temperature is increased, there is a 'dissociation' of trihydrol bonds and an increase in dihydrol molecules. At freezing point, the concentration of dihydrol molecules is minimal whereas at boiling point the concentration of trihydrol molecules is negligible (Collins, 1925). There may exist a 'resonant vibrational effect' which causes a sudden increase in the inter-bond length which may account for the sudden transition observed in the measured data. Furthermore, di-mer molecules absorb comparatively less at 1.064  $\mu\text{m}$  and their concentration increases with temperature (Mezei and Beveri, 1982). At present, there seems no method to determine the relative proportions of the constituents accurately enough for quantitative assessment of the absorption by each component of water (Bassel *et al.*, 1987).

The only other experimental work found in support of this anomalous finding was by Hawkes (1974) which showed an abnormal effect of curling and squirming fringe patterns above 35 °C with sodium light at 0.589  $\mu\text{m}$  wavelength. The anomalous

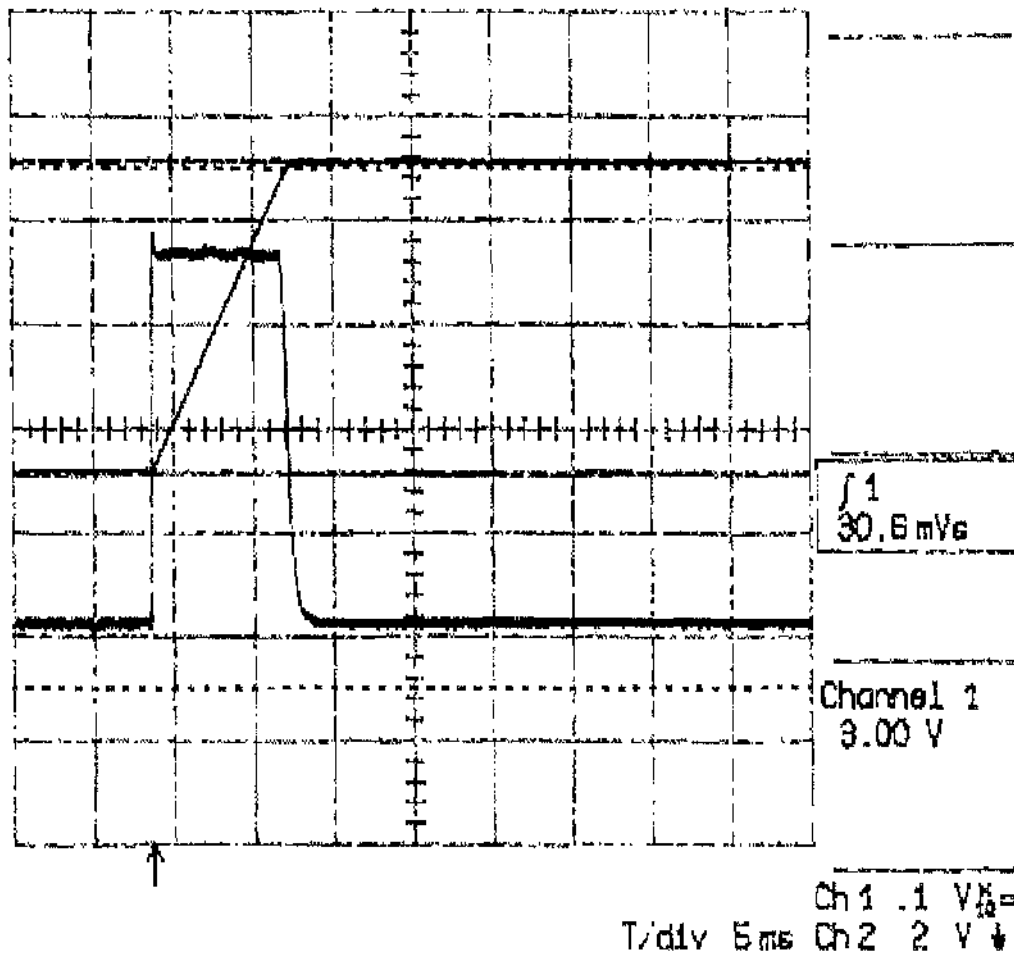


**Figure 2.1.3** Example of trace of a typical transmitted signal detected by the LECROY 9400, 125 Mhz digital oscilloscope from photodiode 2. The integrated voltage showed 30.6 mVs measured at 25 °C at 30 mm water depth in the vessel.

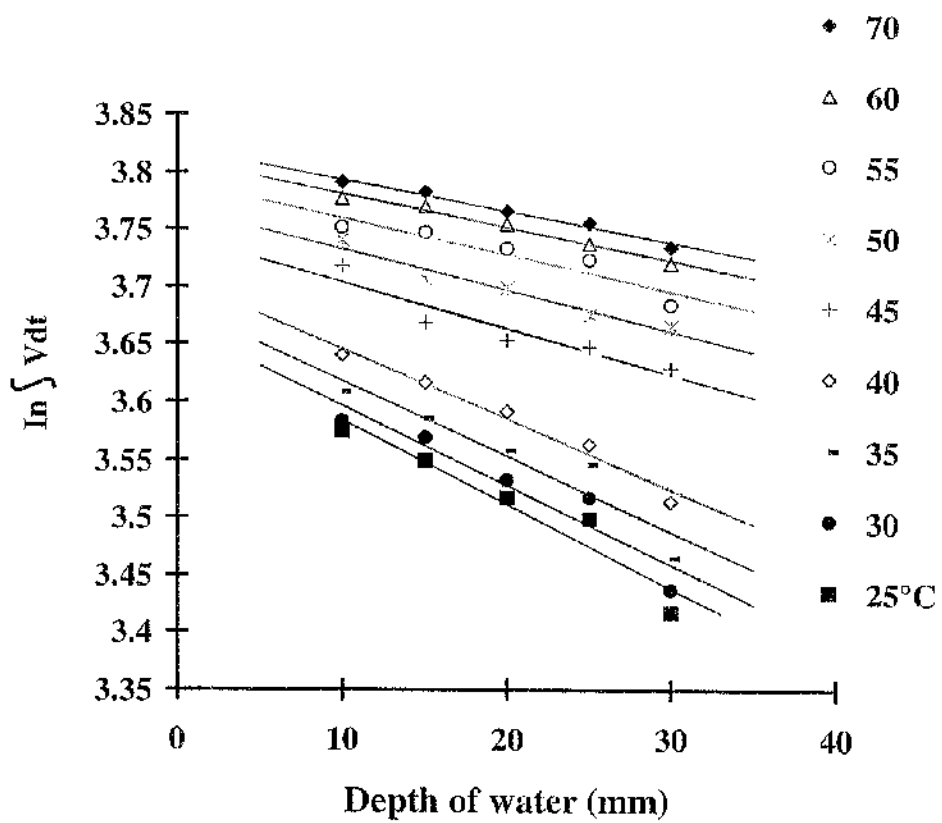
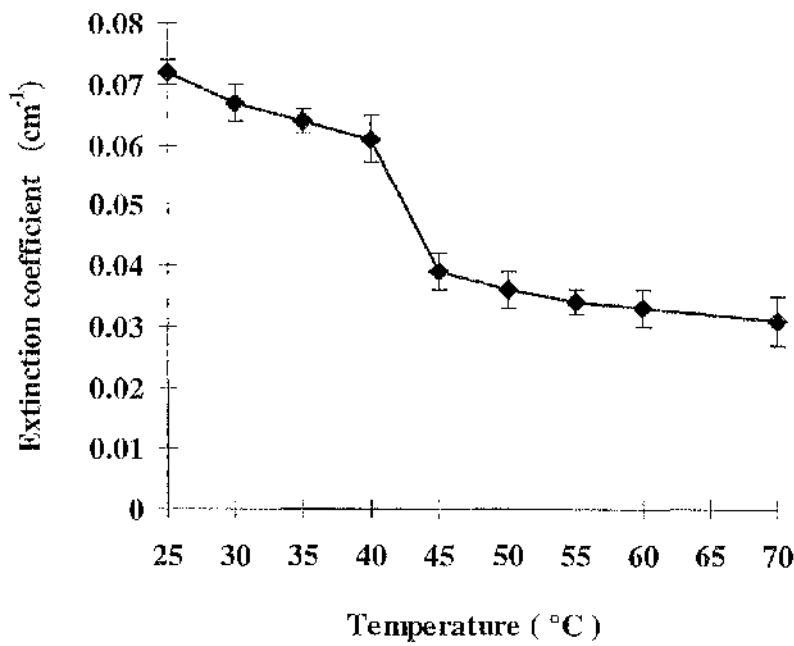
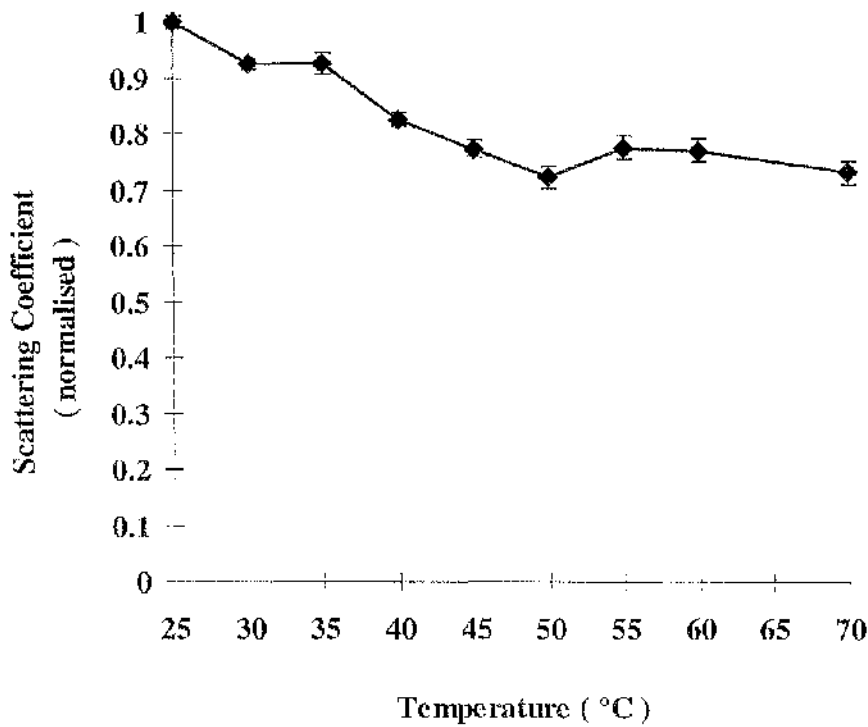


Figure 2.1.4 Graph of  $\ln \int V dt$  versus the depth of water in the vessel.



*Figure 2.1.5* The extinction coefficient,  $\alpha_T$  of water as a function of temperature.



*Figure 2.1.6* The scattering coefficient,  $\alpha_S$  of water versus temperature. The error bar denotes the standard deviation of the mean over two experiments each done in triplicate.

fringe behaviour, observed with a Jamin interferometer, strongly suggested that the optical effects were due to small convection currents, caused by local density (or temperature) inhomogeneities in the liquid. The results of the work presented in this thesis agree with previous work (Collins, 1925). Dobbins and Peck (1973) also reported such phenomena of sudden changes in the structure of water occurring at 35 °C but the discussion was equivocal on the anomaly behaviour.

The optical properties of water can be described as the result of absorption and scattering of radiation by the fundamental stretching and bending vibrations of the O-H bonds in the water molecule, their overtones and combinations of both (Micheal and Marvin, 1972). Moreover, the environment of the water molecule, for example the hydrogen-bond network which forms in any liquid water, has an impact on its optical behaviour. It has been suggested that as the temperature increases, this causes vibrational effects on the different modes of both vibrational and translational motion of the molecular structure in water that weakens the hydrogen-bond network (Bryan and Curnutte, 1972). This could imply that with irradiation by a laser beam, there exists a 'bending' of the hydrogen bonds in the liquid which increases the relative bond length, resulting in a decrease of the extinction coefficient.

It is also worth noting that the coefficients that have been measured vary with wavelength and at other wavelengths, the trend of increasing absorption coefficient with increasing temperature, for example, has been observed (Collins, 1922).

## 2.2 INACTIVATION OF *STAPHYLOCOCCUS AUREUS* ON AGAR MEDIUM

### 2.2.1 INTRODUCTION

Although overshadowed in recent years by Gram-negative bacilli such as *E. coli*, staphylococci are still a major cause of infection in man and animals. *Staph. aureus* is a Gram-positive coccal pathogen which if present in food, secretes enterotoxins, toxins that affect the vomiting centres of the brain and causes gastroenteritis. Disease caused by coagulase-negative staphylococci is increasingly recognised. Few bacteria produce such a wide range of diseases as *S. aureus*. Due to this diversity, the death kinetics of the bacteria have been the subject of much interest and research.

The capacity and benefits of using Nd:YAG laser inactivation was demonstrated by various groups (Cobb *et al.*, 1992; Horton and Lin, 1992; Rooney *et al.*, 1994; Ward *et al.*, 1996). A comparison of the bactericidal capacity of seven different laser wavelengths by Watson *et al.* (1996) showed that a Q-switched Nd:YAG laser, with a mean power of 0.25 W, 5 ns pulses and peak power of 5 MW, did not inactivate *E. coli* lawned on agar but melted the petri dish. By contrast, 8 ms pulse length and much lower peak power (13 KW) produced rapid sterilisation with exposure times up to 16 s. However, comparison with the studies mentioned above and those discussed in **Section 1.2.3.3** indicates that reliance on any one laser parameter is insufficient.

The influence of the different laser parameter settings at 1.06  $\mu\text{m}$  wavelength described above is unknown. However, the killing of microorganisms is partly photothermal. Consequently, the pulse repetitive frequency and pulse energy applied will produce different rates of inactivation because different thermal effects are introduced into the system. This study was initiated because data on the dependency of the laser parameters on inactivation of bacteria are scarce. The effect of Nd:YAG laser radiation on *S. aureus* lawned on agar plates and the influence of PRF, pulse energy, exposure time and the laser beam diameter was examined.

## 2.2.2 MATERIALS AND METHODS

### 2.2.2.1 Culture preparation

*Staphylococcus aureus* 6571 (Oxford strain) was maintained on nutrient agar (CM3, Oxoid) slopes at 4 °C and was subcultured monthly. Bacterial cultures were grown in nutrient broth (10 ml); (CM67, Oxoid) and incubated overnight at 37 °C.

### 2.2.2.2 Preparation of lawned plates

Fresh molten nutrient agar (CM3, Oxoid) was prepared and allowed to flood the surface of the sterile circular plastic plates (9 cm in diameter). They were left to dry and solidify for 40 min in a class 100 laminar air flow cabinet (Flow Laboratories, Germany). Aliquots (1.5 ml) of the overnight culture were pipetted onto the agar plates and allowed to flood the surface. The concentration of these aliquots was determined from serial dilutions at  $4.2 \times 10^9 \text{ ml}^{-1}$ . The excess liquid was decanted and this volume was measured at 1.15 ml. Therefore, a volume of 0.35 ml was left on the plate with a concentration of  $\sim 1.47 \times 10^9 \text{ cfu}$  inoculated per plate. Thus, the concentration per unit area over the petri-dish was  $\sim 2.31 \times 10^7 \text{ cfu cm}^{-2}$ .

### 2.2.2.3 The Nd:YAG laser

A pulsed, 400 W, Nd:YAG laser (Lumonics, MS830) operating at 1064 nm, with a fibre optic beam delivery system and collimating focusing lens assembly was used, **Figure 2.2.1**. The beam was passed through a 20 mm collimating lens and beam expanding telescope onto the agar plate. A total of six exposure sites were performed per agar plate. The absorbing base, a stone brick, absorbed the transmitted output beam while a fraction of the beam was sampled via the wedge and mirror set-up to compare with the burn print obtained on photographic paper as a reference.

The laser output pulse energy was varied between 2 and 30 J over a frequency range of 5 to 30 Hz. The exposure time was adjusted from 8 to 115 s, the pulse width was fixed at 8 ms throughout the experiments. With these parameters, the range of

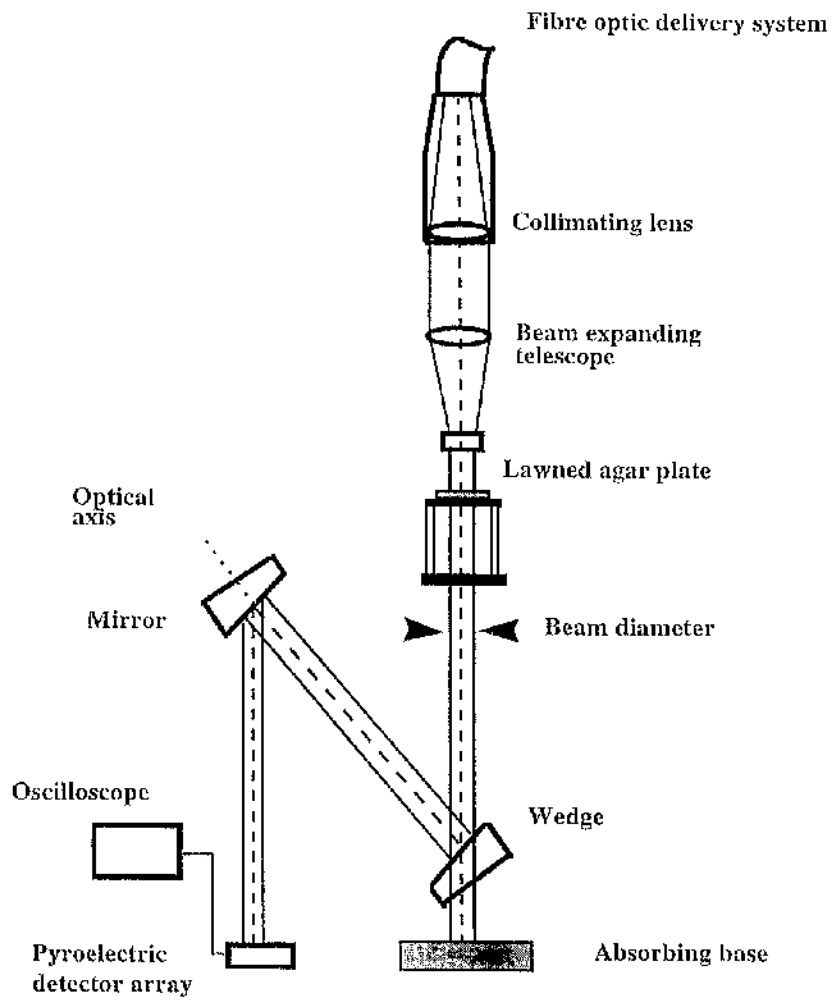


*Figure 2.2.1* Schematic representation of the experimental system

energy densities varied from 800 to 2700 Jcm<sup>-2</sup>. The laser output power was measured with a power/energy meter (FieldMaster™, Coherent, U.K.).

#### 2.2.2.4 Laser output beam area and energy density

The beam diameter of the Nd:YAG laser was measured from burn prints produced on photographic paper (Rypma, 1997) at various laser parameters, and the beam area was calculated. The validity of the burn print diameter was checked against measurement from pyroelectric detector array (PDA), see **Figure 2.2.1**. After laser exposure and incubation of the lawned agar plates at 37°C overnight, the area of inactivation was measured for various laser parameters.

The power output, P<sub>o</sub>, is given by:

$$P_o = f P_e \quad (\text{W}) \quad (2.2.1)$$

where  $f$  is the PRF (s<sup>-1</sup>); P<sub>e</sub>, the pulse energy (J). The energy density, ED, is defined as :

$$ED = \frac{P_o t}{A} \quad (\text{Jcm}^{-2}) \quad (2.2.2)$$

where  $t$  is the exposure time of the laser light (s) and  $A$ , the measured beam area (cm<sup>2</sup>).

#### 2.2.2.5 Laser exposure of lawned plates

The lawned plates were mounted on a stand and positioned beneath the laser beam. Each set of laser parameters was applied in triplicate and each experiment repeated twice. Each lawned plate was divided into six separate exposure sites. After exposure, the plates were incubated overnight at 37 °C and each segment was observed under a Profile Projector (PJ-300, Mitutoyo). The diameters of the cleared zones with no bacterial growth were measured for each set of the laser parameters

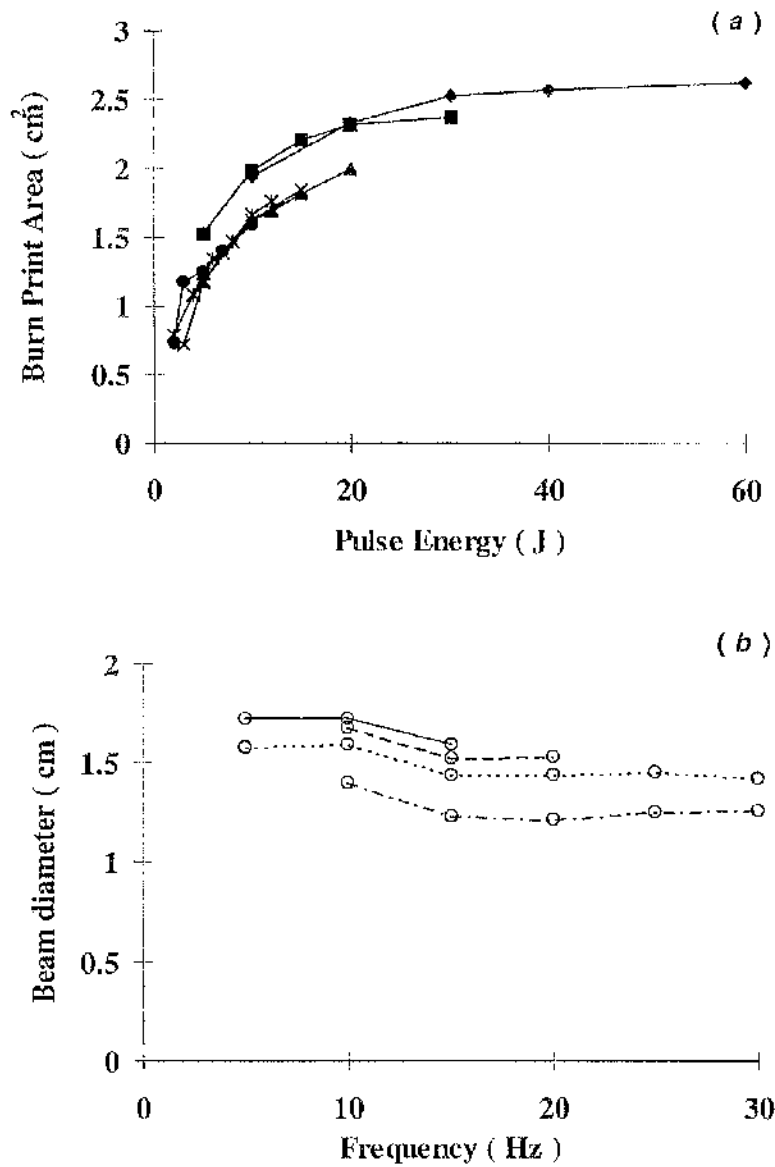
namely: PRF, pulse energy and exposure time. The areas of bacterial inactivation were calculated and these values were plotted as a function of the exposure time. The energy density ( $IA_{50}$ -values) needed to give an area of inactivation (IA) equal to 50 % of the beam area (Ward *et al.*, 1996) was also determined for different laser parameters.

For each experiment, several controls were set-up. A lawned plate was left unexposed to the laser beam and incubated overnight at 37 °C in the normal manner. NA plates without *S. aureus* were exposed to laser radiation of varying energy densities, up to 2700 Jcm<sup>-2</sup> and were incubated at 37 °C with the treated plate. This control was set-up to investigate whether the laser radiation affected the nutrients in the agar and consequently the growth of *S. aureus*. All plates were kept for up to 2 weeks to check for any sign of delayed growth or recovery.

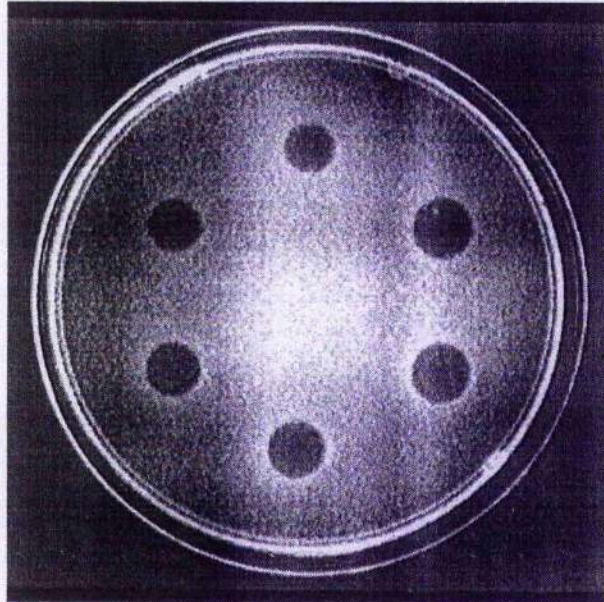
### 2.2.3 RESULTS

The smallest beam diameter on the photographic paper was 0.72 cm observed at 20 Hz and 3 J (60 W) and the largest diameter achieved was 2.62 cm at 5 Hz and 60 J (300 W). **Figure 2.2.2a** shows the laser beam area as a function of pulse energy and **Figure 2.2.2b** shows the laser beam area as a function of pulse repetition frequency (PRF) for different pulse energies. For a given PRF, the beam diameter increased with increasing pulse energy. For any pulse energy applied with and above 15 Hz, the beam diameter was independent of PRF. However, the beam diameter was larger for a PRF below 15Hz.

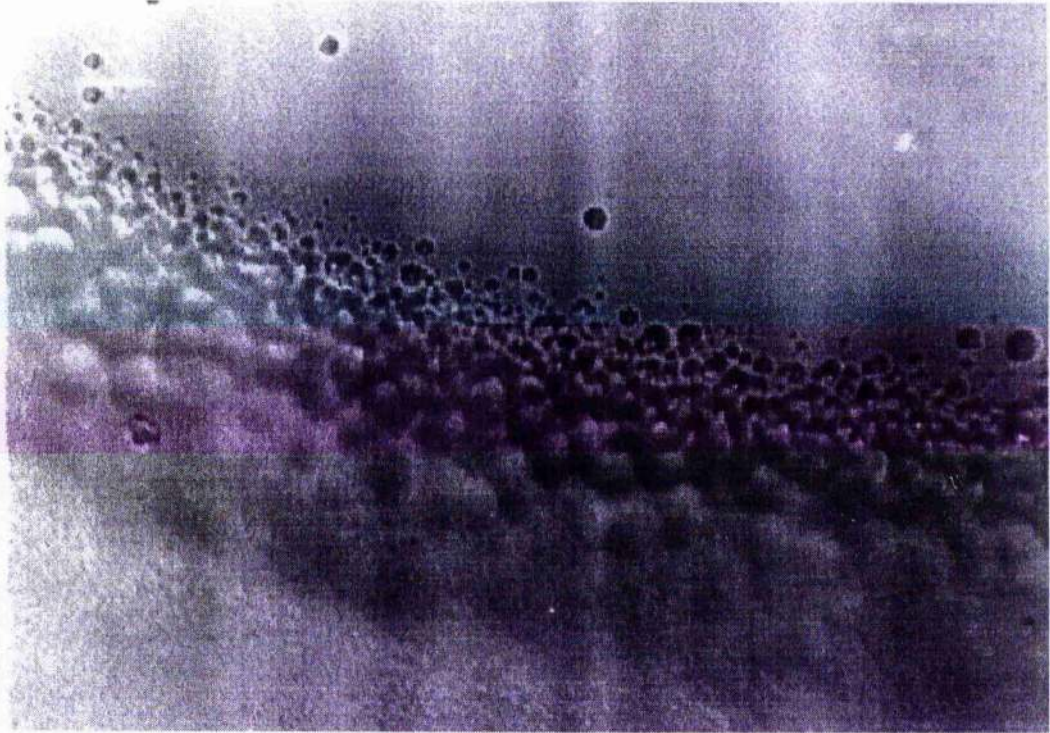
**Figure 2.2.3** shows a lawned plate after 6 laser exposures and incubation for 24 hr after which the cleared areas were measured. A section of the edge of the inactivated area by the laser exposure at 30 J (300 W) was magnified, **Figure 2.2.4**. **Figure 2.2.5** shows the inactivation areas as a function of exposure time respectively for PRF of: 5, 10, 15, 20, 25 and 30 Hz and for pulse energies from 3 to 60 J. For a given frequency and pulse energy, the area of inactivation increased with applied energy density. For a given energy density, a greater area of inactivation was



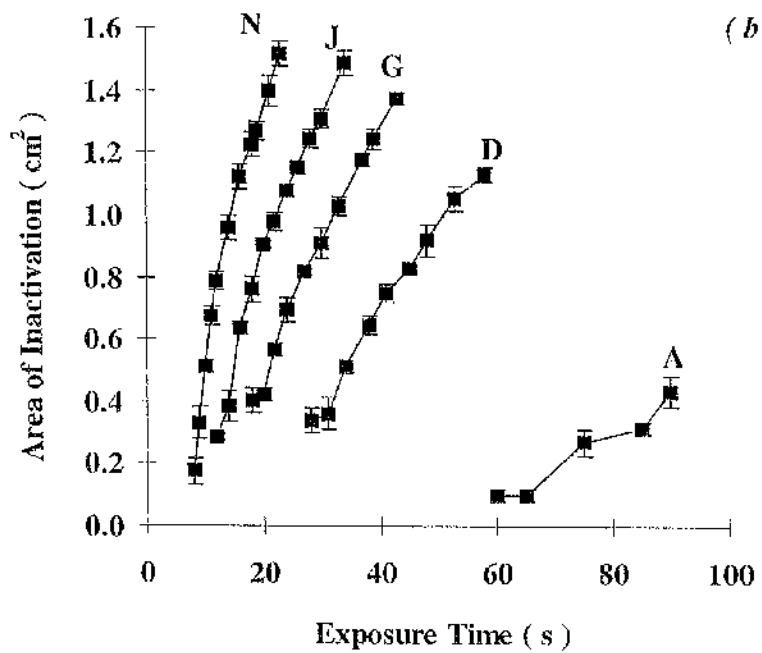
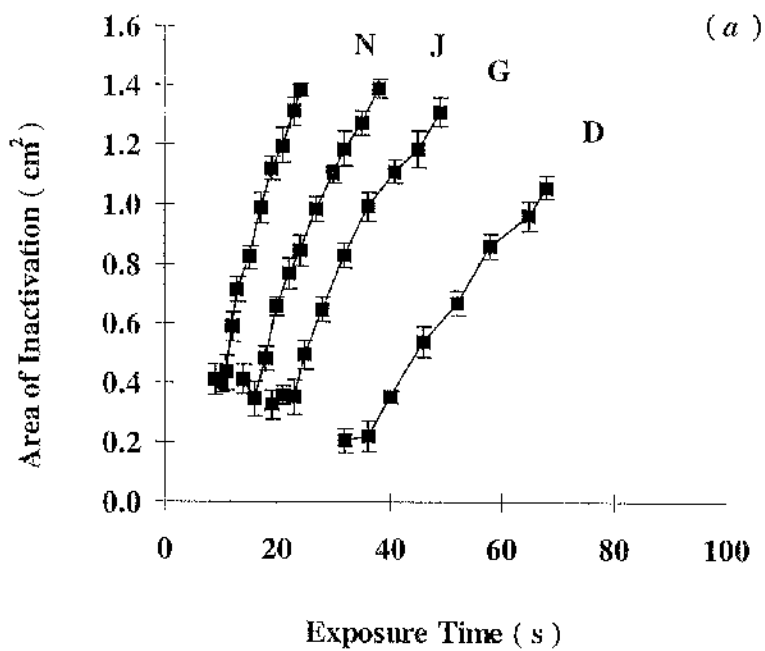
**Figure 2.2.2** Burn print characteristic with 400 W Nd:YAG laser. (a) shows the area of the Nd:YAG beam on the photographic paper as a function of pulse energy and at frequencies of:  $\blacklozenge$ , 5;  $\blacksquare$ , 10;  $\blacktriangle$ , 15;  $\times$ , 20;  $*$ , 25 and  $\bullet$ , 30 Hz. The energy densities covered were from 800 to 2700 Jcm<sup>2</sup>. (b) compares the beam diameter on the photographic paper for a range of frequencies at pulse energies of 5 (---), 10 (.....), 15 (-.-.-), and 20 (—) J. Both experiments were done using a single shot exposure with an 8 ms pulse width individually.

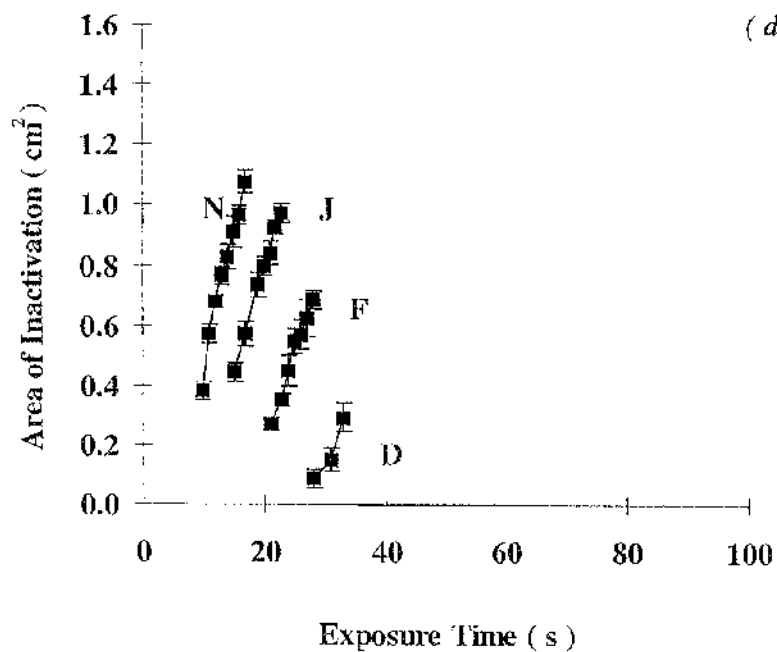
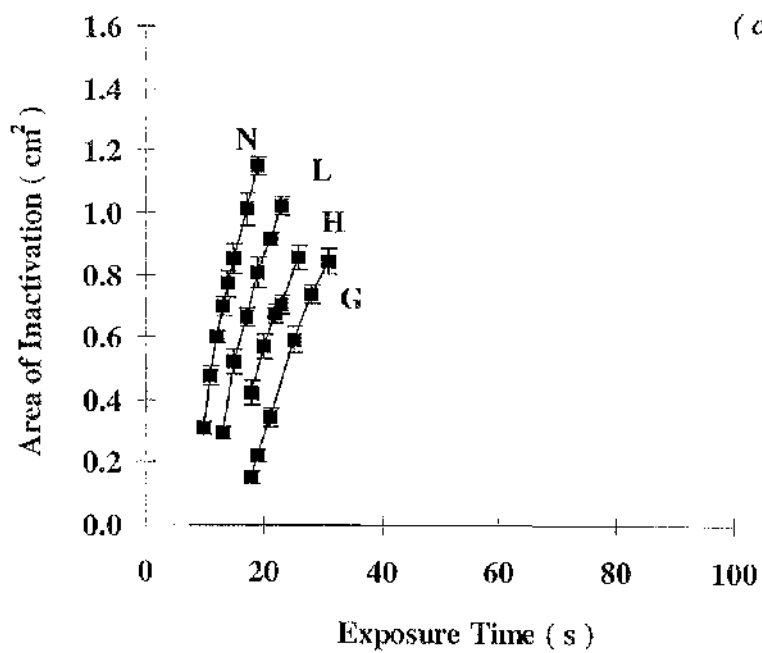


**Figure 2.2.3** A culture plate lawned with *S. aureus* after six Nd:YAG laser exposures and then incubated for 24 hr. The cleared zones indicate areas of bacteria killing. The inactivated areas were exposed in increasing energy density at 30 J (300W) in an anti-clockwise direction starting at the uppermost clear area with 14, 16, 18, 19, 21 and 23 s respectively.



**Figure 2.2.4** Photograph showing section of the lawned plate of *S. aureus* after laser exposure at 30 J (300W) for 16 s. The top-half shows the inactivated area by the laser exposure and the bottom-half indicates the bacteria growth after 24 hr incubation. The miniature colonies along the periphery indicates sub-lethal damage and further away from the irradiated area, there was reduced damage until confluent growth was observed at the bottom of the picture.





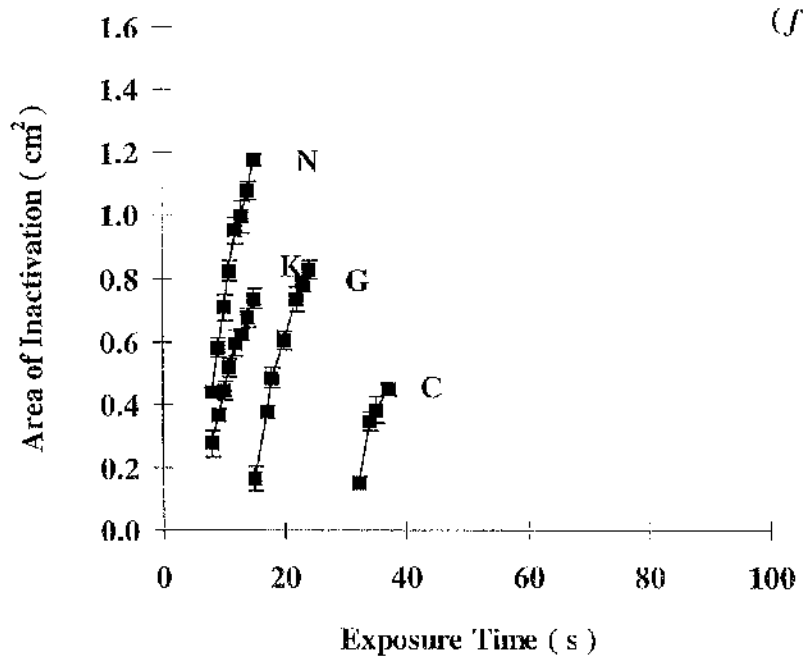
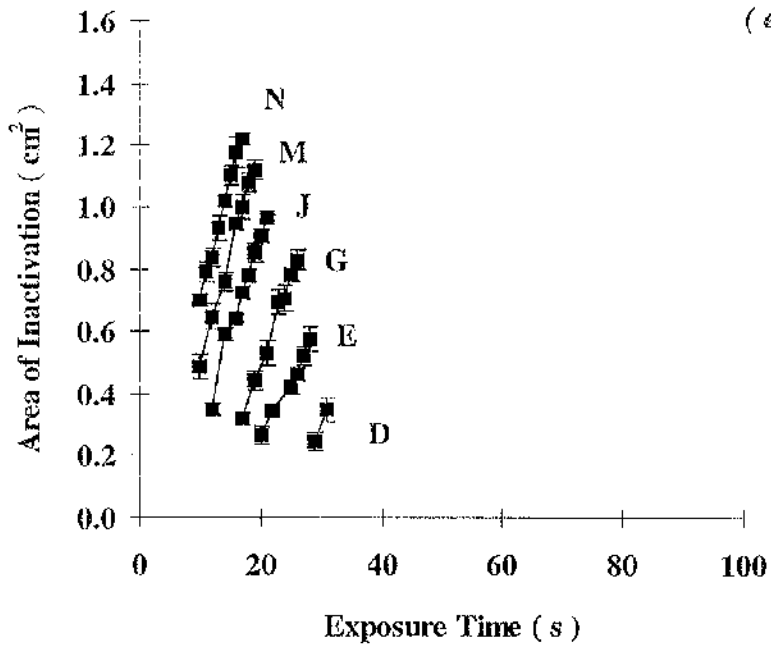


**Figure 2.2.5** Series of graphs showing the area of inactivation of *S. aureus* as a function of the exposure time of Nd:YAG laser at PRF of (a), 5 Hz; (b), 10 Hz; (c), 15Hz; (d), 20 Hz; (e), 25 Hz and (f), 30 Hz with various power output at A, 50 W; B, 75 W; C, 90 W; D, 100 W; E, 125 W; F, 140 W; G, 150 W; H, 180 W; J, 200W; K, 210 W; L, 225 W; M, 250 W; and N, 300 W.

observed with increased pulse energy and frequency. In **Figure 2.2.6**, various pulse energies were plotted as a function of the exposure time to achieve a 50 % area inactivation for PRF of: 5, 10, 15, 20, 25 and 30 Hz.

### 2.2.3.1 Frequency dependence of laser inactivation

At a relatively low output power at 50 W for a PRF of 5 Hz the inactivation areas were 0.31 and 0.41 cm<sup>2</sup> for an exposure time of 115 and 145 s with ED of 2002 and 2524 Jcm<sup>-2</sup> respectively. Whereas at 100 W (**Figure 2.2.5a**), the equivalent killing area of 0.31 cm<sup>2</sup> was achieved after an exposure of 39 s with an ED of 1154 Jcm<sup>-2</sup>. The largest inactivation area of 1.39 cm<sup>2</sup> was observed at 200 and 300 W but with different ED; 2145 and 1902 Jcm<sup>-2</sup> respectively. The smallest inactivation area (0.21 cm<sup>2</sup>) was observed at 100 W with exposure time of 32 s and ED of 953 Jcm<sup>-2</sup>.

At a PRF of 10 Hz and for a given energy density, the areas of inactivation increased with increasing pulse energy, **Figure 2.2.5b**. For example, at 2000 Jcm<sup>-2</sup>, the areas of inactivation for 5, 10, 15, 20 and 30 J were: 0.25, 0.95, 1.20, 1.33 and 1.41 cm<sup>2</sup> respectively. However at higher pulse energies of 15, 20 and 25 J, the percentage inactivation areas were relatively close to one another with values of 0.60, 0.57 and 0.59 respectively. At 300 W, an 18 s exposure was required to achieve the 50 % beam area of inactivation, **Figure 2.2.6**.

The areas of inactivation increased with energy density for a PRF of 15 Hz. For a fixed energy density, the same trend was observed as for the previous frequencies. For pulse energies of: 10, 12, 15 and 20 J, the areas of inactivation were: 0.61, 0.7, 0.88 and 1.03 cm<sup>2</sup>, respectively, whilst the exposure time decreased from: 25.5, 23.0, 20.4 to 17.3 s respectively, **Figure 2.2.5c**. At the highest output power (300 W), the energy density applied was 1942 Jcm<sup>-2</sup> and in just 16.8 s, an inactivation area of 50 % was achieved, **Figure 2.2.6**. The longest exposure time was 44 s with an inactivation area and ED of 0.27 cm<sup>2</sup> and 2371 Jcm<sup>-2</sup> (data not shown).

No inactivation was found at 60 W (20 Hz) for energy densities up to 2452 Jcm<sup>-2</sup> and an exposure time of 34 s. Above pulse energies of 3 J, however, the area of clearing increased with pulse energy (5, 7, 10 and 15 J), **Figure 2.2.5d**.

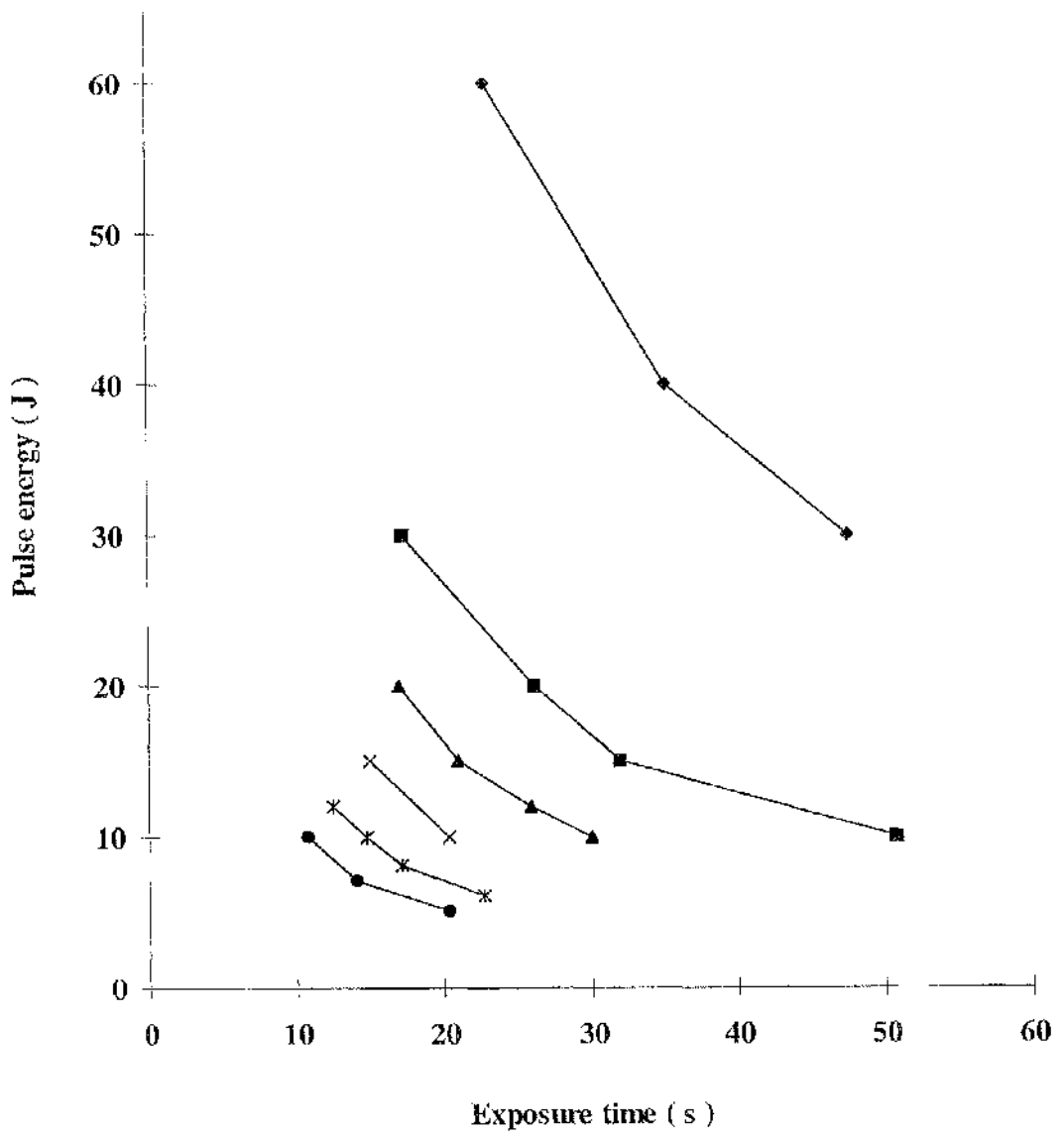


Figure 2.2.6 Graph of pulse energy as a function of the exposure time for IA<sub>50</sub> values for PRF of: ♦,5; ■, 10; ▲,15; ×,20; \*, 25 and ●, 30 Hz.

No inactivation was found at 50 W (25 Hz) for energy densities up to  $2511 \text{ Jcm}^{-2}$ , corresponding to an exposure time of 45 s. For a given pulse energy above 2 J, the areas of clearing increased with energy density and exposure time, **Figure 2.2.5e**. The 50 % areas of inactivation for pulse energies: 6, 8, 10 and 12 J were interpolated as follows:  $2140 \text{ Jcm}^{-2}$  (22.8 s),  $1944 \text{ Jcm}^{-2}$  (17 s),  $1870 \text{ Jcm}^{-2}$  (14.7 s) and  $1783 \text{ Jcm}^{-2}$  (12.5 s), **Figure 2.2.6**. To achieve the  $IA_{50}$  values, the energy density and exposure time both reduced with increasing pulse energy.

No inactivation was observed at 60 W (30Hz) for an applied energy density of up to  $2641 \text{ Jcm}^{-2}$  with an exposure time of 35 s. An increasing area of inactivation was observed with increasing energy density and pulse energy above 60 W (i.e. 90, 150, 210 and 300 W), **Figure 2.2.5f**. It is also seen that to achieve a given area of inactivation, the exposure time reduced with increasing pulse energy. The largest area of inactivation ( $1.18 \text{ cm}^2$ ) was observed for an applied energy density of  $2404 \text{ Jcm}^{-2}$  with an exposure time of 15 s. The shortest exposure time with a 50 % area of inactivation was with an exposure time of 10.75 s, **Figure 2.2.6**.

### **2.2.3.2 Checks for viable but non-culturable microorganisms**

No further growth on the exposed areas was observed under the shadowgraph on the lawned plates after leaving them for incubation for 2 weeks. Similarly, no further growth was seen when sections of the irradiated areas were removed after 2 days, incubated in nutrient broth for 24 hr and imprinted on fresh agar plates; this was done to investigate whether any colony forming units had formed. For unexposed lawned plates, normal growth was observed after 24 hr incubation at  $37^\circ \text{C}$  and similarly for unexposed sections on the irradiated lawned plates. In all cases, confluent growth was observed on control agar plates exposed to laser prior to lawning; indicating that the nutrients of the agar were unaffected by the laser exposure.

## 2.2.4 DISCUSSION

No further growth on the control plates was observed which indicated that the laser had inactivated the bacteria in the exposed areas and no recovery mechanism was operating.

From **Figure 2.2.4**, the distinction between the exposed (top section) and unexposed (bottom section) regions of the plate can be seen clearly. It is interesting to note that clear distinct miniature colonies were seen around the periphery of the exposed zone. Ward *et al.* (1996) also showed that similar microcolonies, which contained auxotrophs, were observed with laser inactivation of *E. coli*. The formation of the miniature colonies near the periphery of the irradiated area may be due to the fact that the laser beam output, and consequently the applied energy density, was not radially constant. The intensity at the centre of the beam is at its maximum and decreases away from the centre. The miniature colonies at the inner edge of the exposed area, where partial killing has taken place, experience an energy density slightly less than the "threshold energy density". Away from the centre of the irradiated area, the organisms receive a lower energy density and less damage occurs, until normal confluent growth was observed where there was no effect on the bacteria. This "transient area" was around the threshold energy density of the exposure. It was suggested by Schultz *et al.* (1986) that these micro-colonies represent cells with sub-lethal damage. The precise damage mechanism to the cells has not been elucidated. However, the widths of the threshold rings varied at different segments further suggest the non-ideal beam profile characteristic of the laser light. This is due to different laser parameter characteristics' interaction with the microorganisms. The energy distribution is further analysed and commented on in **Section 2.3**.

Jacques (1992) broadly divided the laser-tissue/cell interaction into three categories: photochemical, photomechanical and photothermal. No conclusive work has been done to quantify any photochemical effects that may occur due to exposure from IR lasers. Transient stress waves (Dingus and Scammon, 1991) which cause photomechanical damage require short laser pulses (of the order of nanoseconds) to

rapidly heat the bacteria, causing stress-induced damage by thermoelastic expansion. Consequently, photomechanical effects are likely to be ruled out as the pulse width applied (8ms) throughout the experiments, was relatively long. Furthermore, Watson *et al.* (1996) showed that a high power, Q-switched Nd:YAG laser with about 5 ns pulse lengths, were ineffective in inactivating *E. coli* B 10537 lawned on agar; whereas pulse lengths of the order of milli-seconds and much lower peak powers did produce sterilisation. It is likely, therefore, that the inactivation mechanism is at least partly photothermal and it is probable that thermal absorption and diffusion effects of the laser-bacteria interaction dominate the bactericidal action.

Semenov *et al.* (1996) demonstrated the penetrating and bactericidal effects of the Nd:YAG laser beam at 1.06  $\mu\text{m}$  on *E. coli* and *S.aureus* growth at various depths in the nutrient agar. A significant increase in survival number of colonies per unit agar volume was demonstrated at a depth of 25-26 mm from the surface of the agar medium and complete inactivation of the nutrient agar surface was achieved at 1000  $\text{Wcm}^{-2}$ . However, the time taken to achieve this effect was not indicated and at 1000  $\text{Wcm}^{-2}$ , it would be important to know the effect on the agar medium. In comparison, an equivalent lower power density of 300  $\text{Wcm}^{-2}$  operating at 30 Hz, pulse energy of 10 J, with a time of 10.75 s produced complete sterilisation of *S. aureus* in this study.

Ward *et al.* (1997) showed that *E. coli* in liquid culture inactivated by Nd: YAG laser radiation ruptured when the bulk temperature of the liquid was taken to 50°C or higher, whereas at 50°C in the water-bath, the integrity of the cells remained intact. The thermal and *E. coli* bacteria interaction in liquid culture was further investigated by Wang *et al.* (1997). The three dimensional temperature distribution of the bacterial liquid suspension contained in a glass vessel was mathematically modelled. The transient and steady state temperatures of the culture were found. Thus, the lethality of the laser radiation may not be a straightforward thermal inactivation process. Once the lawned area is exposed above the threshold energy density, the process of irreversible thermal denaturation takes place.

From the experiments reported herein, for any given frequency, the area of inactivation increased with pulse energy. This can be explained in that the higher the applied energy density, the greater the heat input into the plate and therefore the greater the thermal damage and the greater the inactivation area. As the laser beam output is not spatially constant, the instantaneous temperature reached will vary spatially and in general it will increase with increasing pulse energy. The Gaussian profile of the output laser beam influences the killing of *S. aureus*. In **Figure 2.2.6**, it can be seen that the higher the PRF over the same output power, the lower the exposure time needed to achieve 50 % killing. Thus inactivation with Nd:YAG laser light is intensity dependent.

For light to exert any effect on the bacteria cell it must first be absorbed by the organism and/or its constituents. The primary effect seems to lead to the disruption of the cell membrane with an extrusion of intracellular contents due to pressure building up from within, as viewed by Ward *et al.* (1997) in a scanning electron microscope (SEM) with *E. coli* after Nd:YAG laser exposure at 50 °C. The inactivation areas on agar plates of *E. coli* and *S. aureus* 6571 with 10 J, 10 Hz (100W) and 8 ms pulse width were relatively close with average IA<sub>50</sub> values of 2123 Jcm<sup>-2</sup> and 2086 Jcm<sup>-2</sup> respectively (Ward *et al.* 1996), indicating that these bacteria have similar susceptibilities to Nd:YAG laser radiation. Furthermore, the IA<sub>50</sub> at 10 J and 10 Hz (100 W) was 2069 Jcm<sup>-2</sup> whilst Ward *et al.* (1996) obtained 2086 Jcm<sup>-2</sup>. With a lower energy density to achieve the same inactivation, *S. aureus* may behave similarly, leading to disruption of the cell membrane with extrusion of intracellular contents. In addition, the lethal effect of the laser radiation may be enhanced by the presence of the naturally occurring golden-yellowish pigment of *S. aureus* (Schultz *et al.* 1986).

A "lattice hypothesis of the absorption capabilities of malignant tumours" was suggested by McGuff and Bell (1966) and this hypothesis could apply to the bactericidal effect of Nd:YAG radiation on *S. aureus*. The extinction coefficient is an important factor which determines the amount of laser energy absorbed by the bacteria (Yeo *et al.* 1996) and to a certain extent the colour of the pigment will determine its absorption rate. Also, the higher the reflectivity of the bacteria and the

medium, the lower the amount of laser energy absorbed. The high powered Nd:YAG laser operating at 1064 nm, emits light with a wavelength that may preferentially be absorbed by the naturally yellowish pigment in *S. aureus*.

## 2.3 BEAM PROFILING/QUALITY ANALYSIS WITH *SERRATIA MARCESCENS*

### 2.3.1 INTRODUCTION

The widespread availability and usage of lasers of varying power levels and wavelengths has kindled the need of manufacturers and researchers or even end-users to maximise and optimise the laser output beam quality for specific applications. In biological systems such as laser sterilisation, understanding the beam characteristics would result in optimising the system's performance, reduce experimental inconsistency and produce conclusive and consistent results. Laser beam diagnostics (Cohen *et al.*, 1984, Cannon *et al.*, 1986 and Wright *et al.*, 1992) is therefore necessary to quantify the quality of the laser light applied with different measurement parameters such as the spatial intensity and its propagation characteristics. It can include measurements such as energy/power, spatial intensity profile, wave-front/propagation, temporal/time dependence and spectral analysis.

Near Gaussian laser beams are generally more useful than beams with multiple modes and often it is important to know the properties of the laser irradiance accurately if useful comparisons of theoretical and experimental results are to be made. For example in the development of hollow waveguides (WG) for mid-infrared spectrum transmission for medical applications, beam analysis is useful as the beam profile measurements supplied data on the contribution of coupling to the mode of propagation which optimises the delivered energy onto the target (Nathan *et al.*, 1997). Ward *et al.* (1996) has shown the bacterial effects of *E. coli* with Nd:YAG laser on lawned agar plates but only the integral energy densities were quoted. However, the spatial and radial laser energy density distributions were not evaluated.

With beam diagnostics, the energy profile across the area of inactivation can be defined and provides vital information which further conclusive understanding of the energy distribution with respect to the inactivation process of the microorganisms.

Moreover, the sub-lethal zones of inhibition (Ward *et al.*, 1996; Yeo *et al.*, 1997) could be mapped onto the beam profile to further gather the threshold energy densities across these transient zones of killing as observed. Additionally, such transient zones were different in widths when measured of different peripheral positions on a single inactivated zone.

In this section, two dimensional spatial intensity profiles of 10 Hz, 10 J and 20 Hz, 5 J on *Serr. marcescens* 2302 microorganisms seeded on nutrient agar medium were evaluated, with comparison of modelling and experimental results on the high-power Nd:YAG laser beam delivery system. A two dimensional plane of integrated energy density profiles at IA<sub>50</sub> values of the mentioned laser parameters were superimposed onto the circular zones of inactivation. The quality of the laser beam output was also evaluated using the M<sup>2</sup> factor.

Such application would yield a better resolution and accurate intensity profile across the area of clearance rather than the integral value of the power output by the laser which is often misleading and many times larger than the method described below.

## **2.3.2 EXPERIMENTAL SET-UP**

The whole set-up comprised the Nd:YAG laser delivery system, a detection system and the signal processing system, **Figure 2.3.1**.

### **2.3.2.1 Nd:YAG laser delivery system**

A pulsed, 400 W, Nd:YAG laser (Lumonics, MS830) operating at 1064 nm, with a fibre optic beam delivery system and collimating focusing lens assembly was used. The laser beam travelled via the step index fibre optic into the collimating lens telescope to produce a collimated beam. Various photographic papers were placed with at different distances from the collimating lens to measure the diameter at different parameters used in the profiling. A wedge was used to reflect a small percentage of the incident beam via a mirror to the signal detection head.

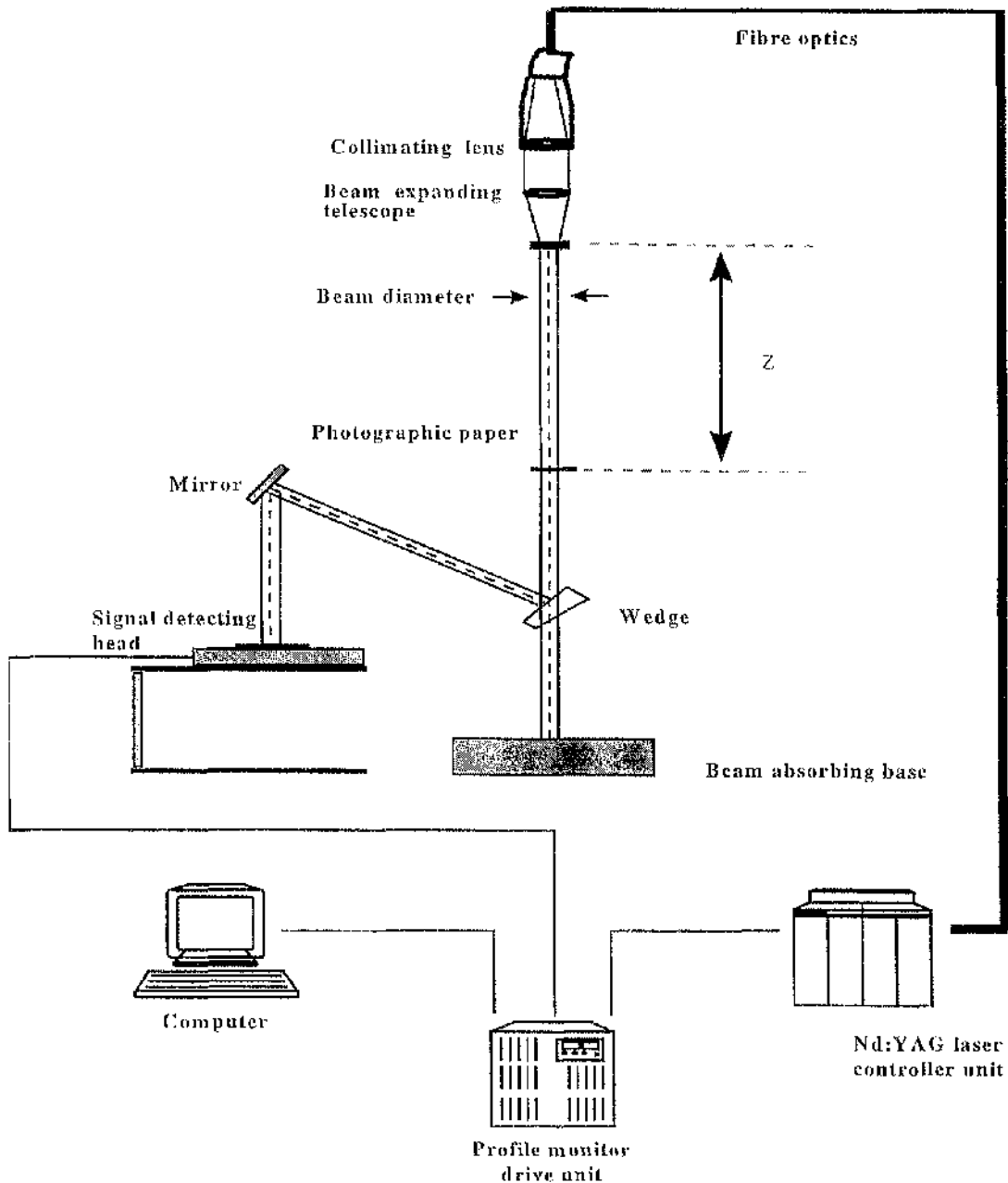


**Figure 2.3.1** Experimental set-up. A fraction,  $R_f$ , of the main beam is reflected via a wedge and a mirror onto a one dimensional pyroelectric detector array located at  $z=1664$  mm. The lawned plate of *Serratia marcescens* was placed at  $z = 323$  mm.

### **2.3.2.2 Signal detecting head**

The detecting head contained a linear array of sixty-four pyroelectric elements together with amplifiers and multiplexers to create a single analogue signal channel back to the drive unit, namely, sixty active pyroelectric elements with two zero references before and after. Each pyroelectric element has a rectangular dimension of 0.375 by 2.67 mm with element pitch of 0.4375 mm gauge. The array size was 26.2 by 2.67 mm, **Figure 2.3.2**.

### **2.3.2.3 Signal processing system**

This comprised of the profile monitor drive unit which linked the Nd:YAG controller unit and interface with the end user PC using software to retrieve the signal.

### **2.3.2.4 Culture preparation**

*Serr. marcescens* 2302 was maintained on nutrient agar (CM3, Oxoid) slopes at 4°C and was sub-cultured once monthly. Bacterial cultures were grown in nutrient broth (15 ml, CM 67, Oxoid) and incubated overnight at 25°C.

### **2.3.2.5 Preparation of lawned plates**

Fresh molten nutrient agar (CM3, Oxoid) was prepared and allowed to flood the surface of the sterile circular plastic plates (9 cm in diameter). They were left to dry and solidify for 40 min in a class 100 laminar air flow cabinet (Flow Laboratories, Germany). Aliquots (1.5 ml) of the overnight culture were pipetted onto the agar plates and allowed to flood the surface. The concentration of these aliquots was determined from serial dilutions at  $4.2 \times 10^9 \text{ ml}^{-1}$ . The excess liquid was decanted and this volume was measured at 1.15 ml. Therefore, a volume of 0.35 ml was left on the plate with a concentration of  $\sim 1.47 \times 10^9 \text{ cfu}$  inoculated per plate. Thus, the concentration per unit area over the petri-dish was  $\sim 2.31 \times 10^7 \text{ cfu cm}^{-2}$ . The lawned plates were dried for 30 min in a Petric Class III microbiological safety cabinet, before starting the experimental work.

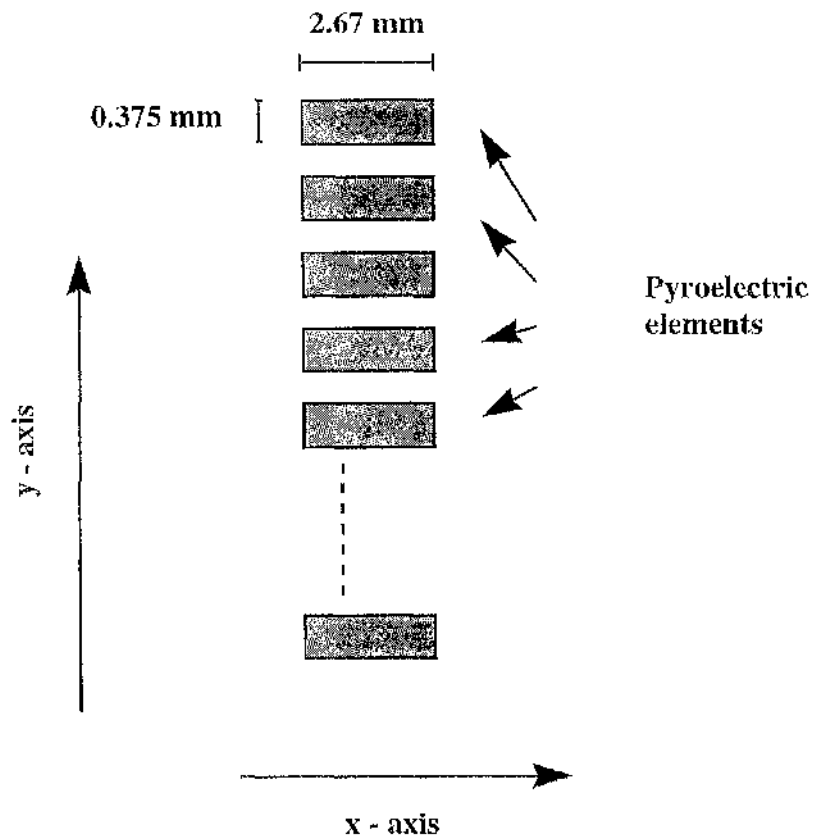


**Figure 2.3.2** Diagram shows the one dimensional series of pyroelectric detector used to capture the intensity profile of both 10 Hz 10 J and 20 Hz 5 J respectively. The overall array size has a dimension of 26.2 by 2.67 mm. At any instance, a two dimensional spatial energy density distribution was captured via the array comprises of 60 pyroelectric detectors; follow by which successive increments of a detector's width length (2.67mm) was made to build the 3-D profile along the x-axis.

## 2.3.3 PRINCIPLES OF OPERATION AND PROCEDURES

### 2.3.3.1 Detector threshold energy density

The laser output beam energy sampled has to be below the damage threshold energy density of the pyroelectric detector array. From **Figure 2.3.3**, the maximum safe energy density for 8 ms sample pulses was  $9 \text{ Jcm}^{-2}$ . The calibration table, **Table 2-3-1** showed the corrected true energy pulse values measured with the FIELDMASTER<sup>TM</sup> (Coherent) power/energy meter for the above laser parameters mentioned. To prevent any damage to the pyroelectric array, a cautious approach was taken to calculate the damage threshold level with the following assumptions:

1. No significant beam divergence; thus the sampled beam diameter on the pyroelectric array was taken to be the reference beam diameter.
2. Reflected ray from the wedge at 5 % of the incident beam onto pyroelectric detector array.

With the above assumptions, a table of energy densities of both pulse energies, namely 10 and 5 J was applied.

### 2.3.3.2 Beam divergence

The reference position was taken with respect to the datum or minimum radius,  $w_0$ , which was taken to be the radius imprinted by the laser shot on the photographic paper at position  $z_0$  where the collimating lens were positioned. Burn prints were taken at  $z$  positions of 87, 150, 199.5, 225.5, 249.5, 323.5, 519, 659, 764 and 851 mm from the collimating lens.

### 2.3.3.3 Beam profile

A fraction of the incident beam,  $R_f$ , was reflected via the  $1^\circ$  fused silica wedge (Virgo Optics) and mirror to the signal detecting head located at a distant,  $z_{\text{unmy}}$ , situated 1664 mm away from the collimating lens. The aim of evaluating  $R_f$  was to enable the mapping of the energy profile on the detector onto the inactivation site of contaminated agar plates. The profile monitor drive unit was set to capture five

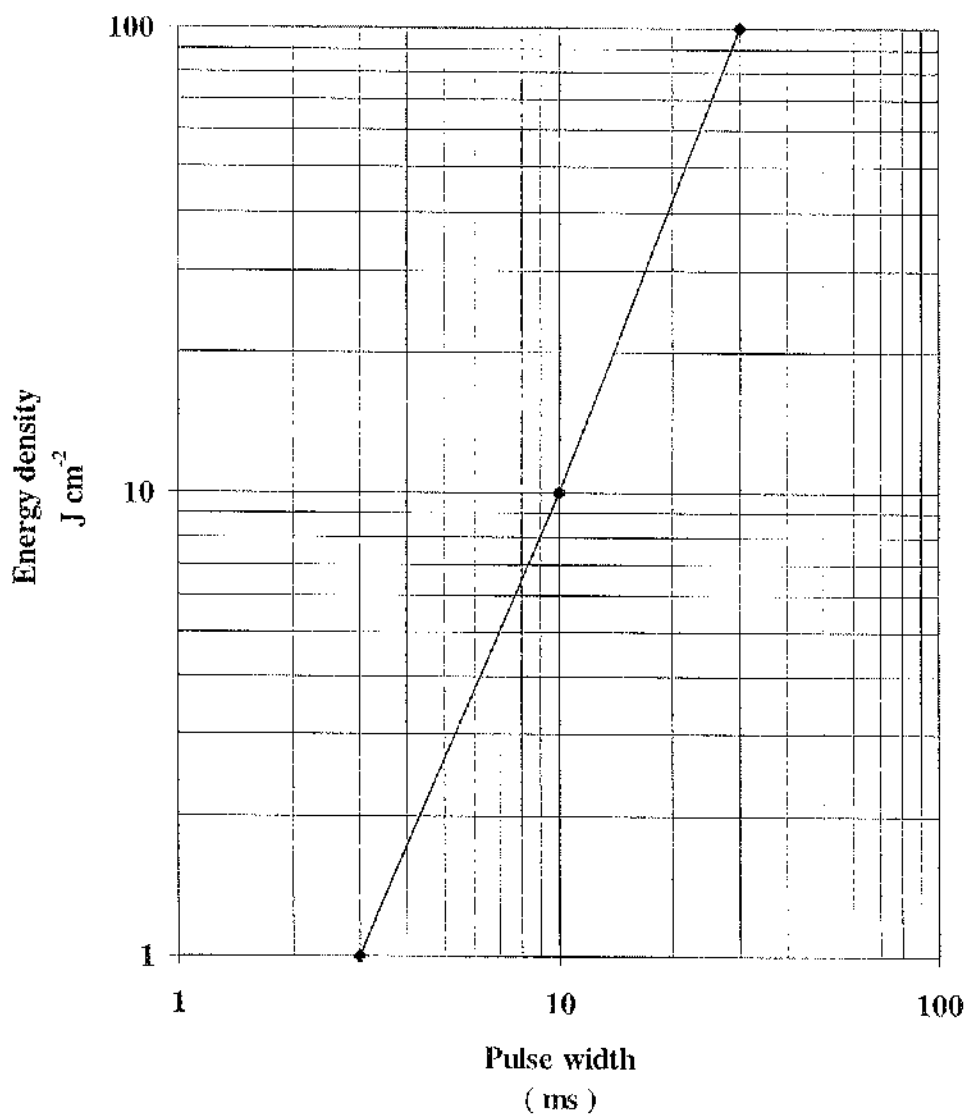


*Figure 2.3.3* Graph showing the threshold energy density of each pyroelectric detector of approximately  $9 \text{ J cm}^{-2}$  at 8 ms pulse width which is used for both 10 Hz 10 J and 20 Hz 5 J.

*Table 2-3-1* The calibration for each set of laser parameters were measured using a power/energy meter (FILEDMASTER™, Coherent, U.K.)

Beam Parameters					
Frequency ( Hz )	Pulse Energy ( J )	Pulse width ( ms )	Set Power ( W )	Actual Power ( W )	Actual Pulse Energy ( J )
10	10	8	100	81	8.1
20	5	8	100	82.67	4.1

pulses at the array which was synchronised with the Nd:YAG controller unit. Noise and unwanted signals were filtered out by taking the difference in the energy pulse signals with pre and post inter-pulsed scans. Thus the average result of the five energy pulses reduced the pulse to pulse signal instability of the pulses sampled. The two dimension pyroelectric array was then shifted incrementally, at 2.5 mm interval, along the x axis direction to achieve the two dimensional pulse energy profile (see **Figure 2.3.2**). The actual beam diameter measured was taken along the pyroelectric array plane. The detector array signals were retrieved in terms of energy density ( $\text{Jmm}^{-2}$ ). By integrating the signal:

$$\int_A ED \, dA = P_e \quad (2.3.1)$$

the pulse energy,  $P_e$  (J) was obtained. The integrals of each successive plane of signals formed the three dimensional energy distribution when combined.  $R_f$  can then be evaluated by taking the ratio of the integrated energy intensity profile to the pulse energy applied.

Using on  $R_f$ , the three dimension energy distribution,  $P_e$  at the agar plate position (i.e. at  $z = 323$  mm) can be estimated. At the agar plate position, the power output,  $P_o$ , was then given by:

$$P_o = f P_e \quad (2.3.2)$$

where  $f$  is the PRF ( $\text{s}^{-1}$ ). The energy density, ED ( $\text{Jcm}^{-2}$ ) applied onto the contaminated agar plates, was defined as:

$$ED = \frac{P_o t}{A} \quad (2.3.3)$$

where  $t$  was the exposure time of the laser light (s) and  $A$ , the measured beam area on burn prints ( $\text{cm}^2$ ). Also, a two dimensional energy density distribution profile

across the plane where the highest peak occurred was then extracted and superimposed on the burn-print diameter and compared with the diameters of inactivation at  $IA_{50}$  values on the agar plates.

#### 2.3.3.4 Beam quality factor, $M^2$

Beam propagation parameters such as  $M^2$  can be determined using a combination of both near and far field measurements. It is a number that expresses the ratio of the beam diameter with that of a pure fundamental Gaussian beam. As few high power lasers operate in their pure fundamental mode ( $TEM_{00}$ ), the  $M^2$  factor is useful in characterising the quality of the laser output beam. The beam radius theoretically,  $w_{theor}$ , at any distant  $z$  away, can be obtained from (Boyd *et al.*, 1996):

$$w_{theor}^2(z) = w_0^2 \left\{ 1 + \left( \frac{\lambda z}{\pi w_0^2} \right)^2 \right\} \quad (2.3.4)$$

However, **Eqn. 2.3.4** does not really give a good approximation to most lasers operating in multi-mode since it is only valid for a pure fundamental Gaussian beam output. Since the transverse extent of any higher-order mode of the beam is a fraction of the underlying Gaussian beam by a constant factor,  $M$  (Wright *et al.*, 1992), we have

$$w_{pract}(z) = M w_{theor}(z) \quad (2.3.5)$$

which yields a closer approximation of the actual beam quality. By substituting **Eqn. 2.3.5** into **2.3.4**;

$$w_{pract}^2(z) = w_0^2 \sqrt{\left\{ 1 + \left( \frac{M^2 \lambda z}{\pi w_0^2} \right)^2 \right\}} \quad (2.3.6)$$

By iteration  $M^2$  was found for the best fit of the data obtained on both sets of burn prints corresponding to the above mentioned laser parameters. The beam diameter,

$w_{\text{exp}}$ , obtained using the pyroelectric array, calculated from the number of pyroelectric detectors activated, was then compared with  $w_{\text{pract}}$ .

### **2.3.3.5 Laser beam parameters**

Two sets of laser output conditions were chosen namely 10 J at 10 Hz, 5 J at 20 Hz with applied energy density up to 2979.4 and 3533.5 Jcm<sup>-2</sup>. The chosen parameters were set to 8 ms pulse width to enable consistency in comparison with profile evaluation. The laser output power was measured with a power/energy meter (FILEDMASTER<sup>TM</sup>, Coherent, U.K.) which calibrated the pulse energy used. As mentioned in **Section 2.2.2.5**, the IA<sub>50</sub> value was used as the standard intercept for comparison with both sets of laser parameter used on *S. marcescens*.

### **2.3.3.6 Irradiation of lawned plates**

The preparation of the lawned plates was described in **Section 2.2.2.2**. The lawned plates were mounted on a stand corresponding to  $z$  at 323.5 mm and positioned along the optical propagation axis of the laser beam. Each lawned plate was divided into six segments which enabled six exposures to be made (similar to the irradiation procedures in **Section 2.2.2.5**). Each designated set of parameters was done in triplicate and repeated twice. After exposure, the plates were incubated overnight at 25 °C and each segment was observed under the Profile Projector (PJ-300, Mitutoyo). The diameters of the cleared regions where no bacterial growth observed were measured. All diameter measurements observed under the Profile Projector gave three decimals accuracy of a millimetre (except  $z$  position, which yielded a tolerance of  $\pm 0.5$  mm). The cleared areas were viewed against the background of the plate where confluent growth was seen. These areas were measured for each set of the laser parameters.

## 2.3.4 RESULTS

### 2.3.4.1 Detector threshold energy density

Table 2-3-2 shows the estimated calculation of both 8.1 and 4.1 J pulse energy, which indicated they are all below the pyroelectric detector array safe energy density limit of  $9 \text{ J cm}^{-2}$  per pixel detector.

### 2.3.4.2 Beam divergence

In Figure 2.3.4, both sets of burn-print diameters measured are plotted against its corresponding z positions. The burn print diameters increased with increasing pulsed energy applied and the same trend was also observed with increasing z positions. The burn print diameters on the agar plate position were measured at 12.8 and 15.0 mm for 20 Hz, 5 J and 10 Hz, 10 J respectively.

### 2.3.4.3 Beam profile

The details of the profiles are shown in Table 2-3-3. The calculated  $R_r$  is seen to be fairly accurate between 1.3 to 1.45 % since the anti-reflection coating (Virgo Optics, #2010) on the mirror was quoted at about 1.5 % reflection. The  $R_r$  ratio was used to transpose the energy profile onto the agar position.

The generated three dimensional energy density profiles on the pyroelectric array of both 10 Hz/10 J and 20 Hz/5 J pulses are shown in Figure 2.3.5 and 2.3.6 respectively. Figure 2.3.7 and 2.3.8 shows similar profiles transposed on the inactivation sites on the agar plates with  $IA_{50}$  values at 2488.04 and  $3022.5 \text{ Jcm}^{-2}$  respectively. The height of the Gaussian distribution describes the intensity of the laser beam output with peaks evaluated at 16.8 and  $19.9 \text{ Jcm}^{-2}$  respectively. The beam radius is defined as the distance between the centre peak of the profile to the  $1/e^2$  position.

### 2.3.4.4 $M^2$

Using the  $M^2$  compensation factor,  $w_{\text{theor}}$  was calculated and compared with the  $w_{\text{detector}}$  for both laser parameters. The numbers of detector activated were 55 and 50

**Table 2-3-2** Table shows the minimum diameter,  $w_0$  corresponding to  $z = 0$  mm with energy density falling on the pyroelectric detector for 8.1 and 4.1 J pulse energy which is below the threshold level of the detector array of  $9 \text{ J cm}^{-2}$ .

Pulse Energy ( J )	Minimum Diameter, $w_0$ ( mm )	Energy Density on pyroelectric array ( $\text{Jcm}^{-2}$ )
8.1	13.511	0.245
4.1	11.532	0.183

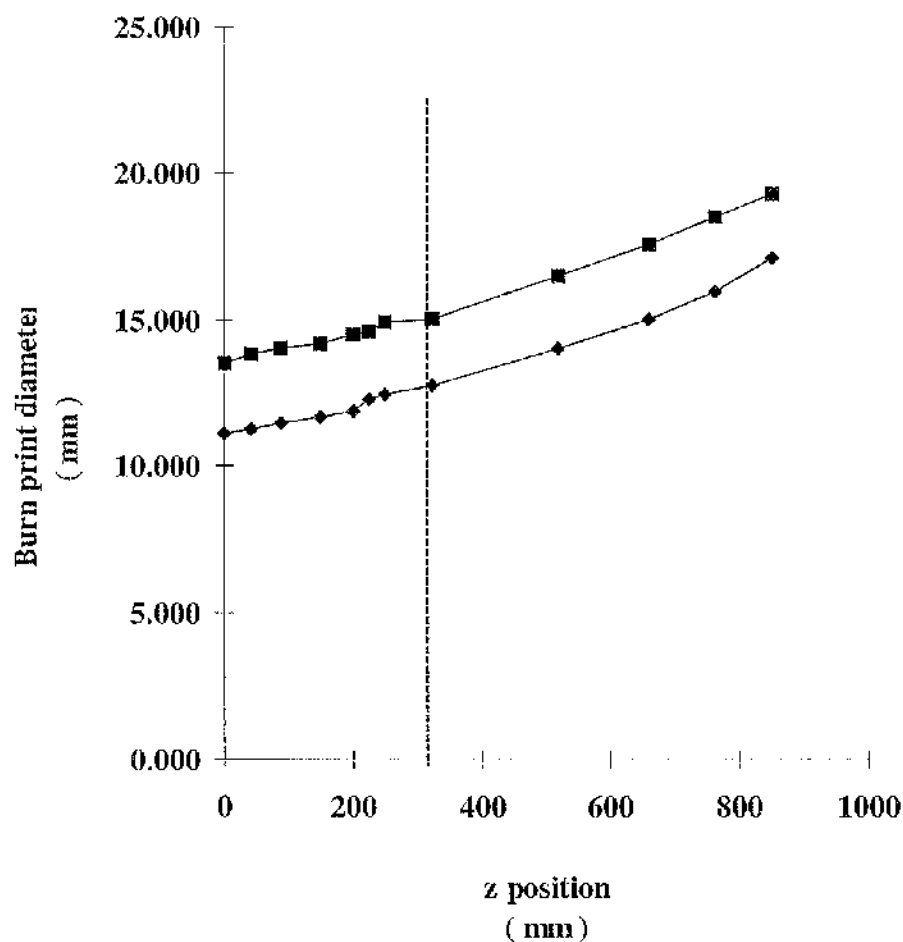


**Figure 2.3.4** The various burn print diameters were plotted as a function of optical z positions away from the collimating lens for 10 Hz 10 J, ■ and 20 Hz 5 J, ◆ at single pulse shot to z = 851 mm. The diameters were measured using a Profile Projector (PJ-300 Mitutoyo) which yields three decimals accuracy of a millimetre. The reference burn print diameters ( $2w_0$ ) for 10 Hz 10 J and 20 Hz 5 J are 13.511 mm (1.43 cm<sup>2</sup> area size) and 11.132 mm (0.97 cm<sup>2</sup> area size) respectively. The dotted line (---) shows the position at which the lawned agar plates of *Serratia marcescens* 2302 were experimented. The correlation coefficient were 0.97 (■) and 0.98 (◆).

**Table 2-3-3** Table shows the detail of the 3-D energy density profile, integrated pulse energy and reflected fraction of the main beam,  $R_r$  for 8.1 and 4.1 J respectively.

3-dimension energy profile					
Pulse energy (J)	Highest intensity identified ( $\mu\text{Jmm}^{-2}$ )	Intensity at 13.5 % of peak intensity ( $\mu\text{Jmm}^{-2}$ )	Integrated total energy per unit area ( $\mu\text{Jmm}^{-2}$ )	Integrated total energy ( $\mu\text{J}$ )	$R_r$ (%)
8.1	726.7	98.1	108190.6	108325.8	1.33
4.1	391.8	52.9	59390.4	59464.6	1.45

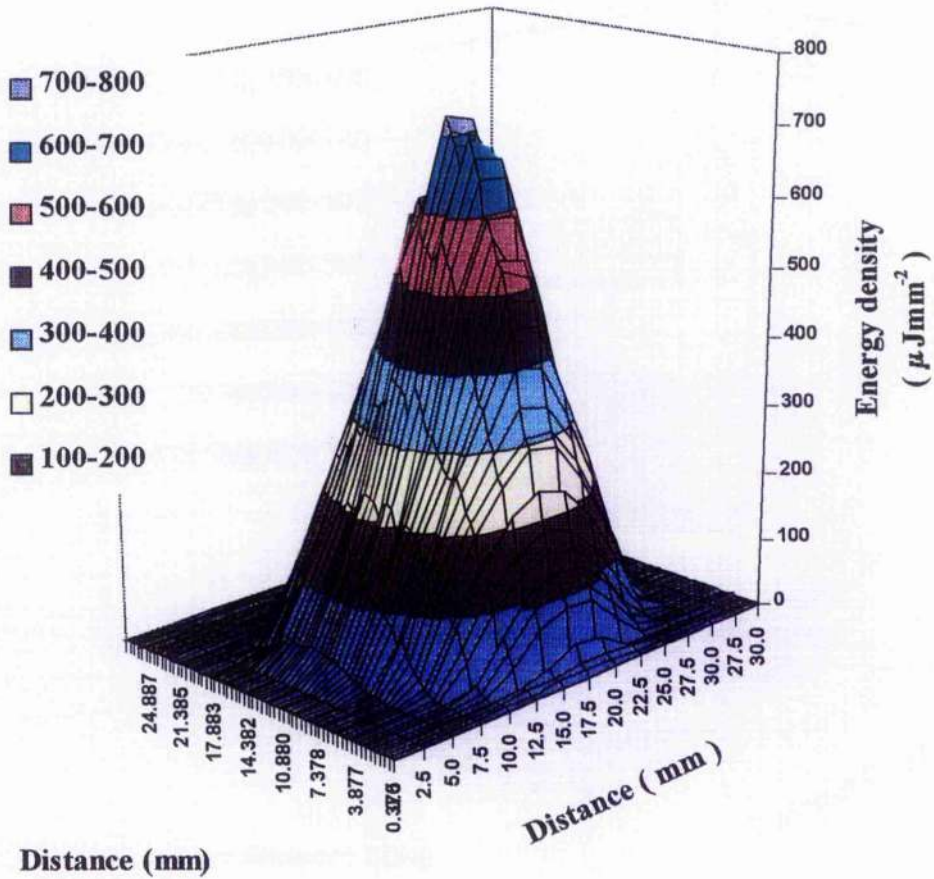


**Figure 2.3.5** Three dimensional view of the energy density profile at pyroelectric detector position ( $z=1664$  mm) of 10 Hz 10 J. The energy density, shown by the height of the profile, increases towards the centre of the beam.

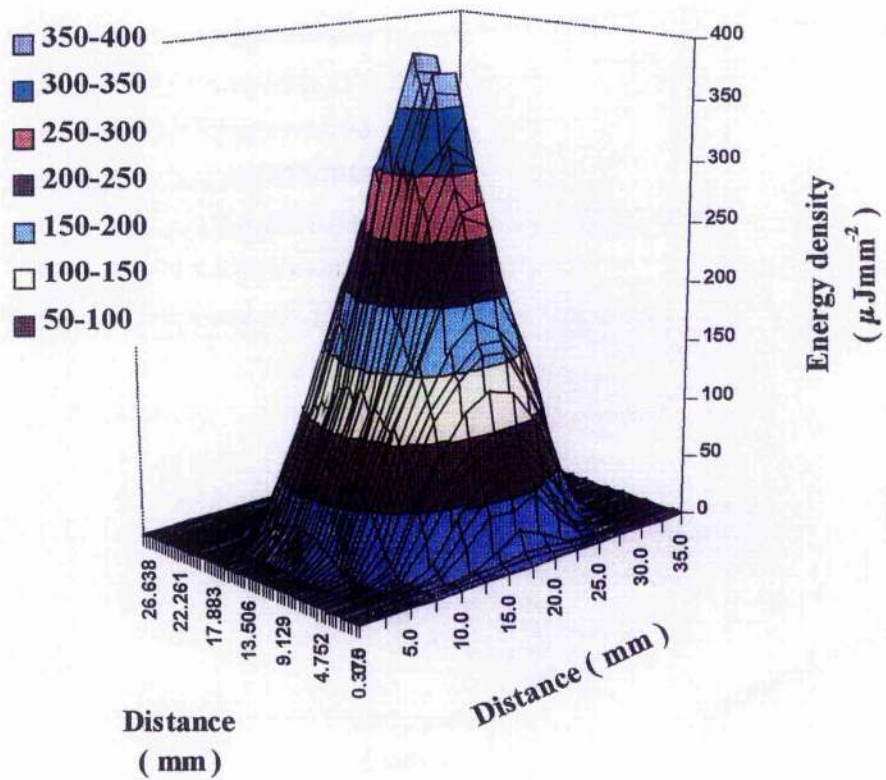


*Figure 2.3.6* Three dimensional view of the energy density profile at pyroelectric detector position ( $z=1664$  mm) of 20 Hz 5 J. The energy density, shown by the height of the profile, increases towards the centre of the beam.

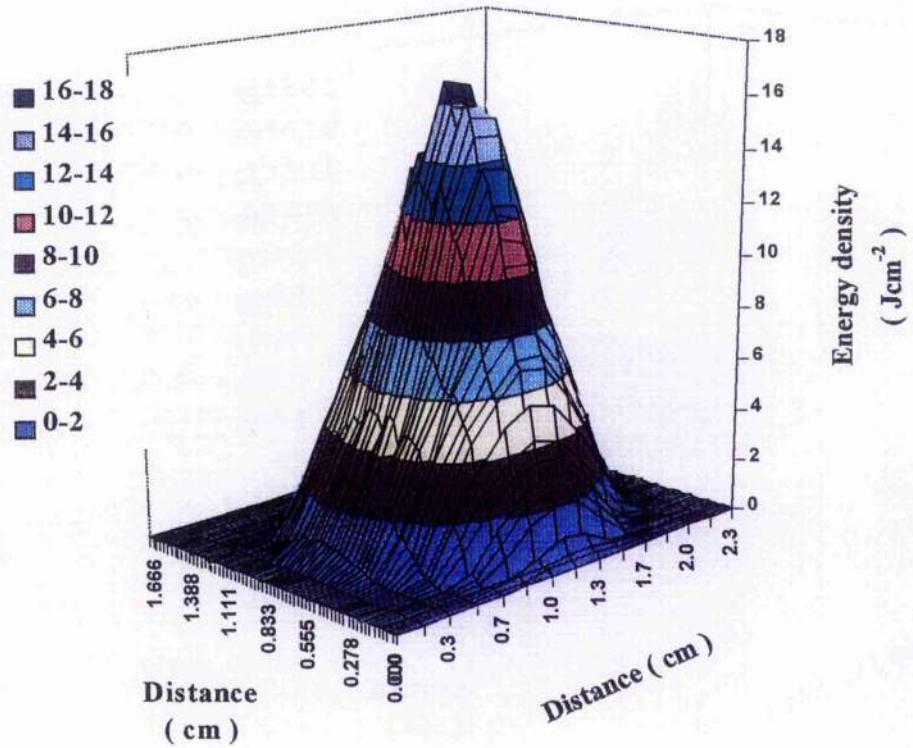


**Figure 2.3.7** Three dimensional view of the energy density ( $IA_{50}$  value= $2488.04 \text{ Jcm}^{-2}$ ) profile of the laser beam at 10 Hz 10 J imposed on *S. marcescens* seeded on nutrient agar plate. The energy density, shown by the height of the profile, increases towards the centre of the beam.

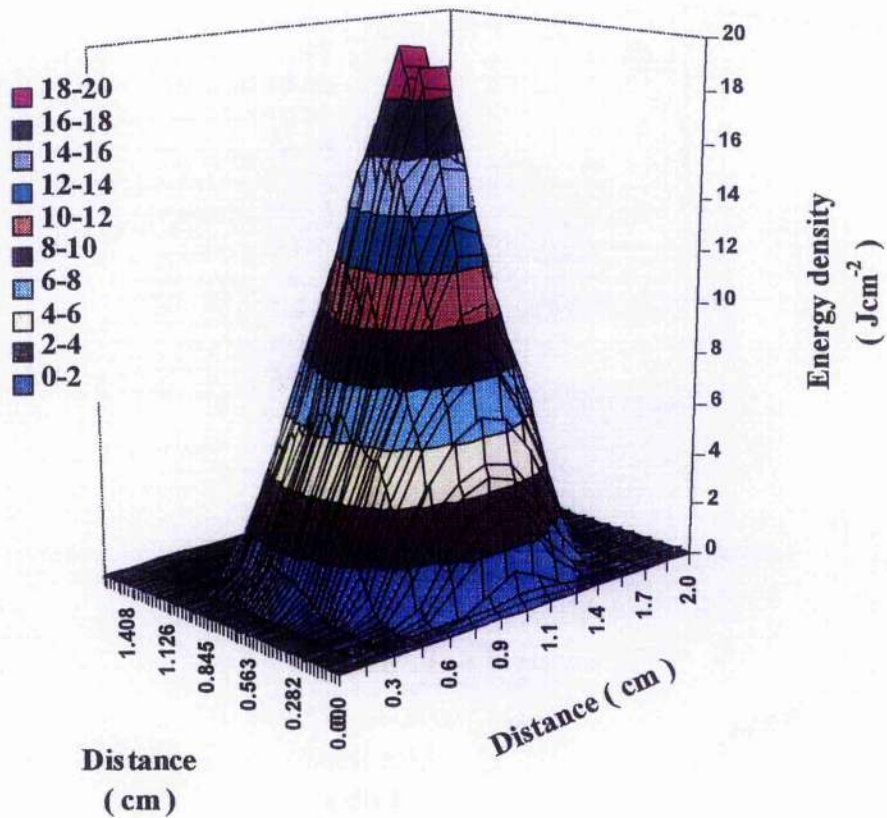


**Figure 2.3.8** Three dimensional view of the energy density ( $IA_{50}$  value=3022.5  $Jcm^{-2}$ ) profile of the laser beam at 20 Hz 5 J imposed on *S. marcescens* seeded on nutrient agar plate. The energy density, shown by the height of the profile, increases towards the centre of the beam.

for the 10 Hz/10 J and 20 Hz/5 J pulses respectively. Since the pyroelectric's element pitch was 0.4375 mm,  $w_{\text{detector}}$  was found to be obtained at 24.1 and 21.9 mm respectively, **Table 2-3-4**.  $M^2$  values were arrived at by iterations with various burn prints obtained at various z positions as shown in **Figure 2.3.9**.  $M^2$  values decreased with pulse energies applied and valued at 150 with 10 Hz/10 J and 120 with 20 Hz/5 J pulses respectively.

#### **2.3.4.5 Laser inactivation of *S. marcescens***

Both the laser settings at 10 Hz/10 J and 20 Hz/5 J achieved inactivation over the range of densities from 2000 to 3500  $\text{Jcm}^{-2}$  without damaging the underlying nutrient agar substrate, **Figure 2.3.10A**. The  $IA_{50}$  values were 2488.0 and 3022.5  $\text{Jcm}^{-2}$  at 10 Hz/10 J and 20 Hz/5 J respectively. The percentage inactivation of the microorganisms increased with increasing energy densities applied and were higher with 10 Hz 10 J pulses than the 20 Hz 5 J pulses. However, with 20 Hz/5 J, for a given exposure time, the inactivation process was achieved quicker than with 10 Hz/10 J. For example, the  $IA_{50}$  values were obtained at 47.7 and 54.3 s respectively, **Figure 2.3.10B**.

The cross section planes of energy densities of both 10 Hz/10 J and 20 Hz/5 J at  $IA_{50}$  values were extracted from **Figure 2.3.7** and **2.3.8**. The two dimension profiles, distributed across the burn print diameters of 1.5 and 1.28 cm, were mapped with the diameter of clearance with values of 1.060 and 0.902 cm respectively, **Figure 2.3.11** and **2.3.12**. The fundamental Gaussian distribution was shown (dotted) to indicate the extent of the deviation of the laser beam output.

### **2.3.5 DISCUSSION**

The use of photographic paper is a simple, economical and fast method for visual inspection of beam diameter of the Nd:YAG laser delivery system (Rypma, 1997). However, it only provides a two dimensional non-critical gauge of the intensity distribution. Nevertheless, it was a good method to predict the divergence with

**Table 2-3-4** Both the beam diameter using Gaussian beam propagation equation with  $M^2$  compensation factor theoretical diameter,  $2w_{\text{theor}}$  and actual diameter,  $2w_{\text{detector}}$  obtained via the pyroelectric detector are shown for 8.1 and 4.1 J respectively.

Pulse energy ( J )	$2w_{\text{theor}}$ ( mm )	No. of pyroelectric detectors activated at highest mean energy plane	$2w_{\text{detector}}$ ( mm )	$M^2$
8.1	28.4	55	24.1	150
4.1	26.6	50	21.9	120

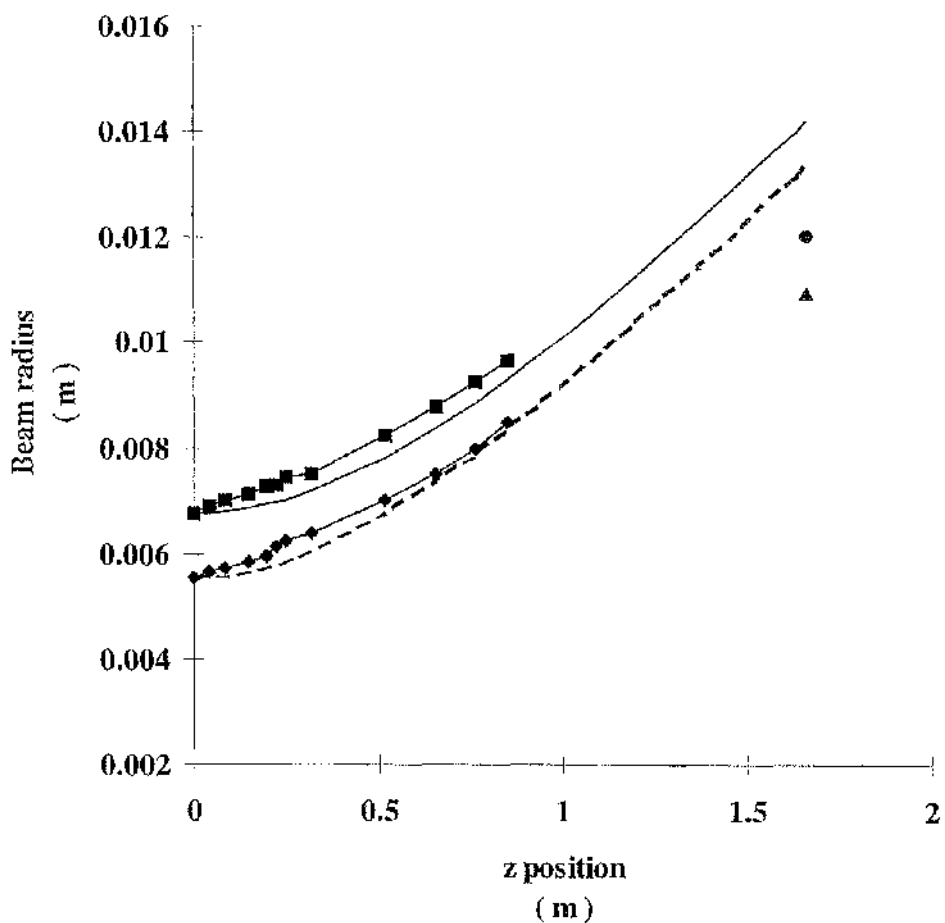


*Figure 2.3.9* Various burn print radii plotted as function of  $z$  from the collimating lens for 10 Hz 10 J, ■ and 20 Hz 5 J, ◆ at single pulse shot to  $z = 851.0$  mm after which no distinct burn print was observed. The theoretical beam radii,  $w_{\text{theor}}$  are also fitted into the burn print radius extrapolated to the pyroelectric detector position at  $z = 1.664$  m for 10 Hz 10 J ( — ) and 20 Hz 5 J ( --- ) respectively. The measured radius on the pyroelectric detector are 0.0125 and 0.0110 m for 10 Hz 10 J ( ▲ ) and 20 Hz 5 J ( ● ) respectively.

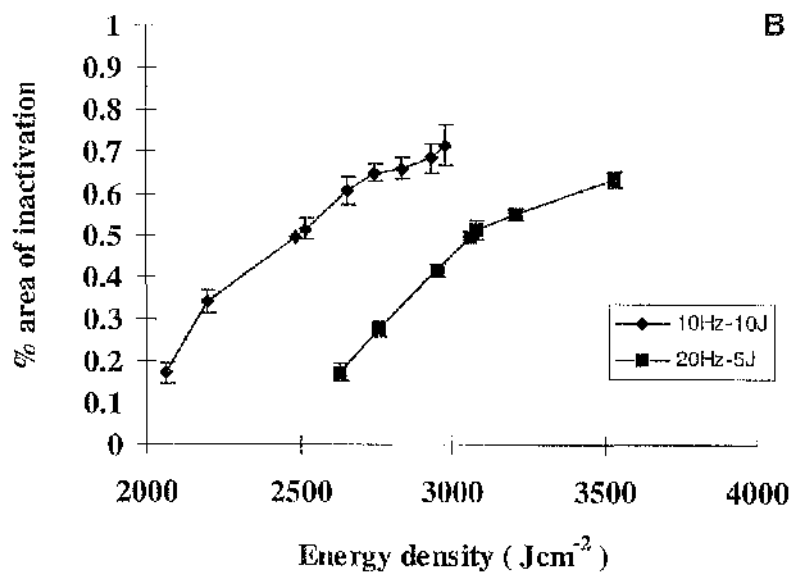
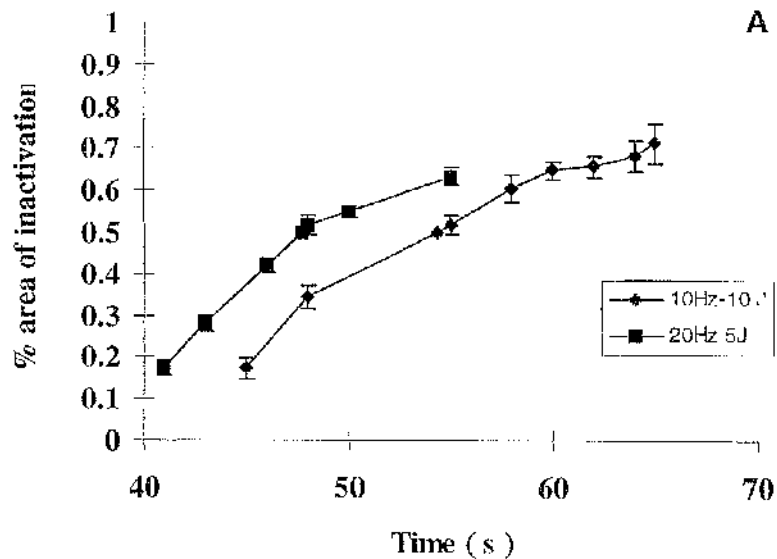


*Figure 2.3.10* Graph of percentage areas of inactivation of *S. marcescens* with respect to exposure times (A) and energy densities applied (B).

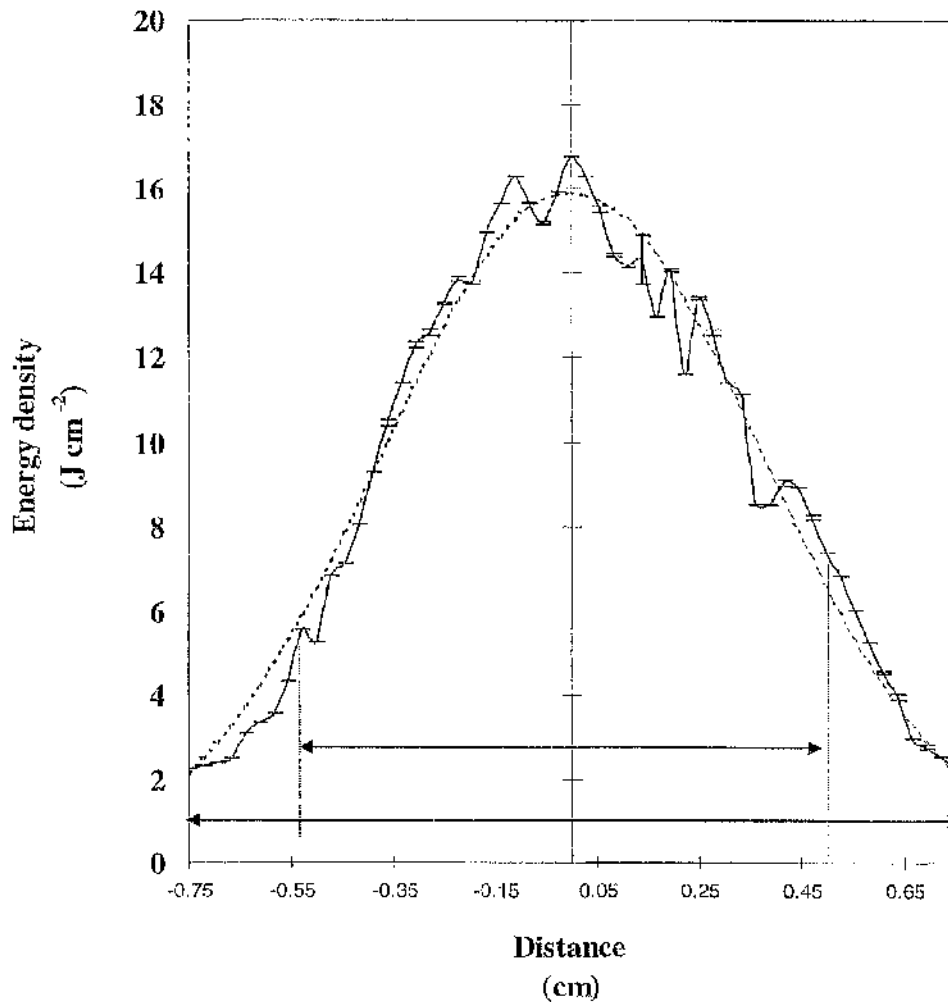


**Figure 2.3.11** The  $1/e^2$  locus gives a beam diameter of 1.5 cm at 10 Hz 10 J with the energy density across as shown with the continuous line. The ideal Gaussian beam profile was plotted as shown with the dotted line using least square fitting method. The diameter of clearance 1.06 cm ( $0.88 \text{ cm}^2$ ) for  $IA_{50}$  value of  $2488.04 \text{ Jcm}^{-2}$  was superimposed onto the 2-D profile which yields value of inactivation between  $5.8$  and  $7 \text{ Jcm}^{-2}$ . The threshold lengths of partial killing observed outside the area of inactivation were measured at  $0.056$  and  $0.068 \text{ cm}$  respectively.

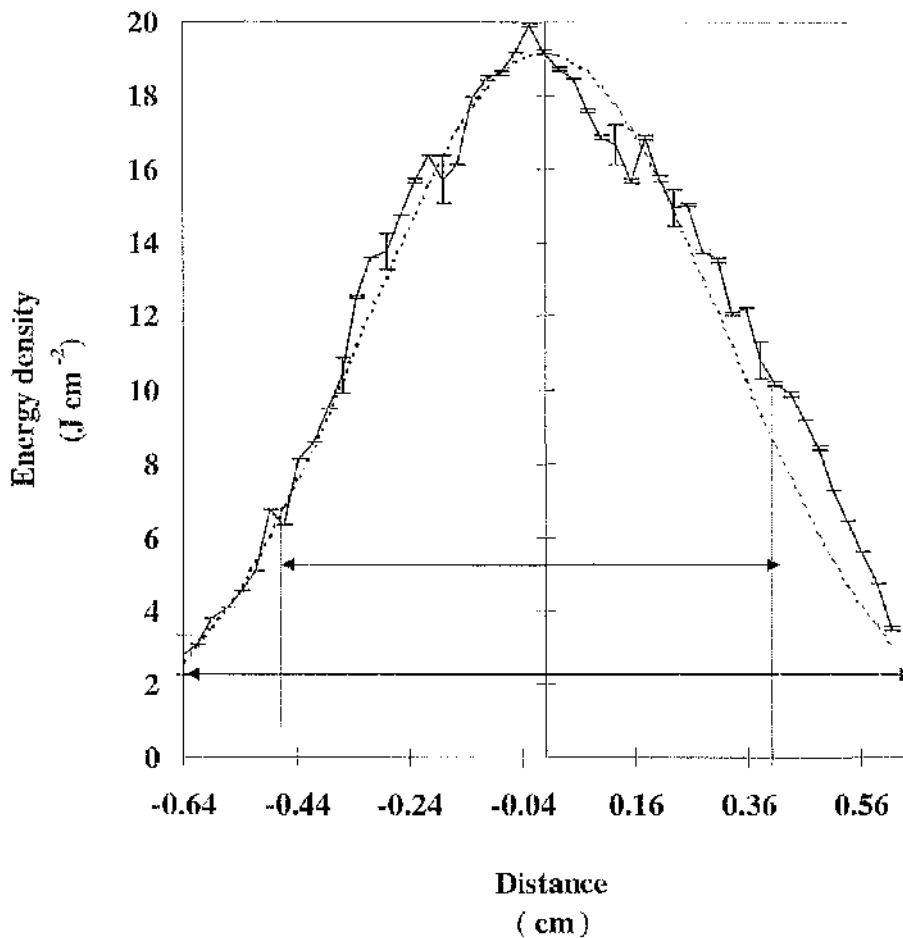


**Figure 2.3.12** The  $1/e^2$  locus gives a beam diameter of 1.28 cm at 20 Hz 5 J with the energy density across as shown with the continuous line. The ideal Gaussian beam profile was plotted as shown with dotted line using least square fitting method. The diameter of clearance of 0.902 cm ( $0.64 \text{ cm}^2$ ) for  $IA_{50}$  value of  $3022.5 \text{ Jcm}^{-2}$  was superimposed onto the 2-D profile which yields value of inactivation between 6.5 and  $10 \text{ Jcm}^{-2}$ . The threshold lengths of partial killing observed outside the area of inactivation were measured at 0.065 and 0.082 cm.

expected diameters and energy density at far-field distances where it is considered 'safe' (in intensity context) to capture the laser beam profile using a scanning slit device such as, the pyroelectric detector array. The pyroelectric detector provides an easy but accurate analysis and above all, low cost as compared to other diagnostic measurements such as CCD imaging system (Philip, 1994). The sensitivity of the photographic paper was fairly consistent as the diameters increased with z distances and with increasing pulse energies. The correlation coefficient between the z distances and the burn print diameters were high for both 10 Hz/10 J pulses and 20 Hz/5 J pulses at 0.97 and 0.98 respectively.

The  $M^2$  values obtained at 150 with 10 Hz/10 J and 120 with 20 Hz/5 J suggested relatively good beam quality output since most high power Nd:YAG lasers usually have  $M^2$  greater than 50. A typical 130 W laser beam Nd:YAG delivery system yields a  $M^2$  value of 55 (Boyd *et al.*, 1996). The larger the  $M^2$  value, the further the delivery system deviates from the pure fundamental Gaussian beam characteristic. The high  $M^2$  could be due to the step-index fibre transmission system and the misalignment of the lens with the fibre-optics to produce the collimated beam. This could suggest the abnormalities of  $w_{\text{detector}}$  are bigger than  $w_{\text{theor}}$  calculated. In a practical system, it may prove beneficial to have a top-hat profile rather than Gaussian distribution to provide a uniform energy distribution on the target sample.

The  $R_f$  value of  $1.38 \pm 0.009 \%$  suggests a relatively consistent total reflection due to the wedge and the mirror set-up. This arrangement enabled the three dimension energy profile to be mapped onto the experimental site where the energy density would be impossible for any detector to withstand. Such sampling techniques could couple with heat-temperature analysis (Wang *et al.*, 1997) to optimise the laser-bacteria interaction when designing laser sterilisation systems.

**Figures 2.3.10A and B** demonstrate the frequency dependence of the microbial killing of *S. macescens* with Nd:YAG laser radiation. At any given energy density, the percentage inactivation was higher with 10 Hz/10 J pulses than with 20 Hz/5 J pulses. However, for any given exposure time, the 20 Hz/5 J pulses achieved a higher percentage of inactivation than the 10 Hz/10 J pulses. From these data, it was

difficult to choose between which was more efficient in microbial killing. 10 Hz/10 J pulses would achieve a given percentage of inactivation with a lower energy density while 20 Hz/5 J took a shorter time to achieve the same percentage area of clearance. However, the heat affected zones or sub-lethal killing areas outside the inactivated areas were larger with 20 Hz/5 J pulses than with 10 Hz/10 J pulses. This suggests that the sub-lethal widths increase with increasing frequency (PRF) for a given power.

With the two dimensional energy density profiles shown in **Figure 2.3.11** and **2.3.12**, the difference in threshold widths with either 10 Hz/10 J or 20 Hz/5 J pulse could be explained in terms of the non-ideal and non-symmetrical beam condition. As seen with 10 Hz/10 J pulses at  $2488.04 \text{ Jcm}^{-2}$  ( $IA_{50}$  value), the threshold widths outside the inactivated zone were measured unequally at 0.056 and 0.068 cm. This was due to a lower energy density applied at  $5.8 \text{ Jcm}^{-2}$  compared with  $7 \text{ Jcm}^{-2}$  respectively. Similar comparison was verified with 20 Hz/5 J pulse measured at 0.065 and 0.082 cm with  $6.5$  and  $10 \text{ Jcm}^{-2}$  respectively. The non-symmetrical beam profile could be non-desirable especially in medical applications such as laser assisted *in situ* kerectomelusus (LASIK), a modern myopia eye correction treatment where applied energy dosage is crucial within a very narrow range on the cornea.

Interestingly, a comparison of the  $IA_{50}$  values at 10 Hz/10 J with Ward *et al.* (1996) revealed a much higher energy density needed for bacteriostasis. In his report,  $IA_{50}$  value was measured at  $1768 \text{ Jcm}^{-2}$  whilst  $2488 \text{ Jcm}^{-2}$  was needed in this study. In both cases, beam diameter was the only variable. This suggests that the beam diameter is a crucial variable with which to optimise the rate of bacterial sterilisation. A smaller beam diameter, with constant energy density, would result in a more rapid with less energy applied to attain  $IA_{50}$  values on the microorganisms. Also, the rate of inactivation, defined over the area of killing per unit time in a decontamination plant could be higher with a smaller beam diameter. This hypothesis was further investigated in the later chapters involving the design of laser scanning systems aiming to optimise the sterilisation process.

### **III. CO<sub>2</sub> LASER**

## 3.1 SPOT TARGET STERILISATION SYSTEM WITH HIGH POWER CO<sub>2</sub> LASER

### 3.1.1 INTRODUCTION

Staphylococci species have been reported to cause infections due to their adherence to various medical materials, for example, intravenous catheters (Maki *et al.* 1973; Gristina 1987). The detrimental effect of the attachment of staphylococci to different materials and plastics has been noted in many medical areas (Espersen *et al.*, 1994; Lewis and Arens, 1995). Different sterilisation techniques have been applied to such medical and polymeric materials e.g., gamma and electron radiation, commonly known as ionisation radiation (Burlinska, 1996) and chemical sterilisation with ethylene oxide (Berkopec and Vidic, 1996). However, as with ionising radiation, which is by far the most widely used industrial scale process, discoloration is a major problem with polymers and deterioration in the optical properties materials when subjected to this process (Clough *et al.*, 1996). Sterilisation of food and medical equipment with ethylene oxide possesses health risks and is potentially explosive. In 1996, Berkopec and Vidic reported ecological problems as a result of ethylene oxide sterilisation. Recently, Ward (1997) has demonstrated the efficacy of sterilisation of various bacteria on glass, plastic and stainless steel with CO<sub>2</sub> laser radiation.

With increasing use of equipment made of plastics, copolymers and stainless steel in the medical and food industry and the scarcity of information in respect to the susceptibility of micro-organisms to CO<sub>2</sub> laser (10.6µm), this section investigates the response of *Staphylococcus aureus* on various substrates; namely stainless steel (SS), polyvinyl chloride (PVC), copolymer Doeflex polypropylene (PP) and ultra high molecular weight polyethylene (PE), to CO<sub>2</sub> laser irradiation.

## 3.1.2 MATERIALS AND METHODS

### 3.1.2.1 Preparation of plastic and stainless steel discs

The culture preparation is as described in **Section 2.2.2.2**. The discs were autoclaved, and placed in a laminar flow hood to dry for an hour. It was essential to provide consistency in all experiments to provide dryness of the materials as H<sub>2</sub>O has a high peak absorbance at 10.6  $\mu\text{m}$ . Aliquots of the bacterial suspension (15  $\mu\text{l}$ ) were pipetted onto the surface of the discs prior to laser exposure, **Figure 3.1.1**. The inoculum's diameter is approximately 3 mm and for each experiment, the laser beam's diameter covers the entire surface area of the inoculum. The discs were then inserted into a sterile anodised aluminium holder with sterile forceps and aligned as required with the laser beam. The aluminium holder was wiped with alcohol after each disc was exposed to prevent any cross contamination with each successive disc. The dimension of the three plastics were 20 dia. mm X 10 mm thickness and 15 dia. mm X 5 mm for stainless steel.

### 3.1.2.3 CO<sub>2</sub> Laser

A high power Ferranti MFK CO<sub>2</sub> laser with a measured output of 1020 W (Lumonics Ltd) was used. The power was set to 'high' or 'low' and the actual power output was calibrated with the power meter (FieldMaster™, Coherent). The laser beam from the resonator was deflected by various water-cooled 45 ° angled mirrors to a focussing lens enclosure onto the work piece.

### 3.1.2.3 Exposure of the prepared discs

The laser was set low (380W) and high (980 W) power with exposures from 0 to 350 and 225 ms respectively. The collimated beam diameter was 11 mm. After exposure, each disc was placed in a 100 ml Duran bottle containing 20 ml of sterile phosphate buffered saline (PBS). A control disc received no laser irradiation. The bottles were shaken at 100 rpm for three hr at 25 °C in a Gallenkamp cooled orbital shaker. Serial ten-fold dilutions were made from each shaking solution, and 20  $\mu\text{l}$  of each dilution was plated out on the surface of a nutrient agar plate in duplicate. At higher exposure times, a 5 ml aliquot of the 20 ml sample was taken and filtered

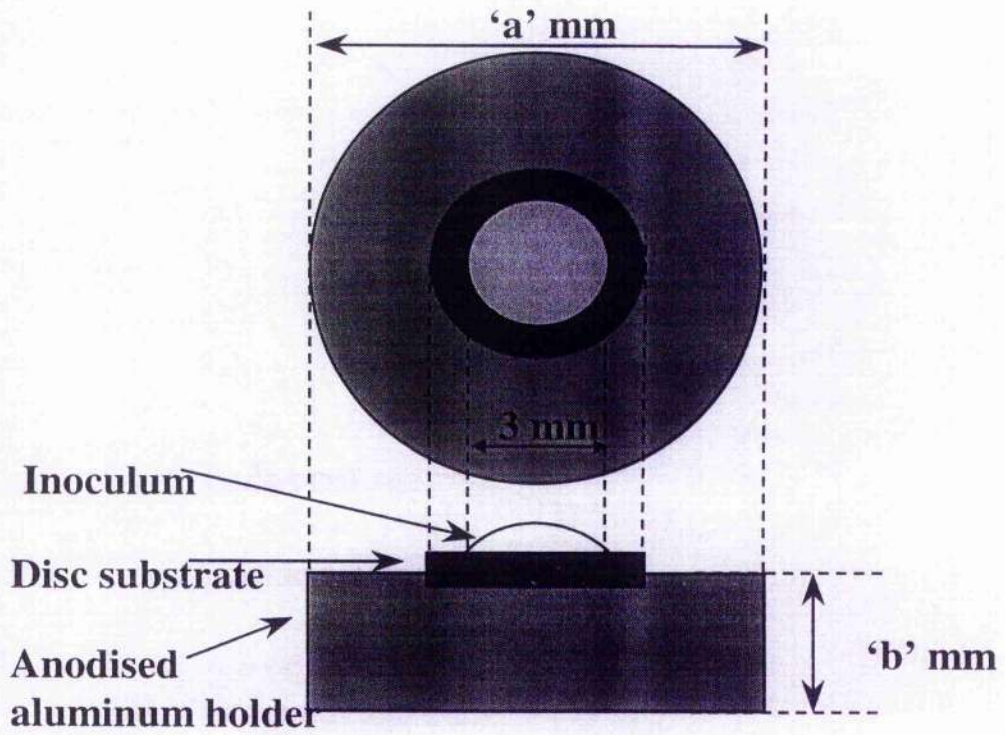


*Figure 3.1.1* Diagram showing the set-up of *S. aureus* on disc substrate with CO<sub>2</sub> laser. The aluminium holder was anodised to reduce any spectral diffusion of the intense coherent laser beam.

through a Millipore 0.45  $\mu\text{m}$  filter. The filter was placed on the nutrient agar plate surface. All plates were incubated at 37 °C for 24 hr, and the colonies were counted with a Gallenkamp colony counter, and compared for each laser treatment.

### 3.1.3 RESULTS

The CO<sub>2</sub> laser, inactivated the micro-organisms before any substantial damage was apparent on the disc of the materials with the exception of PVC where 25 ms exposure did not reduce the viability of *S. aureus*; but damaged and charred the surface. With PP, PE and SS, low power (380W) radiation achieved complete inactivation with exposure times of 175, 200 and 350 ms respectively, **Figure 3.1.2A**. At 980W, a similar killing trend with shorter exposures were observed at 100, 125 and 225 ms respectively, **Figure 3.1.3A**. With PVC, charring occurred with no reduction in microbial viability and a larger radial damage area was observed at 100 ms than at 25 ms with only 1D value reduction in cell viability. With all graphs, the error bars denote the standard error of the mean.

With 380 W, the complete inactivation range for PP, PE and SS were from 0 to 70.0, 80.0, and 140.0  $\text{Jcm}^{-2}$  respectively (**Figure 3.1.2B**). At 980 W, 103.1, 129.0 and 232.0  $\text{Jcm}^{-2}$  (**Figure 3.1.3B**) respectively. The difference in energy input of both the power settings is shown in **Table 3-1-1**.

### 3.1.4 DISCUSSION

With any form of sterilisation treatment, interaction must be made without damaging the disc substrates. CO<sub>2</sub> radiation was effective on PE, PP and SS in achieving 100 % sterilisation before substantial damage to the surface of the materials. With a 15  $\mu\text{l}$  spot of inoculum, the diameter was approximately half of the beam's diameter. In all cases, the CO<sub>2</sub> radiation power had a low penetration power which only affected the disc surfaces after prolonged exposures when the discs became charred. The charring effect of PVC, even with low power and a minimum exposure time of 25

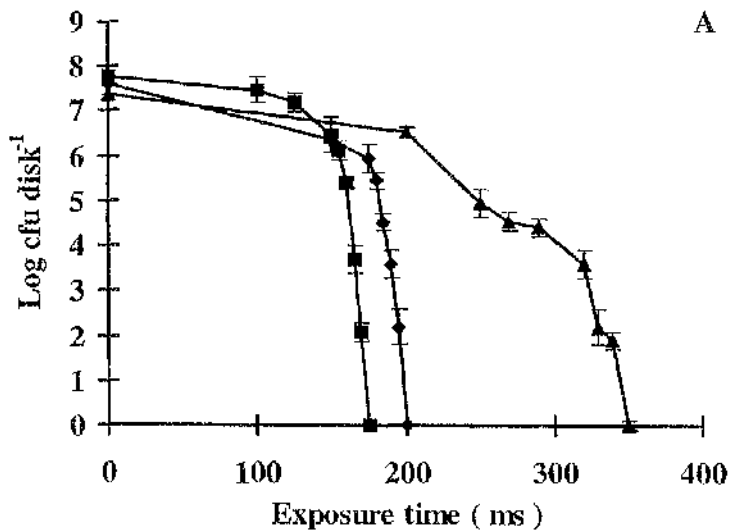
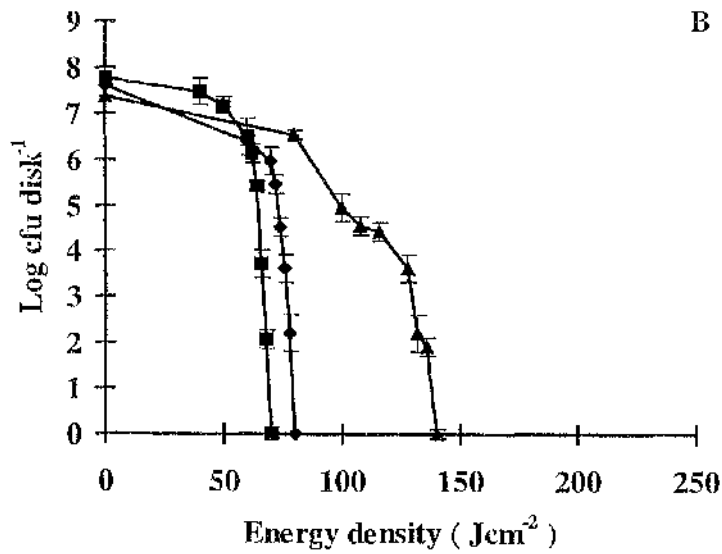


**Figure 3.1.2** Killing pattern curves of overnight cultures of *S. aureus* as wet film with 380 W CO<sub>2</sub> laser on polypropylene, PP (■), polyethylene, PE (◆) and stainless steel (▲). The figures illustrate the killing trend (logarithm to the base 10 microbial reduction) with respect to laser exposure time and energy density applied. Each point is the result of averaging 2 separate experiments

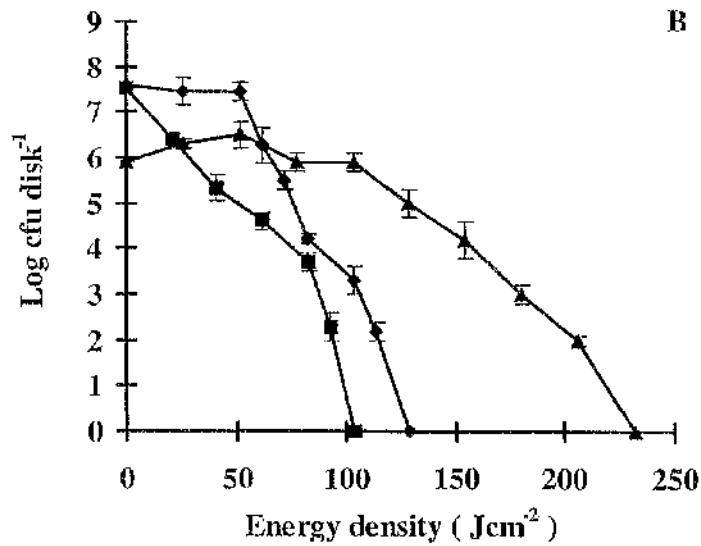
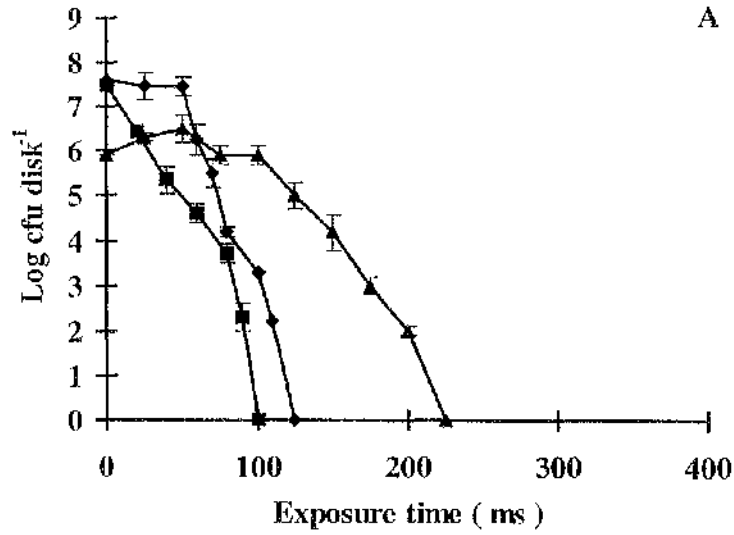


*Figure 3.1.3* Killing pattern curves of overnight cultures of *S. aureus* as wet film with 980 W CO<sub>2</sub> laser on polypropylene, PP (■), polyethylene, PE (◆) and stainless steel (▲). Figure 3A and B illustrate the killing trend with respect to the laser exposure time and energy density applied. Each point is the result of averaging two separate experiments conducted.

**Table 3-1-1 Total inactivation of  $\sim 3 \times 10^7$  cfu ml<sup>-1</sup> of *S. aureus* on polypropylene, PP, polyethylene, PE and stainless steel, SS with CO<sub>2</sub> laser energy applied at 380 and 980 W.** It can be seen that although with both power settings, total inactivation were achieved with the mentioned exposure time, the low power setting was able to deliver a much lower energy.

Substrate	Laser parameter		
	Exposure time (ms)	Power rating (W)	Energy (J)
Polypropylene, PP	175	380	66.5
Polyethylene, PE	200	380	76.0
Stainless steel, SS	350	380	133.0
Polypropylene, PP	100	980	98.0
Polyethylene, PE	125	980	122.5
Stainless steel, SS	250	980	245.0

ms was most likely due to its low thermal conductivity ( $0.14 \text{ Wm}^{-1} \text{ K}^{-1}$ ) and hence low lateral diffusion of heat. At 100 ms, there was only one D-value reduction in viability. The charring area at 100 ms was equivalent to the beam area of 11 mm,  $0.95 \text{ cm}^2$ . The low penetration and undesirable results of  $\text{CO}_2$  laser on PVC was further confirmed when after removing the inoculum, the area where the inoculum was placed was not charred. The inoculum adhered to the surface of the substrates differently, PVC had the lowest surface tension followed by PE, PP and SS, i.e. the inoculum solution sample has the lowest wetting angle on PVC substrate. This suggested that the height or thickness of the drop of inoculum sitting on the substrate, played an important part in determining the amount of radiation absorbed, scattered and transmitted within the bacteria. For all substrates, any damage or melting of the discs started from the surface.

As expected, the survival rate of the organisms decreased with increasing exposure time; a longer exposure time was required at 380 W than with 980 W laser power. However, the equivalent of more than twice the power (from 380 to 980 W) does not imply half the exposure time was needed. Stainless steel was the most resistant substrate and this was probably due to the high reflectance surface and high thermal conductivity ( $15 \text{ Wm}^{-1}\text{K}^{-1}$ ) which dissipated the laser energy very rapidly to the surrounding. As compared with PP and PE with low thermal conductivity ( $0.22$  and  $0.5 \text{ Wm}^{-1}\text{K}^{-1}$  respectively), it was concluded that the infrared radiation killing process was partly thermal by conduction. Complete inactivation were achieved with 70.0, 80.0, and  $140.0 \text{ Jcm}^{-2}$  with 380 W but with 980 W, 103.1, 129.0 and  $232.0 \text{ Jcm}^{-2}$  was needed for PP, PE ad SS respectively.

Interestingly, the energy density applied proved to be more efficient at 380 W than 980 W. The relative shorter laser beam exposure time for the same amount of laser energy applied at high power (980 W) compared to 380 W for complete microbial inactivation suggests the inherent thermal conductivity property of the substrate tested. Although, a much longer exposure time was needed (with constant pulse energy delivered), complete microbial killing was achieved at the lower power setting of 380 W.

The CO<sub>2</sub> laser was more efficient in the inactivation of microbes than the Nd: YAG laser operating at 1064 nm. In 1996, Ward reported similar inactivation system on stainless steel with the Nd:YAG laser. The energy density was 800 and 900 Jcm<sup>-2</sup> for wet and dry inoculum. As with the CO<sub>2</sub> laser, his work was in good agreement as he achieved complete inactivation at 150 Jcm<sup>-2</sup> with dry films whilst in this report, 140 Jcm<sup>-2</sup> were applied to do likewise but with a wet film. This implies that more energy density would be needed for dry than wet films, as far as using laser radiation at these wavelengths is concerned. Thus the amount of laser power utilised in bacterial killing depends on the amount of water present in the sample.

## 3.2 LINEAR SCANNING STERILISATION SYSTEM WITH HIGH POWER CO<sub>2</sub> LASER

### 3.2.1 INTRODUCTION

Because of the high absorption coefficient of water at 10.6  $\mu\text{m}$  and because it is primarily the main constituent of biological cells, the effect at this wavelength is, partly thermal. The basic nature of coherence, the well-controlled beam spot size and the high absorbent peak of water proved to be favourable in demonstrating the biocidal effect on various microorganisms. In **Section 3.1**, results showed rapid sterilisation of using CO<sub>2</sub> laser irradiation on various materials seeded with *S. aureus*. Implicitly, the efficiency of the CO<sub>2</sub> system could be developed into a two-dimensional automated scanning model to inactivate microbes.

As such, initial experiments were done to investigate the effect of translational velocity of two high power CO<sub>2</sub> scanning laser systems, operating at 10.6  $\mu\text{m}$ , on the survival response of *S. aureus* and *E. coli*, seeded on nutrient agar, collagen and stainless steel strips with the aim to optimise and compare the rate of inactivation. Such systems, if feasible, could have applications in industrial sterilisation processes.

### 3.2.2 MATERIALS AND METHOD

#### 3.2.2.1 *S. aureus* on collagen films

The culture preparation is as described in **Section 2.2.2.1**. Nutrient agar plates, which contained iodo-nitro-tetrazolium violet (INT), were required with experiments on collagen film. The INT, dissolved in sterile distilled water, was added to sterile molten agar to a concentration of 0.05 % w/v before pouring into petri-dishes. Squares (~50 x 50 mm) of ethylene oxide sterilized collagen film were reconstituted in sterile distilled water, placed in a petri-dish and dried for 20 min in a laminar air

flow (LAF) cabinet. *S. aureus* suspensions (1.5 ml) were inoculated onto the skins and spread evenly over the surface. The surface of the collagen film was dried again for a further 20 min in the LAF cabinet after which the collagen was placed aseptically onto the agar plate. The procedures for bacterial samples on nutrient agar plates are described in **Section 2.2.2.1**.

### **3.2.2.2 *S. aureus* and *E. coli* on stainless steel strips**

The dimension of the stainless steel strips were 4 x 1 x 0.15 cm. Over-night broth cultures of *E. coli* and *S. aureus* were centrifuged at 4000 rpm and the pellet was resuspended in sterile distilled H<sub>2</sub>O. Bovine serum albumin, BSA, 20 µl solution (0.1% w/v) followed by 15 µl of the suspension were spread onto the central area of the strips which was dried for an hour prior to the experiment, **Figure 3.2.1**.

### **3.2.2.3 CO<sub>2</sub> Laser**

A high power Ferranti MFK CO<sub>2</sub> laser (Lumonics Ltd) was operated at 660 W with stainless steel strips and at 1020 W on nutrient agar and collagen substrate. The unfocused collimated beam produced a diameter of 11 mm and an area of 0.95 cm<sup>2</sup>. The laser system was linked and controlled via a CNC x-y axis arm which translates along the longitudinal length of the stainless steel strip. With the agar plates and collagen skins, alignment was performed to ensure consistent laser beam exposure on the contaminated surfaces with the CO<sub>2</sub> laser, **Figure 3.2.2**.

A total of 6 linear laser scan exposures was performed per plate. Each set of parameters was applied in duplicate and each experiment repeated twice. The linear scan set-up was comprised of a motor controller, a direct current (DC) motor attached to a mounted rotating gold-plated mirror. The motor controller provided rotation of the gold-plated mirror which scanned the incident horizontal laser beam path onto and across the agar plate, **Figure 3.2.2**. The beam diameter,  $D$ , and the frequency of the rotating mirror,  $\omega$ , were set to 10 mm and 0.88 Hz respectively. The width of clearance,  $W_c$  (mm), on the agar plates and collagen films after incubation denotes the inactivation effect. The translational velocity,  $V_t$  (cm s<sup>-1</sup>), is a function of the distance,  $S_r$  (cm) set between the rotating mirror axis and the agar plate or collagen skin given by,

$$V_t = 2 \cdot \pi \cdot S_r \cdot 0.88 \quad (3.2.1)$$

The different values of distance,  $S_r$ , were obtained by shifting the movable base stand vertically to where the target sample was positioned. The effective area inactivated per unit time or the rate of inactivation,  $I_r$  ( $\text{cm}^2\text{s}^{-1}$ ) of the microorganisms was defined as,

$$I_r = W_c \cdot V_t \quad (3.2.2)$$

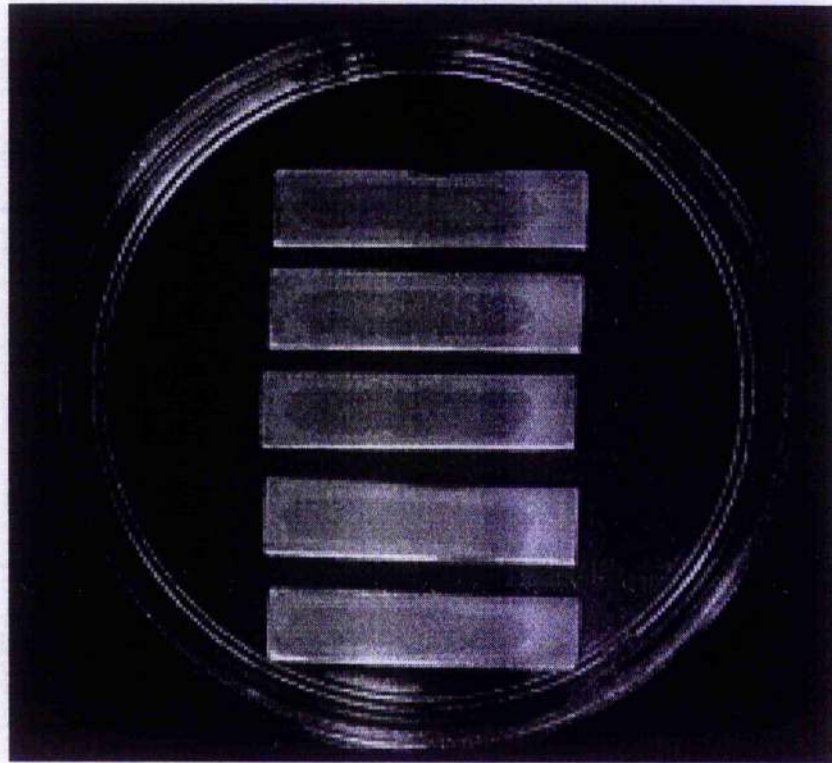
The energy density,  $ED_v$  defined over one beam width, is given as,

$$ED_v = \frac{4 P_o}{\pi V_t D} \quad (3.2.3)$$

where  $P_o$  and  $D$  are the power output and beam diameter of the laser light respectively.

The exposed and unexposed (control) plates were incubated at  $37^\circ\text{C}$  for 24 h and observed under a Profile Projector (PJ-300, Mitutoyo). The diameters of the cleared width with no bacterial growth were measured for each  $S_r$  on nutrient agar and collagen film. The  $W_c$ , %  $W_c$  and  $I_r$  of bacterial inactivation were calculated and these values were plotted as a function of the  $V_t$  and  $ED_v$  respectively.

With another set-up, **Figure 3.2.3**, the contaminated stainless steel strips were aligned so that the laser beam diameter covered the width of the inoculum on the stainless steel strip completely. Different scanning speeds were set to a maximum of  $10 \text{ cm s}^{-1}$ . The laser head enclosure was positioned at least 50 cm away from the sample to ensure constant velocity along the stainless steel strips.



1.1 cm

**Figure 3.2.1** A set of five contaminated unexposed stainless steel strips. The top three and bottom two stainless steel strips are each inoculated with  $1.23 \times 10^7$  and  $1.35 \times 10^6$  cfu of *S. aureus* and *E. coli* respectively.

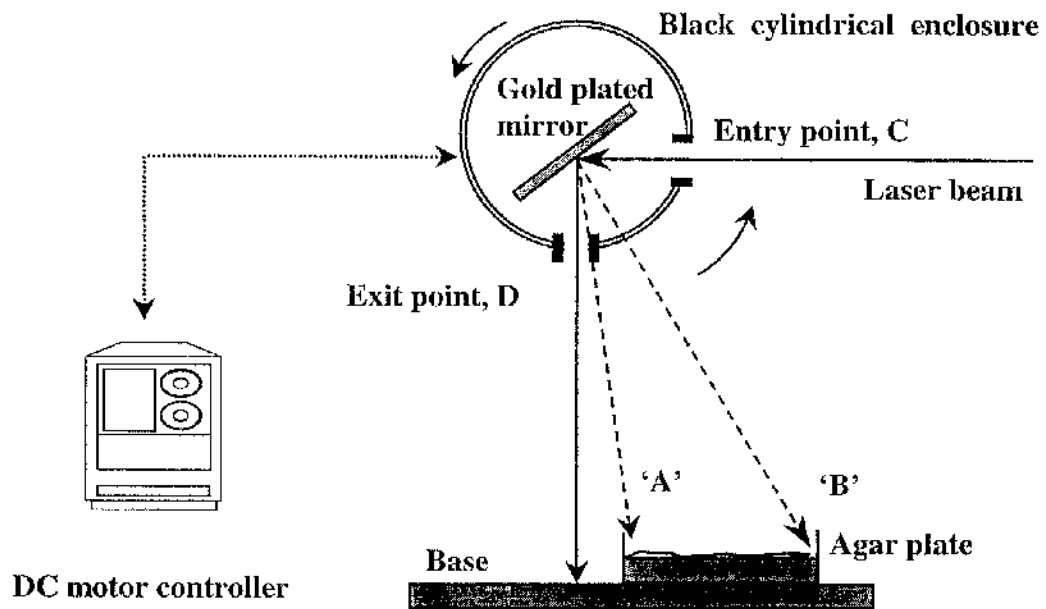


**Figure 3.2.2 Scanning system of contaminated nutrient agar plates and collagen skins.** The laser beam enters via entry point, 'C' and out through 'D' as the enclosure rotated clockwise. At other times, the beam is being hit and absorbed by the matt black cylindrical enclosure. The 90 ° angle between the two points, 'C' and 'D' sweeps a linear distance greater than the agar plate's diameter on the base stand.

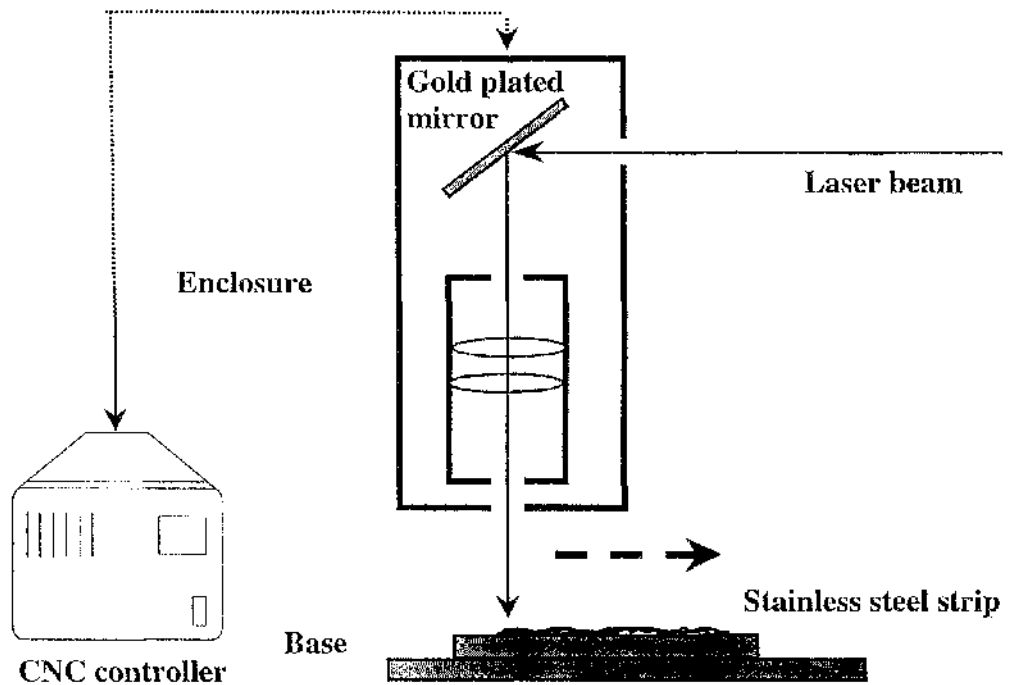


**Figure 3.2.3** Scanning system of *E. coli* and *S. aureus* on stainless steel strips.

The laser beam enters via the enclosure head and passes through a set of focussing lenses before hitting on the stainless steel strips. The laser spot size had an effective area of  $0.95 \text{ cm}^2$ . The enclosure head was translated from left to right to create a linear scanning motion, which inactivated the microbes on the stainless steel strip. The scanning speed is controlled by the CNC controller which was synchronised with the firing of the laser light onto the stainless steel strips.

#### **3.2.2.4 Bacterial viability assessment of dry and wet contaminated stainless steel strip**

Both the wet and dry samples were treated as described in section **Section 3.1.2.3** to assess the bacterial viability. Controls were investigated as described in **Section 2.2.2.5**.

### **3.2.3 RESULTS**

#### **3.2.3.1 Nutrient agar and collagen film**

Different values of  $W_c$  were achieved at different  $S_r$  settings, the standard error of the mean,  $\sigma$ , is shown, **Table 3-2-1**. The SEMs are the result of 2 separate experiments each being the average of three widths obtained from the start, centre and end of the exposed strips of the samples.  $W_c$  and the percentage width of clearance (with respect to the laser beam diameter, 11 mm), %  $W_c$ , decreased with increasing  $S_r$  and  $V_t$ , **Figure 3.2.4** and **3.2.5**. No inactivation or clearance was seen on agar plate and collagen film at height,  $S_r$  of 70 and 80 cm respectively. The same trend was observed with the translational velocities; i.e. the faster the scanning speed, the smaller the inactivation area of width of clearance on the substrate. Full growth was observed at 387.0 for nutrient agar and 442.3  $\text{cm}^2\text{s}^{-1}$  for collagen film plates. However, the converse was true for energy densities which increased with increasing  $W_c$ , **Figure 3.2.6** and %  $W_c$ , **Figure 3.2.7**. Interestingly, the  $I_r$  has a peak value of 151.5  $\text{cm}^2\text{s}^{-1}$  for collagen film at  $V_t$  of 221.2  $\text{cm}^2\text{s}^{-1}$ , **Figure 3.2.8**. **Figure 3.2.9** showed the response with energy densities applied. No growth was observed on the cleared or inactivated zones on both the nutrient agar and collagen films after a few days. However, with scanning velocities at threshold killing levels of the height setting, unequal widths of clearance were observed; the width decreased from the start to the far end of the agar plates, **Table 3-2-2**.

#### **3.2.3.2 Stainless steel strip**

On stainless steel strips, both bacterial species were able to exist in a dry state (with reduced extraneous water) after 1 hr in the laminar air flow cabinet. However, the

drying effect caused some cell viability reduction as shown in **Table 3.2.3**. With this knowledge, additional experiments were conducted to assess the different types of medium suspension namely, bacteria resuspended in sterile distilled water, in overnight culture broth and in saline. The initial bioburden count before exposure was different with both bacterial species. With *S. aureus*, the drying effect reduces 0.75 D-value of the cell viability for all three types of liquid medium; implying high tolerance to salt content. *E. coli* was seen to reduce 3-D values with culture broth and distilled water and 4 D-value with saline.

Total reduction in bacterial viability was observed for both *S. aureus* and *E. coli* seeded on stainless steel strips at 0.83 and 1.33  $\text{cms}^{-1}$  respectively, **Figure 3.2.10**. However, since the initial colony-forming units of both microorganisms were different by approximately 3 log D-values, **Figure 3.2.11** was tabulated using  $N/N_0$  (the ratio of cell population after treatment over the initial concentration without laser exposure) to verify the relative resistance of both species to irradiation; *S. aureus* was more resistant than *E. coli*. The rate of the laser beam scanning at which complete sterilisation occurred was better with *E. coli* (1.3  $\text{cms}^{-1}$ ) than *S. aureus* (0.9  $\text{cms}^{-1}$ ), **Figure 3.2.12**. Complete inactivation was achieved with energy densities 654.8 and 916.7  $\text{Jcm}^{-2}$  respectively, **Figure 3.2.13**. Full inactivation of both species was achieved without damaging the substrate. Slight charring was observed with *S. aureus* and *E. coli* at 1.2 and 1.5  $\text{cms}^{-1}$  respectively and at full inactivation. The error bars were the standard error of mean which reflect the result of two separate experiments each being the average of 3 widths obtained from start, centre and end of the plates' diameters of the scanning processes.

## 3.2.4 DISCUSSION

### 3.2.4.1 Nutrient agar and collagen film

Areas of unexposed sections and exposed sections without inactivation were observed. The normal growth of *S. aureus* showed colonies with golden yellowish pigment on the nutrient agar. As with the collagen films, the area of inactivation was more difficult to quantify. With the INT incorporated into the nutrient agar, the

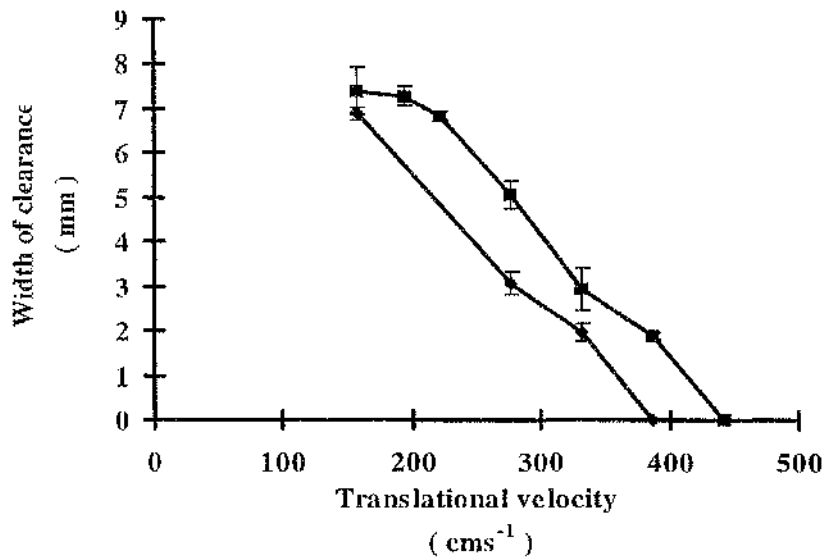


**Figure 3.2.4** Killing pattern of width clearance versus scanning speed with *S. aureus* on sausage skin, (■) and nutrient agar, (◆). The error bars are the standard error or means which reflect the result of two separate experiments each being the average of three widths obtained from start, centre and end of the plates' diameters.

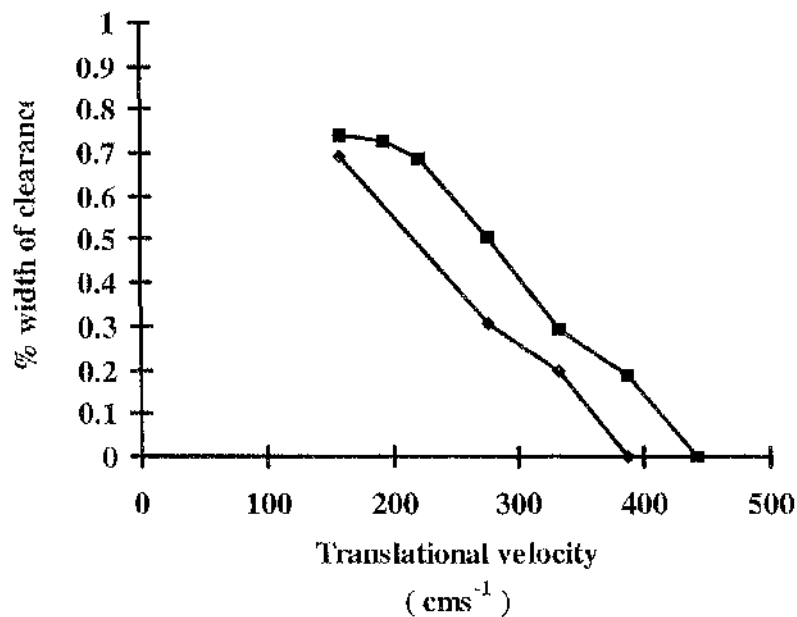


**Figure 3.2.5** Killing pattern of percentage width clearance versus scanning speed with *S. aureus* on sausage skin, (■) and nutrient agar, (◆). Each point is a separate exposure. The results were the average of two separate experiments.

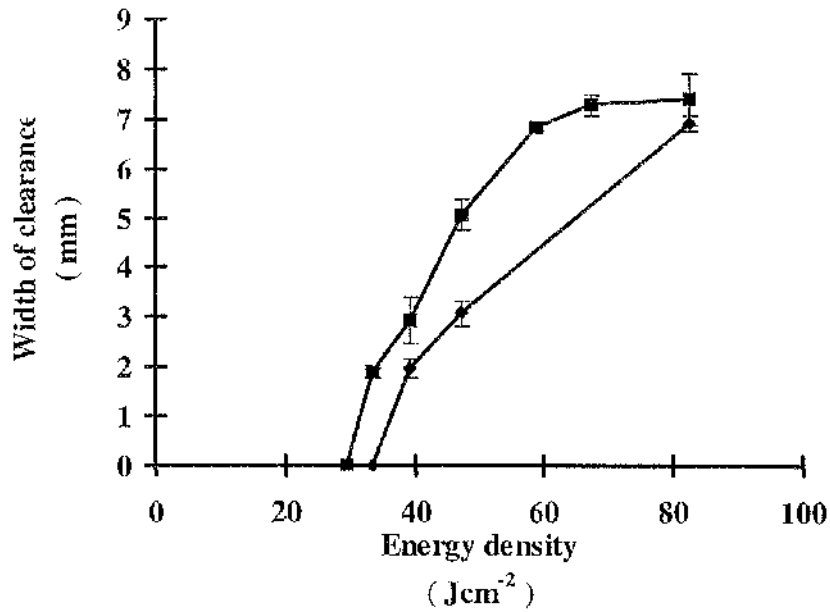


**Figure 3.2.6** Killing pattern of width clearance versus energy density applied with *S. aureus* on sausage skin, (■) and nutrient agar, (◆). Each point is a separate exposure. The results are the average of two separate experiments.

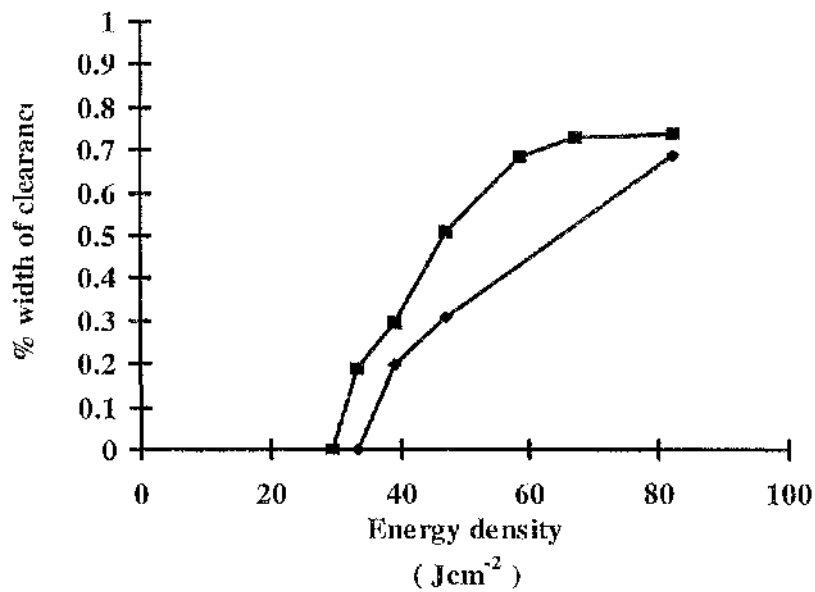


**Figure 3.2.7** Killing pattern of percentage width clearance versus energy density applied with *S. aureus* on sausage skin, (■) and nutrient agar, (◆). Each point is a separate treated exposure.

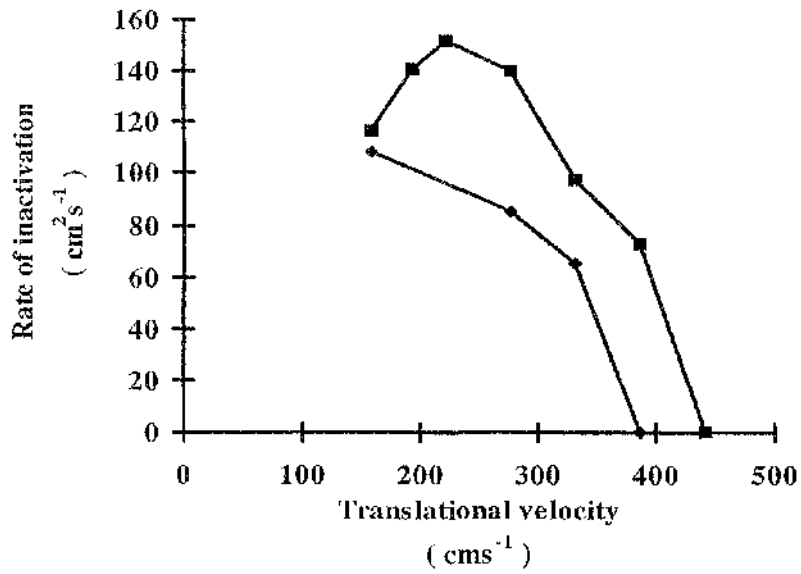


Figure 3.2.8 Killing pattern of rate of inactivation against scanning speed with *S. aureus* on sausage skin, (■) and nutrient agar, (◆).

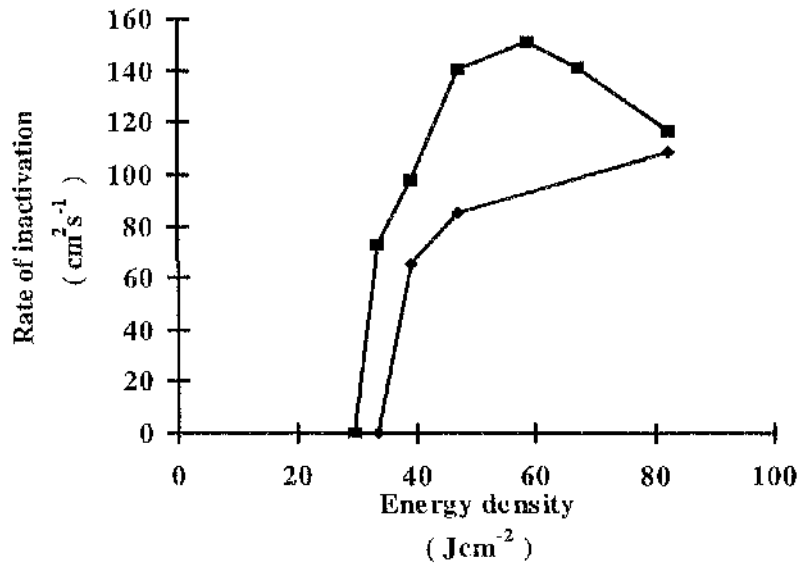


Figure 3.2.9 Killing pattern of rate of inactivation against energy density applied with *S. aureus* on sausage skin, (■) and nutrient agar, (◆).

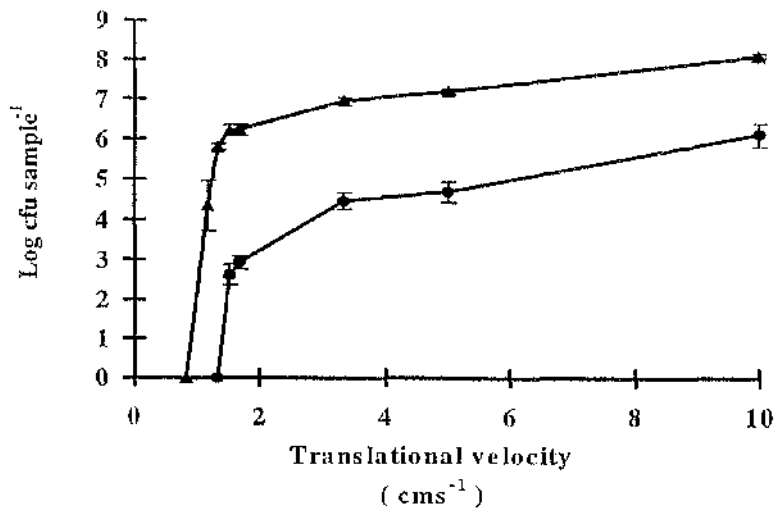


Figure 3.2.10 Killing curve of *E. coli*, (●) and *S. aureus*, (▲) seeded on stainless steel strip with different CO<sub>2</sub> laser beam translational velocities. Each point is a separate exposure. The results are the average of three separate experiments

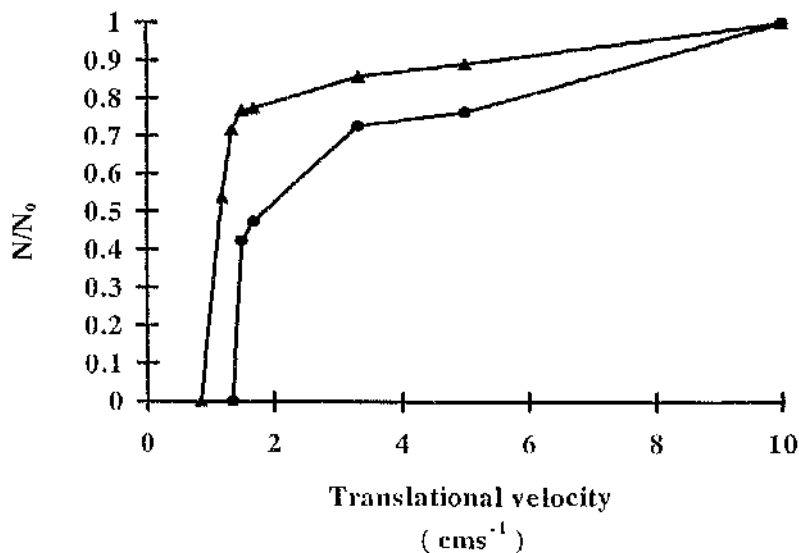


Figure 3.2.11 Response curve of *E. coli*, (●) and *S. aureus*, (▲) seeded on stainless steel strip with different CO<sub>2</sub> laser beam translational velocities. With N/N<sub>0</sub>, the graph shows that *E. coli* is less resistant than *S. aureus* to CO<sub>2</sub> laser light on stainless steel strips.

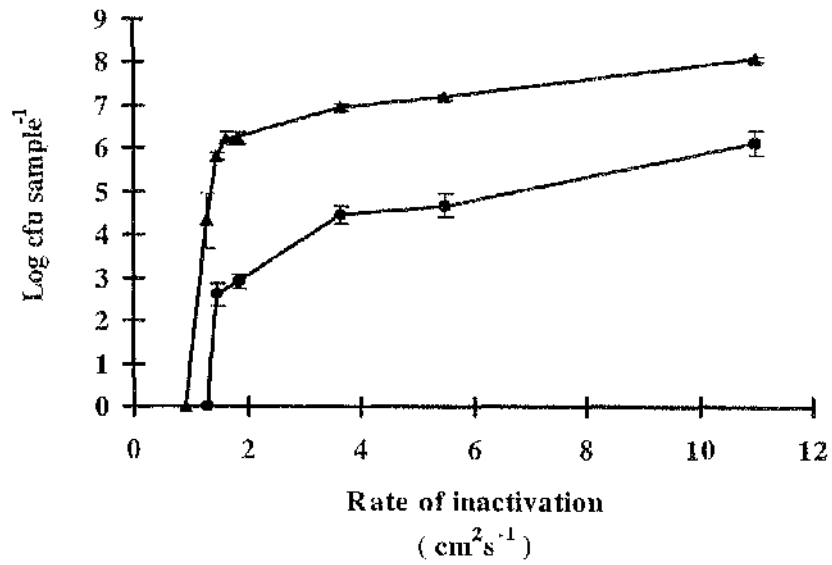


Figure 3.2.12 Response curve of *E. coli*, (●) and *S. aureus*, (▲) seeded on stainless steel strip with rate of inactivation to CO<sub>2</sub> laser irradiation. Each point is a separate exposure. The results are the average of three separate experiments

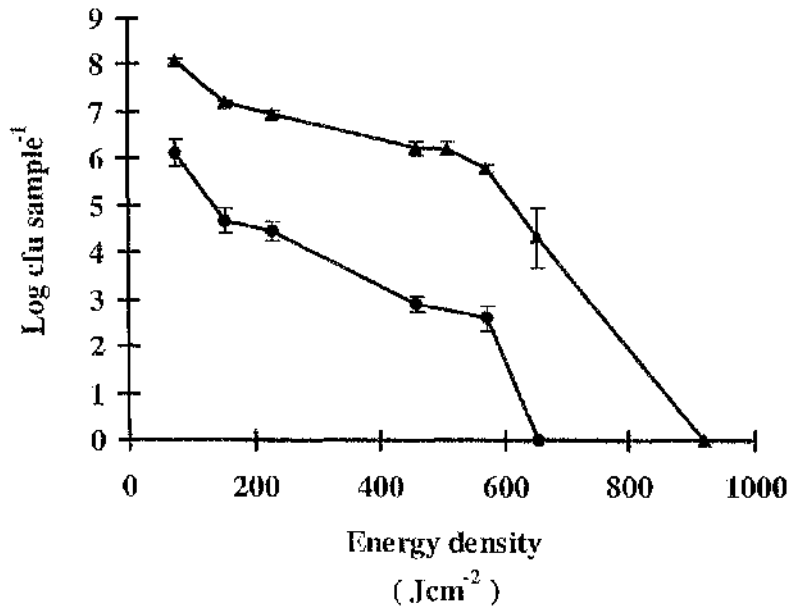


Figure 3.2.13 Killing curve of *E. coli*, (●) and *S. aureus*, (▲) seeded on stainless steel strip with applied CO<sub>2</sub> laser energy density.

**Table 3-2-1** Width of clearance of *S. aureus* lawn on nutrient agar plates. The width of clearance for each  $S_r$  is the average of 3 readings taken at both ends across the diameters of the petri-dishes and the center. On each point, the  $\sigma$  was the calculated result of two separate experiments each being the average of three widths obtained from start, centre and end of the plates' diameters.

$S_r$ (cm)	Width of clearance of <i>S. aureus</i> lawn (mm)			
	Nutrient		Collagen	
	agar plate	$\sigma$	Film	$\sigma$
28.5	6.9	0.15	7.4	0.5
35	NA	NA	7.3	0.2
40	NA	NA	6.9	0.1
50	3.073	0.26	5.1	0.3
60	1.967	0.20	2.9	0.5
70	0	0	1.9	0.1
80	NA	NA	0	0

**Table 3-2-2** Threshold killing level of clearance of *S. aureus* lawn. Widths of clearance were only observed at the start and centre of the plates' diameters. Sub-lethal and irregular width patterns were observed at the end on nutrient agar and collagen films agar plates. The threshold velocity and energy density for both samples were shown below.

<i>S. aureus</i> sample	Parameter		
	$S_r$ (cm)	Velocity ( $\text{cm s}^{-1}$ )	Energy density ( $\text{J cm}^{-2}$ )
Nutrient agar	65	359.4	36.1
Collagen film	75	414.7	31.3

**Table 3-2-3 Bacterial viability reduction of approximately  $4 \times 10^9$  cfu ml<sup>-1</sup> initial bioburden of dried *S. aureus* and *E. coli* inoculum on stainless steel strips with different suspending liquid medium.** Wet sample resuspended in sterile distilled water was used as a standard comparison.

Bacterial viability reduction (D-values) of dried sample with different suspending medium			
Micro-organism	Sterile distilled H <sub>2</sub> O	Culture broth	Saline
<i>S. aureus</i>	0.75	0.75	0.75
<i>E. coli</i>	3	3	4

microorganisms absorbed the dye which implied normal growth had occurred. Inactivation was seen as pale white strips on the collagen film against the red normal growth, on either side of the cleared zones.

From the results, *S. aureus* was less resistant on collagen film than on the agar plate. The effects were significant as shown with error bars plotted. All subsequent graphs shown (y-axis) are derivatives of the width of clearance,  $W_c$ .

The parabolic graph, of the rate of inactivation versus energy density and translational velocity on collagen film can be accounted for from the width of clearance and energy density decreasing non-linearly with increasing translational scanning speed, i.e. the  $W_c$  was inversely proportional to  $V_t$ . With the  $I_r$  being the product of  $W_c$  and  $V_t$ , the rate of inactivation is seen at its optimum value of  $151.5\text{cm}^2\text{s}^{-1}$  at a translational velocity of  $221.2\text{mms}^{-1}$ . Since  $V_t$  was not sufficiently low on nutrient agar, this phenomenon was not observed.  $I_r$  is therefore a good indication of the amount of inactivation with respect to laser scanning speed to obtain optimum sterilisation conditions.

At the threshold killing level, sub-lethal killing was demonstrated by the widths of the inactivation zone decreasing with increasing distance from the reflecting mirror, for example, widths were recorded at position 'A' (start of scan) but not at the end of the laser scan on the plates (position 'B'). This phenomenon reflects the variation in power delivered to the microorganisms. The microorganisms received less irradiation in position 'B' than 'A' by a fraction of the cosine of the angle subtended with respect to the mirror. Therefore the microorganisms received less energy density in position 'B' than 'A'. Nevertheless, the compromise of having such a system yields a much faster scanning velocity without moving the work sample. Such a scanning system is deemed suitable for laser sterilisation without damaging the nutrient agar and collagen films within the energy densities used.

#### **3.2.4.2 Stainless steel strip**

The assessment of dried microorganisms in different suspension liquids on stainless steel strips subjected to laser treatment will have significant industrial and medical

implications since different levels of moisture can exist in contaminated samples. The results suggest that the level of viability of *S. aureus* in the dry state was higher than *E. coli* due to its high tolerance to the drying effect. As shown in **Table 3-2-3**, there was a relatively big difference in survival of organisms when dried on stainless steel strip in different suspending medium. However, the cells were deliberately resuspended in sterile distilled water to enable a maximum amount of contaminant to be seeded on the stainless steel strips subjected to irradiation. Such high levels of contamination mimics a pessimistic but possibly practical situation where the level of hygiene might be extremely low.

The inoculum dried uniformly implying that the microorganisms had good adherence properties and surface tension with the substrate. The BSA was introduced to enhance adherence so that more control of the spreading of the inoculum over an equal area on the stainless steel strips was achieved. In so doing, the dried inoculum area is exposed to the laser beam more consistently. Although charring was observed after laser exposure which was due to the BSA, sterilisation was effective with CO<sub>2</sub> laser irradiation. Work has also been done which showed similar inactivation without BSA (data not shown). It can be concluded that BSA enhanced the feasibility and not the actual inactivation process of the experiment.

Such a scanning system has the advantage of providing constant energy density and beam intensity. Total bacterial destruction was achieved at 0.8 and 1.3 cms<sup>-1</sup> with *S. aureus* and *E. coli* respectively. The rate of microbial destruction was nevertheless much smaller than that with nutrient agar or collagen skins as the amount of liquid in these experiments were much smaller in volume, if not completely dry.

The extinction coefficient, which is a function of the absorption coefficient provides the plausible explanation as to the big differences in translational velocities to achieve microbial destruction. Firstly, both the nutrient agar and collagen skin (semi-dry) have reasonably high water content in contrast to dried inoculum on stainless steel strips. Secondly, the inactivation effect is believed to be thermal since water has a relatively high extinction coefficient at 10.6 μm wavelength which absorb the radiation and inactivates the microorganisms. Last but not least, the

substrate in which the inoculum was seeded plays an important role in assisting the inactivation via optical properties such as spectral diffusion, reflection, penetration and heat conducted upwards and sideways to the cells. With stainless steel, heat is conducted and diffused more rapidly than on agar plates. Thus a lower translational velocity with higher energy density was needed than on agar surfaces. Nevertheless, microbial inactivation was achieved efficaciously without damaging the substrate with such a scanning system. Thus, it is believed that the bactericidal effect of CO<sub>2</sub> laser irradiation on selective micro-organisms was due to the bacterial cell size, wall thickness and/or the water content leading to a difference in energy absorption of the cells Ward, 1997).

### **3.3 LINEAR SCANNING STERILISATION SYSTEM WITH LOW POWER CO<sub>2</sub> LASER**

#### **3.3.1 INTRODUCTION**

As described previously, inactivation of microorganisms at 10.6  $\mu\text{m}$  was achieved with different scanning systems. The rate at which inactivation occurred and the systems' efficacy as well as its non-invasive characteristic makes it very promising procedure.

A similar approach, but with a different set-up was used to investigate the possibility of sterilising *E. coli* and *S. aureus* on nutrient agar and stainless steel strips. The aim was to use a much smaller, relatively much lower cost and low-power CO<sub>2</sub> laser system, operating at the same wavelength, to investigate the feasibility of scaling down the high-power CO<sub>2</sub> system and if successful, to optimise the rate of inactivation and optimum laser parameters of sterilisation. The complete physical size of the 15 W pulsed CO<sub>2</sub> laser with its electronic systems is at least 5-fold smaller and lighter. Such a system will enable sterilisation processes with a relatively smaller cost to size and space ratio.

#### **3.3.2 MATERIALS AND METHODS**

##### **3.3.2.1 CO<sub>2</sub> Laser**

The laser (Synrad, Inc., 48-1 'F' version) operates at 10.6  $\mu\text{m}$  wavelength with a maximum output power of 13.4 W (after calibration); the laser has dimension of width, height and length of 2.8, 3.89 and 17 inch respectively. It consists of a radio frequency (RF) excited plasma tube with an adjustable mirror on each end, mounted together with the RF drive assembly in a single aluminium chassis that is water-cooled. The optical resonator consists of a reflector (three metres radius of curvature) and a flat zinc selenium (ZnSe) output coupler with reflectivities of 95 and 92 % respectively. The laser beam is generated horizontally via the resonator and reflected onto the work samples via a highly reflective gold-plated mirror. The

laser beam has an effective diameter of 3.5 mm measured by a burn-print on photographic paper. The largest distance between the laser output and the work sample is approximately 90 cm. The beam has a near Gaussian beam profile in the far field with 4 milliradians (mrad) divergent angle due to diffraction at the output aperture.

### *System design*

Controlling software was written using Delphi IV compiler (computer software) to provide the required energy exposures and translational scans by synchronising the movement of the mirror with the firing of the laser beam exposure time and length of contact of the work samples.

### *Experimental set-up*

The experimental set-up is shown in **Figure 3.3.1**. The laser output beam was reflected off a gold-plated mirror and, because the power output was not relatively large, the mirror was only air-cooled and targeted on the biological sample on the turntable base. The turntable base was anodised to prevent any scattering of stray reflections. The mirror was attached to a stepper motor and interfaced along with the laser resonator to the computer via a microprocessor. As such, the angular movement of the mirror was well-controlled and synchronised with the power output of the laser unit to provide linear translational scans of various velocities on the turntable base.

### *Laser output beam area and energy density*

The beam diameter and the area of the laser beam were measured from the burn print produced on photographic paper. These were found to be at 3.5 mm and 0.096 cm<sup>2</sup> respectively. The energy density, is given by,

$$\begin{aligned}
 ED_1 &= \frac{4 P_a}{\pi D^2} \cdot \frac{D}{V_t} \\
 &= K_1 \frac{P_a}{V_t}
 \end{aligned}
 \tag{3.3.1}$$

where  $K_1$  is a constant =  $4 \pi^{-1} D^{-1}$ .

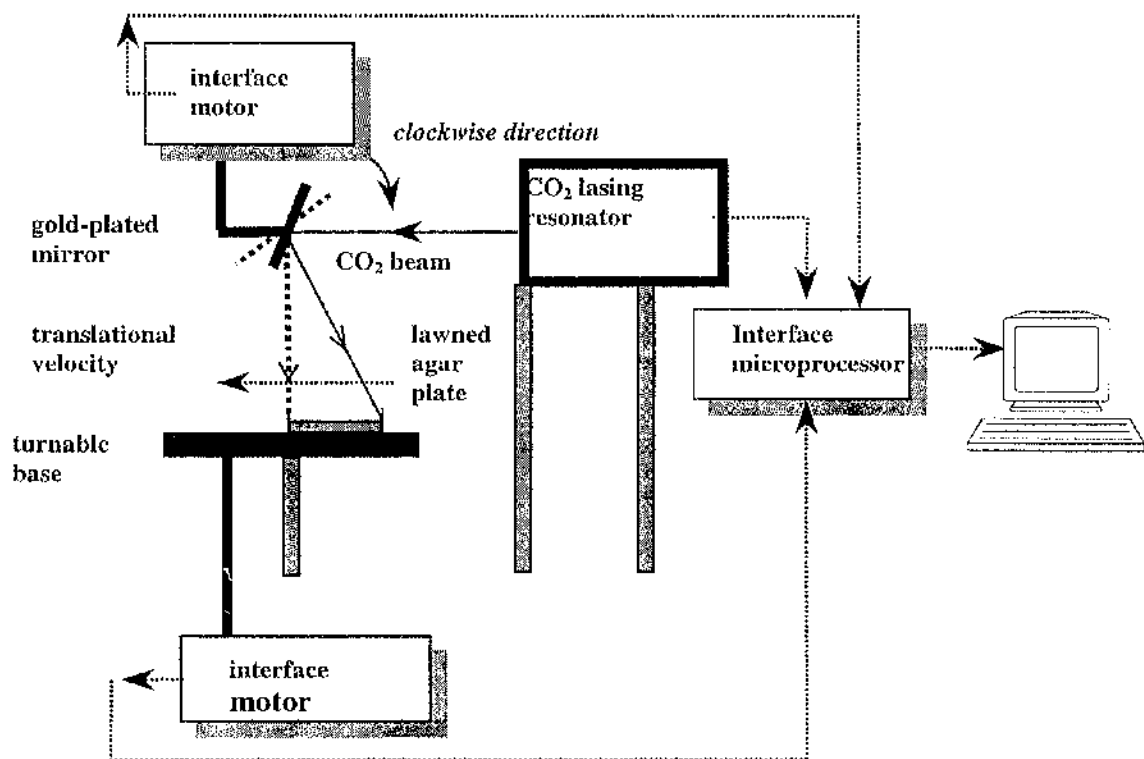


**Figure 3.3.1** Experimental set-up of low power, 15 W CO<sub>2</sub> laser scanning system. The laser beam output was synchronised with the angular speed of rotation of the gold-plated mirror to provide linear scans across the lawned nutrient agar plates on the turnable base at various translational velocity,  $V_t$  and power,  $P_o$ .

### ***Laser parameters***

Translational velocities,  $V_t$  of the laser beam of 100, 80, 60 and 40  $\text{mins}^{-1}$  were used with laser output power of incremented from 2 to 13 W. The clearance widths of bacterial inactivation,  $W_c$  (mm), were calculated and these values were plotted as a function of the laser power, energy density and  $IA_{50}$  values were also determined for different parameters for both microorganisms. The rate of inactivation,  $I_r$ , was also plotted with various speed and laser output powers to investigate the efficacy of inactivating both organisms.

#### **3.3.2.2 *S. aureus* and *E. coli* on nutrient agar plates**

The lawned plates were placed on the turntable base. Since the diameters of the agar plates were 90 mm, the plates were placed to allow the laser beam to completely scan across them. The culture samples were prepared as described in **Section 2.2.2.1** and **2.2.2.2**. The diameters of the cleared width with no bacterial growth were measured for each set, averaging over three measurements made randomly at a different place on the path of laser scan, of the parameters mentioned.

#### **3.3.2.3 *S. aureus* and *E. coli* on stainless steel strips**

The dimension of the stainless steel strips were 4 x 1 x 0.15 cm with a centred rectangular groove of 1.5 mm width and 0.5 mm depth in the centre where the microorganisms were inoculated. The preparation procedures were as described in **Section 3.3.2**. The microorganisms were completely exposed to the laser beam as it had an effective diameter of 3.5 mm. Overnight broth cultures of both microorganisms were centrifuged at 4000 rpm and the pellet was resuspended in sterile distilled water. A volume of 15  $\mu\text{l}$  of the suspension (approximately  $5 \times 10^8$  cfu  $\text{ml}^{-1}$ ) was spread evenly onto the groove with about 5 mm gap at each end of the strip.

In another set of experiments, the stainless steel strip surfaces were sand-blasted to obtain fine matt finish to investigate the sensitivity of the biocidal effect on different surface finish and compare with untreated ones. The abrasive material used was super saftigrain 'F' (Guyson) at 100 p.s.i, **Figure 3.3.2**. After laser treatments the stainless steel strips were analysed as described in **Section 3.2.2.6**.

### 3.3.3 RESULTS

#### 3.3.3.1 Laser exposed nutrient agar plates

Generally, both organisms showed similar responses and inactivation pattern curves after exposure to CO<sub>2</sub> laser light. *S. aureus* was more resistant than *E. coli* lawned on nutrient agar plates. Overnight incubation of the lawned plates showed the distinct contrast of lethal, sub-lethal and normal growth sections. Lethal sections, **Figure 3.3.3** were marked by applying lethal dosage of laser power across the lawned plates while normal growth sections were either subjected to too low an energy density or control areas without the laser scan treatment.

Lethal inactivation of *S. aureus* were observed in all cases except for sub-lethal inactivation at 4 W/40 mms<sup>-1</sup>, **Figure 3.3.4**. No killing or normal growth scans were observed at 2, 3, 4 and 5 W with 100 mms<sup>-1</sup>, 2, 3, 4 W with 60 and 80 mms<sup>-1</sup> and 2 and 3 W with 40 mms<sup>-1</sup>. The width of inactivation or clearance, W<sub>c</sub>, at various power levels are shown in **Figure 3.3.5**. The error bars were the standard errors of the mean which reflects the average of two separate experiments each being the mean of three widths obtained at both ends and centre of the lawned plates after laser treatments. With *E. coli*, similar killing trends were observed with various translational velocities at different power applied. No inactivation was observed at 2 W with sub-lethal effects at 3 W 40 mms<sup>-1</sup>.

In **Figure 3.3.6**, the areas of inactivation of both organisms were plotted against the power applied with IA<sub>50</sub> value (0.048 cm<sup>2</sup>) shown. The area of inactivation was achieved above 0.048 cm<sup>2</sup> for all translational velocities set, namely 40, 60, 80 and 100 mms<sup>-1</sup> for *E. coli* whereas only at lower velocities, namely, 40 and 60 mms<sup>-1</sup>, for *S. aureus*.

The energy density applied is a function of power output but inversely proportional to the translational velocities. The biggest energy density applied was 11.82 Jcm<sup>-2</sup> at 13 W, 40 mms<sup>-1</sup>; with the width of clearance at 2.93 mm for *S. aureus* and 2.97 mm for *E. coli*. Sub-lethal energy densities were only observed at 40 mms<sup>-1</sup>; 2.73 and 3.64 Jcm<sup>-2</sup> on *E. coli* and *S. aureus*, **Figure 3.3.7**.

The relationship between the rate of inactivation,  $I_r$ , and energy densities applied is shown in **Figure 3.3.8**. The highest rate of inactivation was achieved at  $2.49 \text{ cm}^2\text{s}^{-1}$  with a scan velocity at  $100 \text{ mms}^{-1}$ ,  $4.73 \text{ Jcm}^{-2}$  for *E. coli*. With the largest energy density applied at  $11.82 \text{ Jcm}^{-2}$  at  $40 \text{ mms}^{-1}$ ,  $I_r$  was only achieved at 1.19 and  $1.17 \text{ cm}^2\text{s}^{-1}$  for *E. coli* and *S. aureus* respectively.

The curve trend of  $I_r$  varied with increasing scanning velocities at each different power output, **Figure 3.3.9**. With *E. coli* (**Figure 3.3.9A**),  $I_r$  increased with increasing speed from  $40$  to  $100 \text{ mms}^{-1}$  at 13, 12, 11, 10, 9, 8 and 7 W.  $I_r$  values increased slightly from 0.73 to  $0.91 \text{ cm}^2\text{s}^{-1}$  with increasing  $V_t$  at 6 W. However,  $I_r$  decreased after  $60 \text{ mms}^{-1}$ , with no bactericidal effects at  $100 \text{ mms}^{-1}$  at 5 W laser power. Since sub-lethal killing was not considered to be bactericidal in  $I_r$  context, laser treatment at 3 W was not included with  $40 \text{ mms}^{-1}$ . As with *S. aureus* (**Figure 3.3.9B**), similar trends were observed.  $I_r$  increased with increasing  $V_t$  up to  $100 \text{ mms}^{-1}$  but decreased with increasing  $V_t$  at low power output, namely 5 and 6 W.

The relationship between power supplied,  $V_t$  and  $I_r$  of the linear scans is shown in **Figure 3.3.10**. The points represent the  $IA_{50}$  values obtained.  $IA_{50}$  values were attained for all the translational velocities at each respective power output with *E. coli* but only  $40$  and  $60 \text{ mms}^{-1}$  with *S. aureus*. The corresponding  $I_r$  showed approximately the same values obtained with  $40$  and  $60 \text{ mms}^{-1}$  for both the organisms.  $I_r$  values were only attained with *E. coli* at  $80$  and  $100 \text{ mms}^{-1}$ .

Nutrient agar plates, which were exposed to laser irradiation at various settings and then inoculated with both separate organisms showed normal growth after overnight incubation at  $37^\circ\text{C}$ . No localised melting of the nutrient agar medium was observed up to an applied energy density of  $12 \text{ Jcm}^{-2}$ . Lawned plates which were laser exposed which showed inactivation did not show any signs of recovery growth. Similarly, areas of inactivation of the nutrient agar plates were removed and imprinted onto fresh nutrient agar but there was no further growth after 14 days incubation. These areas were able to support fresh culture growth when re-contaminated with microorganisms. Thus the inactivation processes on both organisms were bactericidal, lethal and not bacteriostatic.

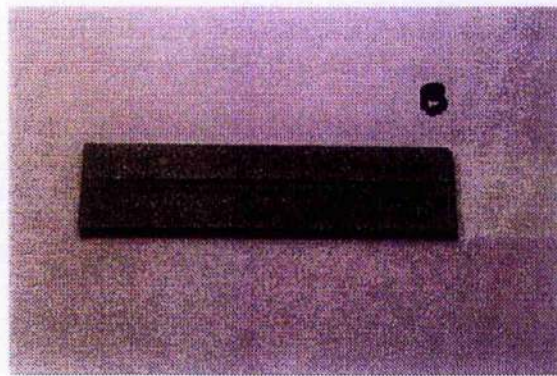
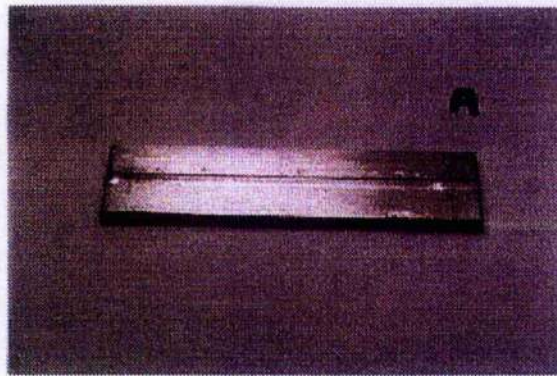


**Figure 3.3.2** Diagram of stainless steel strips for laser scans. The top picture, A, showed a polished strip. The dimension of the stainless steel strips were 4 X 1 X 0.15 cm with a centred rectangular groove of 1.5 mm width and 0.5 mm thickness in the centre where the microorganisms were being inoculated. The stainless steel strip surfaces, B, was sand-blasted to obtain fine matt finish to investigate and compare with untreated ones. The abrasive material used was super safti-grain 'F' (Guyson) at 100 p.s.i.

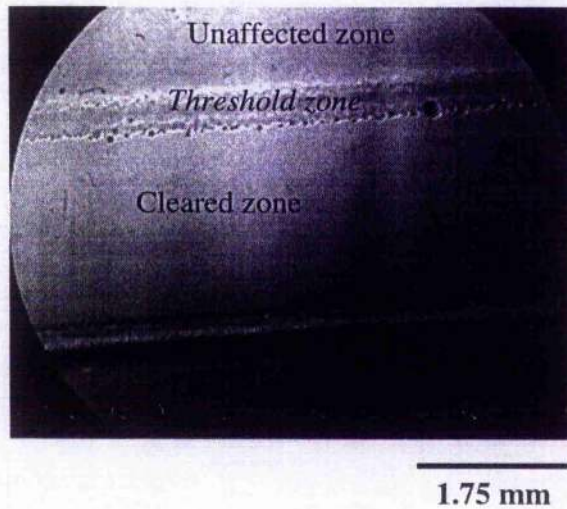


**Figure 3.3.3** Figure showed a section of a laser treated zone of *E. coli* lawned on nutrient agar plate at laser setting  $10\text{ W } 60\text{ mms}^{-1}$  after overnight incubation at  $37\text{ }^{\circ}\text{C}$ . The unaffected zone shows normal confluent growth while the microorganisms had been inactivated on the cleared zone. The threshold region along the peripheral is due to the Gaussian profile intensity of the laser where sub-lethal killing occurred.

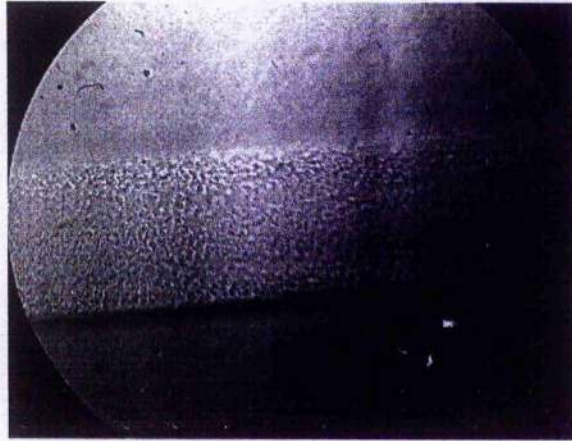


**Figure 3.3.4** Sub-lethal inactivation shown on the laser scanning track with  $40 \text{ mms}^{-1}$  occurred at 4 and 3 W for both *S. aureus* and *E. coli*. Both microorganisms showed similar sub-lethal visible killing effect on the scanned track. Normal confluent growth was observed on both side of the track.

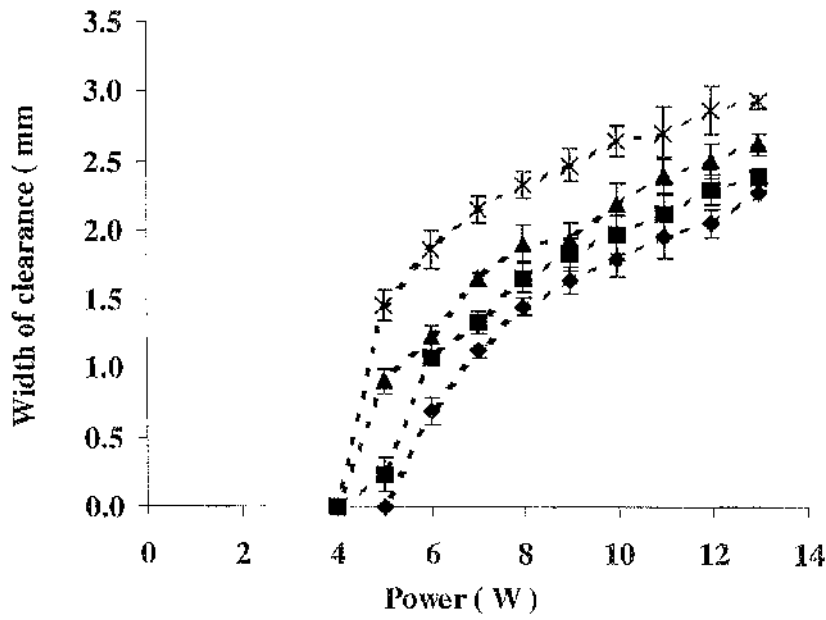
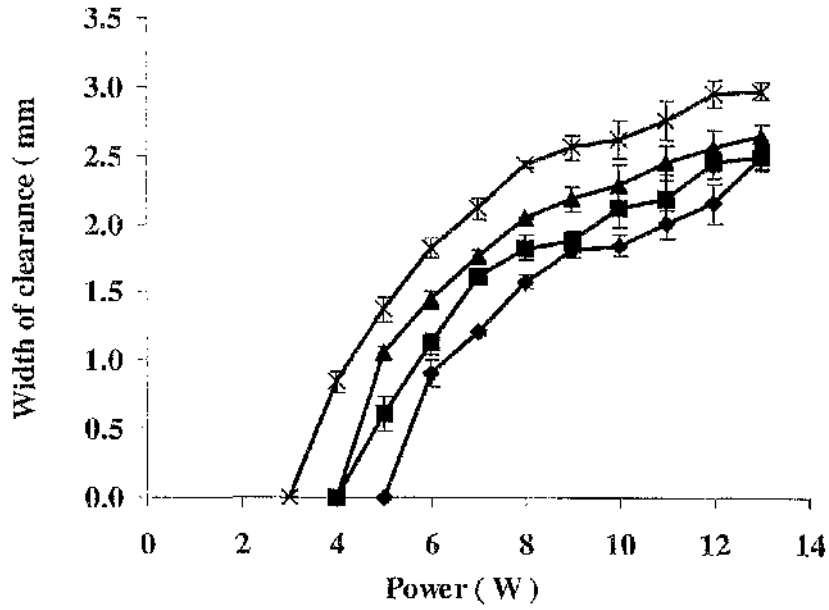
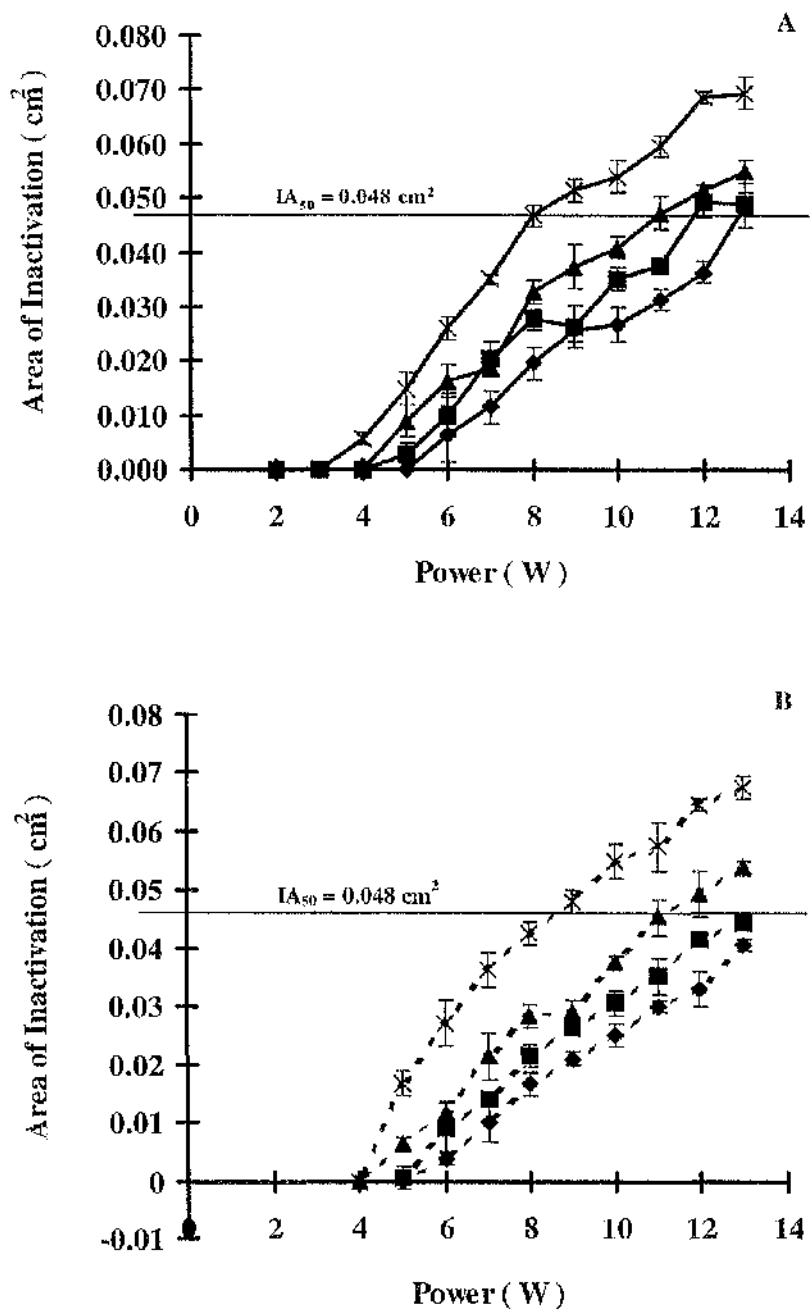
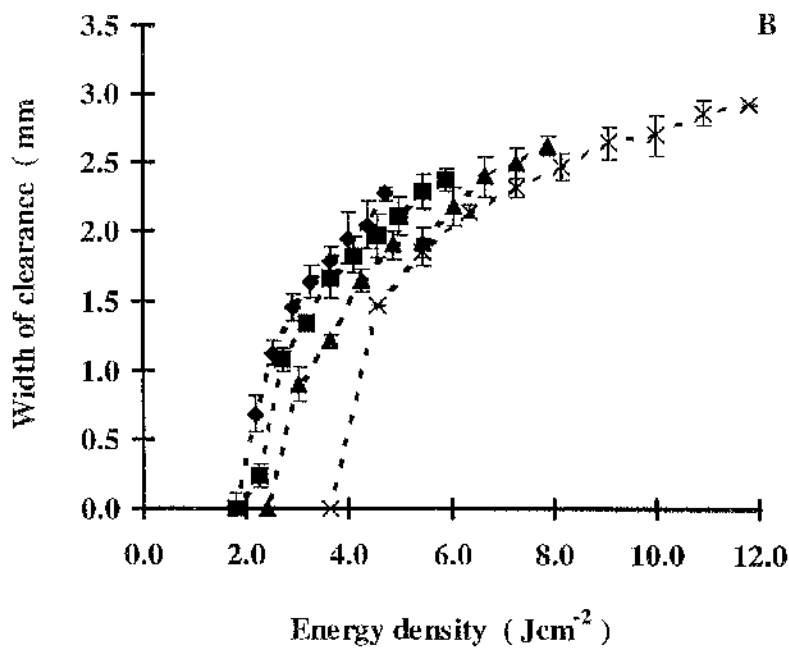
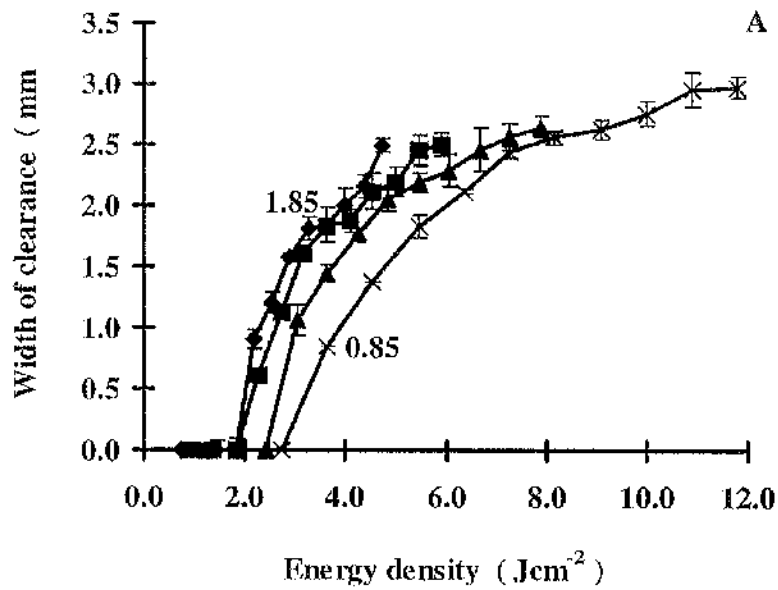


Figure 3.3.5 Width of clearance,  $W_c$  on nutrient agar plates seeded with *E. coli* (solid line) and *S. aureus* (dotted line) over a range of laser power output with  $V_t$  at 40 (×), 60 (▲), 80 (■) and 100  $\text{mm s}^{-1}$  (◆).



**Figure 3.3.6** Graph of area of inactivation versus power output at various  $V_t$ , namely, at 40 (×), 60 (▲), 80 (■) and 100  $\text{mms}^{-1}$  (◆) with *E. coli* (solid line; A) and *S. aureus* (dotted line; B). The  $IA_{50}$  value of the laser beam area is shown at  $0.048 \text{ cm}^2$ ; this is indicated by the horizontal dotted line.



**Figure 3.3.7** Relationship of varying laser energy density with the inactivated width of clearance,  $W_c$  with *E. coli* (solid line; A) and *S. aureus* (dotted line; B) at 40 ( $\times$ ), 60 ( $\blacktriangle$ ), 80 ( $\blacksquare$ ) and 100  $\text{mms}^{-1}$  ( $\blacklozenge$ ). For example with *E. coli*, both laser parameters at 10 W 100  $\text{mms}^{-1}$  and 4 W 40  $\text{mms}^{-1}$  yields the same energy density of  $3.64 \text{ Jcm}^{-2}$ . However, the width of inactivation was 1.85 and 0.85 mm respectively.

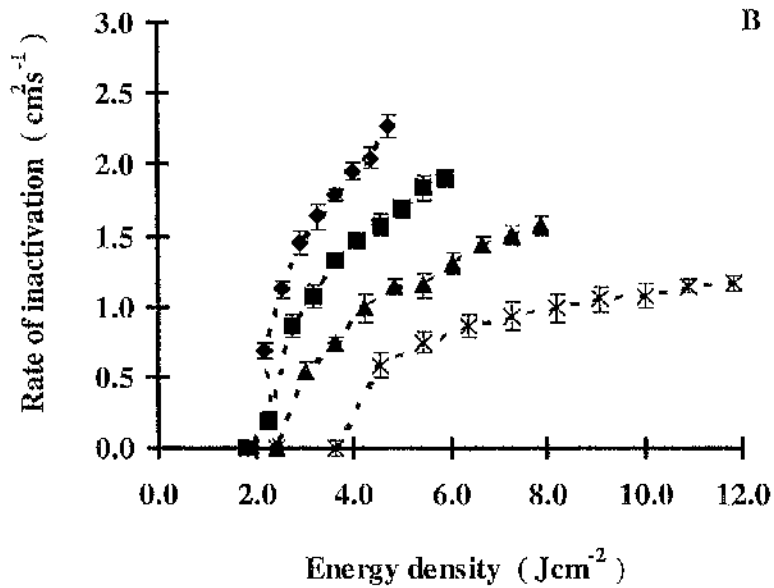
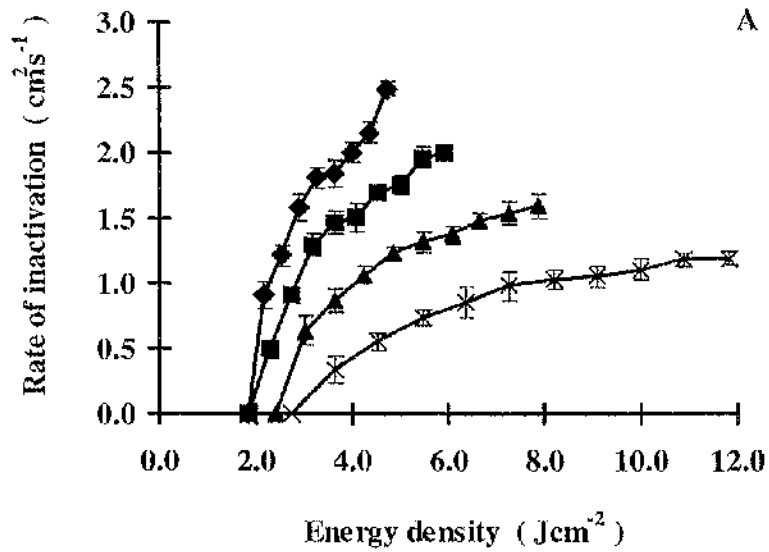


Figure 3.3.8 Rate of inactivation,  $I_r$ , of *E. coli* (solid line; A) and *S. aureus* (dotted line; B) against energy density applied with various  $V_1$  at 40 ( $\times$ ), 60 ( $\blacktriangle$ ), 80 ( $\blacksquare$ ) and 100  $\text{mms}^{-1}$  ( $\blacklozenge$ ).

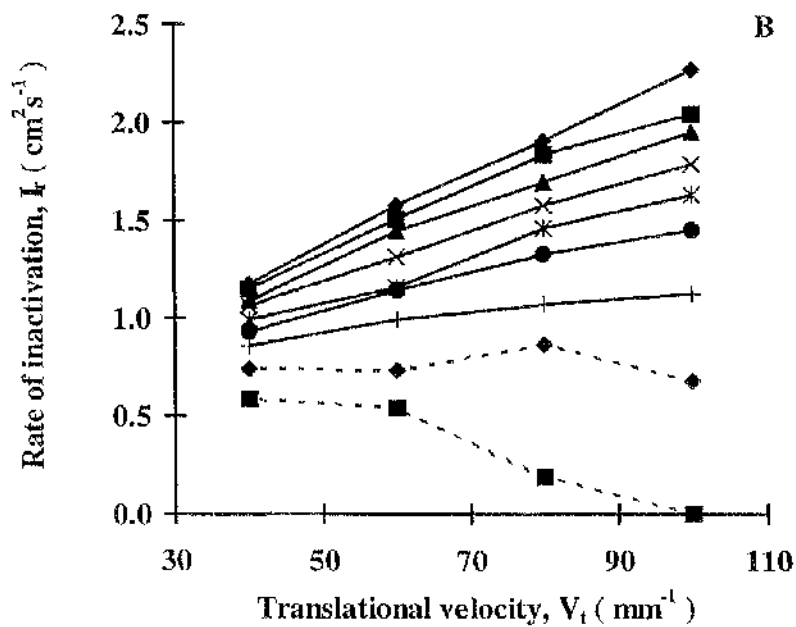
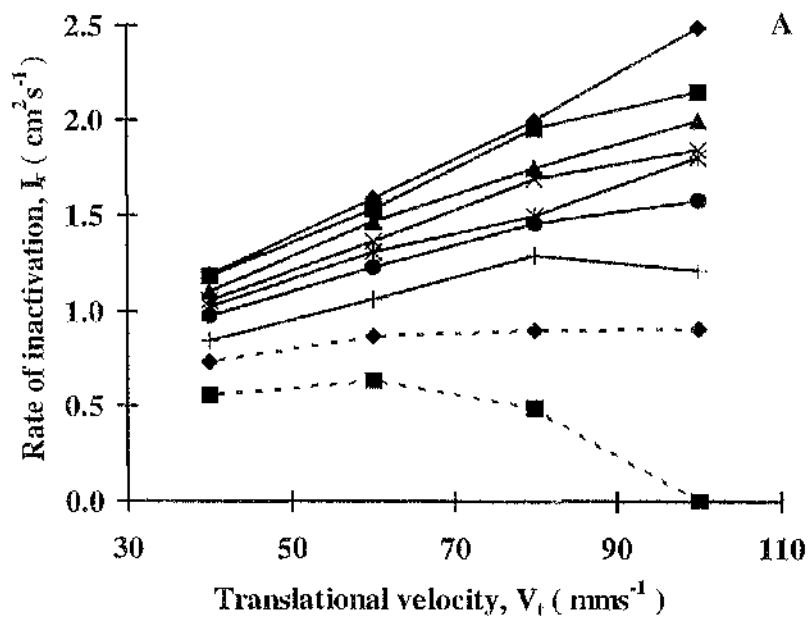
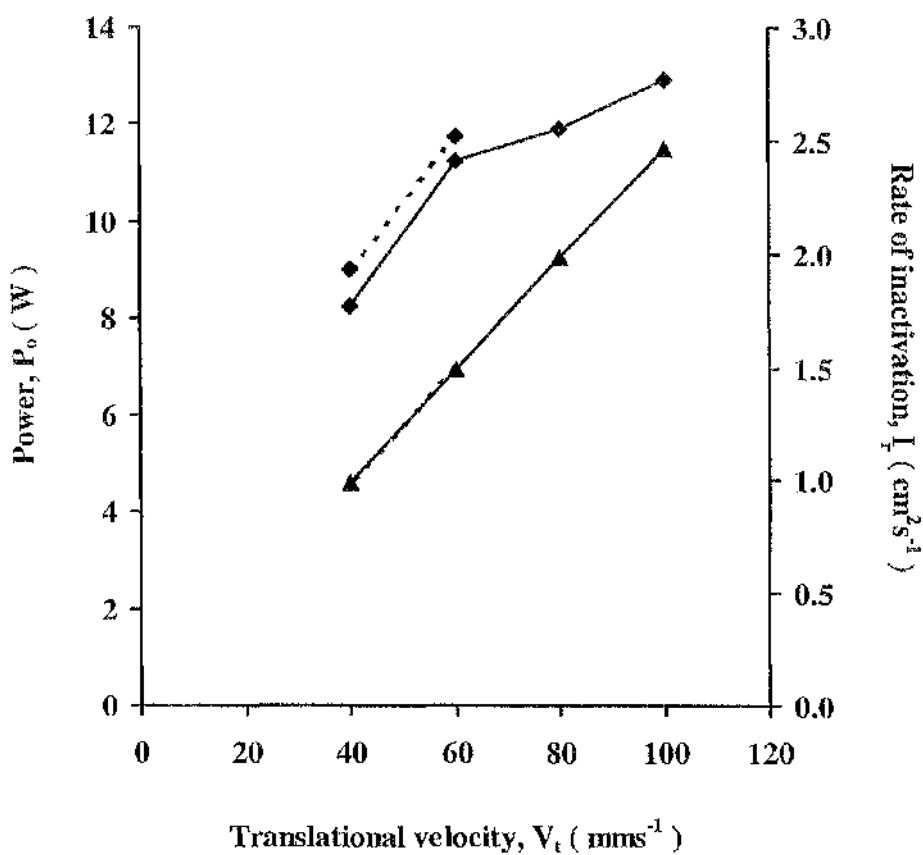


Figure 3.3.9 Rate of inactivation,  $I_r$  against translational velocity,  $V_t$  with *E. coli* (A) and *S. aureus* (B) at 13 (solid line; ◆), 12 (solid line; ■), 11 (▲), 10 (×), 9 (\*), 8 (●), 7 (+), 6 (dotted line; ◆) and 5 W (dotted line; ■).



*Figure 3.3.10* Graph showed the relationship of laser inactivation parameters of *S. aureus* ( -- $\blacklozenge$ -- ) and *E. coli* (solid line;  $\blacklozenge$ ) between power,  $P_0$  and translational velocity,  $V_t$  corresponding to  $IA_{50}$  value of the beam characteristic. Similar relationship was shown with rate of inactivation,  $I_r$  and  $V_t$  for *S. aureus* ( -- $\blacktriangle$ -- ) and *E. coli* (solid line;  $\blacktriangle$ ).

### 3.3.3.2 Laser exposed stainless steel strips

When treated with laser, both organisms did not show any viable reduction up to 13.4 W at 3 mms<sup>-1</sup> (162.5 Jcm<sup>-2</sup>). With sand-blasted stainless steel strips, one D-value microbial reduction was observed with 13 W at 5 mms<sup>-1</sup> (94.6 Jcm<sup>-2</sup>) and 13 W at 10 mms<sup>-1</sup> (47.3 Jcm<sup>-2</sup>) for *S. aureus* and *E. coli* respectively. No viable reduction was observed with unexposed bacteria-seeded sand-blasted strips which indicated that the one D-value reduction was solely due to laser action.

### 3.3.4 DISCUSSION

The low power CO<sub>2</sub> laser proved to be effective in sterilising microorganisms on nutrient agar with relatively low energy densities applied; comparatively more efficient in terms of applied energy densities than the high power CO<sub>2</sub>. In all cases, the scanned paths showed two distinct section results under the microscope; namely bactericidal and sub-lethal or threshold zones, **Figure 3.3.3** and **3.3.4**. The sub-lethal region along the periphery was due to the Gaussian beam profile intensity. The heat dissipated from the beam could have caused such effects, which results in a gradual impact on the microorganisms away from the peak of the laser beam profile. Nevertheless, the clear zones have been tested to be bactericidal and lethal.

From the results in **Figure 3.3.7**, *S. aureus* (dotted line) was only slightly more resistant than *E. coli* (solid line). Nevertheless, inactivation was achieved on nutrient agar plates with as low as 2.18 Jcm<sup>-2</sup> (6 W at 100 mms<sup>-1</sup>) with *E. coli*. In general, the width of clearance,  $W_c$  of the scan increases with increasing power output for a particular  $V_t$ ; and for any power output, the slower the  $V_t$ , the greater the  $W_c$ .

It was interesting to note in **Figure 3.3.7**, for a fixed  $ED_v$ , in this example 3.64Jcm<sup>-2</sup>, two sets of laser parameters at 100 mms<sup>-1</sup>/10 W and 40 mms<sup>-1</sup>/4 W yielded inactivation widths at 1.85 and 0.85 mm respectively with *E. coli*. From **Eqn. 3.3.1**, the  $ED_v$  value is proportional to power output and inversely related to  $V_t$ . The relationship allowed two possible combinations of  $P_o$  and  $V_t$  for any given  $ED_v$  or

the ratio  $P_0/V_t$ . This implied that the domineering variable for any given  $ED_v$  was the  $P_0$  and not  $V_t$  since the expected result of increasing  $V_t$  should decrease  $W_c$ . However, for a given  $ED_v$ , greater  $W_c$  was achieved with faster  $V_t$  than lower ones.

The rate of inactivation,  $I_r$ , is a good measure of the effective area of inactivation of the organisms per unit time, **Figure 3.3.8**. For a given  $ED_v$ ,  $I_r$  increased significantly with increasing  $V_t$ . The largest  $I_r$  achieved was at  $2.49 \text{ cm}^2\text{s}^{-1}$  at a low  $ED_v$  of  $4.73 \text{ Jcm}^{-2}$  with *E. coli*. For a given  $I_r$ , the energy density increased with decreasing  $V_t$ . However, due to the system configuration, the  $V_t$  could not be increased. It would be worthwhile to investigate further to find the optimum speed, greater than  $100 \text{ mms}^{-1}$ , to produce higher  $I_r$  as this would mean greater efficiency of the laser sterilisation.

Interestingly, the power output of such scanning system was crucial in determining the  $I_r$ . In **Figure 3.3.9**, both *E. coli* and *S. aureus* showed similar killing trend. Generally,  $I_r$  increased with increasing  $V_t$  and power,  $P_0$ , except at 5 and 6 W. In fact, at  $100 \text{ mms}^{-1}$ , no killing was observed with 5 W but optimum value of  $2.49$  and  $2.48 \text{ cm}^2\text{s}^{-1}$  with *E. coli* and *S. aureus* at 13 W respectively. This supports the suggestion that power output in such scanning is a more important and decisive variable than  $V_t$ . Judging from the trend of the graphs,  $I_r$  will be optimised at  $V_t$  greater than  $100 \text{ mms}^{-1}$  for 13, 12, 11, 10, 9, 8, and 7 W. As seen with 6 W, the optimum  $I_r$  was achieved at  $0.91$  for *E. coli* and  $0.86 \text{ cm}^2\text{s}^{-1}$  for *S. aureus*. Thus, if a wider range of  $V_t$  was applied, a single peak 'mountain' shape trend curve of  $I_r$  should be observed.

It may have been predicted that such a low power laser might not produce any microbial inactivation since the maximum energy density applied at  $162.6 \text{ Jcm}^{-2}$  was at least a few hundred-fold smaller than that with the high-power  $\text{CO}_2$  system shown previously, **Section 3.2**. The aim was for rapid sterilisation, therefore, it was not feasible to increase the energy density applied by reducing the scanning speed further at  $3 \text{ mms}^{-1}$ . Nevertheless, the degree of microbial killing on different surfaces with laser light was (previously shown in **Section 3.2**) also dependent on the surface optical properties of the underlying substrate. With the same stainless steel strips but undergone sand-blasting, one D-value viable reduction was observed

at relatively lower energy densities with *S. aureus* (94.6 Jcm<sup>-2</sup>) and *E. coli* (47.3 Jcm<sup>-2</sup>). However, it will be interesting to know the level of viable reduction with respect to the different initial bioburden.

**IV. LASER, ULTRA-VIOLET  
AND MICROWAVE  
SYSTEM**

## 4.1 MINIMAL PROCESSES FOR BACTERIAL INACTIVATION WITH COMBINED UNIT OPERATION WITH LASER, ULTRA-VIOLET AND MICROWAVES

### 4.1.1 INTRODUCTION

The inadequacy of adopting appropriate sterilisation processes has been seen with an increase in the severity of food poisoning outbreaks and deaths. A succession of food crises from *Salmonella* to BSE and *E. coli* has been seen which has heightened the public's concern on food safety and a call for tighter reliability on food standards.

Such demands can be better met by introducing reliable control of novel decontamination processes which might result in improved food quality and extended shelf-life over conventional techniques and processes.

As seen in previous chapters, laser light has been proven to be effective in inactivating food pathogens with fast scanning laser systems without damaging the underlying substrate. Such novel sterilisation methods may prove to be a possibility to food processing industries on vegetables and fruits. There may be the potential for the development of reliable and cost-effective sterilisation systems by combining lasers with emerging methods of bactericidal radiation, for example ultra-violet and microwaves, to effectively minimise the decontamination process with no compromise to the quality standard of the treated samples.

In this section, the performance of the sub-systems, namely CO<sub>2</sub> laser (L), ultra-violet (UV) and microwave radiation ( $\mu$ wave) and the combined system of all three were evaluated on sections of apple, potato and tomato seeded with *Staphylococcus aureus*.

## 4.1.2 MATERIALS AND METHODS

### 4.1.2.1 Laser, ultra-violet and microwave system

The system was comprised of a high power Ferranti MFK, CO<sub>2</sub> laser (Lumonics Ltd), a dual germicidal UV lamp system (2 X 4 W tube; BDH) and a conventional microwave oven (800 W, SANYO-EM-S153), operating at wavelengths of 10.6 μm, 0.254 μm and 12 cm respectively. The dual UV lamps were placed on top of the microwaves in which the laser beam entered between the lamps via an aluminium aperture. Samples were placed in the centre of the microwave turntable equidistant (21 cm) from the dual UV lamps. The intensity of the UV lamps on the samples was measured at 500 μWcm<sup>-2</sup>.

The effects of the sub-systems (L, UV and μwave) and their combined effects were assessed simultaneously and sequentially. **Figure 4.1.1** shows the combined system with a tomato sample inside the microwave cavity. The system was built in such a way that each radiation source was able to irradiate independently, therefore, all the bacterial experiments with the sub and combined systems' were conducted within the set-up as shown.

### 4.1.2.2 Preparation of fruit samples

'Granny Smith' green apples (**Figure 4.1.2**), 'English Grade 1' potatoes (**Figure 4.1.3**) and 'Dutch Class 1' tomatoes (**Figure 4.1.4**) were used in each experiment. The fruits were cut into square shapes of 2 x 2 cm in dimension with at least a few mm of underlying flesh. The prepared samples were washed in 70 % v/v ethanol for 5 min and resuspended in sterile distilled water thrice. Excess water was removed aseptically and left to dry in an air-flow cabinet for 20 min. Controls were included at each stage of preparation; i.e. unprocessed and processed.

### 4.1.2.3 Inoculum

The preparation of the inoculum was described in **Section 2.2.2.1**. Aliquots of the bacterial suspension (15 μl) were pipetted onto the surface of the sample prior to radiation exposure. The samples were placed with sterile forceps on a

microwaveable pyrex glass dish, aseptically cleaned with 70 % v/v ethanol, and aligned with the laser beam. With the UV and microwave, the samples were placed 20 cm below and equidistant to the dual UV lamps on the centre of the rotating glass plate.

#### **4.1.2.4 Exposure of prepared samples**

Prior to evaluating the combined system's performance, experimental works on the sub-systems, namely laser, UV and  $\mu$ wave, were examined with the contaminated fruit samples. With the combined system, both 'sequential' and 'simultaneous' treatments were initiated to monitor and compare the bactericidal effects of the individual radiation sources. The microbiological analysis on irradiated samples can be found in **Section 3.2.2.6**.

#### ***Sub-systems exposures***

The CO<sub>2</sub> laser was set to low power (380W output with 200 W after 'clipping effect') for all samples with an exposure time of up to 10 ms. The ultra-violet lamps were set from 0 to approximately 80 s for all samples while the microwave was set to 800 W with a maximum of 8 s exposure time.

The CO<sub>2</sub> laser had to be activated 1 hr prior to the experiments while the UV lamps were activated and left for 8 min prior to experiments and must not be cooled for more 1 min between experiments to ensure constant intensity. The microwave was cooled for 5 min after each experiment to prevent any compound effects due to heat generation. After exposure, each sample was placed in a 100 ml Duran bottle containing 20 ml of sterile PBS. A control sample received no radiation.

#### ***Sequentially combined system exposure***

The CO<sub>2</sub> laser was set to a maximum exposure time of 10 ms. The ultra violet lamps (UV) were set to 50, 20 and 30 s for apple, potato and tomato respectively to produce the bactericidal effect. The microwave was set to 800 W with exposure of 4 s for all samples. With three different irradiation sources and each fruit sample has to be exposed from each source one after the other, a total of six possible sequential combinations is possible for each fruit sample experiment, **Table 4-1-1. Figure 1**



**Figure 4.1.1** Experimental set-up of single and combined treatment with CO<sub>2</sub> laser light, UV and microwave radiation. The laser delivery system stands at the top cover between the two sets of UV lamps of the microwaves. The tomato sample was aligned at the centre of the microwave pyrex plate as shown.

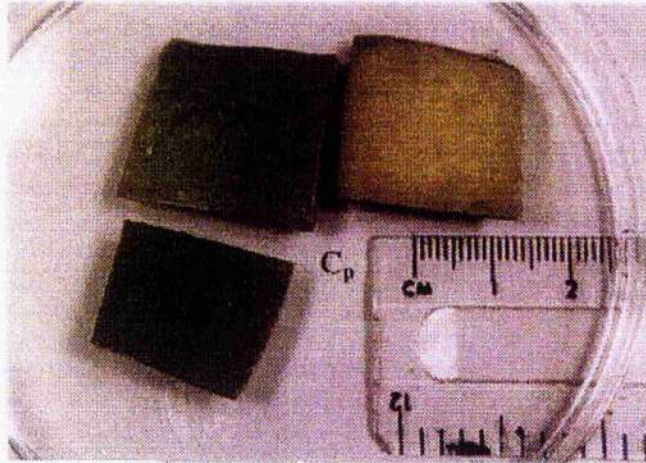


*Figure 4.1.2* Samples of unexposed apple

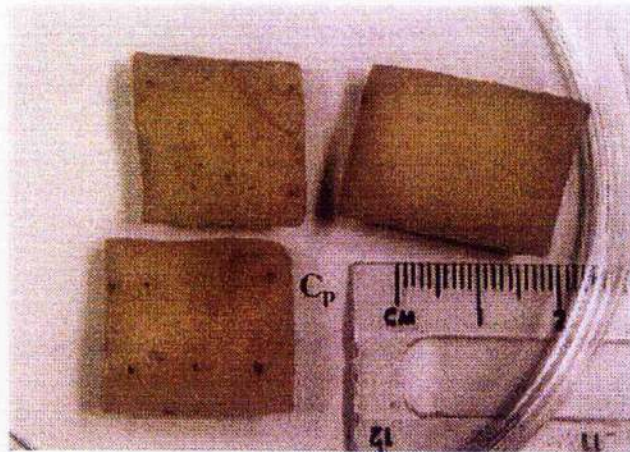


*Figure 4.1.3* Samples of unexposed potato

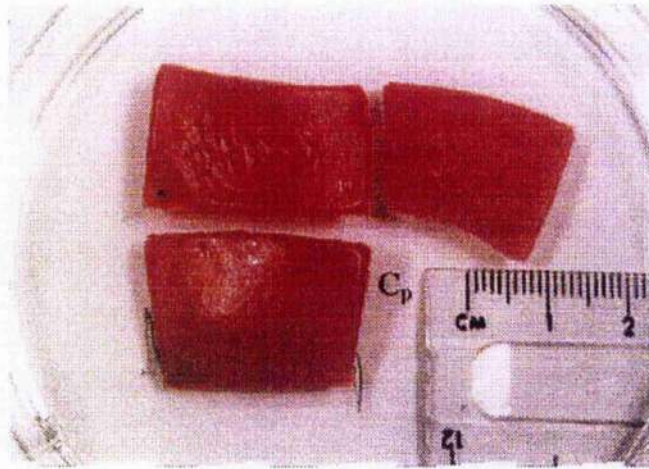


**Figure 4.1.4** Samples of unexposed tomato

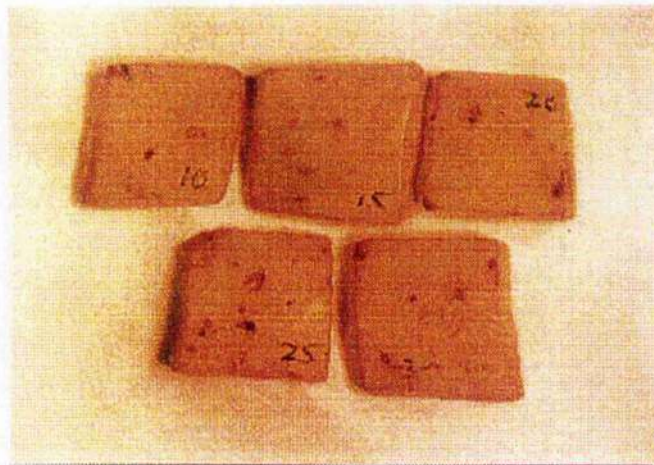


**Figure 4.1.5** Samples of uncontaminated potato cuts with exposure time up to 30 ms with 200 W CO<sub>2</sub> laser. Damages were seen with exposure time of 15 ms and above.

After each exposure, 1  $\mu$ l of the inoculum was pipetted into 10 ml of sterile distilled water (a single 1000 fold dilution; i.e.  $10^{-4}$ ) followed by 3 serial 10-fold dilutions ( $10^{-5}$ ,  $10^{-6}$  and  $10^{-7}$ ) were made, i.e. 0.2 in 1.8 ml sterile distilled water dilution. The delay was to allow time between each treatment to prepare dilutions and plating out. For example, with the apple in **Table 4-1-1**, experiment three, the contaminated fruit sample received 4 s of  $\mu$ wave, delay for 2 min, then 50 s of UV with a 2 min delay followed finally by 10 ms of laser irradiation after where each irradiation (namely sequentially  $\mu$ wave  $\rightarrow$ UV $\rightarrow$ L), 1  $\mu$ l of the inoculum was sampled for dilution. A control disc or fruit sample received no irradiation.

### *Simultaneously combined system exposures*

The CO<sub>2</sub> laser was set to low power as described above for all fruit samples at 10 ms exposure time. The ultra violet lamps were set to 50, 20 and 30 s for apple, potato and tomato respectively. The microwave was set to 800 W with 4 s exposure time for all contaminated samples.

As the exposure time was not comparatively equal, the combined exposure has to start off with the longest irradiation source, the ultra-violet, follow by microwave and the laser. With three different irradiation sources to create the combined effect, the sequence of activating the individual radiation source was shown below for each kind of sample, for example;

#### APPLE

50 s of UV after which  $\mu$ wave and laser radiation were activated at the 23<sup>rd</sup> s for 4 s and 25<sup>th</sup> s for 10 ms respectively

#### POTATO

20 s of UV after which  $\mu$ w and laser radiation were activated at the 8<sup>th</sup> s for 4 s and 10<sup>th</sup> s for 10 ms respectively.

## TOMATO

30 s of UV after which microwaves and CO<sub>2</sub> laser radiation were activated at the 13<sup>th</sup> s for 4 s and 15<sup>th</sup> s for 10 ms respectively.

A control of each kind of sample received no irradiation.

### 4.1.3 RESULTS

#### 4.1.3.1 Sub-systems

##### *CO<sub>2</sub> laser*

The CO<sub>2</sub> laser exposure was limited to 10 ms with the unfocused beam for all contaminated fruit samples. A preliminary experiment was conducted to investigate the threshold exposure time of the radiation before substantial damage was done to the surface of the samples. **Figure 4.1.5, 4.1.6 and 4.1.7** showed the uncontaminated potato, apple and tomato samples of various exposure time up to 30 ms. The darker rings on the samples were the result of irradiation. It is clearly seen that damage was done with 15 ms or longer exposure time. As such, the exposure time of irradiation on the contaminated fruit samples were set to a maximum of 10 ms to investigate the bactericidal effect.

The laser exposure time, up to 10 ms, was not relatively effective in killing the microorganisms, **Figure 4.1.8**. No microbial reduction was seen with potato and tomato samples. However, with apple samples, 0.3 D-values was observed.

##### *Microwaves*

It was observed that microwave radiation was emitted after two s from the onset of activation. The microorganisms have good surface tension which enable the contaminated areas to be inoculated fairly consistently on the samples.

**Table 4-1-1 Combined sequential experiments.** For each experiment, the sequential process of CO<sub>2</sub> laser (L), ultra-violet (UV) and microwave ( $\mu$ wave) was done as shown on contaminated fruit samples.

Experiment	Sequential irradiation				
1	UV	→	$\mu$ wave	→	L
2	UV	→	L	→	$\mu$ wave
3	$\mu$ wave	→	UV	→	L
4	$\mu$ wave	→	L	→	UV
5	L	→	$\mu$ wave	→	UV
6	L	→	UV	→	$\mu$ wave

The response pattern of *S. aureus* with microwave radiation is illustrated in **Figure 4.1.9** for all three samples. No visible effects were seen on any of the three contaminated samples with 3 and 4 s exposure times. With 5, 6 and 7 s, damage was seen in all three samples as underlying flesh was cooked which caused a distinctly darker area on the surface as heat being conducted upwards. For example, **Figure 4.1.10a, b, and c** shows the damage done to the tomato samples. Slight log bacterial reduction was observed at 4 s for apple and potato samples but approximately 0.75 log D-value reduction with potato. Full inactivation was achieved at 7 and 8 s for apple and tomato samples. With potato samples, a 4.5 log D-value bacterial reduction was observed with 8 s exposure where the sample was completely cooked.

### ***Ultra-violet***

There was no apparent heat generated or apparent changes with the inoculum or substrates when subjected to UV radiation. Relatively, higher inactivation was achieved with UV than microwave or the laser although the exposure time was longer without damaging the substrates. **Figure 4.1.11** showed the killing pattern of the 3 contaminated fruit samples subjected to various UV irradiation times. With the apple and tomato, both the bacterial log D-reduction can be approximately by a single linear rate of inactivation with exposure time. However, with the potato, a steeper (0 to 30 s) and plateau (30 to 90 s) rate of microbial population decline was observed. A 4 D-value log reduction was achieved for both apple and tomato contaminated samples with an 80 s exposure time. With potato samples, the bacterial reduction fluctuated approximately at 5 log cfu sample<sup>-1</sup> with 30 to 90 s irradiation time.

### **4.1.3.2 Combined simultaneous system**

The results from **Figure 4.1.8, 4.1.9 and 4.1.11** were used to determine the experimental parameters for the combined simultaneous treatments. For each substrate, the combined effects of the subsystem and systems were found, **Table 4-1-2**.



**Figure 4.1.6** Samples of uncontaminated apple cut with exposure time up to 30 ms with 200 W CO<sub>2</sub> laser. Damages were seen on the surface of the skin with exposure time of 15, 20, 30 and 50 ms.



**Figure 4.1.7** Samples of uncontaminated tomato cut with exposure time up to 50 ms with 200 W CO<sub>2</sub> laser.

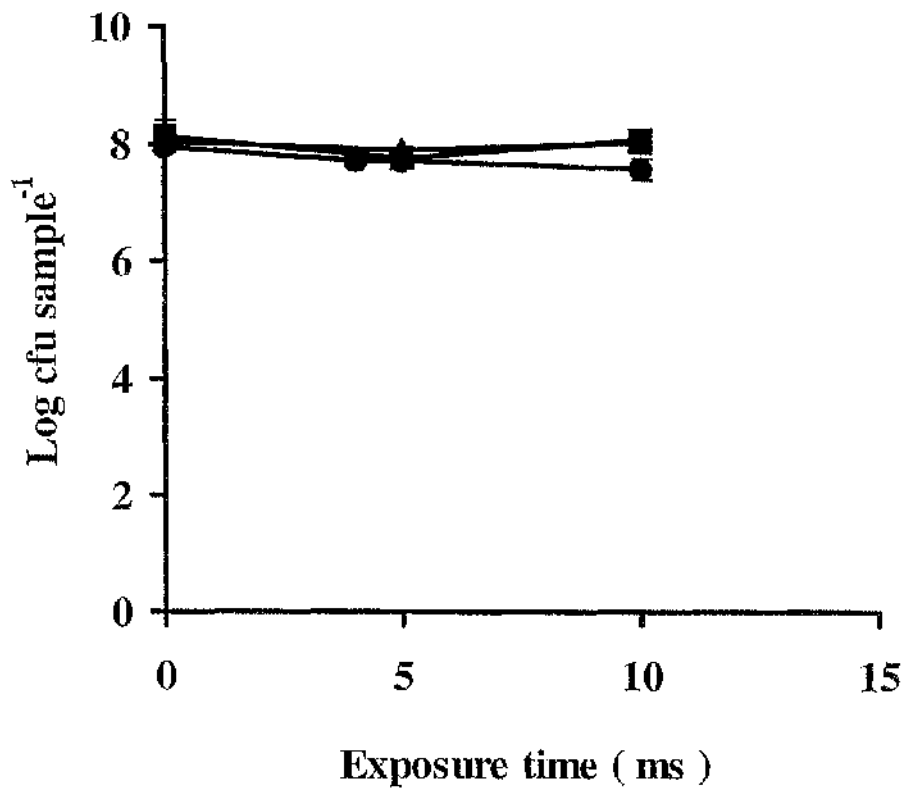


*Figure 4.1.8* Bacterial viable reduction of contaminated samples namely, apple; ●, potato; ■, tomato; ▲, with initial bioburden of approximately  $6 \times 10^7$  cfu *S. aureus* (15  $\mu$ l) exposed to 200 W CO<sub>2</sub> laser up to 30 ms.

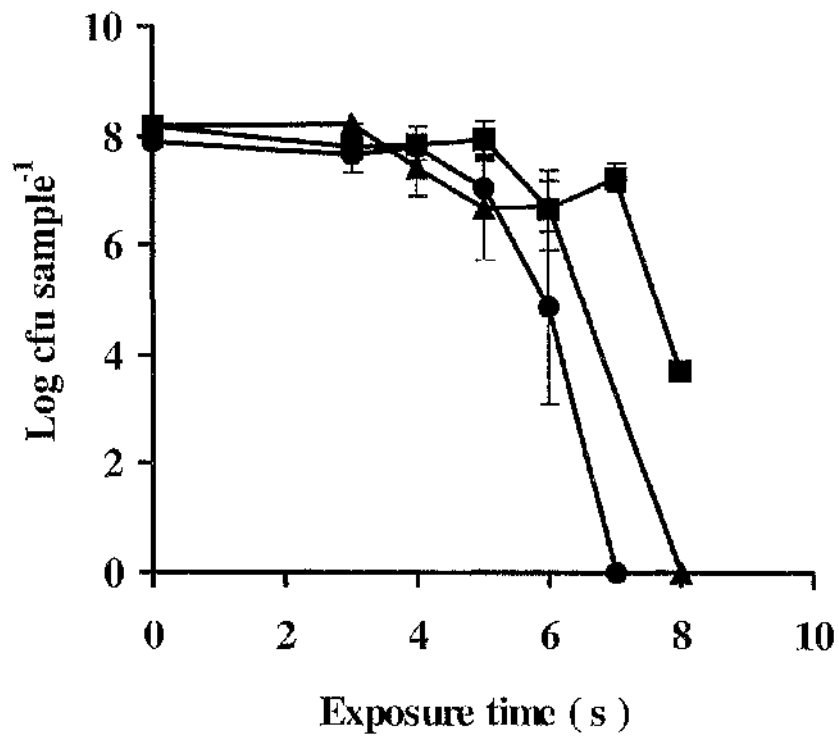


*Figure 4.1.9* Response killing patterns of *S. aureus* on apple; ●, potato; ■, and tomato; ▲ samples with 800 W conventional microwave oven.

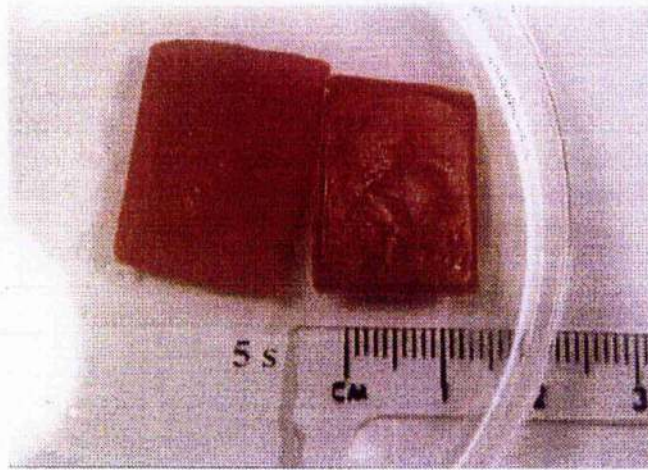


**Figure 4.1.10a** Tomato sample exposed to 5 s microwave radiation. The left and right cut showed the underneath and surface view of the sample.

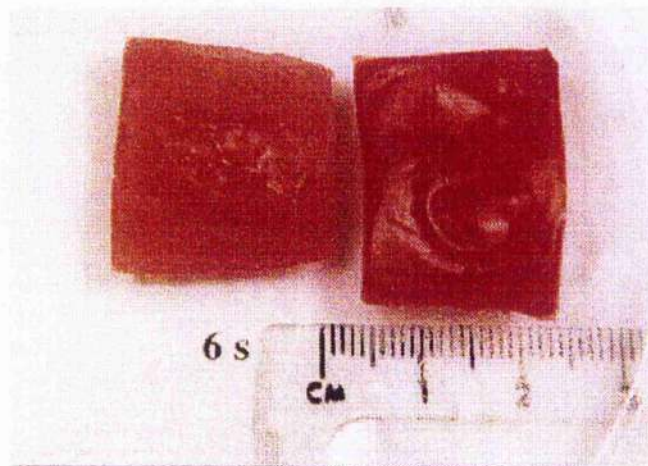


**Figure 4.1.10b** Tomato sample exposed to 6 s microwave radiation. The left and right cut showed the underneath and surface view of the sample.

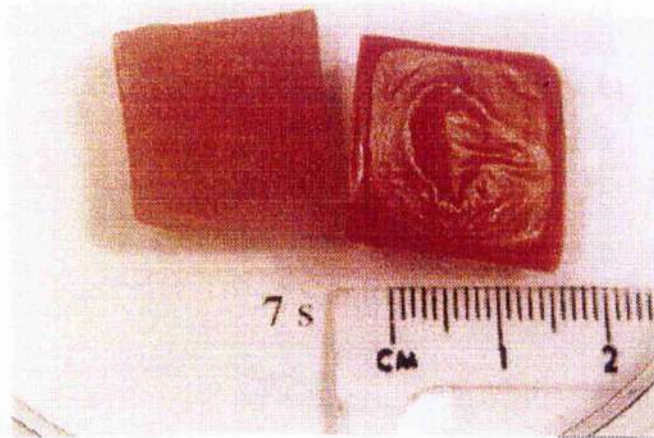


**Figure 4.1.10c** Tomato sample exposed to 7 s microwave radiation. The left and right cut showed the underneath and surface view of the sample.

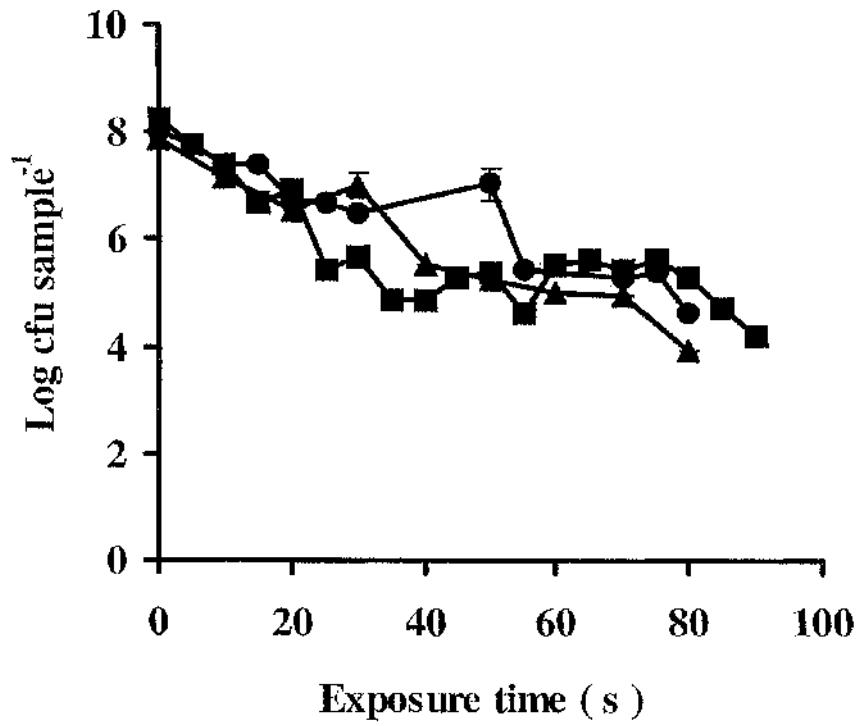


*Figure 4.1.11* Graph of *S. aureus* response killing pattern with ultra-violet radiation up to 90 s exposure time with apple; ●, potato; ■, and tomato; ▲, sample.

The CO<sub>2</sub> laser was set to low (200 W) or high (540 W) power for 10 ms for all samples with the exception of PE discs when 100 ms was used. The UV lamps were set for 50 s for apple, 20 for potato, and 30 for tomato samples. The microwave was set to 800 W with 4 s for all the samples. The log reduction values for the CO<sub>2</sub> laser were shown (Table 4-1-2, items 1, 5, and 9) for all the treated samples. The comparative values were for microwave radiation, (Table 4-1-2, items 2, 6, and 10) and for ultra-violet radiation (Table 4-1-2, items 3, 7, and 11).

For the combination of the three treatments, a breadboard prototype test bed was constructed which enabled the samples to be exposed to the three treatments with the above mentioned parameters simultaneously, Table 4-1-2, items 4, 8, and 12. Untreated controls were added at each stage, combined in Table 4-1-2, item 13.

The boxplots of the individual results from the multiple experiments are shown in Figure 4.1.12a and b. The numbers at the left side indicate the treatment received by the *S. aureus* organisms from Table 4-1-2 as mentioned.

The largest standard error of mean (SEMEAN) of the viable counts following laser treatment was potato (0.208), apple (0.197) and tomato (0.058). With microwaves, the order was tomato (0.486), potato (0.292) and apple (0.143). Similarly with UV, they were apple (0.304), tomato (0.249) and potato (0.154). The SFMEAN was reduced considerably with the combined treatment process compared to the individual sub systems' effects namely: potato (0.160), apple (0.086) and tomato (0.074).

#### 4.1.3.3 Combined sequential system

The effect of exposing the inoculated samples to sequential treatments from each sub-system and the importance of the order of the treatment process was assessed. The counts surviving in the treated sample are shown below (in brackets), see Table 4-1-3.

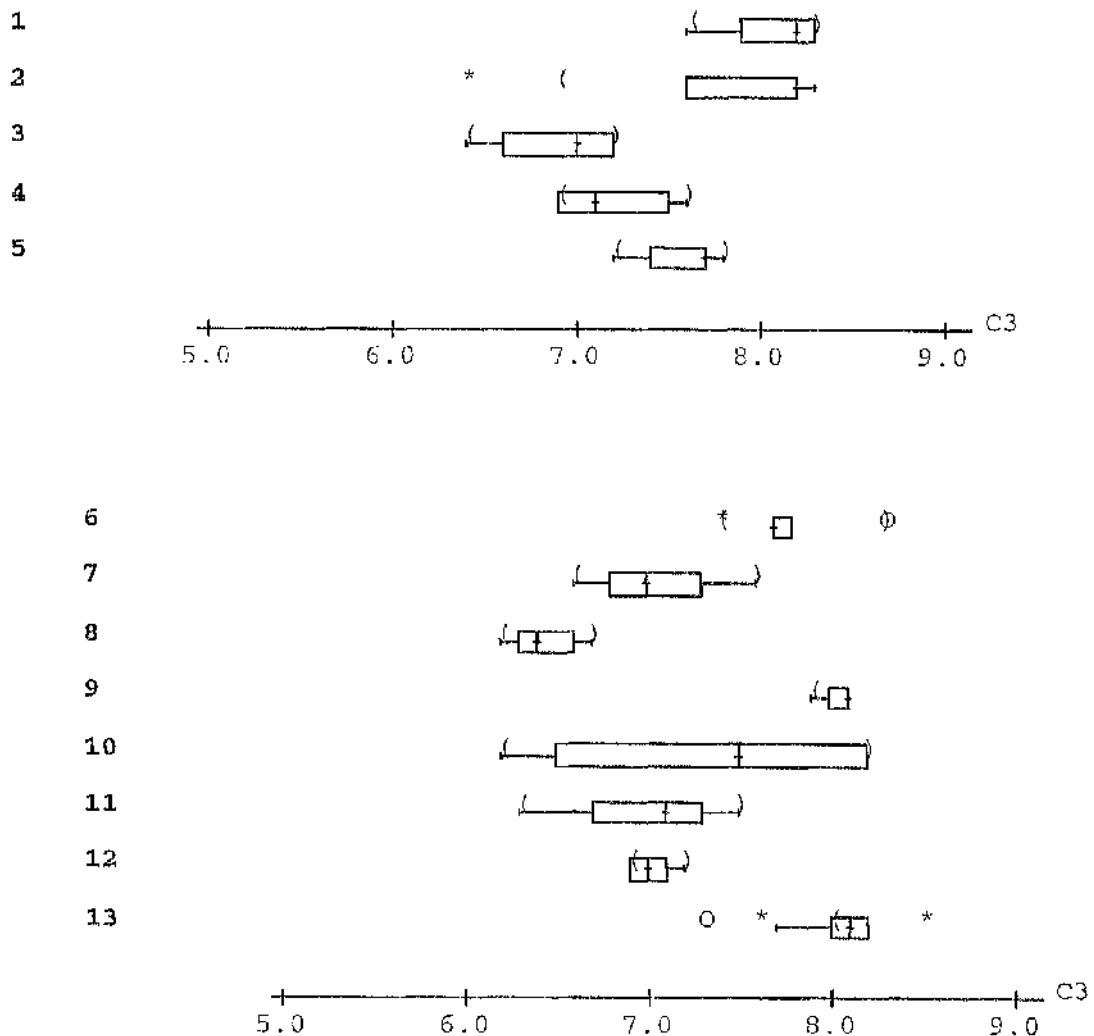


**Figure 4.1.12** Boxplots of the individual results extracted from Table 4-1-2 with potato, no. 1, 2, 3; apple, no. 5, 6, 7 and tomato, 9, 10, 11, and the permutations of combined treatments with potato, no. 4; apple, no. 8 and tomato, no. 12. No. 13 showed the statistical results for the controls. The ends of the boxes represent the inter-quartile range, the horizontal line the range, the vertical line inside each box is the median and the curved brackets are the 95% confidence limits of the median; asterisks are outliers (Minitab, reference manual).

**Table 4-1-2 Simultaneously combined (COMB) effect of CO<sub>2</sub> laser, ultraviolet and microwaves radiation on *S. aureus* with potato, apple and tomato.** (N is the number of experiments conducted. TRMEAN is the 5 % trimmed result of the MEAN value where Minitab removes the smallest 5 % (rounded to the nearest integer) and the largest 5 % of the mean value and then average the rest. SEMEAN is the standard error of MEAN calculated as the ratio of the standard deviation (STDEV), to the square root of N).

TREATMENT	N	MEAN	MEDIAN	TRMEAN	STDEV	SEMEAN
1. POTATO/ CO <sub>2</sub>	3	8.091	8.230	8.091	0.361	0.208
2. POTATO/μwave	6	7.856	8.230	7.856	0.714	0.292
3. POTATO/UV	5	6.926	7.000	6.926	0.344	0.154
4. POTATO/COMB	4	7.237	7.181	7.237	0.321	0.160
5. APPLE/CO <sub>2</sub>	3	7.603	7.710	7.603	0.333	0.192
6. APPLE/μwave	5	7.813	7.785	7.813	0.319	0.143
7. APPLE/UV	3	7.106	7.041	7.106	0.526	0.304
8. APPLE/COMB	4	6.490	6.491	6.49	0.172	0.086
9. TOMATO/CO <sub>2</sub>	3	8.068	8.105	8.068	0.101	0.058
10. TOMATO/μwave	4	7.404	7.554	7.404	0.973	0.486
11. TOMATO/UV	4	7.02	7.096	7.02	0.499	0.249
12. TOMATO/COMB	4	7.05	7.021	7.05	0.149	0.074
13. CONTROLS	33	8.041	8.114	8.044	0.277	0.048

**Table 4-1-3** Sequential treatment of samples and the number of *S. aureus* which survived at each time and stage (in brackets). The exposure times were as described in Section 4.1.2 in 'Sequentially combined system exposure'.

Treatment (cfu surviving)			
	First	Second	Third
<i>S. aureus</i>	Control Inoculum ( $4 \times 10^9$ )ml <sup>-1</sup>		
<b>Apple</b>	UV (0)	$\mu$ wave (0)	Laser (0)
	UV (0)	Laser (0)	$\mu$ wave (0)
	$\mu$ wave ( $1.4 \times 10^6$ )	UV (0)	Laser (0)
	MW ( $3.3 \times 10^7$ )	Laser ( $6.4 \times 10^7$ )	UV (0)
	Laser ( $1.3 \times 10^8$ )	$\mu$ wave ( $3.8 \times 10^7$ )	UV (0)
	Laser ( $2.9 \times 10^8$ )	UV (0)	MW (0)
	Untreated left for 45 min ( $3.8 \times 10^7$ )		
<b>Potato</b>	UV ( $1.7 \times 10^5$ )	MW ( $1.2 \times 10^6$ )	Laser ( $5.3 \times 10^5$ )
	UV (0)	Laser (0)	MW (0)
	MW ( $4.2 \times 10^7$ )	UV ( $6.6 \times 10^4$ )	Laser ( $1.4 \times 10^4$ )
	MW ( $8.4 \times 10^5$ )	Laser ( $6.3 \times 10^5$ )	UV (0)
	Laser ( $3.5 \times 10^7$ )	MW ( $5.2 \times 10^7$ )	UV ( $3.5 \times 10^3$ )
	Laser ( $6.0 \times 10^7$ )	UV ( $3.2 \times 10^4$ )	MW ( $6.3 \times 10^4$ )
	Untreated left for 45 min ( $9 \times 10^6$ )		
<b>Tomato</b>	UV ( $2.0 \times 10^5$ )	MW ( $4.6 \times 10^4$ )	Laser ( $6.8 \times 10^4$ )
	UV (0)	Laser (0)	MW (0)
	MW ( $4 \times 10^6$ )	UV (0)	Laser (0)
	MW ( $4 \times 10^7$ )	Laser ( $5.5 \times 10^7$ )	UV (0)
	Laser ( $4.2 \times 10^7$ )	MW ( $3.6 \times 10^7$ )	UV (0)
	Laser ( $2.3 \times 10^7$ )	UV (0)	MW (0)
	Untreated left for 45 min ( $3.4 \times 10^7$ ) cfu in 15 $\mu$ l		
<i>S. aureus</i>	Inoculum at the end of experiment ( $1.0 \times 10^8$ )		

#### 4.1.4 DISCUSSION

It is worthwhile to appreciate that inoculum was far in excess of any average contaminated fruit samples possibly found in practice (approximately  $4 \times 10^8$  cfu

sample<sup>-1</sup>). With a lower contamination level, laser sterilisation was more efficacious. For example, the ratio of logarithmic bacterial reduction after laser treatment over initial bacterial concentration ( $N/N_0$ ) was 0.25 and 0.6 with initial log bacterial counts of 7.7 and 4.0 respectively (Ward, 1997). Moreover, complete inactivation will be achieved with a lower energy density and lesser exposure time with lesser amount of contamination.

An interesting perspective can be gathered from the killing pattern of microorganisms with microwaves and UV as compared with laser. Presumably, the rate of bacterial decline of laser treatment was higher at the last phase before complete inactivation was achieved (see **Chapter 3.2**) although minimal or no killing was achieved with 10 ms of high power CO<sub>2</sub> before the surface was burnt. Conversely, due to the fluorescing irradiation effects of the UV lamps, the microorganisms were inactivated in a more predictable gradual manner while the microwave radiation exhibited intermediary killing.

#### **4.1.4.1 Sub systems**

##### *CO<sub>2</sub> laser*

A possible approach to increase the killing effect with the laser is to decrease the power and increase the exposure time. It has been demonstrated that with the same energy density applied, the efficacy was higher with 380 to 980 W laser irradiation (**Section 3.1**). This could be due to the compound heat generated over a longer time of exposure, which enhanced the inactivation process on the microorganisms. However, with an extended study, the optimum killing parameters of the laser could be better achieved.

Microbial reduction on fruit samples with laser irradiation can be attributed to the physiological shape and texture of the fruit sample. As with apple, a 0.3 D-value reduction was observed which indicated that more radiation must have been absorbed and rendered the microorganisms inactive; whereas no killing was observed with potato and tomato samples. As observed, the surface of the apple was

much smoother and comparatively more reflective than the other two contaminated substrates. The crumpled and wrinkled surfaces of the cut tomato samples could also prevent direct laser-bacteria interaction.

### *Microwaves*

At any instant, the radiation on each given area of treated sample was unequal due to the rotating action of the pyrex dish and the nature of the microwave field pattern. This could account for the high SEMEAN calculated over 4, 5 and 6 separated experiments conducted for tomato, apple and potato respectively. Nevertheless, viable reduction was achieved for all treated samples.

### *Ultra-violet*

The visible tolerances of the microbial seeded substrates were independent of the UV dosage applied, unlike the response with microwaves or lasers. The maximum UV energy density applied was  $40 \text{ mJcm}^{-2}$  with 80 s exposure time. With potato samples, the bacterial population was constant after 40 s of UV exposure. Due to the 'eyes' of the potato surfaces, the microorganisms were able to penetrate into the skin, which shielded the UV radiation. Since the number of 'eyes' of the random potato samples was unequal from one sample to the next, this could account for the inconsistency of the bactericidal effect with UV light. With tomato and apple samples, the epidermis were less porous, resulting in incremental bactericidal effects with increasing UV dosage. Although the 'eyes' hindered the radiation effect, increase the intensity and energy density will increase the probability of killing.

#### **4.1.4.2 Combined system**

There was no significant killing with the laser set to low power (380 W) and 10 ms pulse length. This exposure, however, was used in the combined treatment process to see if significant killing could be achieved with little killing from the sub-system, but with an enhanced effect above that of the microwaves and ultraviolet.

### *Simultaneous effect*

The combined test with potato samples gave an equivocal result as there was an increase in the effect of laser treatment alone, boxplot 1, but a slight decrease in the result of UV treatment alone, boxplot 3. However, with apple and tomato samples the conditions of this trial produced the best results with the combined treatment, boxplots 8 and 12. It was noticed that the results of repetitive experiments showed test values within a narrow range. This series of experiments revealed that the unit parts of the system were less effective than the combined treatment. The results also indicated that the variable response to the microwave field was reduced in the combined treatment. This implied that for the same level of killing, the thermal load could be reduced with the combined system as compared to the microwave or laser alone.

In any conventional microwave oven, the incident electro-magnetic field waves are unequal in the cavity. This is why microwaves have rotating tables to enhance equal distribution of its radiation on treated food. Thus from the results above, the combined system development has important implications. For example, the uniformity of the field from the microwave source will not be such a critical design issue.

### *Sequential effect*

The results with the apple indicate that the dose of UV irradiation gives complete inactivation of the organisms. This was probably because the irradiance from the UV lamps was found to be dependent on the warm up time. For the simultaneous treatment process, the warm up time was less than for the sequential treatments. However it is noticeable that the effect was not additive with microwave and then laser or laser and then microwaves. The experiment shows that there is a need to explore further the relationship observed with the three treatments applied simultaneously in the combined experiment mentioned above.

**V. MICROWAVE  
IRRADIATION ON  
*STAPHYLOCOCCUS*  
*AUREUS***

## 5.1 HEAT TRANSFER ANALYSIS OF *STAPHYLOCOCCUS AUREUS* ON STAINLESS STEEL WITH MICROWAVE IRRADIATION

### 5.1.1 INTRODUCTION

With the work done in **Section 4**, understanding the bactericidal effects of microwaves and its mechanism will enhance the combined system's sterilisation process. Moreover, the kinetics of microbial killing with microwave radiation are not understood fully. It is believed that the microorganisms absorb microwave energy, resulting in thermal death (Corelli *et al.*, 1977; Jeng *et al.*, 1987). Interestingly, it was suggested in several reports that there exists a significant temperature difference between particles and suspension liquid medium with thermal treatments in several food processing applications (Amato and Tien, 1972; Culkin and Fung, 1975; Fernandez *et al.*, 1988; Harrison and Carpenter, 1989). Sastry and Palaniappan (1991) suggested that the bactericidal effects with microwaves were due to the fact that the temperature rise in the microorganisms was higher than that of the surrounding medium but no experimental investigation was done. The Expert Panel on Food Safety and Nutrition has referred to this explanation in their Scientific Status Summary (1989), stating that "...it is not possible to prove or disprove such claims, since the internal temperature of a bacterial cell cannot be measured accurately...".

This work reported in this section of the thesis was done to investigate and understand the transient heat transfer mechanism of *Staphylococcus aureus* microorganisms with its suspending liquid medium and underlying substrate (stainless steel disc) when irradiated with 2450 MHz microwave radiation. There were two objectives in modelling the microwave-bacteria interactions. First, to establish the heat transfer relationship between *S. aureus* and the surrounding liquid medium (distilled water) due to the microwave radiation. Second, to calculate and compare the temperature rise due to the direct heat transfer to the microorganisms from the microwave irradiation to that caused via heat conduction from the microwave-heated stainless steel underlying substrate in the microwave oven.

## 5.1.2 MATERIALS AND METHODS

### 5.1.2.1 Bacterial samples

The preparation of the culture samples and stainless steel discs can be found in **Section 2.2.2.1** and **3.1.2.1**. The viability assessment of the microorganisms was described in **Section 3.1.2.3**. The stainless steel discs (AISI 316) were 15 mm in diameter and 5 mm thickness.

### 5.1.2.2 Microwaves

A conventional microwave oven, with a capacity of 0.7 cubic ft (800 W, SANYO EM S153) operating at 2450 MHz was used. The bacterial suspension in sterile distilled water or sterile nutrient broth (15  $\mu$ l), were pipetted onto the surface of the stainless steel disc prior to microwave irradiation. The samples were placed on a microwavable pyrex glass dish, aseptically cleaned with 70% v/v ethanol, with sterile forceps and placed at the centre of the rotating glass plate.

### 5.1.2.3 Temperature measurements

Temperature adhesive indicators (RS Components, U.K.) of 14 mm diameter were placed on the stainless steel disc to record the temperature rise due to microwaves as a function of exposure time. These sensors changed to black irreversibly depending on the surface temperature with accuracy to  $\pm 1$  °C below 100 °C with less than 1 sec response time. With the inoculum, sterile distilled water and sterile nutrient broth, the temperatures recorded were assumed to be that of the interface temperature between the temperature indicator and the liquid. The linear rate of temperature rise (based on least square linear fitting),  $R_T$ , of stainless steel discs, stainless steel discs with bacterial inoculum, nutrient broth and distilled water were tabulated.

#### 5.1.2.4 Heat transfer analysis

##### *Thermal heat conduction*

The power absorbed,  $Q$ , by the stainless steel disc and bacterial-liquid suspension in one-dimensional steady state heat conduction, assuming no heat losses, is governed by;

$$Q = k A \frac{dT}{dx} \quad (5.1.1)$$

where  $k$  is the thermal conductivity,  $A$ , area and  $x$ , effective heat transfer width.

For stainless steel  $k=16.3 \text{ Wm}^{-1}\text{K}^{-1}$  and was taken as being independent over the range of temperature investigated. The thickness of the discs was 5 mm. The thermal properties of the inoculum was taken as that of distilled water and varied with temperature, i.e. the  $k$  values at 50, 55, 60 61.4 and 65 °C are 0.643, 0.648, 0.653, 0.654 (interpolated) and 0.658  $\text{Wm}^{-1}\text{K}^{-1}$  respectively (Rogers and Mayhew, 1988) while  $x$  is defined as the radius of the zone of the bacterial sample; 1.93 mm.

##### *Lumped analysis*

Due to the microscopic size of the bacterium, it was assumed that the resistance to heat conduction within the microorganism was small compared with the resistance to heat transfer between the microorganism and the distilled water. Such a phenomenon can be quantified by the 'lumped heat analysis' method to determine the time dependent energy absorption rate of the bacteria and its surrounding liquid (distilled water) under the conditions for which the temperature gradient within the microorganism is small or negligible. Such analysis assumes fundamental Newtonian heating and cooling with 'Biot number' less than 0.1 (Alhamdan *et al.*, 1990).

When the 15  $\mu\text{l}$  inoculum sits on top of the stainless steel disc in the microwave (wet sample), it was assumed to be hemispherical in shape. The distilled water and

microorganism are assumed to heat at different but uniform rates of energy absorption. A low Biot number was assumed in the calculations due to the fact that the organism is of microscopic size (Eastop and McConkey, 1986).

The transient temperature response was determined by formulating an overall energy balance on the microorganism such that: *"The sum rate of energy absorbed by the microorganism per unit volume was equal to the rate of change of the internal energy and heat loss through convection to the surrounding medium"*

The rate of temperature rise,  $dT/dt$ , of the microorganism (with subscript 'm' representing microorganism), can then be represented by,

$$q_m V_m = \rho_m C_{p_m} V_m \frac{dT}{dt} + h_m A_m [T - T_f] \quad (5.1.2)$$

where  $q_m$ ,  $V_m$ ,  $\rho_m$ ,  $C_{p_m}$ ,  $h_m$  and  $A_m$  are the energy absorption rate per volume (absorbed power density), volume, density, specific heat capacity, convective heat transfer coefficient and cross sectional area of the bacterium respectively. The final equilibrium temperature,  $T_f$ , of the bacteria-liquid sample, can be determined from the following energy analysis of the surrounding liquid medium (distilled water) assuming negligible heat losses,

$$q_l = \rho_l C_{p_l} \frac{dT_f}{dt} \quad (5.1.3)$$

where  $q_l$  is the power density;  $\rho_l$ , density of water; and  $C_{p_l}$ , the specific heat capacity of distilled water. Solving **Eqn. 5.1.3** yields,

$$T_f = \frac{q_l t}{\rho_l C_{p_l}} + T_i \quad (5.1.4)$$

where  $T_i$  is the initial temperature of the bacteria-liquid sample. Substituting **Eqn. 5.1.4** into **Eqn. 5.1.2** gives,

$$\frac{dT}{dt} = \frac{q_m}{\rho_m C_{p_m}} - \frac{h_m A_m}{\rho_m C_{p_m} V_m} \left[ T - \frac{q_l t}{\rho_l C_{p_l}} - T_i \right] \quad (5.1.5)$$

re-arranging;

$$\frac{dT}{dt} + \frac{h_m A_m T}{\rho_m C_{p_m} V_m} = \frac{q_m}{\rho_m C_{p_m}} + \frac{h_m A_m}{\rho_m C_{p_m} V_m} \left[ \frac{q_l t}{\rho_l C_{p_l}} + T_i \right] \quad (5.1.6)$$

**Eqn. 5.1.6** is solved (**Appendix 9.1**) by means of integrating factors which yields,

$$T = \frac{q_m V_m}{h_m A_m} + T_i + \frac{q_l t}{\rho_l C_{p_l}} - \frac{q_l}{\rho_l C_{p_l}} \frac{\rho_m C_{p_m} V_m}{h_m A_m} + \left( \frac{V_m}{h_m A_m} \right) \left[ \left( \frac{\rho_m C_{p_m}}{\rho_l C_{p_l}} \right) q_l - q_m \right] \exp \left\{ - \left[ \frac{h_m A_m t}{\rho_m C_{p_m} V_m} \right] \right\} \quad (5.1.7)$$

Subtracting **Eqn. (5.1.4)** from **Eqn. (5.1.7)**, the temperature difference between the microorganism and its surrounding liquid medium can be found, and is given by,

$$T - T_f = \left( \frac{r_m}{3 h_m} \right) \left[ q_m - q_l \left( \frac{\rho_m C_{p_m}}{\rho_l C_{p_l}} \right) \right] \left\{ 1 - \exp \left( \frac{-3 h_m t}{r_m \rho_m C_{p_m}} \right) \right\} \quad (5.1.8)$$

where  $r_m (=V_m/A_m)$  is the radius of the microorganism.

The properties of the microorganism,  $\rho_m$  and  $C_{p_m}$ , and that of the distilled water,  $\rho_l$  and  $C_{p_l}$ , are temperature dependent. The value of the specific heat capacity will be of the same order for both the microorganism and distilled water; taking into consideration that the temperature concerned is less than 100°C. During irradiation, the density of the microorganism is expected to increase with decreasing moisture content while the specific heat would increase with increasing water content. Thus the ratio of  $\rho_m C_{p_m}$  to  $\rho_l C_{p_l}$  can be set to unity (Sastry and Palaniappan 1991), yielding,

$$T - T_f = \left( \frac{r_m}{3h_m} \right) [q_m - q_l] \left\{ 1 - \exp \left( \frac{-3h_m t}{r_m \rho_m C_{p_m}} \right) \right\} \quad (5.1.9)$$

In all cases, because of the microscopic radius of the microorganism, approximately 1  $\mu\text{m}$ , the exponential time expression in **Eqn. 5.1.9** can be reduced infinitesimally; which simplifies to,

$$T - T_f = \left( \frac{r_m}{3h_m} \right) [q_m - q_l] \quad (5.1.10)$$

Therefore, the power density difference ( $q_m - q_l$ ) of bacteria and distilled water (surrounding suspending liquid medium) needed to obtain a 1  $^{\circ}\text{C}$  temperature difference can be found; reducing **Eqn. 5.1.10** to,

$$q_m - q_l = \frac{3h_m}{r_m} \quad (5.1.11)$$

The ratio of absorbed power density for the microorganism to the surrounding distilled water,  $q_m / q_l$  is given by;

$$\frac{q_m}{q_l} = \frac{3h_m}{q_l r_m} + 1 \quad (5.1.12)$$

Thus at each temperature reached due to microwave irradiation,  $q_m$  and  $q_l$  can be determined.

### 5.1.3 RESULTS

Complete bacterial inactivation was achieved in 110 s with microwave radiation on the bacterial suspension at 61.4  $^{\circ}\text{C}$ . Similar comparisons at this temperature were made with temperature measurements without the inoculum for: sterile distilled water; broth; and sterile stainless steel discs, obtaining at 65, 102 and 114 s

respectively (**Figure 5.1.1**). It can be seen that the nature of the prepared inoculum in sterile distilled water affects the rate of temperature rise,  $R_T$ , with microwave radiation as compared with distilled water and broth solution alone (**Table 5-1-1**). Due to the metallic nature of stainless steel, the  $R_T$  was low ( $0.3\text{ }^\circ\text{C s}^{-1}$ ) whereas that of the broth and distilled water have corresponding  $R_T$  values of  $0.5$  and  $0.4\text{ }^\circ\text{C s}^{-1}$  respectively.

The shape of the inoculum drop was assumed to be a hemisphere sitting on the stainless steel disc. With an inoculum volume of  $15\text{ }\mu\text{l}$  ( $1.5 \times 10^{-8}\text{ m}^3$ ), the effective radius was calculated to be  $1.53 \times 10^{-3}\text{ m}$ . The initial temperature was taken at  $20\text{ }^\circ\text{C}$  prior to microwave exposure. With increasing exposure time, the power conducted through the stainless steel and inoculum increased with temperatures, **Table 5-1-2**. Due to the small volume, both the stainless steel disc and inoculum exhibited low power density values. Nevertheless, the relative different rate of thermal conduction between the inoculum and stainless steel disc was significant at each respective temperature; for example, the stainless steel disc conducts approximately 145 times more than the bacterial-heated sample. Full sterilisation corresponded with thermal absorption power at  $23.8\text{ W}$  for stainless steel disc and  $0.16\text{ W}$  inoculum were achieved.

The value of  $h_m$  was dependent on the heat flow conditions on the microorganism. It is a time-temperature variable which can only be determined empirically.

Reasonably, it is assumed to range between  $100$  to  $500\text{ Wm}^{-2}\text{K}^{-1}$  in this analysis (Alhamdan *et al.* 1990) taking into account that the microorganism is suspended in over 90 % by weight of sterile distilled water. The result of the power densities of  $q_m$  and  $q_l$  was calculated at  $50$ ,  $55$ ,  $60$  and  $65\text{ }^\circ\text{C}$  as these were shown to be lethal temperatures, **Figure 5.1.1**. With the corresponding  $q_l$  (**Table 5-1-2**) and taking the radius of the microorganism to be  $0.5\text{ }\mu\text{m}$  ( $5.0 \times 10^{-7}\text{ m}$ ), the respective power density ratios of microorganism to distilled water are shown in **Table 5-1-3**. The rate of energy absorption of *S. aureus* microorganism is at least 51 times more than its surrounding medium and increases with the increasing  $h_m$  assumed. In all cases, the ratio of  $q_m/q_l$  decreases with increasing temperature for a given  $h_m$  but increases

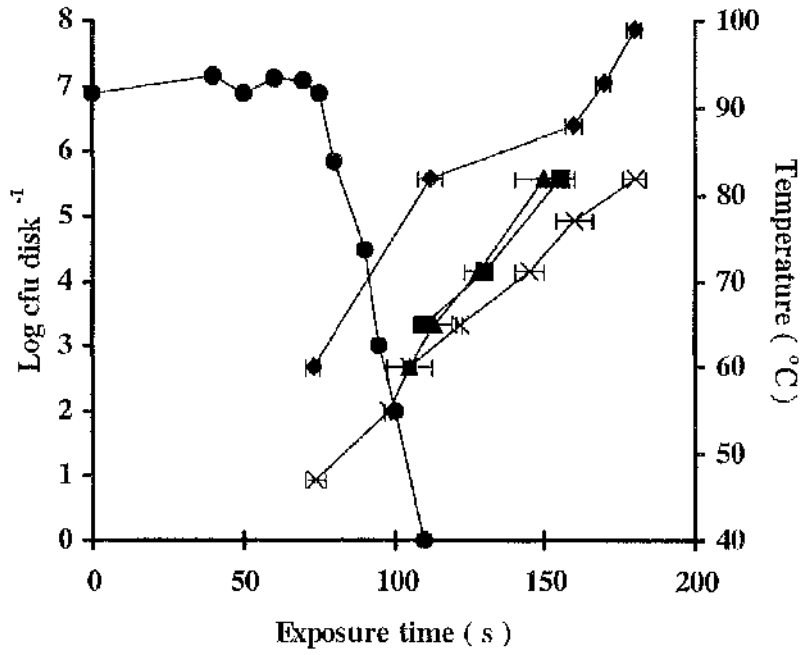


*Figure 5.1.1* Representation of cell viability, ● (primary, left y-axis) and temperature measurements (secondary, right y-axis) of stainless steel, ◆; with broth, ▲; distilled water, ■ and bacteria-liquid suspension, × against microwave exposure time.

**Table 5-1-1** Rate of temperature rise,  $R_T$ , with and without culture broth, distilled water or inoculum on stainless steel disc.  $R_T$  is based on a least square linear regression approximation of the data obtained from **Figure 5.1.1** .

	Stainless steel disc with:			
	Un-inoculated	Broth	Distilled water	Inoculated
Rate of temperature rise, $R_T$ ( $^{\circ}\text{C}\cdot\text{s}^{-1}$ )	0.3	0.5	0.4	0.3

with increasing  $h_m$  for a particular temperature. However, at all temperatures, the power density ratio difference between  $h_m$  of 100 and 500  $\text{Wm}^{-2}\text{K}^{-1}$  was approximately 5 times. Total cell reduction was seen with  $q_m$  ranging from 56 to 274 times more than its surrounding liquid at 61.4 °C.

#### 5.1.4 DISCUSSION

It is worthwhile to know that for a given power input with different volumes of inoculum or substrate used with microwave exposure there would be different rate of temperature rise. A larger volume mass of liquid generally absorbs more microwaves power than smaller ones. However, a larger mass will usually take longer to heat in a microwave cavity as more time will be needed for conduction to cause the temperature gradient to equilibrate. The rate of temperature rise or energy absorbed increases with lesser volumes of sample used. It was reported that less microwave energy would be absorbed with increasing temperature and exposure time in pure water (Ohlsson 1983).

The exposure time required to raise the temperature to 61.4 °C was 65 s for sterile distilled water and 102 s for broth solution. However, the resuspended bacterial sample in sterile distilled water took 110 s, shown **Figure 5.1.1**. Thus the rate of temperature rise is significantly different and smaller with sterile distilled water and nutrient broth alone when compared to the bacterial-suspension sample. This implies that the microorganisms themselves possess thermal properties which are directly involved with microbial destruction. Moreover, the results showed that the microorganisms absorb microwave thermal heat at a much greater rate than the surrounding liquid medium. The thermal conductivity of a bacterium is believed to be of several orders higher than sterile distilled water. The power conductance of the stainless steel was many times higher than the inoculum which suggests that the bactericidal action is more likely to be due to the heating conducted from the stainless steel to the inoculum. Also, the density affects the rate of temperature rise with microwaves which determines the viability of the microorganisms; since the resuspended inoculum was denser than the distilled water and nutrient broth.

Moreover, the rate of temperature rise was rapid for such a small volume, 15  $\mu$ l of inoculum which accounts for the rapid sterilisation after 110 s. Although the microbes absorb many times faster with thermal conductivity of several orders of magnitude higher than the liquid suspension, the relative time taken for sterilisation is longer. It is believed to be due to the extremely low percentage of dry weight of the microorganisms to liquid suspension.

As the temperature increases, the absorbed power density of the liquid medium increases at a rate higher than that of the microorganism, thus reducing the ratio as the temperature rises. This phenomenon can be explained since the cellular constituents were exposed to gradual thermal increment effects and final lethal temperatures 61.4 °C or greater.

Thus full inactivation of  $8 \times 10^6$  cfu of *S. aureus* was achieved at 61.4 °C with the conventional microwave oven. *S. aureus* possesses thermal properties which allow the absorption of the thermal microwave heat at least 51-fold greater than its suspending sterile distilled water medium at 65 °C. Heat transfer via conduction through the underlying stainless steel substrate inactivates the microbes with lethal microwave exposures.

**Table 5-1-2 Comparison of power and power density conducted through stainless steel disc and inoculum with increasing temperature and microwaves irradiation. ' \* ' denotes the temperature at which complete sterilisation of approximately  $8.0 \times 10^6$  cfu *S. aureus* bacteria was achieved.**

Heat conduction				
Temperature (°C)	Stainless steel disc		Inoculum	
	Power, $Q_{ss}$ (W)	Power density, $q_{ss}$ ( $Wm^{-3}$ )	Power, $Q_{ino}$ (W)	Power density, $q_{ino}$ ( $Wm^{-3}$ )
50	17.3	$1.9 \times 10^7$	0.12	$8.0 \times 10^6$
55	20.2	$2.3 \times 10^7$	0.14	$9.3 \times 10^6$
60	23.0	$2.6 \times 10^7$	0.16	$1.1 \times 10^7$
61.4*	23.8	$2.7 \times 10^7$	0.16	$1.1 \times 10^7$
65	26.0	$2.9 \times 10^7$	0.18	$1.2 \times 10^7$

**Table 5-1-3** Energy absorption rate ratio of *S. aureus* microorganism to its surrounding suspending liquid, sterile distilled water,  $q_m/q_l$ , with microwave irradiation at 50 to 65 °C. The calculated ratios assumed a temperature difference maintained at 1 ° between the microorganism and the suspending sterile distilled water. ' \* ' denotes the lethal condition in which complete bacterial inactivation occurred.

Convective heat transfer coefficient, $h_m$ ( $Wm^{-2}K^{-1}$ )	Power density ratio, $q_m/q_l$				
	50°C	55°C	60°C	61.4°C*	65°C
100	76.0	62.2	55.5	55.5	51.0
200	150.0	123.4	110.1	110.1	101.0
300	226.0	184.7	164.6	164.6	151.0
400	301.0	245.9	219.1	219.1	201.0
500	376.0	307.1	273.7	273.7	251.0

**VI. LASER SPECKLE FOR  
CONTROLLING &  
MONITORING  
CONTAMINATION  
SYSTEM**

## 6.1 BIODYNAMIC LASER-BACTERIA SPECKLE INTERACTION

### 6.1.1 INTRODUCTION

When diffuse objects are illuminated with laser light, a characteristic granular pattern is seen in the reflected or transmitted light (Rigden and Gordon, 1962). This effect is known as speckle. Fundamentally, it is caused by interference between light scattered from adjacent points on the object (Goodman, 1975 and 1963). This pattern may be observed either in the near or far field by intercepting the light scattered from the surface. An object that moves as a whole or movements caused by microscopic components with a certain velocity in its constituents will result in an orderly structured speckle pattern formation. As such, living objects produce dynamic speckles that generally fluctuate in a space-time random fashion owing to the complex and inconsistent physiological activity of its constituent/s.

Laser speckle effects can be determined statistically (Briers, 1993). The statistical properties of speckle can be divided into the first-order statistics, which describes the contrast of the speckles, and second-order statistics, which describes the size distribution and inter-pixel correlation of the speckles. Efforts have been made in applications based on speckle fluctuation properties including laser doppler velocimetry (Riva *et al.*, 1972; Tanaka *et al.*, 1974; Stern *et al.*, 1977; Riva *et al.*, 1989), use to measure the blood flow in major human organs. In some medical establishments, techniques based on speckle phenomenon have become almost a routine tool to discriminate between arterial and capillary blood flow (Gush and King, 1991). However both the above described methodologies using speckle involve substantial, sophisticated and expensive equipment.

From studies carried out by Zheng *et al.* (1994), information related to the vitality and identity of Gyrodinium and Salmonella cultures could be extracted from the dynamical and statistical characteristics of the observed speckle phenomenon. With speckle applications such as time correlation length  $T_c$  of the time-varying

autocorrelation function applied, positive indication of the motility and vitality of microbiological species were reported. Work has also been carried out by Xu *et al.* (1995) using various speckle techniques on botanical specimens such as orange, tomatoes and radishes, where these techniques were shown to exhibit information about the shelf-life and ageing of these specimens due to the state of living cells present on and in them.

Conventionally, different microbial disinfectants are known to inactivate different genera of microorganisms and the strength of such disinfectants are based more often than not, on the concentration needed rather than on how fast the inactivation on the microbial species takes place. Present day methods of characterising and monitoring the microbial communities are generally known to be time-consuming and often ambiguous (Zheng *et al.*, 1994). Techniques for overcoming these difficulties are in general, in their infant stage. Thus, no elucidatory time varying definitions have been made on the exact state of microbiological activities of the species when in contact with disinfectant with respect to time.

In this report, speckle patterns are used to provide an inexpensive and distinctive alternative method to model the state of biological activities using time varying dependent analysis in *E.coli* liquid suspension with and without Hibitane disinfectant solution with a hybrid opto-electronic system. Most microscopic sectioned sample techniques are destructive, this may interfere with the life process of the sample; speckle methodology, however, is non-invasive. The system constructed enabled the biospeckles to be captured through transmission of laser beam and seen on a TV monitor with a CCD camera. Unlike normal plating technique (i.e. Miles & Misra method) which requires 24 hr incubation period and only then exhibits the surviving colonies forming unit, the speckle analysis provides almost instant analytical imaging results and vital information about the living organisms within minutes. Such method is only limited by the speed of the computer hardware and software in the present cases.

## 6.1.2 MATERIALS AND METHODS

### 6.1.2.1 Experimental Set-up

The experimental set-up was shown in **Figure 6.1.1**. A continuous (CW) 10 mW, He-Ne laser was used as the source of illumination operating at 632.8 nm wavelength. This was focused onto a curvette (semi-micro visible 1938) sample. The transmitted and scattered rays from the curvette were detected by the CCD camera which interfaced to an image processing system. The images of the biospeckle can be observed directly on a TV monitor. After being digitized with an analog to digital converter and frame grabber, the biospeckles can be evaluated by the image processing system in the computer to extract its characteristic. The resolution of the CCD camera was 768 X 572 pixels, each pixel being 13  $\mu\text{m}$  X 13  $\mu\text{m}$  in size. The present imaging system used consisted of a 2 Dimensional CCD Camera with a scan rate of 70 Hz, interfaced to a computer with an image processing program. The experiments were conducted on an optical bench.

### 6.1.2.2 Data Acquisition of Spatial Time Speckle (STS) pattern

#### *STS Pattern*

The CCD camera, interfaced to an image processor in a variable scan mode, was used for measuring the spatial intensity distributions of the speckle patterns. A two-dimensional image was constructed in the memory of the image processor with the horizontal axis displaying the intensity distribution of the scanned line of the image and the vertical axis representing the time evolution of the fixed line image. Such line records showed both the spatial and temporal characteristics of the time varying speckle and therefore can be referred to as the space-time speckle (STS) patterns (Briers, 1975), **Figure 6.1.2**.

STS patterns combine the spatial and temporal features of the time varying speckle pattern in a single two-dimensional image. Its x-direction (horizontal-direction) consists of 128 pixels which records the spatial intensity distribution of one fixed line of speckles in the speckle pattern per time instant, and its y-direction (vertical-

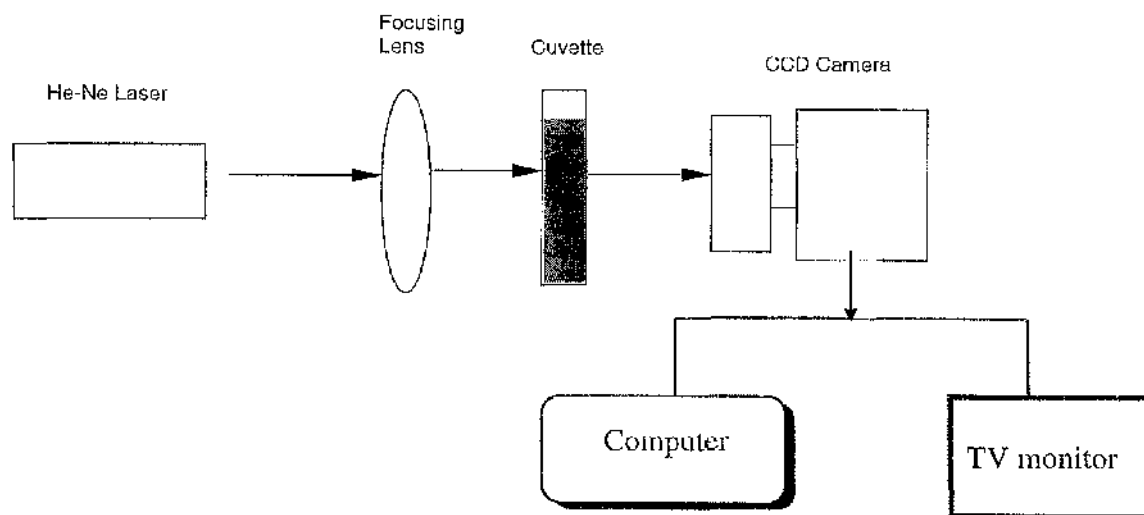


**Figure 6.1.1** Experiment set-up for detecting the state of bioactivity in *E. coli* suspension with and without disinfectant solution.

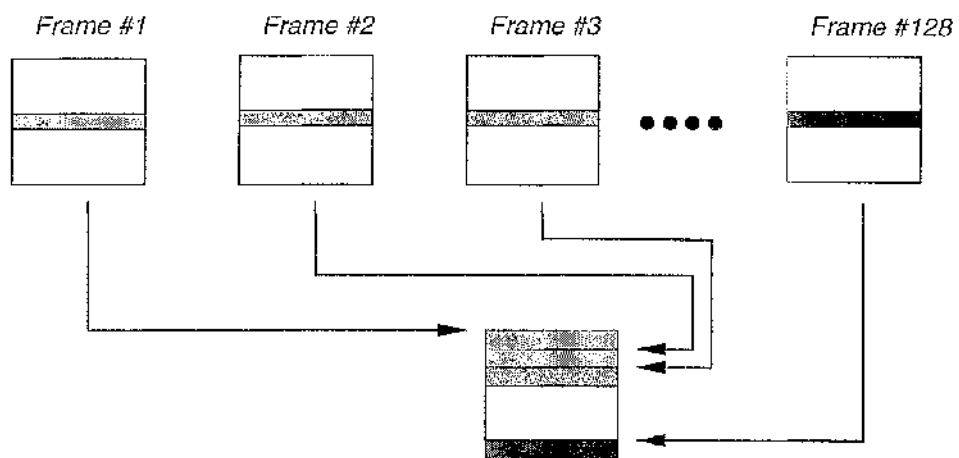


*Figure 6.1.2* From each frame, each horizontal line consisting of 128 pixel at 25<sup>th</sup> position was extracted (at 3 s interval) and group to form a resultant STS image which contains both spatial and temporal information.

direction), of 128 pixels which records the temporal evolution of the biospeckles formed. Thus in the present case, a STS pattern will have a matrix of 128 by 128 pixel domain.

### ***Data Acquisition***

A line frame region of interest (ROI) was selected to capture a line spatial intensity profile with time using a Dynamic Data Exchange (DDE) macro in 'OPTIMAS' software. Intervals of 3 s was set to capture a total of 128 temporal line images and stored into the buffer memory. The time taken for a full STS image formed was 6.4 min. The 128 temporal line images will be retrieved and grouped to form the matrix of 128 by 128 pixel by extracting the buffer memory.

### ***Data Transfer***

The intensity of each pixel was transported to 'EXCEL 5.0' software to be converted to numerical values written in DDE macro code using 'OPTIMAS' software.

### ***Image Processing***

Arrays of both spatial and temporal intensity distribution will be transported as text files to 'MATHCAD professional 6.0' software for statistical analysis.

## **6.1.2.3 Sample Preparation**

*E. coli* B 10537 microorganisms were used and the preparation protocol was as described in Section 2.2.2.1. For each experiment, a fresh pipetted volume of 0.9 ml of fresh bacterial culture was mixed with 2.7 ml of the respective concentration of disinfectant solution in cuvettes; volume ratio of 1:3.

## **6.1.2.4 Hibitane Disinfectant solution**

Hibitane, consists of chlorhexidine gluconate 5% w/v (equivalent to Chlorhexidine Gluconate solution Ph. Eur. 25 % v/v), which is an antimicrobial solution for general antiseptic purposes like disinfection of wounds and burns or swabbing on patients at a dilution rate of 1 in 2000 aqueous (0.05 % w/v). It is one of a family of  $N^1$ ,  $N^5$ -substituted biguanides which has emerged from synthetic and screening studies

primarily by research workers at Imperial Chemical Industries (Curd and Rose, 1946; Davies *et al.*, 1954; Rose and Swain, 1956). It is also suitable for normal microbiological laboratory clean ups and storage of sterile instruments with sodium nitrite (1g per litre) to prevent corrosion. In all descriptions throughout this thesis, concentrated disinfectant solution will mean undiluted Hibitane.

#### **6.1.2.5 Optical Density (OD) Measurement**

The absorbency of the sample in the curvette was measured with UV/VIS spectrometer (UNICAM 8625) at 600 nm wavelength. The absorbency of the sample was given by the logarithmic ratio of the percentage of the incident intensity over the transmitted intensity. For example, a 1 % transmitted intensity yields a high absorbance value of 2. For pure *E.coli* suspension, sterile saline was used as blank whilst concentration strength of 1/6000, 1/4000, 1/40 and concentrated disinfectant were used as blank for mixture of *E.coli* with 1/6000, 1/4000, 1/40 and concentrated disinfectant solution respectively for obtaining the absorbance values. Experiments with 1/6000, 1/4000, 1/40 and concentrated disinfectant against blank sterile saline were also carried out to measure the absorbance values.

#### **6.1.2.6 Laser Speckle Statistical Analysis Techniques**

The structure of the analysis can be broadly divided into two speckle techniques, namely first order speckle contrast,  $c_1$  (dimensionless) and second order temporal decorrelation speed,  $V_{uk}$  ( $s^{-1}$ ) with each giving results of a series of experiments conducted with *E. coli* suspensions combined with various concentrations of Hibitane solution.

##### ***First-Order Statistics analysis: Spatial Contrast Analysis***

Speckle is an interference effect, it was assumed that any movement of the experimental sample producing the speckle patterns resulted from differences in the relative phases between light scattered and absorbed from different points and angles on the sample. Similar implicit deductions can also be made with the laser beam angle of incidence and whether any external light has an adverse effect on the speckle. As such, all experiments were conducted in minimum external light

conditions with precise optical alignment to avoid inconsistency and the laser beam was incident normally to the surface of the bacterial-filled cuvettes.

The first-order statistics describe the properties of a speckle pattern point by point and it is independent between intensities at different points of a speckle pattern. In a fully coherent speckle pattern, the standard deviation,  $\sigma_I$ , of the (spatial) intensity variations is equal to the mean intensity of the pattern,  $\langle I \rangle$ . The ratio of the standard deviation to the mean intensity can be used as a measure of the contrast of the speckle pattern; this will, in practice, usually be less than unity (Perdersen 1974);

$$c_t = \frac{\sigma_I}{\langle I \rangle} \quad (6.1.1)$$

Hence for a fully developed speckle pattern the contrast is defined to be unity (Goodman, 1975; Briers, 1996) whereas a partially developed speckle patterns exhibit lower speckle contrast, with  $c_t < 1$ .

A total of 128 average spatial contrast values against 128 temporal horizontal line pixels was formed for any given sample tested.

### ***Second-Order Statistics:-Temporal Decorrelation speed effect***

Decorrelation of the mean speed of the global movement of the particles was used to compute the relationship between the intensity of the light and the velocity (Oulamara *et al.*, 1989).

A total of 128 block of STS images taken at successive interval of 3 s delay was captured by the system. Each block of images consists of 128 x 128 signal pixels. The arbitrary image row of interest was extracted at  $u^{\text{th}}$  line where the  $u = 25$  and each signal pixel line was taken to form the resultant 128 x 128 pixel STS image. Each pixel signal can then be represented by  $S_{k(i)}$  where  $k$  and  $i$  represents the row and column coordinates' system. The signals were then normalized by their energies, ie  $E_0, \dots, E_k$

$$(E_k)_u = \sum_{i=1}^N S_k^2(X_i) \quad k = 0, \dots, N-1; N = 128 \quad (6.1.2)$$

The signals were normalised signals, for example at the zero<sup>th</sup> pixel line, became:

$$^*S_0(X_i) = \frac{S_0(X_i)}{E_0} \quad i = 1 \text{ to } N \quad (6.1.3)$$

or in general, the 128 x 128 pixel formation takes the form of:

$$^*S_k(X_i) = \frac{S_k(X_i)}{E_k} \quad i = 1 \text{ to } N \quad (6.1.4)$$

The decorrelation coefficients  $C_{10}, C_{11}, C_{12}, C_{13}, \dots$ , and  $C_{1127}$  were computed as the square difference between the signals, the first being taken as a reference. For a given intensity  $I_u$  the coefficients were expressed by

$$(C_{1k})_u = \sum_{j=1}^{j=n} [^*S_0(j) - ^*S_k(j)]^2 \quad (6.1.5)$$

where  $k = 0, \dots, 127$ ;  $n$  and  $j = 1, \dots, 128$  with  $(C_{10})_u = 0$ . Consider successive delays  $(\Delta t), (2\Delta t), (3\Delta t), \dots, (128\Delta t)$ , from the instant  $t$ , and define the decorrelation speed as the ratio:

$$v_{uk}(t) = \left( \frac{C_{1k}}{k\Delta t} \right)_u \quad (6.1.6)$$

The resultant  $V_{uk}$ , was the computed intensity correlation of the whole 128 temporal lines of STS image pattern with respect to the first temporal horizontal pixel line having units of correlated intensity coefficient per unit time. As such, it is known as temporal decorrelation speed ( $s^{-1}$ ) (Oulamara *et al.*, 1989).

## 6.1.3 RESULTS

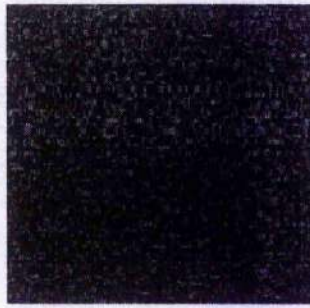
For the speckle patterns and  $C_t$  calculations, the viable count of the original culture was  $8 \times 10^9$  cfu ml<sup>-1</sup>. With the temporal decorrelation speed,  $V_{uk}$ , the viability was measured at  $8 \times 10^9$  cfu ml<sup>-1</sup> with 1/6000, 1/4000 and  $2 \times 10^8$  cfu ml<sup>-1</sup> with 1/40, concentrated Hibitane solution.

### 6.1.3.1 Spatial Time Speckle (STS) Pattern

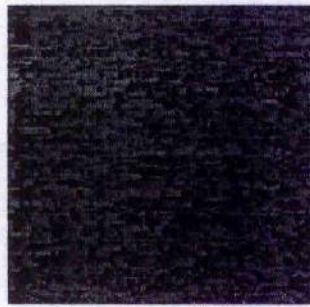
The 128 by 128 pixel STS patterns formed as described in Section 6.1.2.2 with various conditions with time are illustrated in Figure 6.1.3. The images are scaled between 0 to 255 grey levels.

Visibly, the intensity of the STS pattern images increased with concentration of disinfectant solution added. This phenomenon can be attributed to a higher level of scattering towards the CCD camera. The high fluctuation random image as shown in pure *E. coli* suspension was due to the high bioactivity movements and the overall darker image can be associated with the high absorption rate of the 632.8 nm He-Ne wavelength, such that less light was being transmitted and reached the imaging system. By contrast, adding clear concentrated disinfectant solution inactivates and inhibits the bioactivity of the microorganisms which results in a smoother, more orderly structured STS pattern image.

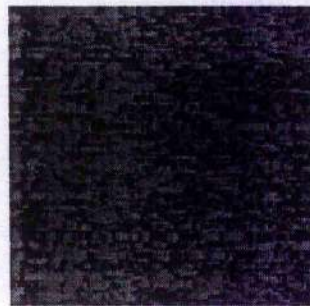
The similar phenomenon was also observed with increasing time for all the different concentrations added. The image intensity increased with time and concentration of disinfectant solution added. Clearly, visible contrast can be seen with 1/40 and concentrated disinfectant added over the time difference of 15 min due to anti-bactericidal effects. The random disorientation and distinct black and white spots were found with lower concentration of disinfectant added, compared with higher concentration with smoother and brighter appearance. Note that particular points on the speckle pattern appear dark or bright depending on whether the rays scattered from the object interfere destructively or constructively at that point.



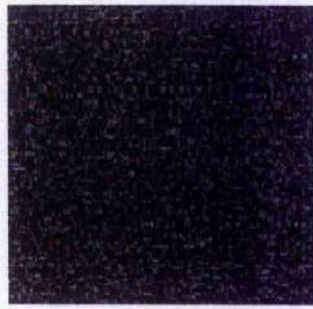
( a1 )



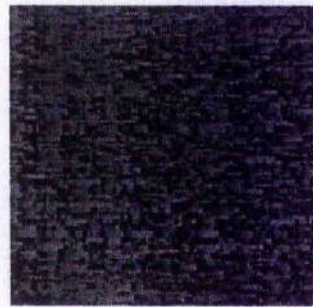
( b1 )



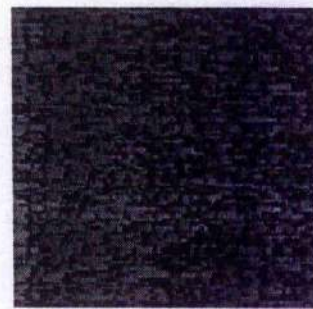
( c1 )



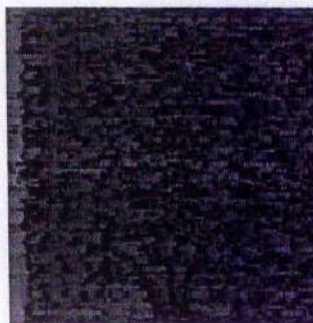
( a2 )



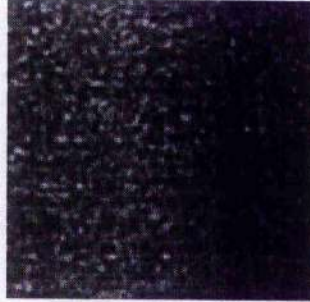
( b2 )



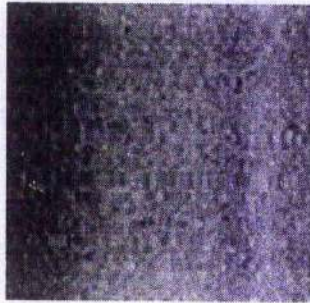
( c2 )



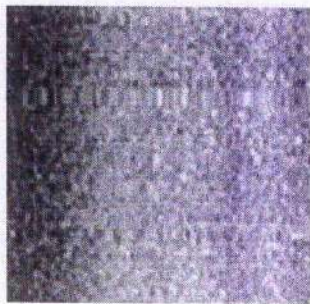
( d2 )



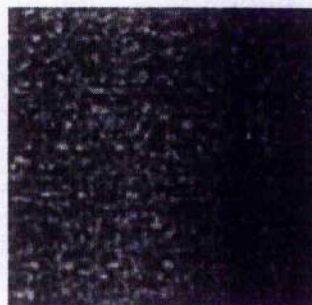
( a3 )



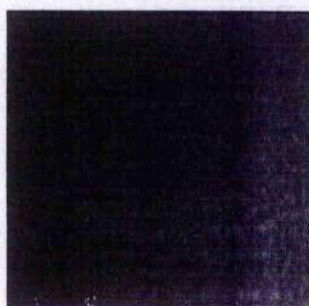
( b3 )



( c3 )



( a4 )



( b4 )



( c4 )

**Figure 6.1.3** STS patterns of *Escherichia coli* suspension with 1/6000 at T<sub>0</sub> (b1) and T<sub>30</sub> (c1) min; 1/4000 at T<sub>0</sub> (b2), T<sub>15</sub> (c2) and T<sub>30</sub> (d2) min; 1/40 at T<sub>0</sub> (b3) and T<sub>15</sub> (c3) min and concentrated Hibitane disinfectant solution at T<sub>0</sub> (b4) and T<sub>15</sub> (c4) min. The STS patterns of **Figure a1, a2 and a3, a4** correspond to  $8 \times 10^9$  and  $2 \times 10^8$  cfu ml<sup>-1</sup> *E. coli* suspension before treated with Hibitane solution.

### 6.1.3.2 Optical density measurements

Spectrometric work was carried out to investigate the optical density of *E. coli* suspension mixture with Chlorhexidine. **Figure 6.1.4** showed that pure *E. coli* suspension had a constant OD value of 1.902 with time over 30 min. With 1/6000 and 1/4000 concentration disinfectant solution added, the absorbant values decreased sharply to 0.654 and 0.684 respectively and remained almost constant after 30 min. However with 1/40 and concentrated concentration disinfectant solution, an increase was seen which implied that less transmitted light at 600 nm wavelength has occurred.

Further experiments were carried out on these four different concentrations against sterile saline as blank without *E. coli* suspension added to validate the dependency characteristic of the dilution and colour with absorbant values, **Table 6-1-1**. It can be seen that only 1/40 and concentrated disinfectant solution contribute a small fraction to the absorbency of *E. coli* mixture with the above mentioned disinfectant dilutions.

### 6.1.3.3 First-Order statistics analysis: Spatial Contrast Analysis

The random fluctuation of the contrast level can be seen with all mixture conditions over each STS image. An average contrast level value was calculated over the 128 spatial line pixel for each sample. High contrast level was observed with pure *E.coli* suspension as can be visually seen in the STS patterns with less intensity reaching the CCD camera and higher dilutions of Hibitane solution as seen in **Figure 6.1.5**.

When pure *E. coli* suspension was mixed with 1/6000 and 1/4000 concentration disinfectant solution added, the contrast level dropped from an average value of 0.721 to 0.522 and 0.508 respectively, **Table 6-1-2**. The same trend was also observed with 1/40 and concentrated disinfectant solution with contrast level dropping to 0.299 and 0.277 respectively, **Table 6-1-2**.

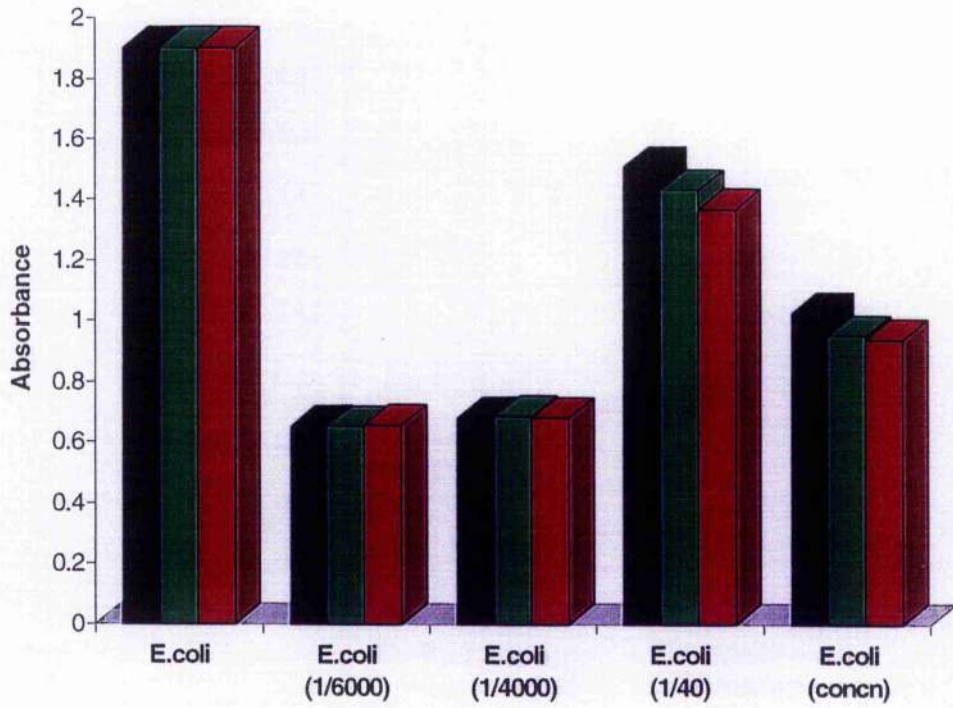


*Figure 6.1.4* Absorbance values for *E.coli* liquid culture with increasing concentration of HIBITANE disinfectant solution added at T<sub>0</sub> min ( ■ ), T<sub>15</sub> min ( ■ ) and T<sub>30</sub> min ( ■ ).

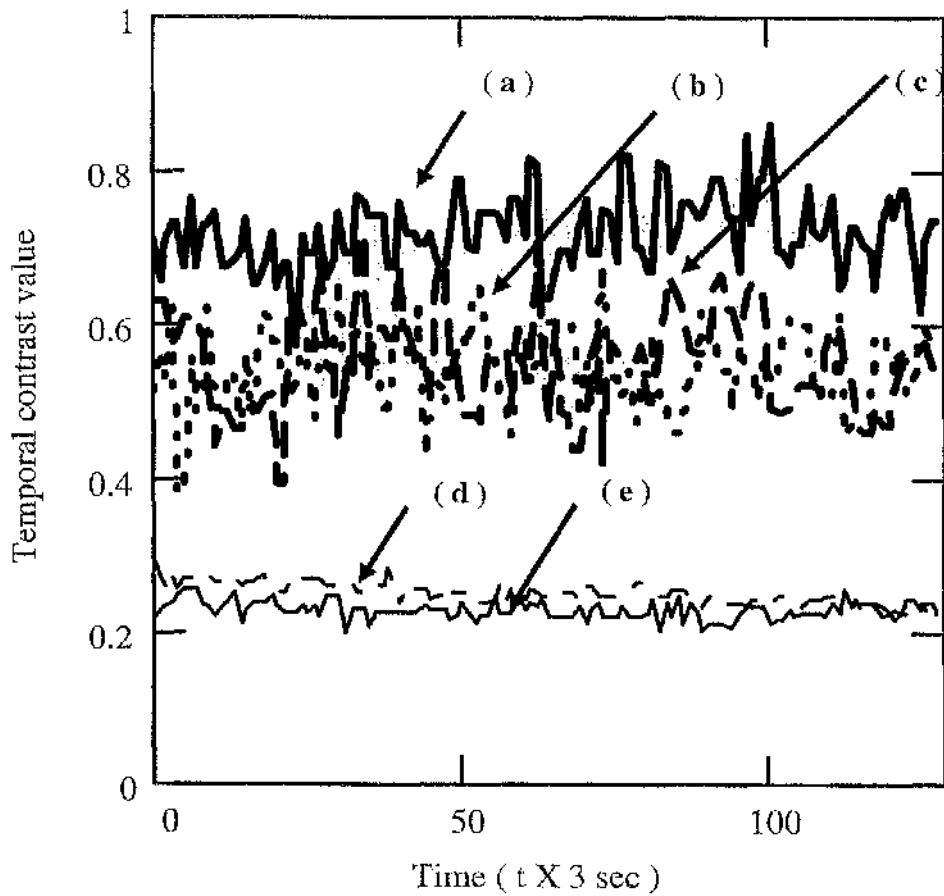


**Figure 6.1.5** Contrast level characteristics of pure *E.coli* suspension (a), with 1/6000 (b), 1/4000 (c), 1/40 (d) and concentrated (e) Hibitane disinfectant solution at  $T_0$  min corresponding to 128 temporal positions or array element number of 3 s interval.

**Table 6-1-1** Absorbant values measured at 600 nm wavelength of various dilutions concentration and concentrated HIBITANE disinfectant solution against sterile saline as blank.

Various HIBITANE disinfectant concentration	Absorbance
1 / 6000	0
1 / 4000	0
1 / 40	0.007
concentrated	0.174

With 1/6000 dilution added, a slight increase was observed at  $T_{15}$  min with  $c_t$  at 0.553. With 1/4000 dilution, intervals of 15 min were taken and the contrast levels were 0.521 and 0.545 at  $T_{15}$  min and  $T_{30}$  min respectively. As with 1/40 and concentrated disinfectant solution added,  $c_t$  were 0.25 and 0.227 at 15 min respectively.

#### 6.1.3.4 Second-Order statistics: Temporal decorrelation speed effect

Figure 6.1.6 shows the  $V_{uk}$  variations with time for 1/6000, 1/4000, 1/40 and undiluted disinfectant. The solid line represents the pure *E. coli* culture with cell viability of  $8 \times 10^9$  cfu ml<sup>-1</sup>. Figures 6.1.7, 8, 9 and 10 shows each dilution with *E. coli* over a time period of 30 min respectively. With 1/6000 and 1/4000 disinfectant solution dilutions added, there was a declining trend with  $V_{uk}$  at  $4 \times 10^{-8}$  and  $2.5 \times 10^{-8}$  s<sup>-1</sup> as compared with pure *E.coli* suspension at  $1.2 \times 10^{-7}$  s<sup>-1</sup> measured at the 5<sup>th</sup> temporal variation (15 s), Table 6-1-3.

With 1/40 and concentrated disinfectant added, a clear distinction was observed with a much smoother exponential decline as compared to the pure *E. coli* suspension. Due to the greater bactericidal effect with greater rate of inactivation of the cells, a drastic drop in  $V_{uk}$  was observed with values of  $1.7 \times 10^{-9}$  s<sup>-1</sup> and  $2.8 \times 10^{-9}$  s<sup>-1</sup> for 1/40 and concentrated dilutions as compared with pure *E.coli* suspension at  $3.8 \times 10^{-8}$  s<sup>-1</sup> respectively. With concentrated disinfectant, the temporal positions with the corresponding temporal decorrelation speed varies much the same at  $T_0$  and  $T_{15}$  min, Table 6-1-3.

### 6.1.4 DISCUSSION

The optical density measurement gave a good indication of the transmissivity and a good prediction of the extinction coefficient properties of the sample for different conditions as illustrated in Figure 6.1.4. With irradiation of wavelength approximately the same as the cell diameter, in this case 600 nm, it was believed that the scattering coefficient was comparable to the absorption coefficient.

Chlorhexidine behaved in many ways like antibacterial agents with surface-active properties such as, for example, cetyltrimethylammonium bromide and polymyxin (Hugo and Longworth, 1964). With 1/6000 and 1/4000 dilution on *E. coli* suspension, a sharp drop in absorbant values from 1.902 to 0.653 was seen, **Figure 6.1.4**. This indicated that the absorbate molecules of chlorhexidine readily adhered to the microorganisms' cell wall which then promote intracellular leakages by damaging the cytoplasmic membrane. Gale (1963) suggested that the mode of action of chlorhexidine was to react with the cell causing a disorientation of the lipoprotein membrane, by virtue of the lipophilic groups of the drug molecule, so that the membrane no longer fulfilled its function as an osmotic barrier. Thus the debris or intracellular debris formed as a result could have decreased the extinction coefficient which in turn increased the transmittivity at 600 nm wavelength.

However, with the high concentration of 1/40 and concentrated disinfectant solution added, the absorbency increased. This anomalous behaviour has been reported by Hugo and Longworth (1964), that with a higher addition of chlorhexidine, an increased in leakage inhibition was seen although the source of illumination was not at 600 nm. This implies that the absorbate molecules were at first readily taken up and adhered to the surface of the cell wall but as the sites or surface area became filled, the probability of further adsorption decreased. This results in building up multilayers of the chlorhexidine molecules which was a feature of the leakage inhibition phenomenon, or, alternatively, to penetration of the chlorhexidine molecules into the interior (cytoplasm) of the cell. As seen with 1/40 and concentrated disinfectant on *E. coli* in **Figure 6.1.4**, the absorbencies decreased with increasing time; suggesting secondary or outer layers of adhering chlorhexidine molecules could have started to induce more adverse bactericidal effects on the cell. Thus, the absorbency was dependent on the mode of action of the bactericidal agent and the physical orientated state at which the microorganisms were in.

The contrast method provided a qualitative statistical analysis of the STS pattern formed at each different condition as described above; illustrating the bactericidal effects of adding disinfectant with time. Adding of 1/6000, 1/4000, 1/40 and concentrated disinfectant solution exceed the threshold dosage to inactivate and

**Table 6-1-2 Average temporal contrast values of *Escherichia coli* and with various strength of Iibitane disinfectant solution added.**

Time ( min )	Pure <i>E.coli</i>	with 1/6000 disinfectant	with 1/4000 disinfectant	with 1/40 disinfectant	with concentrated disinfectant
T <sub>0</sub>	0.721	0.522	0.508	0.299	0.277
<b>Average temporal contrast value</b> T <sub>15</sub>	0.720	0.553	0.521	0.25	0.227
T <sub>30</sub>	0.724	NA	0.545	NA	NA

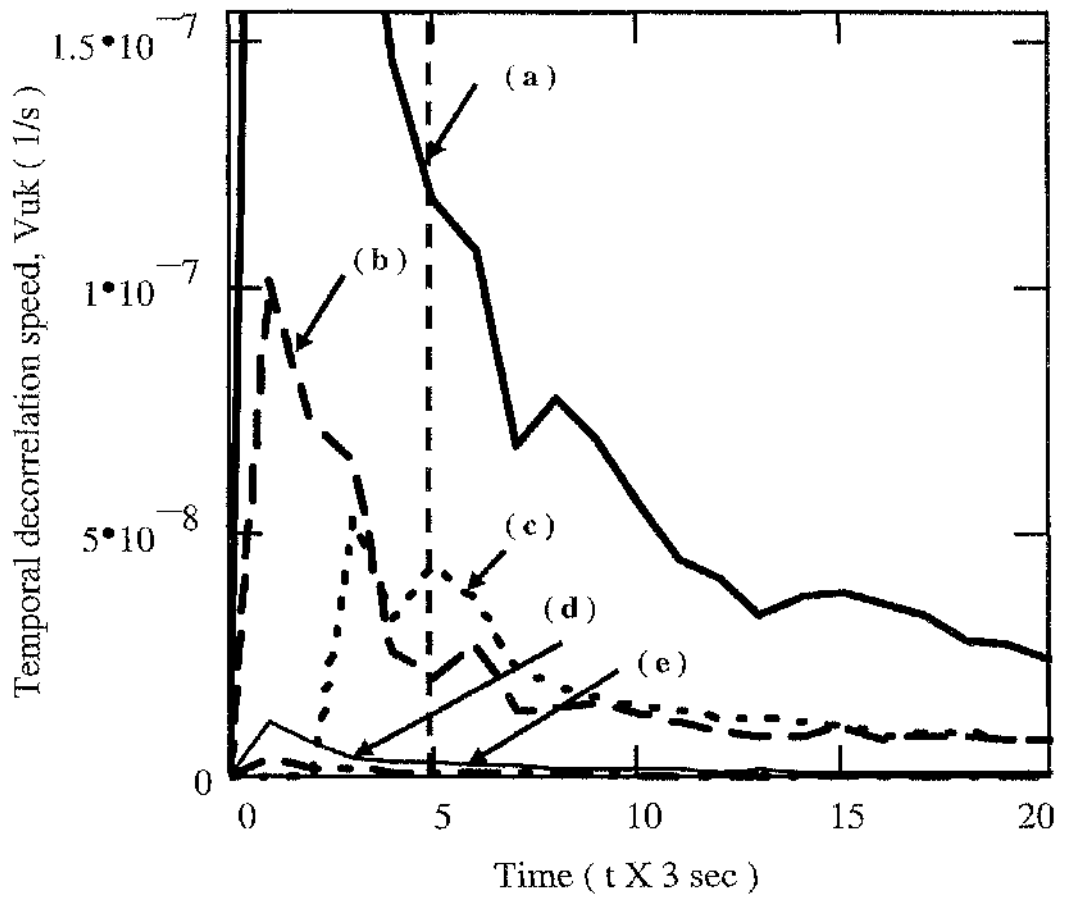
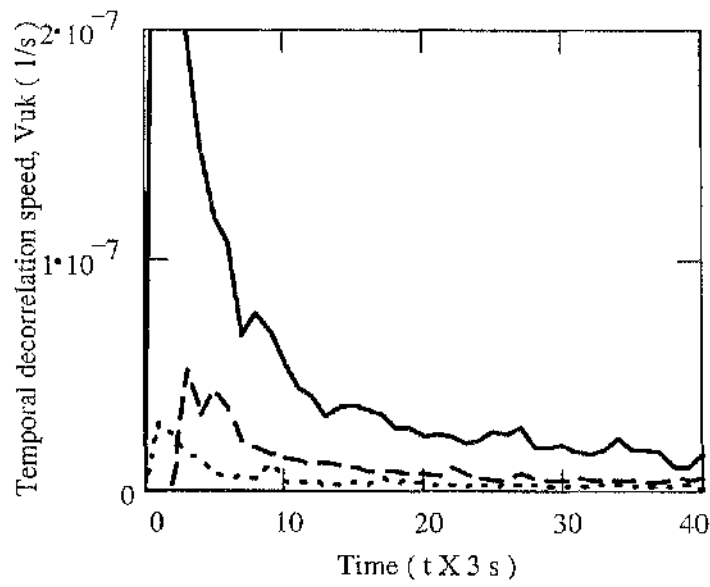
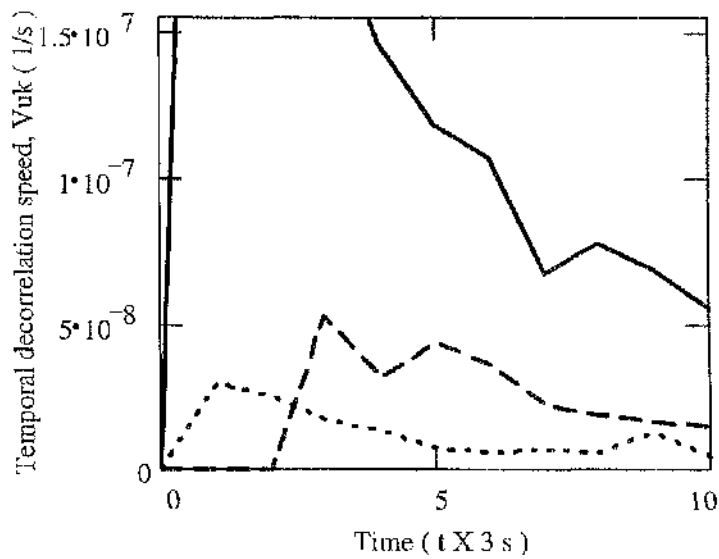


**Figure 6.1.6** Temporal decorrelation speed,  $V_{uk}$  of pure *E.coli* suspension (a), with 1/6000 (b), 1/4000 (c), 1/40 (d) and concentrated (e) Hibitane disinfectant solution at  $T_0$  min corresponding to 128 temporal positions or array element number of 3 s interval.

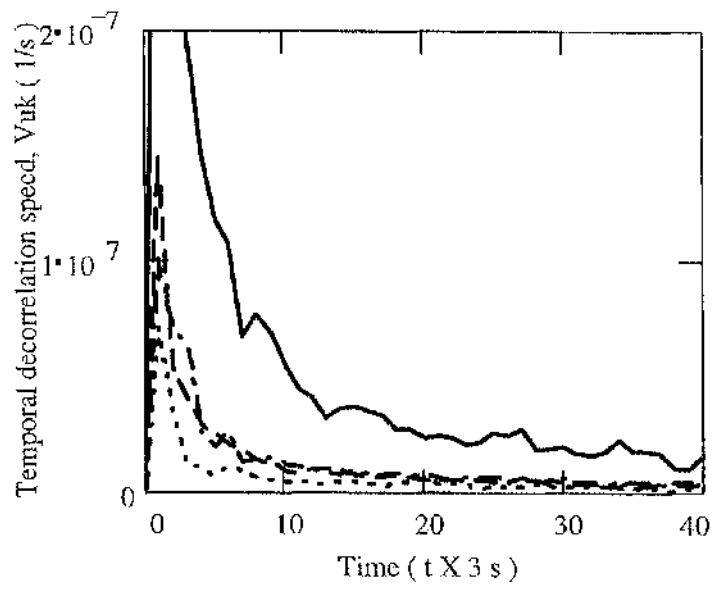


(a)

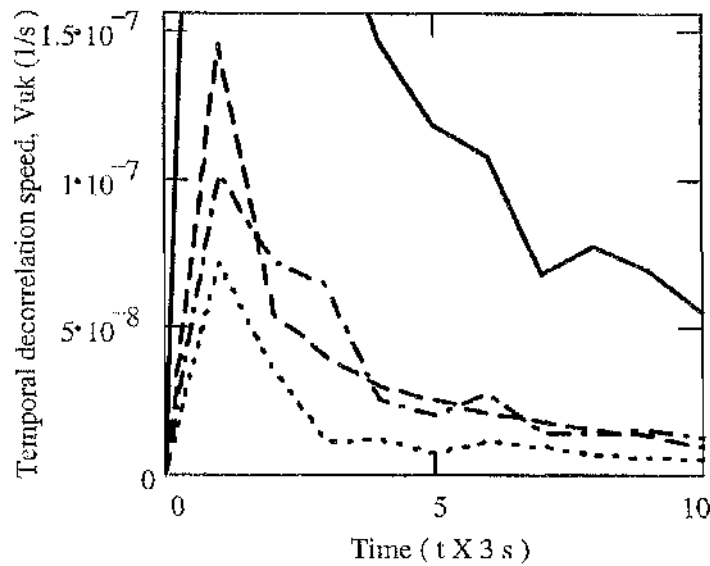


(b)

**Figure 6.1.7** Temporal decorrelation speed,  $V_{uk}$  of *E. coli* (solid line) with 1/6000 diluted Hibitane disinfectant solution at  $T_0$  (dash line) and  $T_{15}$  (dotted line) min corresponding to 128 temporal positions of 3 s interval. **Figure 6.1.7b** showed the detail trend of  $V_{uk}$  from 0 to 10 temporal positions.

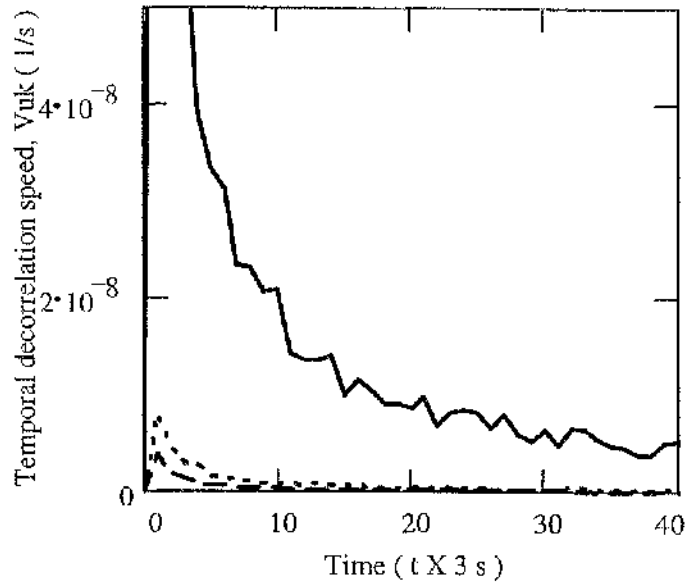


(a)

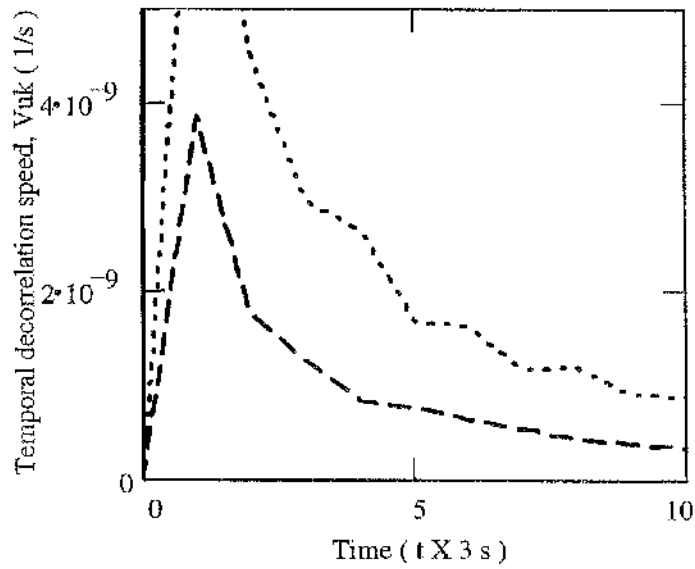


(b)

**Figure 6.1.8** Temporal decorrelation speed,  $V_{uk}$  of *E. coli* (solid line) with 1/4000 diluted Hibitane disinfectant solution at  $T_0$  (dash line) and  $T_{15}$  (dot-dashed line) and  $T_{30}$  (dotted) min corresponding to 128 temporal positions of 3 s interval. **Figure 6.1.8b** showed the detail trend of  $V_{uk}$  from 0 to 10 temporal positions.

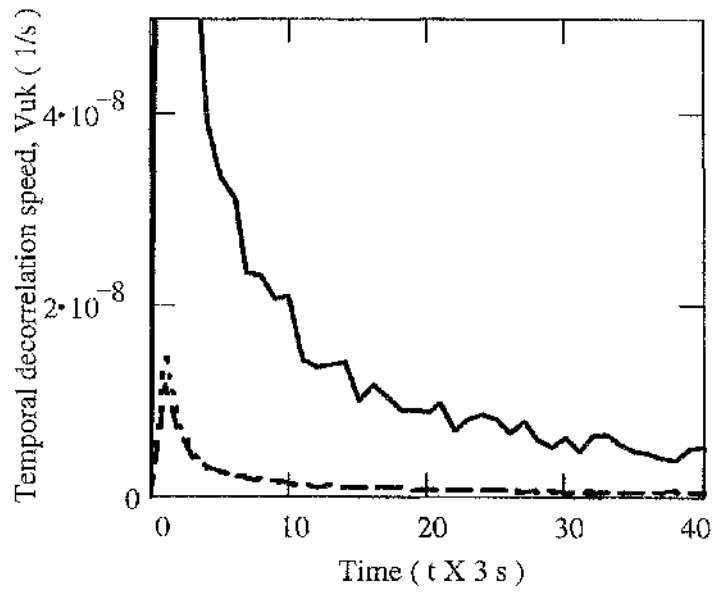


( a )

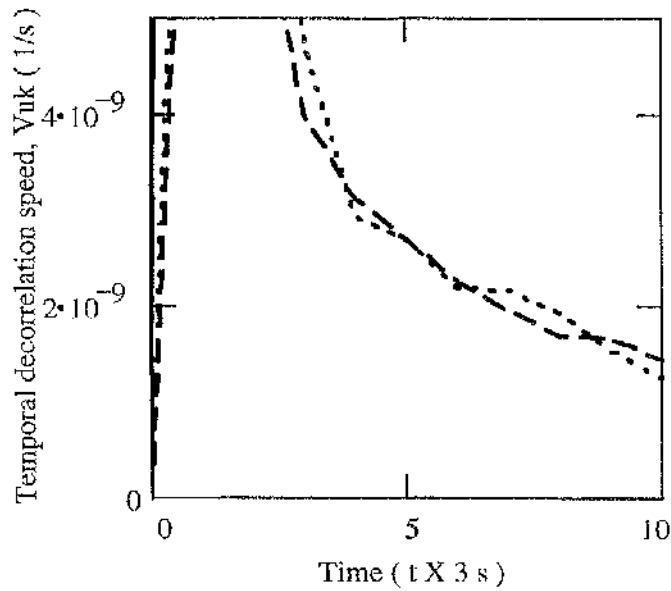


( b )

**Figure 6.1.9** Temporal decorrelation speed,  $V_{uk}$  of *E. coli* (solid line) with 1/40 diluted Hibitane disinfectant solution at  $T_0$  (dotted line) and  $T_{15}$  (dashed line) min corresponding to 128 temporal positions of 3 s interval. Figure 6.1.9b showed the detail trend of  $V_{uk}$  from 0 to 10 temporal positions.



(a)



(b)

**Figure 6.1.10** Temporal decorrelation speed,  $V_{uk}$  of *E. coli* (solid line) with undiluted Hibitane disinfectant solution at  $T_0$  (dotted line) and  $T_{15}$  (dashed line) min corresponding to 128 temporal positions of 3 s interval. Figure 6.1.9b showed the detail trend of  $V_{uk}$  from 0 to 10 temporal positions.

**Table 6-1-3 Temporal decorrelation speed,  $V_{uk}$ , of *Escherichia coli* and with various strength of Hibitane disinfectant solution added.** The  $V_{uk}$  obtained correspond at time 15<sup>th</sup> s at each sampling interval namely,  $T_0$ ,  $T_{15}$  and  $T_{30}$  min. The values in brackets and bold represented the  $V_{uk}$  values of pure *E. coli* suspension without Hibitane solution. The initial viabilities of the microorganisms were  $8 \times 10^9$  cfu ml<sup>-1</sup> with 1/6000 and 1/4000 diluted disinfectant and  $2 \times 10^8$  cfu ml<sup>-1</sup> with 1/40 and undiluted Hibitane.

Temporal decorrelation speed, $V_{uk}$ ( s <sup>-1</sup> )				
Time, $T_{min}$	with 1/6000 disinfectant	with 1/4000 disinfectant	With 1/40 disinfectant	With undiluted disinfectant
	<b>(<math>1.2 \times 10^{-7}</math>)</b>	<b>(<math>1.2 \times 10^{-7}</math>)</b>	<b>(<math>3.8 \times 10^{-8}</math>)</b>	<b>(<math>3.8 \times 10^{-8}</math>)</b>
$T_0$	$4 \times 10^{-8}$	$2.5 \times 10^{-8}$	$1.7 \times 10^{-9}$	$2.8 \times 10^{-9}$
$T_{15}$	NA	$2 \times 10^{-8}$	$9 \times 10^{-10}$	$2.8 \times 10^{-9}$
$T_{30}$	$1 \times 10^{-8}$	$1 \times 10^{-8}$	NA	NA

induce bactericidal effects (Russell A.D. *et al*, 1982). To effectively kill 99.9 % of *E. coli* cells, 1 part of the disinfectant in 50 000 dilution was needed but the bactericidal effect was not elucidated with time. Cell viability was often measured via plating techniques which requires a minimum of 24 hr incubation.

As shown in **Figure 6.1.5**, a decrease in contrast level implied a reduction in the bioactivity of the organisms with increasing coherent light reaching the imaging system. With 1/6000 and 1/4000 added to *E.coli* suspension, similar reduction trend in contrast levels were observed. The mode of action of chlorhexidine on *E. coli* (Hugo and Longworth, 1964), resulted in breaking of the cytoplasmic membrane, could lead to multiple scattering effect (Briers 1993) which hindered transmittivity and thus causes a slight increase in the absorbance value. This could account for the slight increase of the samples tested with 1/6000 and 1/4000 at  $T_{15}$  min and  $T_{30}$  min, **Table 6-1-2**. The unstable fluctuations of the contrast patterns with 1/6000 and 1/4000 implied that the bacteria viability were relatively high and the cells were not fully inactivated over 6.4 min.

With a much stronger Hibitane concentration of 1/40 and undiluted solution, much less irregular patterns and lower contrast values were observed, implying that the rate of cell viable reduction was decreasing rapidly. After 150 s ( $t \times 50$  s), the patterns were stable at around a contrast value of 0.3, which could indicate minimal cell viability. The contrast level will not reach zero as with 632.8 nm wavelength, transmission was observed in all sample conditions.

The temporal decorrelation speed measurements of the time-varying speckle demonstrated the relationship between the correlated inter-pixel intensity of the STS pattern and the velocity of the global movement of the particles. In all experiments, declining exponential trends were observed, even with pure *E.coli* suspension. With pure *E. coli* suspension, this phenomenon should not be associated with a decrease in bioactivity of the cellular viability (although it could be over a longer period of time) but possibly be due to the fact that it exhibits a more orientated state of random motion within the sample, resulting in more coherent light reaching the imaging system in 6.4 min. Environmental effects like external noise and vibration were also

negligible since in another experiment under the same experimental conditions, no reflection speckle patterns were observed with a piece of metal.

A large difference in the magnitude decrement of the temporal decorrelation speed of pure *E. coli* solution with disinfectant added could be seen implying the rate of anti-bacterial action was in the time frame of a few tens of seconds, **Figures 6.1.6. Figure 6.1.7, 8, 9, 10** show the bactericidal effects on the cells, sampled at time intervals of 15 min, up to 30 min. With concentrated disinfectant solution added, both  $T_0$  and  $T_{15}$  min showed almost identical curves with huge differences in the temporal decorrelation speed with pure *E. coli* suspension, implying great reduction in cell viability and thus bioactivity. With almost the same value throughout the temporal positions at  $T_0$  and  $T_{15}$  min, implying the concentrated disinfectant solution exceeded the threshold dosage needed to inactivate the microorganisms, **Figure 6.1.10**. The difference in initial  $V_{uk}$  for 1/6000 and 1/4000 compared to 1/40 and undiluted Hibitane solution was due to the initial cell viability at  $8 \times 10^9$  and  $2 \times 10^8$  cfu ml<sup>-1</sup> respectively.

It is also worth noting that the temporal decorrelation speed decreased with decreasing incident intensity of the laser beam and this was also observed by Oulamara *et al.* (1989). However, the magnitude of the decorrelation effect was proportional to the light intensity but the shape of the decorrelation curve still characterised the microbiological activity of the cell sample.

The speckle properties and fluctuations from microbiological species are dependent on the laser wavelength applied, the viewing direction and the colour pigment found in the sample. For example in speckle specular reflection technique, a red tomato produces more rapid fluctuations than a green tomato observed in red light from a helium-neon laser (wavelength 633 nm), but the effect was reversed when the green line of an argon-ion laser (wavelength 514 nm) was used (Briers, 1975). Implicitly, a tentative explanation of this phenomenon was that the colour of the sample was due to the presence of discrete, pigmented bodies that selectively scatter and absorb. The direction and incidence of the laser light propagation on the microorganisms will also produces different speckle intensity distributions.

Preliminary experiments were also carried out to show the spatial intensity distribution of any given time of a STS pattern of a horizontal line pixel with intensity level versus spatial pixel positions (data not shown). Huge variations of the intensity were observed but were not distinctive and unique under different conditions with disinfectant. Thus no significant conclusions of the characteristics of the spatial distribution for any given sample conditions can be drawn but this is essential to form the building block of a full STS pattern for further statistical analysis.

## **VII. CONCLUSION**

The aim of the work in this thesis is to build and optimise both Nd: YAG and CO<sub>2</sub> laser-bacteria inactivation processes with laser parameters which lead to a greater understanding in laser-microbial interaction.

The temperature dependence of the optical properties of the extinction coefficient,  $\alpha_T$  and the scattering coefficient,  $\alpha_S$  of water were measured at 1.064  $\mu\text{m}$  between 25 °C to 70 °C. In general, both the extinction coefficient and the scattering coefficient decreased with increasing temperature. Between 40°C to 45°C however, the extinction coefficient decreased more rapidly. No corresponding increase was observed in the scattering coefficient, measured normal to the incident beam. The investigation of the temperature dependence of the optical properties of water provides an important role in understanding laser-bacteria and laser-tissue interaction.

The effect of laser radiation on *Staphylococcus aureus* 6571 (Oxford strain) was studied with high power Nd:YAG laser radiation between 50 and 300 W. A range of laser pulse repetition frequencies (PRF) from 5 to 30 Hz, with a combination of pulse energies from 2 to 30 J were applied; this covered a range of energy densities from 800 to 2700  $\text{Jcm}^{-2}$ . The area of inactivation of *S. aureus*, lawned on nutrient agar plates was quantified as a function of energy density and exposure time. The shortest exposure time which produced an area of inactivation equal to 50 % of the beam area was achieved at a PRF of 30 Hz, pulse energy of 10 J, and with an exposure time of 10.75 s; this was equivalent to an applied energy density of 1723  $\text{Jcm}^{-2}$ . No bacterial inactivation was observed at relatively low power settings for PRF, pulse energies and exposure time of: 20 Hz, 3 J and 34 s; 25 Hz, 2 J and 45 s and 30 Hz, 2 J and 35 s respectively. Thus, high power Nd:YAG lasers offer the capacity of achieving rapid inactivation or sterilisation at lower temperatures than traditional methods.

Although Nd:YAG laser could produce a killing effect on microorganisms on agar plates, a transient sub-lethal area at the periphery of the zone was observed. This suggested the nature of the distribution of the beam profile; a Gaussian distribution. Hence, further investigation of the effect of Nd:YAG laser light on *Serratia*

*marcescens* was done to elucidate and quantify the energy density distribution. Three dimensional energy density profiles of laser parameters at 100 W, namely 10 Hz, 10 J and 20 Hz, 5 J were evaluated using a one dimensional pyroelectric detector array set-up. The inactivation effects of *S. marcescens* on nutrient agar plates were demonstrated over a range of applied energy densities from 2000 to 3500 Jcm<sup>-2</sup>. At IA<sub>50</sub> values, 10 Hz, 10 J achieved inactivation at a lower energy density but longer exposure time compared to 20 Hz, 5 J. The cross-sectional energy density profiles of the burn print diameters were mapped onto the diameters of microbial inactivated zones to demonstrate the energy distribution at 10 Hz, 10 J and 20 Hz, 5 J at IA<sub>50</sub> values applied. The differences in widths measured on different peripheral positions on a single inactivated zone were due to the non-symmetrical and non-ideal energy density distribution of the laser beam. Such detailed mapping of the laser's output energy on the targeted microbial area reveals the true energy distribution and not the integrated value on the microorganisms.

High power CO<sub>2</sub> laser irradiation inactivated micro-organisms before any substantial damage was done to polypropylene (PP) and stainless steel (SS) discs except for PVC, at which 25 ms exposure did not reduce the viability of *S. aureus* but damaged and charred the surfaces. Complete inactivation was achieved with 70.0, 80.0, and 140.0 Jcm<sup>-2</sup> using 380 W but with 980 W, 103.1, 129.0 and 232.0 Jcm<sup>-2</sup> was needed for PP, PE and SS respectively. With pulse energy kept constant, the minimum exposure time for complete microbial killing will be longer for 380 than 980 W. It is thus more efficient then, to use the lower power setting since both settings produced total bacterial killing. The plausible explanation lied in the inherent thermal conductivity property of the substrates since variable exposure times were needed with constant applied energy to induce a substantial heating effect. This investigation shows the dependence of substrates with microorganisms with CO<sub>2</sub> laser irradiation.

The efficacy and bactericidal effect of two different high power CO<sub>2</sub> laser scanning systems was investigated. *S. aureus* was more resistant than *E. coli*. With nutrient agar, collagen film and stainless steel, the inactivation process, increased with decreasing scanning speed,  $V_t$  and increasing energy density. No killing was observed at 387.0 (~30 Jcm<sup>-2</sup>) and 442.3 cms<sup>-1</sup> (~34 Jcm<sup>-2</sup>) scanning speed with

nutrient agar and collagen film respectively. The rate of inactivation,  $I_r$ , peaked at  $151.5 \text{ cm}^2\text{s}^{-1}$ ,  $221.2 \text{ cms}^{-1}$  with collagen film, corresponding to an applied energy density of  $60 \text{ Jcm}^{-2}$ . This phenomenon was not observed on nutrient agar plates since the maximum  $V_t$  applied was not sufficiently low. The bactericidal effects on stainless steel strips were quantified by a viable count plating method. No reduction in bacterial viability was observed with  $80 \text{ Jcm}^{-2}$  for both organisms but with full inactivation at  $0.83 (916.7 \text{ Jcm}^{-2})$  and  $1.33 (654.8 \text{ Jcm}^{-2}) \text{ cms}^{-1}$  respectively. The rate of the laser scanning systems at which sterilisation occurs was better achieved with *E. coli* than *S. aureus*. Such laser scanning systems can be envisaged into automated decontamination processes.

A similar but lower power  $\text{CO}_2$  laser scanning system was designed and built in the laboratory to investigate bacterial sterilisation at  $10.6 \mu\text{m}$ . Laser power of 2 to 13.4 W, scanning speed of 3 to  $100 \text{ mms}^{-1}$  was used on nutrient agar and stainless steel strips inoculated with *S. aureus* and *E. coli*. Sub lethal killing was observed at 4 W,  $40 \text{ mms}^{-1}$  ( $3.64 \text{ Jcm}^{-2}$ ) and 3 W,  $40 \text{ mms}^{-1}$  ( $2.73 \text{ Jcm}^{-2}$ ) respectively. Notably,  $I_r$  increased with increasing  $V_t$  for a given energy density. However, no inactivation was observed with stainless steel strips up to an applied energy density of  $162.5 \text{ Jcm}^{-2}$  at 13.4 W,  $3 \text{ mms}^{-1}$ . With sand-blasted stainless steel strips, one D-value microbial reduction was observed with 13 W,  $5 \text{ mms}^{-1}$  ( $94.6 \text{ Jcm}^{-2}$ ) and 13 W,  $10 \text{ mms}^{-1}$  ( $47.3 \text{ Jcm}^{-2}$ ) for *S. aureus* and *E. coli* respectively. No viable reduction was observed with unexposed bacteria-seeded sand-blasted strips which indicated that the one D-value reduction was solely due to laser action. Although the speed of sterilisation was much higher with 1020 than 15 W  $\text{CO}_2$  laser, the relatively energy density input was smaller with 15 W able to achieve minimum sterilisation which makes the low power laser more energy efficient. Thus the efficacy and optimisation of sterilisation between both systems are dependent on whether energy density or speed of laser scan (or total killing time taken) are used as the main experimental variable.

A test-bed was built combining  $\text{CO}_2$  laser, ultra-violet and microwaves radiation to investigate any synergism or additive effect.  $\text{CO}_2$  laser irradiation did not reduce microbial viability without damaging the produce. This was reversed with an

increase in the exposure time with a larger beam diameter. Microwaves induced microbial killing (a few log D-values) but the power variability within the chamber was inconsistent. With ultra-violet irradiation, killing was observed without appreciable heat rise. However, in most experiments, the median value of the cell viable reduction was greater with the combined simultaneous treatment than individual sub-systems, indicating an enhanced effect. Statistically, the combined effect reduced the variability of microbial inactivation.

The thermal inactivation kinetics between *S. aureus* microorganism and its resuspending liquid medium with microwave radiation was evaluated to understand the bactericidal mechanism. Full inactivation of  $8 \times 10^6$  cfu of *S. aureus* was achieved in 61.4 °C. *S. aureus* microorganisms possess thermal properties which absorb the thermal microwave heat at least 51-fold greater than its suspending sterile distilled water medium at 65 °C. Heat transfer via conduction through the underlying stainless steel substrate inactivates the microbes with lethal microwave exposures. The stainless steel disc conducts approximately 145 times more than the bacterial sample. Full sterilisation corresponding with thermal absorption power at 23.8 and 0.16 W for stainless steel disc and inoculum respectively were achieved. The investigation shows that heat transfer from the underlying substrate was the mode of bacteriostasis and not the direct microwave irradiation.

The fluctuation of speckle patterns of *E. coli* with and without disinfectant can be understood as the result of a time-varying distribution effect of individual scatters within a unique but random structure of sample concerned. Speckle imaging has proved to be sensitive in picking up small changes in the movements and the ability to detect the viability of the cells through the fluctuating image component. High disinfectant concentration induced lesser bioactivity movement within the liquid sample and this resulted in a lower rate of fluctuation of the speckle intensity with a brighter and smoother STS pattern. The killing effect with respect to time was also being identified through the correlation measurement. Microorganisms were plated out to determine their viability and the results were compared with speckle predictions. Thus, speckle imaging was able to measure the bioactivity of microorganisms instantaneously with temporal and spatial variations in contrast to

normal plating techniques. This technique was useful in detecting and quantifying the bacteria population and its viability. Such procedures could be useful in many applications such as decontamination processes and food quality control plants. Speckle algorithms provide a fast, objective and non-invasive alternative methodology for distinguishing the vitality or motility of the state of bioactivites of the living microorganisms. Realise that this system provides a real time analysis, *in situ* without any probe into the sample which might have an adverse effect of the state of microbial bioactivity.

## VIII. REFERENCES

- Adrian J C and Gross Arthur** (1979) A new method of sterilisation: the carbon dioxide laser, *Journal of Oral Pathology*, **8**, 60-61
- Alhamdan A, Sastry S K and Blaisdell J L** (1990) Natural convection heat transfer between water and an irregular-shaped particle, *Transactions ASAE*, **33**, 2, 620-624
- Allwood M C, Hambleton R and Beverly S** (1975) Pressure changes in bottles during sterilisation by autoclaving, *Journal of Pharmaceuticals Science*, **64**, 333-334
- Amato W and Tien C** (1972) Free convection heat transfer from isothermal spheres in water, *Journal of Heat Mass Transfer*, **15**, 327-339
- Amato W. and Tien C** (1972) Free convection heat transfer from isothermal spheres in water, *Journal of Heat Mass Transfer*, **15**, 327-339
- Antipa C, Bruckner I I, Crangulescu N, Moldovan C I, Podoleanu A G, Stanciulescu V and Ionescu E** (1996) Our clinical experience in low-energy laser medical treatments, *Optical Engineering*, **35**, 5, 1367-1371
- Artandi C and Winkle V W** (1959) Electron beam sterilisation of surgical sutures, *Nucleonics*, **17**, 86-90
- Bassel M P, Lee J and Robinson C W** (1987) Is liquid water really anomalous, *J. Phys. Chem.*, (**91**), 5818-5825
- Bedwell J, Holton J, Vaira D, MacRobert A J and Bown S G** (1990) *In vitro* killing of *Helicobacter pylori* with photodynamic therapy, *Lancet*, **335**, 1287
- Berkopcc B and Vidic A** (1996) Ecological problems of sterilisation oxide in Slovenia, **56**, 73-76
- Blackman C F, Beane S G Weil C M and Ali J S** (1968) Effects of non-ionising electromagnetic radiation of single cell biologic systems, *Ann. of N.Y. Acad. of Science*, **247**, 352-366
- Blenkarn J I** (1995) The disposal of clinical waste, *Journal of Hospital Infection*, **30**, 514-520
- Boyd V H, Leong K H, Miller C B, Golden J, Robert D. Glesias and Patrick J. Laverty** (1996) Understanding high-power fibre-optics laser beam delivery, *Journal of Laser Applications*, **8**, 307-316
- Briers J D** (1975) Wavelength dependence of intensity fluctuations in laser speckle patterns from biological specimens, *Optical Communication*, **13**, 3, 324-326
- Briers J D** (1993) Speckle fluctuations and biomedical optics: implications and applications, *Optical Engineering*, **32**, 2, 277-283

- Briers J D** (1996) Monitoring biomedical motion and flow by means of coherent light fluctuations, *Proceedings, SPIE*, **2732**, 2-15
- Brown G H and Morrison W C** (1954) An exploration of the effects of strong radio-frequency fields on micro-organisms in aqueous solutions, *Food Technology*, **8**, 361-366
- Bruck S D and Mueller E P** (1988) Radiation sterilization of polymeric implant materials, *Journal of Biomedical Materials Research*, **22**, no. A2, 133-144
- Bryan J B and Curnutte B** (1972) A normal coordinate analysis based on the local structure of liquid water, *Journal of Molecular Spectrum*, **41**, 512-532
- Burlinska G, Bojarski J and Michalik J** (1996) Studies of irradiated polypropylene, its copolymers and blends- I. ESR studies, *Radiat. Phys. Chem.*, **47**, no. 3, 449-451
- Burns T, Wilson M and Pearson G** (1992) Laser induced killing of photosensitized cariogenic bacteria, *Journal of Dental Research*, **71**, 675
- Burns T, Wilson M and Pearson G** (1993) Sensitisation of cariogenic bacteria to killing by light from a helium/neon laser, *Journal of Medical Microbiology*, **38**, 401-405
- Cannon B, Gardner T S and Cohen D K** (1986) Measurement of 1  $\mu\text{m}$  diameter beams, *Applied Optics*, **25**, 2981-2983
- Chapple P** (1994) Beam waist and  $M^2$  measurement using a finite slit, *Optical Engineering*, **33**, 2461-2466
- Clough R L, Gillen K T, Malone G M and Wallace J S** (1996) Color formation in irradiated polymers, **48(5)**, 583-594
- Clothiaux E J** (1983) Inactivation of bacterial spores by a microwave discharge, *Journal of Environmental Science and Health*, **A18**, 1, 51-57
- Cobb C M, McCawley T K and Killoy W J** (1992) A preliminary study on the effects of the Nd:YAG laser on root surfaces and subgingival microflora *in vivo*, *Journal of Periodontology*, **63**, 701-707
- Cohen D C, Little B and Luecke F S** (1984) Techniques for measuring 1  $\mu\text{m}$  diameter Gaussian beams, *Applied Optics*, **23**, 637-640
- Colebrook L** (1955) *Lancet*, **269**, 885
- Collins J R** (1922), The effect of certain dissolved substances on the infra-red absorption of water, **20**, 486-498

- Collins J R** (1925) Infrared absorption spectrum of water, *Physics Review*, **26**, 771-779
- Corelli J C, Gutmann R J, Kohazi S and Levy J** (1977) Effects of 2.6 - 4.0 GHz microwave radiation on E-Coli B, *Journal of Microwave Power*, **12**, 2, 141-144
- Cortelyou J R, McWhinnie M A, Riddiford M S and Semrad T E** (1954) *Appl. Microbiol.*, **2**, 269
- Cremer M L and Chipley J R** (1980a) Hospital ready-prepared type foodservice system: Time and temperature conditions, sensory and microbiological quality of scrambled eggs, *Journal of Food Science*, **45**, 1422-1424, 1429
- Cremer M L and Chipley J R** (1980b) Time and temperature, microbiological and sensory assessment of roast beef in a hospital foodservice system, *Journal of Food Science*, **45**, 1472-1477
- Crespo F L and Ockerman H W** (1977) Thermal destruction of microorganisms in meat by microwaves and conventional cooking, *Journal of Food Protection*, **40**, 442-444
- Culkin K A and Fung Y C D** (1975) Destruction of *Escherichia coli* and *Salmonella typhimurium* in microwave-cooked soups, *Journal of Milk Food Technology*, **38**, 1, 8-15
- Curd F H S and Rose F L** (1946) Synthetic antimalarials. Part X. Some aryl-diaguanide ('-biguanide') derivative, *Journal of the Chemical Society*, 729-737
- Curnutte B and Bandekar J** (1972) The intramolecular vibration of the water molecule in the liquid state, *Journal of Molecular Spectrum*, **41**, 500-511
- Curran H R** (1952) *Bacteriology Review*, **16**, 111
- Darmady E M, Hughes K E A and Jones J D** (1958) *Lancet*, **2**, 766
- Darmady E M, Hughes K E A and Tuke W** (1957) Sterilization of syringes by infra-red radiation, *Journal of Clinical Pathology*, **10**, 291
- Darmady E M, Hughes K E A, Jones J D, Prince D and Winfred T** (1961) *Journal of Clinical Pathology*, **14**, 39
- Das P** (1991) Light amplifier-Population inversion, In *Lasers and Optical Engineering* (Springler-Verlag), 226-229
- Davis G E, Francis J, Martin A R, Rose F L and Swain G** (1954) 1:6-di-4 chlorophenyl-diguanidino-hexane ('Hibitane'): a laboratory investigation of a new antibacterial agency of high potency, *British Journal of Pharmacology*, **9**, 192-196

- Dayoub M and Devine M J** (1976) Endodontic dry-heat steriliser effectiveness, *Journal of Endodontic*, **2**, 343-344
- Dederich D N, Pickard M A, Vaughn A S, Tulip J and Zakariassen K L** (1990) Comparative bactericidal exposures for selected oral bacteria using carbon dioxide laser radiation, *Lasers in Surgery and Medicine*, **10**, 591-594
- Dingus R S and Scammon R J** (1991), *SPIE Proc.*, **1427** p 45-54
- Dobbins H M and Peck E R** (1973) Change of refractive index of water as a function of temperature, *J. Opt. Soc. Am.*, (**63**), 318-320
- Draeger D A, Stone N W B, Curnutte B and Williams D** (1966) Far-infrared spectrum of water, *J. Opt. Soc. Am.*, **56**, 64-69
- Dreyfuss M S and Chipley H** (1980) Comparison of effects of sublethal microwave radiation and conventional heating on metabolic activity of *Staphylococcus aureus*, *Applied Environmental Microbiology*, **39**, 13-16
- Duggar B M and Hollaender A** (1934) *Journal of Bacteriology*, **27**, 241
- Dunn C G, Campbell W L, Fram H and Adelia H** (1948), *Journal of applied Physics*, **19**, 605
- Eastop T D and McConkey A** (1986) Heat flow through a cylinder and a sphere, In *Applied Thermodynamics*, fourth edition: Longman Scientific Technical Press Ltd, 683-690
- Ernst R R** (1977) Sterilisation by heat. In *Disinfection, Sterilisation and Preservation* (ed. Block, S.S.) 2<sup>nd</sup> ed., 481-739
- Espersen F, Wurr M, Corneliussen L, Hog A L, Rosdahl V T, Moller N F and Skinhoj P** (1994) Attachment of staphylococci to different plastic tubes in vitro, *Journal of Medical Microbiology*, **40**, 37-42
- Esty J R and Meyer K F** (1922) The heat resistance of the spores of *B. Botulinus* and allied anaerobes. XI, *Journal of Infectious Diseases*, **31**, 650-663
- Fernandez C I., Rao M A, Rajavasireddy S P and Sastry S K** (1988) Particulate heat transfer to canned snap beams in a steriort, *Journal of Food Processing Engineering*, **10**, 183-198
- Fitzpartrick J A, Kwao-Paul J and Massey J** (1978) Sterilization of bacteria by means of microwave heating, *Journal of Clinical Engineering*, **3**, 1, 44-47
- Ford T A and Falk M** (1968) Hydrogen bonding in water and ice, *Canad. J. of Chemistry*, (**46**), 3579-3586

- Frank M W** (1984) Lumped system with uniform temperature, In *Heat Transfer*, 162-166, Reading: Addison-Wesley Press Ltd
- Frucht-Pery J, Mor M, Evron R, Lewis A and Zauberman H** (1993) The effect of the ARF excimer laser on *Candida albicans* in vitro, *Graefe's Archives for Clinical and Experimental Ophthalmology*, **231**, 413-415
- Gale E F** (1963) *Pharmacology Reviews*, **15**, 481-530
- Galuska P J, Kolarik R W and Vasavada P C** (1988) Inactivation of *Listeria monocytogenes* by microwave treatment, *Journal of Annual Science*, **Suppl. 1**, 139
- Gartner K** (1947) *Z. Hyg. InfektKr.*, **127**, 273
- Gates F L** (1929) *Journal of General Physiology*, **13**, 231
- Gates F L** (1930) A study of the bactericidal action of ultra-violet light. III. The absorption of ultra-violet light by bacteria, *Journal of General Physiology*, **14**, 31-42
- Goldman I, Gray J, Goldman J, Goldman B and Meyer R** (1965) Effect of laser beam impact of teeth, *Journal of American Dental Association*, **70**, 601-606
- Goodman J W** (1963) Statistical properties of laser speckle patterns, *Stanford Electrical Laboratory Technical Report*, 2303-1
- Goodman J W** (1975) Statistical properties of laser speckle in *Laser Speckle and Related Phenomena*, Springer-Verlag, Berlin-Heidelberg-New York, 9-75.
- Gordon T E and Smith D L** (1970) Laser welding of prostheses, *Journal of Prosthetic Dentistry*, **24**, 472-6
- Gristina A** (1987) Biomaterial-centred infection: microbial adhesion versus tissue intergration, *Science*, **237**, 1588-1595
- Gush R J and King T A** (1991) Discrimination of capillary and arterio-venular blood flow in skin by Laser Doppler flowmetry, *Medical & Biological engineering & Computation*, **29**, 387-392
- Gutknecht N, Moritz A, Condras G, Sievert T and Lampert F** (1996) Bactericidal effect of the Nd:YAG laser in in vitro root canals, *Journal of Clinical Laser Medicine & Surgery*, **14**, 2, 77-80
- Hale G M and Querry M R** (1973) Optical constants of water in the 200 nm to 200  $\mu\text{m}$  wavelength region, *Applied Optics*, **12**, 555-563
- Hambleton R and Allwood M C** (1976) Containers and closures, In *Microbiological Hazards of Infusion Therapy*, 3-12, Lancaster: MTP Press Ltd

- Hannan R S** (1955) *Scientific and Technological Problems involving in using Ionising Radiations for the Preservation of Food* : H.M.S.O London
- Hansen N H and Riemann H** (1963) Factors affecting the heat resistance of non-sporing organisms, *Journal of Applied Bacteriology*, **26**, 314-333
- Harrison M A and Carpenter S L** (1989) Survival of *Listeria monocytogenes* on microwave cooked poultry, *Food Microbiology*, **6**, 153-157
- Hawkes J B and Astheimer R W** (1974) Optical properties of water in the neighbourhood of 35°C, *J. Opt. Soc. Am.*, **64**, 105-106
- Hoerter J and Eisenstark A** (1988) Synergistic killing of bacteria and phage by polystyrene and ultraviolet radiation, *Environmental and Molecular Mutagenesis*, **12**, 261-264
- Hooks T W, Adrian J C, Gross A and Bernier W E** (1980) Use of carbon dioxide laser in sterilisation of endodontic reamers, *Oral. Surg.*, **49**, 3, 263-265
- Horton J E and Lin P P** (1992) *Proc. of the 3rd International Congress on Lasers in Dentistry, Salt Lake City, U.S.A., Abstract 46. Salt Lake City: International Society for Lasers in Dentistry*
- Hossain M A and Dutta S K** (1982) Comparison of bacterial growth to high-intensity microwave exposure and conventional heating, *Bioelectromagnetics*, **3**, 471-474
- Hugo W B and Longworth A R** (1964) Some aspects of the mode of action of chlorhexidine, *Journal of Pharmacy and Pharmacology*, **16**, 655-662
- Humphrey A E and Nickerson J T P** (1961) Testing thermal death data for significant non-logarithmic behaviour, *Applied Microbiology*, **9**, 282-286
- IFT** (1989) Microwave food processing, *Food Technology*, **43** (1), 117-126
- Ingram M** (1971) *Goteborg: Svenska Institutet for Konserveringsforskning*, **292** p A1-A43
- Iziak E S** (1973) Radiation sensitivity of microorganisms. Effects on radiations on microorganisms, *International Journal of Radiation sterilisation*, **1**, 45-59
- Jacques S L** (1992) *Lasers in General Surgery*, **72** p 531-558
- Jagger J** (1973) Ultraviolet effects, *Medical Radiation Biology*, 44-51
- Javan A, Benette W R and Herriott D R** (1961) *Physics Review Letters*, **6**, 106
- Jeng K H D Kaczmarek K A, Woodworth A G and Balasky G** (1987) Mechanism of microwave sterilization in dry state, *Applied and Environmental Microbiology*, **53**, 2133-2137

- Karoutis A D, Guiti Z, Charvalous E, Tselentis I and Helidonis E** (1996) Bactericidal effect of ArF excimer laser radiation. I. Negative bacteria, *Lasers in the Life Science*, **7**(1), 59-70
- Kazbekov E N and Vyacheslavov L G** (1987) Effects of microwave irradiation on some membrane-related processes in bacteria, *General Physiology and Biophysics*, **6**, 57-64
- Keates R H, Drago P C and Rothchild E J** (1988) Effect of excimer laser on microbiological organisms, *Ophthalmic Surgery*, **19**, 715-718
- Kelsey J C** (1958) *Lancet*, **1**, 306
- Kennedy J C, Pottier R H and Pross D C** (1990), *Journal of Photochemistry and Photobiology*, **6**, 143-148
- Khalil H and Villota R** (1986) A comparative study on the thermal inactivation of *B. Stearothermophilus* spores in microwave and conventional heating, In *Food Engineering and Process Applications*, Vol. 1, Transport phenomena, Elsevier Applied Science Publisher, New York, NY
- Khalil H and Villota R** (1988) Comparative study on injury and recovery of *Staphylococcus aureus* using microwaves and conventional heating, *Journal of Food Protection*, **51**, 181-186
- Khosrofian J M and Garetz B A** (1983) Measurement of a Gaussian laser beam diameter through the direct inversion of knife-edge data, *Applied Optics*, **22**, 3406-3410
- Kidd S, Chris C and Wayne Y** (1997) Aligning lasers to fibre the automatic way, *Europhotonics*, **Jun/July**, 53-55
- Kirschner R A and Unger M** (1984) *Surgery Clinical of North America*, **64** p 939-940
- Klein E, Fine S, Ambrus J, Cohen A E, Neter E, Ambrus C, Bardos T and Lyman R** (1965) Interaction of laser light with biological systems. III . Studies on biological systems *in vitro*, *Fed. Proc.*, **24**, Supplement 14, S104-S110
- Klinke T, Klimm W and Gutknecht N** (1997) Antibacterial effects of Nd:YAG laser irradiation within root canal dentin, *Journal of Clinical Laser Medicine & Surgery*, **15**, 1, 29-31
- Klinke T, Klimm W and Gutknecht N** (1997) Antibacterial effects of Nd:YAG laser irradiation within root canal dentin, *Journal of Clinical Laser Medicine & Surgery*, **15**, 1, 29-31

- Kochewar I** (1992) Biological effects of excimer laser irradiation, *Proceedings of IEEE*, **80(6)**, 833-837
- Lary W, Pinkley P P, Seta and Williams D** (1977) Optical constants of water in the infrared: Influence of temperature, *J. Opt. Soc. Am.*, **67(4)**, 494-499
- Latimer J M and Matsen J M** (1977) Microwave oven as a method for bacterial decontamination in clinical microbiological laboratory, *Journal of Clinical Microbiology*, **6**, 340-342
- Lenz M K and Lund D B** (1978) The lethality-Fourier number method. Heating rate variations and lethality confidence intervals for forced convection heated foods in containers, *Journal of Food Process Engineering*, **2(3)**, 227-271
- Levy J G** (1994) Photodynamic therapy of cancer, *Proceedings of SPIE*, **2078**, 91-101
- Lewis D L and Arens M** (1995) Resistance of micro-organisms to disinfection in dental and medical devices, *Nature Medical*, **1**, no. 9, 956-958
- Lin C K, Kennick W H, Sandine W E and Kootharaic M** (1984) Effect of electrical stimulation on meat microflora: Observations on agar media, in suspensions and on beef carcasses, *Journal of Food Protection*, **56**, 279-283
- Loh C S, MacRobert A J, Bedwell J, Regula J, Krasner N and Bown S G** (1993), *Journal of Brain Cancer*, **68**, 41-51
- Lyman R** (1965) Interaction of laser radiation with biological systems. III. Studies on biologic systems *in vitro*, *Federal Proceedings*, **24**, Supplement 14, S104-S110
- Macmillan J D, Maxwell W A and Chichester C O** (1966) Lethal photosensitization of microorganisms with light from a continuous wave gas laser, *Photochemistry and Photobiology*, **5**, 555-565
- McCaughan J S, Barabash R D, Penn G M and Glavan B J** (1990) *Chest*, **98**, 1374-1378
- Maiman T H** (1960) Stimulated optical radiation in ruby, *Nature*, **187**, 493-494
- Maki D, Goldman D and Rhame F** (1973) Infection control in intravenous therapy, *Ann Intern Med*, **79**, 867-887
- Marcus S** (1992) in *Photodynamic Therapy: Basics Principle and Clinical Applications* (Henderson B W and Dougherty T J), 219-268
- Martin B C, Kenneth W D, Gary M, Caroline D H and Derrick C K** (1993) A vitalistic model to describe the thermal inactivation of *listeria monocytogenes*, *Journal of Industrial Microbiology*, **12**, 232-239

- Martinetto P, Gariglio M, Lombard G F, Fiscella B and Boggio F** (1986) Bactericidal effects induced by laser irradiation and haematoporphyrin against Gram positive and Gram-negative microorganisms, *Drugs in Experimental Clinical Research*, **12**, 335-342
- Mauck M** (1979) Knife-edge profiling of Q-switched Nd:YAG laser beam and waist, *Applied Optics*, **18**, 599-600
- McCaughan J S, Barabash R D, Penn G M and Glavan B J** (1990) *Chest* **98**, 1374-1378
- M<sup>c</sup>Guff P and Bell E J** (1966) The effect of laser energy radiation on bacteria, *Medical & Biological illustration*, **16**, 191-194
- Mertens B and Knorr D** (1992) Developments of non-thermal processes for food preservation, *Food Technology*, **46**, 124-133
- Mezei M and Beveri D L** (1982) Further Quasicomponent distribution function analysis of liquid water. Temperature dependence of the results, *J. Chem. Phys.*, (**76**), 593-600
- Micheal G H and Marvin R** (1972) Influence of temperature on the spectrum of water, *J. Opt. Soc. Am.*, **62**, 1103-1108
- Micheal B and Mullarky M A** (1985) The efficacy of the CO<sub>2</sub> laser in the sterilisation of skin seeded with bacteria: Survival at the skin surface and in the plume emissions, *Laryngoscope*, **95**, 186-187
- Milne D** (1964) Scottish Home and Health Department. The Aberdeen typhoid outbreak, report by the *Department Committee of Enquiry*, Edinburgh, HMSO
- Miserendino I J, Kos W, Miserendino C A, Luebke N** (1988) Sterilisation of bacterially contami-root by CO<sub>2</sub> irradiation, *Abstracts of papers submitted to the America association of endodontists*, **45**, 193
- Mullarky M B, Norris C W and Goldberg I D** (1985) The efficacy of the CO<sub>2</sub> laser in the sterilization of skin seeded with bacteria : Survival at the skin surface and in the plume emission, *Laryngoscope* **95**, 186-187
- Nathan I, Croitoru, Alexandra I, Reuben D and Moshe B D** (1997) Scattering and beam profile measurements of plastic, silica and metal radiation waveguides, *Journal of Biomedical Optics*, **2(2)**, 235-242
- Nelson S O, Forbus W R and Lawrence K C** (1994) Microwave permittivities of fresh fruits and vegetables from 0.2 to 2 GHz, *Transaction of the ASAE*, **37**, 1, 183-189

- Nordgren G** (1939) Formaldehyde sterilisation, *Acta Pathologica et Microbiologica Scandinavica I, Suppl*, 38-41
- Ohlsson T** (1983) Fundamentals of microwave cooking, *Microwave World*, **4**, 4-9
- Okamoto H, Iwase T and Morioka T** (1992) Dye medicated bactericidal effect of He-Ne laser irradiation on Oral microorganisms, *Lasers in Surgery and Medicine*, **12**, 450-458
- Oulamara A, Tribillon G and Duvernoy J** (1988) Subpixel speckle displacement measurement using a digital processing technique, *Journal of modern optics*, **35**, 7, 1201-1211
- Oulamara A, Tribillon G and Duvernoy J** (1989) Biological activity measurement on botanical specimen surfaces using a temporal decorrelation effect of laser speckle, *Journal of Modern Optics*, **36**, 1650-179
- Pedersen H M** (1974) The roughness dependence of partially developed monochromatic speckle patterns, *Optical Communication*, **12**, 156-159
- Philip B C** (1994) Beam waist and  $M^2$  measurement using a finite slit, *Optical Engineering*, **33**(7), 2461-2466
- Phillips C R** (1977) Gaseous sterilisation, In *Disinfection, Sterilisation and Preservation* (ed. Block, S.S.) 2<sup>nd</sup> ed., 592-611
- Pikaev A** (1990) Radiation processing in the U.S.S.R., *Radiat. Phys. Chem.*, **35**, nos. 4-6, 870-878
- Polanyi T G** (1983) Laser physics, *Otolaryngology Clinical North America*, **16**, 753-774
- Powell G and Whisenant B K** (1991) Comparison of three lasers for dental instrument sterilisation, *Lasers in Surgery and Medicine*, **11**, 69-71
- Reed J M, Bohrer C W and Cameron E J** (1951) *Food Research*, **16**, 383
- Ridgen J D and Gordon E I** (1962) The granularity of scattered optical maser light, *Proceedings of IEEE*, **50**, 2367-2368
- Riva C E, Petrig B L, Shonat R D and Pournaras C J** (1989) Scattering process in LDV from retinal vessels, *Appl. Opt.*, **28**, 1078-1083
- Riva C, Ross B and Benedek G** (1972) Laser Doppler measurements of blood flow in capillary tubes and retinal arteries, *Invest. Ophthalmol.*, **11**, 936-944
- Rogers G F C and Mayhew Y R** (1988) Thermodynamics and transport properties of fluids, In *SI Units*, fourth edition, Blackwell publisher.

- Rooney J, Midda M and Leeming J** (1994) A laboratory investigation of the bactericidal effect of a Nd:YAG laser, *British Dental Journal*, **176**, 61-64
- Rose F L and Swain G** (1956) Bisguanides having antibacterial activity, *Journal of Chemical Society*, **23**, 4422-4425
- Ruff J A and Siegman A E** (1992) Single-pulse laser beam quality measurements using a CCD camera system, *Applied Optics*, **31**, 4970-4909
- Russell A D and Harries D** (1967) Some aspects of thermal injury in *Escherichia coli*, *Applied Microbiology*, **15**, 407-410
- Russell A D, Hugo W B and Ayliffe G J** (1982) Anti-bactericidal agent, In *Principles and practice of disinfection, preservation and sterilisation*, 5<sup>th</sup> edition, 40-42
- Rypma R** (1997) Beam diagnostics, *The Photonics Design and Applications Handbook*<sup>®</sup>, **43**, H297-300
- Saks N and Roth C** (1963) Ruby laser as a microbiological instrument, *Science*, **141**, 46-47
- Sams A R and Ferria R** (1991) Microbial effects of ultrasonication of broiler drumstick skin, *Journal of Food Science*, **56**, 247-248
- Sanborn M R, Wan S K and Bulard R** (1982) Microwave sterilisation of plastic tissue culture vessels for reuse, *Applied Environmental Microbiology*, **44**, 960-964
- Sastry S K and Palaniappan S** (1991) The temperature difference between a microorganism and a liquid medium during microwave heating, *Journal of Food Processing and Preservation*, **15**, 3, 225-230
- Sato Y, Takahashi T, Saito T, Sato T and Takehisa** (1993) Sterilisation of health care products by 5 Mev bremsstrahlung, *Radiation Physics and Chemistry*, **42**, 621-624
- Schultz R J, Harvey G P, Fernandez-Beros M E, Krishnamurthy S, Rodriguez J E and Cabello F** (1986) Bactericidal effects of the Neodymium:YAG Laser: in vitro study, *Lasers in Surgery and Medicine*, **6**, 445-448
- Scientific status summary** (1989) Microwave food processing, *Food Technology*, **43** (1), 117-126
- Sedarevic O, Darell R W, Krueger R R and Trokel S L** (1985) Excimer laser therapy for experimental *Candida keratitis*, *American Journal of Ophthalmology*, **99**, 534-538

- Semenov F V, Galenko-Yaroshevskii P A and Babichev S A** (1996) Bactericidal properties of a defocused Nd:YAG laser beam, *Bulletin of Experimental Biology and Medicine*, **121**, 6, 654-656
- Shaban A M, El-Taweel G E and Ali G H** (1997) UV ability to inactivate microorganisms combined with factors affecting radiation, *Water Science and Technology*, **35**, 11, 107-112
- Siegman A E, Sasnett M W and Johnston T F** (1991) Choice of clip levels for beam width measurements using knife-edge techniques, *IEEE Journal Quantum Electronic*, **27**, 1098-1104
- Skyles G** (1965) Radiation sterilization, In *Disinfection and sterilisation*, 2<sup>nd</sup> edition, London, 178-182
- Sobotka J** (1992) Application of ultraviolet radiation for water disinfection and purification in Poland, *Water Science Technology*, **26**, 9-11, 2313-2316
- Soren L and Flemming M** (1986) Microwave sterilization of vials, *Journal of Parenter Science Technology*, **40**, 1, 25-30
- Speckle and Related Phenomena, *J. C. Dainty (Springer-Verlag, Berlin)* 9-75
- Stabholz A, Kettering J, Neev J and Torabinejad** (1993) Effects of the XeCl excimer laser on *Streptococcus mutans*, *Journal of Endodontics*, **19**, 5, 232-235
- Stellar S, Polanyi T G and Bredemeier H C** (1974) Laser in surgery: Lasers Applications in Medicine and Biology, **2**, New York, Plenum Press, 265-268
- Stern M, Lappe D L, Bowen P D, Chinovsky J E, Holloway G A, Kaiser H R and Bowman R L** (1977) Continuous measurement of tissue blood flow by laser doppler, *America Journal of Physiology*, **232**, 441-448
- Strong M S and Jako G J** (1972) Laser surgery in the larynx, *Archives of Otolaryngology*, **81**, 791-798
- Takabashi P K, Toups H J, Greenburg D B, Dimopoulos G T and Rusoff L L** (1975) Irradiation of *Escherichia coli* in the visible spectrum with a turnable organic-dye laser energy source, *Applied Microbiology*, **29**, 63-67
- Talebzadeh N, Morrison P R and Fried M P** (1994) Comparative cell target in vitro using the CO<sub>2</sub> laser, *Laser in Surgery and Medicine*, **14**, 164-167
- Tanaka T, Riva C and Ben-Sira I** (1974) Blood velocity measurements in human retinal vessels, *Science*, **186**, 830-832
- Wang R K, Watson I A, Ward G D, Stewart-Tull D E S and Wardlaw A C** (1997) Temperature distribution in *Escherichia coli* liquid suspensions during

irradiation by a high-power Nd:YAG laser for sterilization applications, *Journal of Biomedical Optics*, **2**, 3, 295-303

**Ward G D** (1996) Exposure of bacteria on plastic, stainless steel and glass surfaces, *Laser Sterilisation of Microorganisms (thesis)*, 203-206

**Ward G D, Watson I A, Stewart-Tull D E, Wardlaw A C and Chatwin C R** (1996) Inactivation of bacteria and yeasts on agar surfaces with high power Nd:YAG laser light, *Letter in Applied Microbiology*, **23** p 136-40

**Ward G D, Watson I A, Stewart-Tull D E, Wardlaw A C and Wang R K** (1997) Lethal effect of high power Nd:YAG laser light on *Escherichia coli* in liquid culture, *Journal of Applied and Environmental Microbiology*; submitted

**Watson I A, Gstettner S and Stewart-Tull D E** (1995) Nd: YAG laser sterilisation of *Escherichia coli* and *Bacillus stearotherophilus*, *Cleo/Pacific Rim*, **Thl 4**, 143-144

**Watson I A, Ward G A, Wang R K, Sharp J H, Budgett D M, Stewart-Tull D E, Wardlaw A C and Chatwin C R** (1996) Comparative bactericidal activities of lasers at seven different wavelengths, *Journal of Biomedical Optics*, **1**, 4, 466-472

**Weichman J A and Johnson F M** (1971) *Oral Pathology*, **31** p 416-20

**Weiman T J, Fingar V H and Johnston M N** (1994), *Proceedings 5<sup>th</sup> Institute of Photodynamic Association*, **Sept. 21-24**, 43

**Weymes C and White J D** (1975) Studies in the use of low concentrations of formaldehyde with steam at sub-atmospheric pressures as a method of sterilising non-porous heat-sensitive items, *Glasgow Greater Health Board, Sterile Supply Service*

**Whitters C J, Macfarlane T W, Mackenzie D, Moseley H and Strang R** (1994) The bactericidal activity of pulsed Nd:YAG laser radiation in vitro, *Lasers in Medical Science*, **9**, 297-303

**Wilson J and Hawkes J F B** (1987) The optical resonator, In *Lasers:- Principles and Applications (Prentice Hall Publications)*, 21-24

**Wilson M** (1993) A Review:- Photolysis of oral bacteria and its potential use in the treatment of caries and periodontal diseases, *Journal of Applied Bacteriology*, **75**, 299-306

**Wilson M, Dobson J and Harvey W** (1992) Sensitisation of oral bacteria to killing by low power laser radiation, *Current Microbiology*, **25**, 77-81

- Windeler A S and Walter R G** (1975) The sporicidal activity of glass bead steriliser, *Journal of Endodontic*, **1**, 273-275
- Wright D, Greve P, Fleischer J and Austin L** (1992) Laser beam width, divergence and beam propagation factor- an international standardization approach, *Optical Quantum Electronic*, **24**, s993-s1000
- Wright R L Walker H W and Parish F C** (1986) Survival of *Clostridium perfringens* and aerobic bacteria in ground beef patties during microwave and conventional cookery, *Journal of Food Protection*, **49**, 203-206
- Wu Q** (1996) Effect of high-power microwave on indicator bacteria for sterilisation, *IEEE Transactions on Biomedical Engineering*, **43(7)**, 752-754
- Xu Z, Joenathan C and Khorana B M** (1995) Temporal and spatial properties of the time-varying speckles of botanical specimens, *Opt. Eng.*, **34 (5)**, 1487-1501
- Yanagawa T, Koike K A, Yamada I and Hashimoto K** (1992) Bactericidal effects of argon laser on various organisms, *Lasers in the Life Science*, **4, 4**, 201-207
- Yeo C B Allen, Watson I A and Wang R K** (1996) Temperature dependency of the optical properties of water at 1.064  $\mu\text{m}$ , *OSA Trends in Optics and Photonics Series; Medical and Biological Applications*, **6** p 14-17
- Yuge T** (1960) Experiments on heat transfer from spheres including natural and forced convection, *Journal of Heat Transfer*, **82**, 214-220
- Zakariasen K L, Dererich D N, Tulip J, Decoste S, Jensen S E and Pickard M A** (1986) Bactericidal action of CO<sub>2</sub> laser radiation in experiment dental root canals, *Canadian Journal of Microbiology*, **32**, 942-946
- Zheng B, Pleass C M and Lee C S** (1994) Feature information extraction from dynamic biospeckle, *Appl Opt.*, **33**, 231-237
- Zimmermann U** (1986) Electrical breakdown, electro-permeabilisation and electrofusion, *Review Physiology Biochem. Pharmacol.*, **105**, 175-256

## **IX. APPENDICES**

## 9.1 HEAT TRANSFER ANALYSIS

Eqn. 5.1.6 is solved by means of integrating factors. Using the condition that the initial temperature of the microorganism is the same as that of the fluid; i.e.  $t=0$  ( $T(0) = T_i$ )

$$\frac{dT}{dt} + \frac{h_m A_m T}{\rho_m C_{pm} V_m} = \frac{q_m}{\rho_m C_{pm}} + \frac{h_m A_m}{\rho_m C_{pm} V_m} \left[ \frac{q_l t}{\rho_l C_{pl}} + T_i \right] \quad (5.1.6)$$

Eqn. (5.1.6) can be represented by;

$$\frac{dT}{dt} + P(t)T = Q(t)$$

Integrating factor is given by :

$$\exp\left[\int P(t)dt\right] = G(t) \text{ and } \frac{d}{dt}[TG(t)] = Q(t)G(t) \quad (5.1.6A)$$

implies :

$$\int P(t)dt = \int \frac{[h_m A_m]}{[\rho_m C_{pm} V_m]} dt = \frac{h_m A_m t}{\rho_m C_{pm} V_m}$$

and

$$G(t) = \exp\left[\frac{h_m A_m t}{\rho_m C_{pm} V_m}\right]$$

Substitute into Eqn. 5.1.6A;

$$\frac{d}{dt} \left\{ T \exp\left[\frac{h_m A_m t}{\rho_m C_{pm} V_m}\right] \right\} = \left\{ \left[ \frac{q_m}{\rho_m C_{pm}} \right] + \left[ \frac{h_m A_m}{\rho_m C_{pm} V_m} \right] \left[ \frac{q_l t}{\rho_l C_{pl}} + T_i \right] \right\} \exp\left[\frac{h_m A_m t}{\rho_m C_{pm} V_m}\right]$$

Integrating both sides,

$$\begin{aligned}
 T \exp\left[\frac{h_m A_m t}{\rho_m C_{pm} V_m}\right] &= \int \frac{q_m}{\rho_m C_{pm}} \exp\left[\frac{h_m A_m t}{\rho_m C_{pm} V_m}\right] dt + \\
 &\quad \int \left[\frac{h_m A_m}{\rho_m C_{pm} V_m}\right] \left[\frac{q_l t}{\rho_l C_{pl}}\right] \exp\left[\frac{h_m A_m t}{\rho_m C_{pm} V_m}\right] dt + \\
 &\quad \int \left[\frac{h_m A_m}{\rho_m C_{pm} V_m}\right] T_i \exp\left[\frac{h_m A_m t}{\rho_m C_{pm} V_m}\right] dt \\
 &= \left[\frac{q_m}{\rho_m C_{pm}}\right] \frac{\rho_m C_{pm} V_m}{h_m A_m} \exp\left[\frac{h_m A_m t}{\rho_m C_{pm} V_m}\right] + \\
 &\quad \int \left[\frac{h_m A_m}{\rho_m C_{pm} V_m}\right] \left[\frac{q_l t}{\rho_l C_{pl}}\right] \exp\left[\frac{h_m A_m t}{\rho_m C_{pm} V_m}\right] dt + \\
 &\quad \frac{h_m A_m T_i}{\rho_m C_{pm} V_m} \times \frac{\rho_m C_{pm} V_m}{h_m A_m} \exp\left[\frac{h_m A_m t}{\rho_m C_{pm} V_m}\right] \quad (5.1.6B)
 \end{aligned}$$

Now, let 
$$\int \left[\frac{h_m A_m}{\rho_m C_{pm} V_m}\right] \left[\frac{q_l t}{\rho_l C_{pl}}\right] \exp\left[\frac{h_m A_m t}{\rho_m C_{pm} V_m}\right] dt =$$

$$\int AB \exp(At) dt = AB \int \exp(At) dt$$

Implies that;

$$A = \frac{h_m A_m}{\rho_m C_{pm} V_m} \quad \text{and} \quad B = \frac{q_l}{\rho_l C_{pl}}$$

Using integration by parts, i.e.  $\int u dv = [uv] - \int v du$

Let  $t = u$ , so  $dt = du$

Implies  $dv = \exp(At) dt$ , so  $\frac{dv}{dt} = \exp(At)$  and  $v = \frac{\exp(At)}{A}$

Therefore;  $AB \int \text{texp}(At) dt = AB \left\{ \left[ \frac{\text{texp}(At)}{A} \right] - \int \frac{\text{exp}(At)}{A} dt \right\} =$

$$AB \left[ \frac{\text{texp}(At)}{A} - \frac{\text{exp}(At)}{A^2} \right] + \text{Const.} = B \text{texp}(At) - \frac{B \text{exp}(At)}{A} + \text{Const.} \quad (5.1.6C)$$

Substitute A and B into (5.1.6C) :

$$\therefore AB \int \text{texp}(At) dt = \frac{q_1 t}{\rho_l C_{pl}} \exp \left[ \frac{h_m A_m t}{\rho_m C_{pm} V_m} \right] - \frac{q_1}{\rho_l C_{pl}} \left[ \frac{\rho_m C_{pm} V_m}{h_m A_m} \right] \exp \left[ \frac{h_m A_m t}{\rho_m C_{pm} V_m} \right] + \text{Const.}$$

From Eqn. 5.1.6B,

$$\begin{aligned} T \exp \left[ \frac{h_m A_m t}{\rho_m C_{pm} V_m} \right] &= \frac{q_m}{\rho_m C_{pm}} \exp \left[ \frac{h_m A_m t}{\rho_m C_{pm} V_m} \right] \left[ \frac{\rho_m C_{pm} V_m}{h_m A_m} \right] + \\ &\quad \frac{h_m A_m T_i}{\rho_m C_{pm} V_m} \exp \left[ \frac{h_m A_m t}{\rho_m C_{pm} V_m} \right] \left[ \frac{\rho_m C_{pm} V_m}{h_m A_m} \right] + \\ &\quad \frac{q_1 t}{\rho_l C_{pl}} \exp \left[ \frac{h_m A_m t}{\rho_m C_{pm} V_m} \right] - \\ &\quad \frac{q_1}{\rho_l C_{pl}} \left[ \frac{\rho_m C_{pm} V_m}{h_m A_m} \right] \exp \left[ \frac{h_m A_m t}{\rho_m C_{pm} V_m} \right] + \text{Const.} \end{aligned}$$

which can be simplified to :

$$\begin{aligned} T \exp \left[ \frac{h_m A_m t}{\rho_m C_{pm} V_m} \right] &= \frac{q_m V_m}{h_m A_m} \exp \left[ \frac{h_m A_m t}{\rho_m C_{pm} V_m} \right] + T_i \exp \left[ \frac{h_m A_m t}{\rho_m C_{pm} V_m} \right] + \\ &\quad \frac{q_1 t}{\rho_l C_{pl}} \exp \left[ \frac{h_m A_m t}{\rho_m C_{pm} V_m} \right] - \end{aligned}$$

$$\frac{q_l}{\rho_l C_{pl}} \frac{\rho_m C_{pm} V_m}{h_m A_m} \exp\left[\frac{h_m A_m t}{\rho_m C_{pm} V_m}\right] + \text{Const.}$$

Using the condition that the initial temperature of the microorganism is the same as the fluid i.e.  $T(0) = T_i$  implies;

$$\text{Const.} = \frac{V_m}{h_m A_m} \left[ \left( \frac{\rho_m C_{pm}}{\rho_l C_{pl}} \right) q_l - q_m \right]$$

yielding;

$$\begin{aligned} T \exp\left[\frac{h_m A_m t}{\rho_m C_{pm} V_m}\right] &= \frac{q_m V_m}{h_m A_m} \exp\left[\frac{h_m A_m t}{\rho_m C_{pm} V_m}\right] + T_i \exp\left[\frac{h_m A_m t}{\rho_m C_{pm} V_m}\right] + \\ &\frac{q_l t}{\rho_l C_{pl}} \exp\left[\frac{h_m A_m t}{\rho_m C_{pm} V_m}\right] - \frac{q_l}{\rho_l C_{pl}} \frac{\rho_m C_{pm} V_m}{h_m A_m} \exp\left[\frac{h_m A_m t}{\rho_m C_{pm} V_m}\right] + \\ &\frac{V_m}{h_m A_m} \left[ \left( \frac{\rho_m C_{pm}}{\rho_l C_{pl}} \right) q_l - q_m \right] \end{aligned}$$

Finally;

$$\begin{aligned} T &= \frac{q_m V_m}{h_m A_m} + T_i + \frac{q_l t}{\rho_l C_{pl}} - \frac{q_l}{\rho_l C_{pl}} \frac{\rho_m C_{pm} V_m}{h_m A_m} + \\ &\left( \frac{V_m}{h_m A_m} \right) \left[ \left( \frac{\rho_m C_{pm}}{\rho_l C_{pl}} \right) q_l - q_m \right] \exp\left\{ - \left[ \frac{h_m A_m t}{\rho_m C_{pm} V_m} \right] \right\} \end{aligned} \quad (5.1.7)$$